

Master thesis

Underground mine design Mazy

Golzinne, Belgium

Vielkind Moritz Stefan, BSc

Date(09/11/2012)



Chair of Mining Engineering and Mineral Economics
Department Mineral Resources and Petroleum Engineering
Montanuniversitaet Leoben

A-8700 LEOBEN, Franz Josef Straße 18
Phone: +43/(0)3842-402-2001
Fax: +43/(0)3842-402-2002
bergbau@unileoben.ac.at

Declaration of authorship

„I declare in lieu of oath that this thesis is entirely my own work except where otherwise indicated. The presence of quoted or paraphrased material has been clearly signaled and all sources have been referred. The thesis has not been submitted for a degree at any other institution and has not been published yet.”

(Date)

(Moritz Stefan Vielkind)

Preface, Dedication, Acknowledgement

First of all I want to thank Francis Kezirian from Solubema that he gave me/us the opportunity to work on this interesting and challenging topic. Thank you!

Secondly, a special thank to Dr. Hannes Blaha for his excellent supervision and for his 'always open door' for my questions. The thesis would not exist in that manner without his tremendous guidance. Thank you!

I also want to thank Dr. Horst Wagner, for spending his time to support and guide me through critical questions. Furthermore I want to thank him for his motivation. Thank you!

The laboratory tests would not have been possible without the introduction, the encouragement and support of DI Wolfgang Hohl and Mr. Klaus Lackner. Thank You!

Finally I want to say thank you to my parents who supported me and gave me the opportunity to do my studies at the Montanuniversitaet Leoben. Thank you!

Abstract

The aim of the work is on the one side, to describe the current geomechanical status of the underground mine of black marble and on the other side to design possible future mining areas.

The current status of the room and pillar operation is described by using the results of the fieldwork and the results of the laboratory tests. With this data the stability of the pillars and the rooms are evaluated, using the concept of the factor of safety and rock mass classification systems. Besides the structure of the deposit, geological discontinuities are also described and documented.

In consideration of external influences, like water or quality, possible future mining areas are reported and possible mining geometries are shown. With all this information and the results of the analysis of the current status, a pre-design for the future mining operations is done. The current status and the results for the possible future mining areas are visualized by a 3D model in Surpac.

Zusammenfassung

Ziel dieser Arbeit ist es einerseits den geomechanischen Ist-Zustand des untertägigen Abbaus von schwarzem Marmor zu beschreiben und andererseits mögliche zukünftige Abbaubereiche zu dimensionieren.

Der Ist-Zustand des Örtlerbaus wird mittels der Untersuchungen vor Ort und die durch Tests im Labor gefundenen Ergebnisse kalibriert. Dabei wurden die Stabilität der Festen mittels des Ansatzes des Sicherheitsfaktors sowie die der Örtler mittels Gebirgsklassifikationssysteme evaluiert. Des Weiteren wurden neben dem Aufbau der Lagerstätte, die geologischen Diskontinuitäten beschrieben und dokumentiert.

Unter Berücksichtigung der externen Einflüsse, wie Wasser oder Qualität, wurden mögliche zukünftige Abbaubereiche verglichen und möglich Abbaugeometrien aufgezeigt. Mit den Erkenntnissen von der Analyse des Ist-Zustandes wurde eine Vordimensionierung für zukünftige Abbaue erstellt. Der Ist-Zustandes und die Ergebnisse der möglichen zukünftigen Abbaue wurden mittels 3D Modell in Surpac visualisiert.

Table of contents

Declaration of authorship	II
Preface, Dedication, Acknowledgement	III
Abstract	IV
Zusammenfassung	V
Table of contents	VI
1 Executive summary	1
2 Introduction	3
3 Tasks	4
4 Documentation of the current status	5
4.1 Position	6
4.2 Geology.....	11
4.2.1 Structure of Deposit.....	12
4.2.2 Major Faults	16
4.2.3 Geophysics	25
4.2.4 Geological discontinuities	27
4.3 Underground mine.....	30
4.3.1 General aspects	30
4.3.2 3D Model.....	34
4.3.3 Historical development of the mine.....	44
4.3.4 External influences	47
5 Geotechnical investigations	50
5.1 Rock strength parameter	55
5.1.1 Uniaxial compressive strength (UCS)	55
5.1.2 Bending tension strength (BTS).....	64
5.2 Pillar strength	67
5.2.1 Factor of safety (FOS) – theory	67
5.2.2 Factor of safety (FOS) – applied to the mine	73
5.2.3 Effect on the panel width	82
5.2.4 Result of the stability of the pillars	86
5.3 Stability of the roof.....	88
5.3.1 Hangingwall stability rating (HSR)	90
5.3.2 Bieniawski (Rock Mass Rating (RMR)) & Laubscher (Mining Rock Mass Rating (MRMR))	95
5.3.3 Barton (Q-System) → Mathew (N – Stability Number)	103

5.3.4	Summary of the geomechanical classification systems	115
5.3.5	Width of roof plate	116
5.4	Strength of the geological discontinuities.....	122
6	Possible future mining areas	123
6.1	Planned deployed machinery	124
6.2	Lower Levels	131
6.3	Area East	133
6.4	Area West	133
6.5	Area South	134
6.6	Area North.....	136
6.7	Basic access	138
7	South field	140
7.1	Access to South field.....	143
7.2	Dimensioning roof	146
7.2.1	Geomechanical classification systems - Global stability of the roof.....	146
7.2.2	Cantilever beam calculation.....	160
7.2.3	Summary of the global dimensioning of the room width.....	161
7.3	Dimensioning Pillar.....	162
7.4	Outlay of field south.....	170
7.4.1	Comparison to other variants.....	176
7.5	Width barrier pillar major fault “south” – main development “south”	185
7.6	Support	191
7.6.1	Support roof	193
7.6.2	Support walls.....	204
7.6.3	Support floor.....	211
7.7	Summary – south	212
8	Northfield	213
8.1	Access to future mining area north	214
8.2	Outlay – future mining area north	217
8.3	Summary – north.....	221
9	General Safety aspects	222
9.1	Equipment employees.....	222
9.2	Installations	224
9.3	Weathering.....	227
9.4	Additional machinery	228
10	Discussion	231
11	Bibliography.....	233

12	List of figures	236
13	List of tables	243
14	List of abbreviations and definitions	246
15	Annex	I
15.1	Provided Map of the company – total	I
15.2	Provided Map of the company – left part, enlarged.....	II
15.3	Provided Map of the company – right part, enlarged	III
15.4	Discontinuities distance distribution – overview map	IV
15.5	Exemplary photo documentation for UCS laboratory tests.....	V
15.5.1	BBK 81 – base material.....	V
15.5.2	BBK 81-1 – sample – perpendicular to layering	VI
15.5.3	BBK 81-5 – sample – parallel to layering	VI
15.6	Calculation and results of pillar stability (FOS)	VII
15.6.1	Pillar 1 – 43 (incl. Database 1 and 2).....	VII
15.6.2	Pillar 44 – 265 (only Database 3 available).....	IX
15.7	Effect on the panel width – alignment map	XVI
15.8	Calculation rock quality designation (RQD – value)	XVII
15.9	Tables for Barton’s – Q-System.....	XVIII
15.10	Calculation of pillar 1, future mining area south	XXIII
15.11	Values for the calculation of the example for volume comparison/contrast of different Variants, future mining area south.....	XXIV
15.12	Fieldwork report	XXV

1 Executive summary

The aim of the work is on the one side, to describe the current geomechanical status of the underground mine of black marble, located in Mazy, Glozinne – Belgium, and on the other side to design possible future mining areas for the further mining of dimension stones. The outlay of the future mining area is basically done to mine the whole thickness of the deposit (12 [m]).

The current status of the room and pillar operation is described by using the results of the fieldwork, the provided data from the company and the results of the laboratory tests. With this data, the stability of the pillars are evaluated by using the concept of the factor of safety including the tributary area theory. Furthermore the stability of the current rooms are described by using rock mass classification systems and the classical approach of the cantilever beam, with the ulterior motive to gain a basis for determining the span width for the possible future mining areas. Additionally the structure of the deposit, geological discontinuities and external influences are described and documented.

In consideration of the investigations and of the external influences, like water or quality, two possible future mining areas result:

- possible future mining area south (southern the current mining area)
- possible future mining area north (northern the current mining area, beyond the major fault named “17m”, which shifts the northern and southern current mining area around 17 [m])

Possible future mining area south

The room width for the future mining operation is 8 [m], based on the investigation of the rock mass classification systems and the cantilever beam approach. The mining heights for the possible future mining area south is for the main developments 6 [m], at an inclination of 3 [°] (main development south) and 1 [°] (main development north) into ~east. The mining height for the stopes are (with an inclination ~11 [°] into ~ south) during the first phase 6 [m] and after applying the second phase up to 12 [m]. The mining height of 6 [m] results from the constraint, that the planned deployed cutting machine, reaches a cutting height of 6 [m]. The suggested type of pillar is a strip pillar which follow ~ the dip direction of the deposit (north – south). The width of the pillar is 6 [m] and was determined by taking once, the classical approach of the factor of safety as well as the influence of the geological discontinuity into consideration. The width of the future mining area south is determined by the uncertain major fault “south”. The determination of the major fault is crucial to complement the layout for the possible future mining area south, e.g. by a core drilling program. Between the main development north and the current mine a barrier pillar with 8 [m] width is suggested. Based on the available data base, a barrier pillar between

the major fault “south” and the main development south of 8 [m] is suggested (depending on the position and the experienced quality of the rock mass near the fault).

Possible future mining area north

The room width is, as for the possible future mining area south, 8 [m]. The general mining height for the future mining area north is 6 [m]. The main developments have a length of 64 [m] and an inclination of 5 [°] into ~east. The stopes have length of 32 [m] and an inclination of 14 [°] into ~south. The mining operation is situated in the lower layers of the deposit since quality of the upper layers is uncertain due to the nearness to the surface. The suggested type of pillar is a strip pillar which follow ~ the dip direction of the deposit (north – south). The width of the pillar is 6 [m]. The pillar dimension allows, with the proper investigations, an expansion of the mining height to mine in a second step the upper layers and thereof the whole deposit. Between the major fault 17 [m] and the main development north a barrier pillar with a width of 8 [m] is suggested (depending on the experienced quality of the rock mass near the fault)

The current status and the results for the possible future mining areas are visualized by a 3D model in Surpac and are presented on basis of the plan view below (see Figure 1).

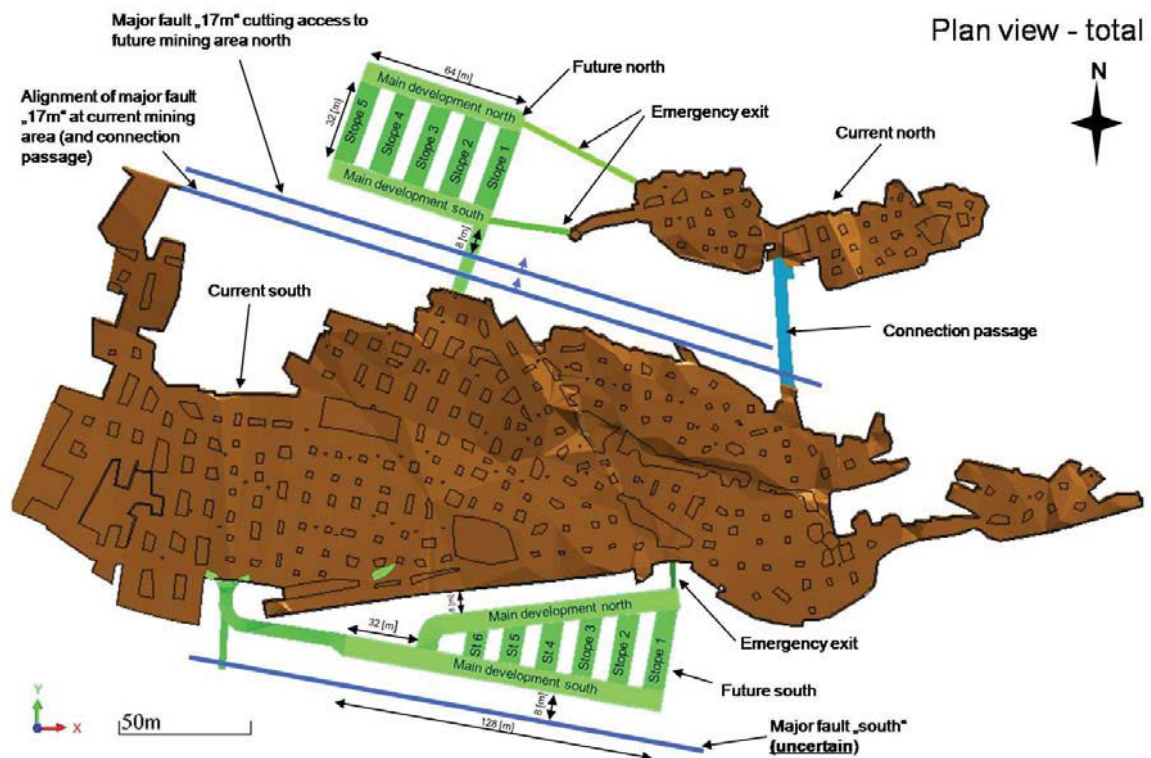


Figure 1: Plan view total, executive summary

Note: The above presented values and results are first approaches and require further investigations combined with supervision at the real mining situation to be valid and complemented.

2 Introduction

This master thesis deals with a black marble underground mine Mazy in Belgium, near Golzinne. The mine is operated by the Belgium company Merbes-Sprimont, originally established in 1779, which is today a subsidiary of the Portuguese company Solubema. The company produces dimension stones out of the unique black marble deposit by room and pillar mining. The material is also called "Noir Belge" or "Belgian Black" and the end product can be found, among other products, all over Europe's most famous royal castles and churches (e.g. Westminster Abbey, UK).

Two main characteristics give the rock the capacity to obtain a mirror-like polish and its unmistakable color. Once, the virtually vein- and fossil free occurrence, caused by the peculiar sedimentation conditions and the absence of tectonic deformations. Second, a pure chemical composition of 98,5 [%] calcium carbonate. (cp. Galiotto 2011, p. 71)

An example of the shift from the dimension stone into a modern work of art is shown in Figure 2.

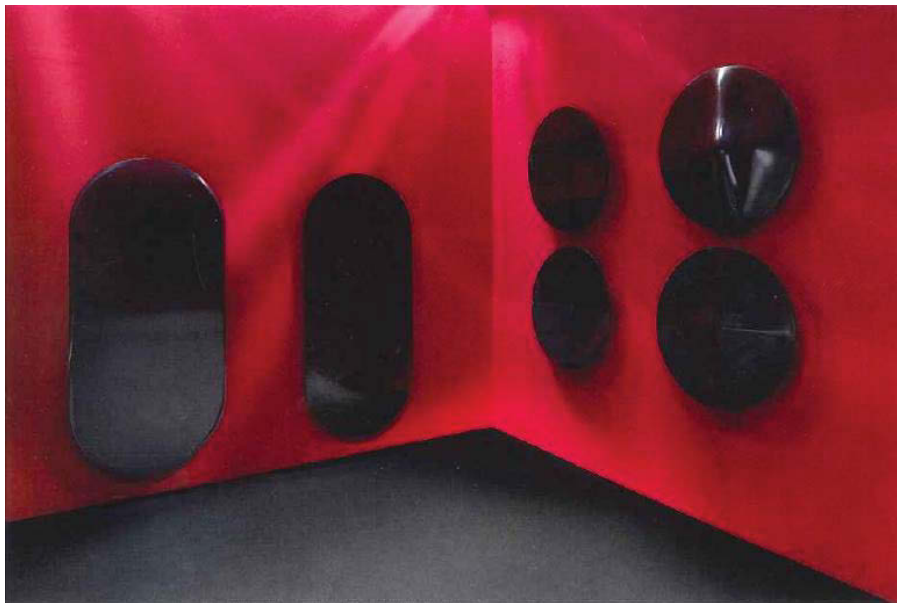


Figure 2: Distorting mirrors (Galiotto 2011, p. 39)

The master thesis is part of a slivered offer between the company and the Montanuniversität Leoben, Austria. It is used for getting to know each other and to deliver a base work for the possible further studies.

The contact and the communication with the company were achieved by Francis Kezirian, a geologist and a member of the board of the company.

3 Tasks

The aim of the work is to describe the current geomechanical status of the underground mine of black marble and to design possible future mining areas.

To describe the current geomechanical status, the first task contains to describe the mine in general – including the position, the principle structure of the deposit, the geological discontinuities and the external influences. Therefore the gained data and results from the fieldwork and the provided data from the company are taken into consideration. The second task is to gain values for describing the stability of the room and pillar operation. Therefore laboratory tests for the uniaxial compressive strength and the bending tension strength are performed. With these data the stability of the pillars are described by using the classical approach of the factor of safety. To describe the stability of the rooms, in special the roof, rock mass classification systems are used. A special task is to describe the influence of the geological discontinuities on the span width of the roof plates.

The third main task is to define and layout possible future mining areas, including the access to them. Therefore the gained knowledge and information of the current status, the external influences and the changing mining method (blast and cut to exclusive cutting) and as a consequence thereof the change of the profile (e.g. mining height), are taken into consideration. The layout is realized in that manner that the same tools for describing the stability of the room and pillar for the current mine are used to define the dimensions of the rooms (rock mass classification system) and the pillars (factor of safety). A special task is to describe the increasing influence of the geological discontinuities due to the change of the mining profile – especially the mining height – and include these results into the final layout. A further task is to design a first approach concerning the necessary reinforcement.

An overall accompanying task is to visualize the current status and the possible future mining areas into a 3D model.

The final task is to present suggestions of general safety aspects which are detected at the fieldwork.

4 Documentation of the current status

In this chapter the current status of the mining operation will be presented, including a general presentation of the underground mine. For this the information gained in the fieldwork, observations and measured data will be used. Furthermore the from the company provided material will be taken into consideration.

In Figure 3 the naming of the areas within the mine is declared.

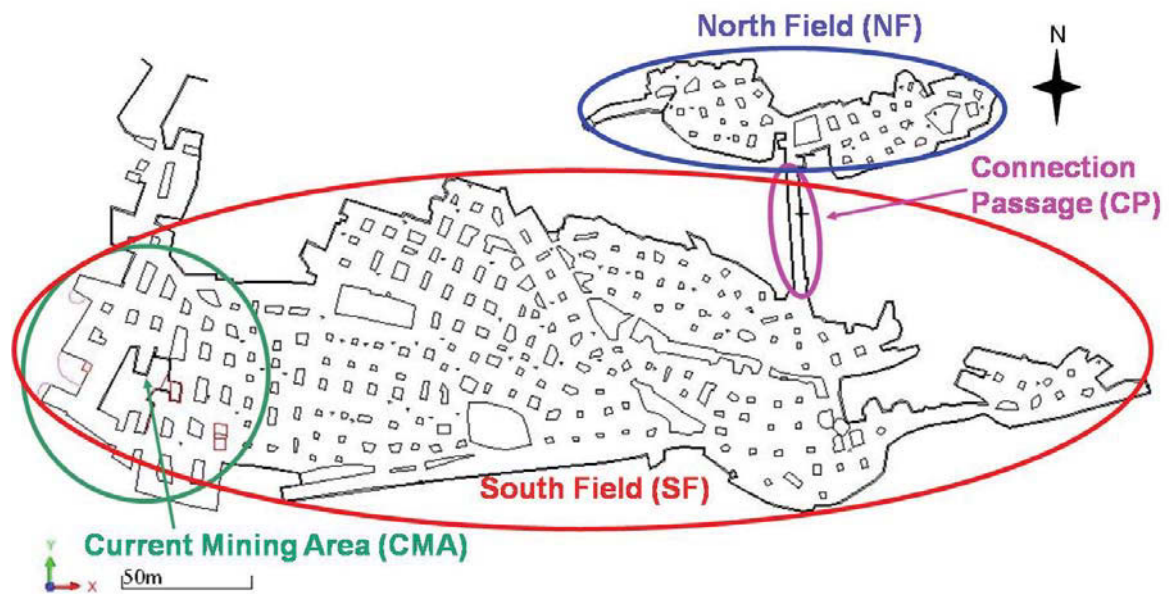


Figure 3: Naming of mining areas

4.1 Position

The mine is located in Belgium, Golzinne. Golzinne is around 45 km away from Brussels into south eastern direction. The location of the mine belongs to the district 5032 Bossière. In the following the location will be presented on the basis of 3 figures, which were taken from Google maps.

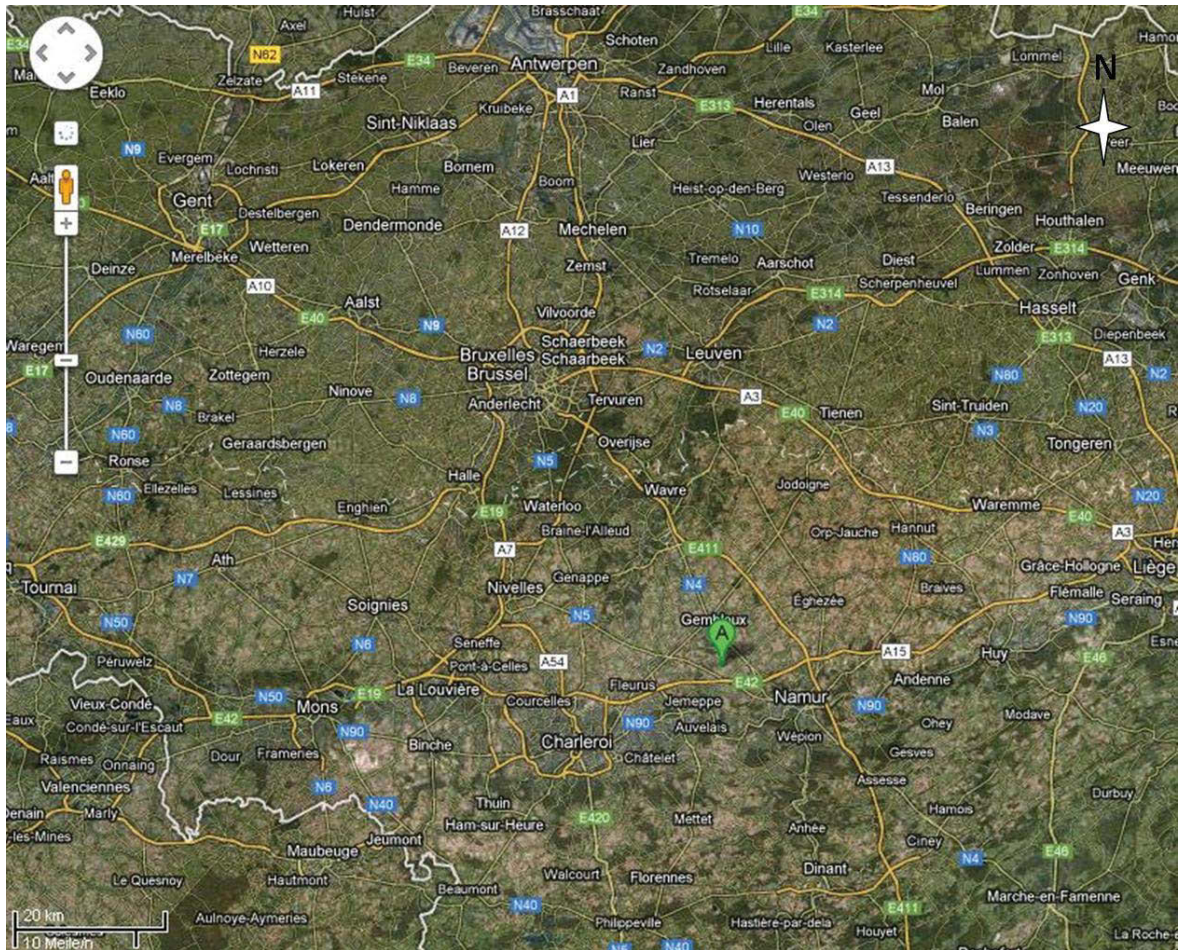


Figure 4: Location of the mine 1, Google maps 2012

As shown in Figure 4 the location is marked with the “green A”. In the following Figure 5 an enlargement of the area is shown.



Figure 5: Location of the mine, Google maps 2012

In Figure 6 a further enlargement of the surface area of the underground mine is shown. On basis of Figure 6 the main infrastructure will be presented.

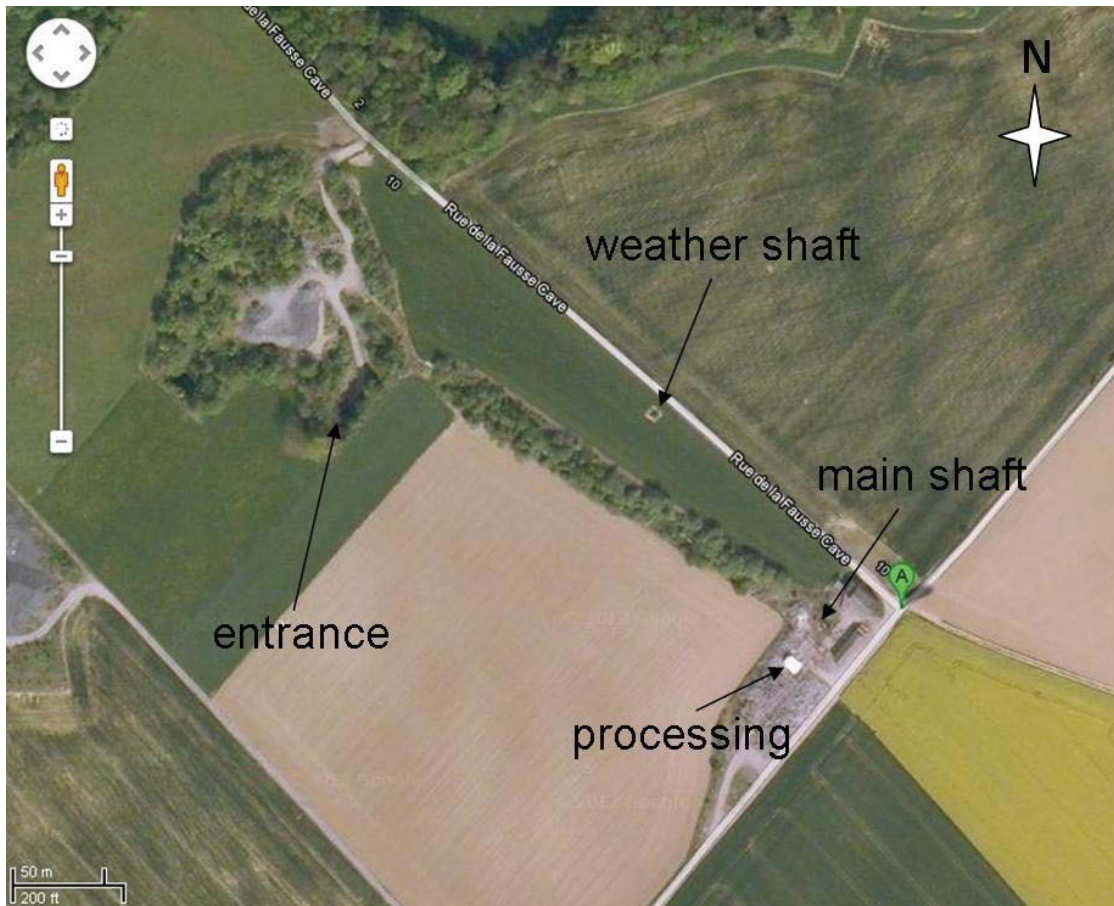


Figure 6: Location of the mine 3, Google maps 2012

The main access to the mine is given by the entrance, as shown in Figure 6. The main shaft and the weather shaft are secondary accesses. The final cutting of mined dimension stones/blocks is done at the processing. In the figures below, the mine itself is shown on the basis of the in Surpac¹ built 3D model. The description of the position of the mine will be stated after the figures. The visualization of the surface is adapted by draping an ortho-photo over the topography. Figure 7 presents the plan view.

(The procedure how the 3D model and the topography was built is shown in chapter 4.3.2)

¹ Mining software; Surpac Minex Group Pty Ltd (a Gemcom Company); www.gemcomsoftware.com

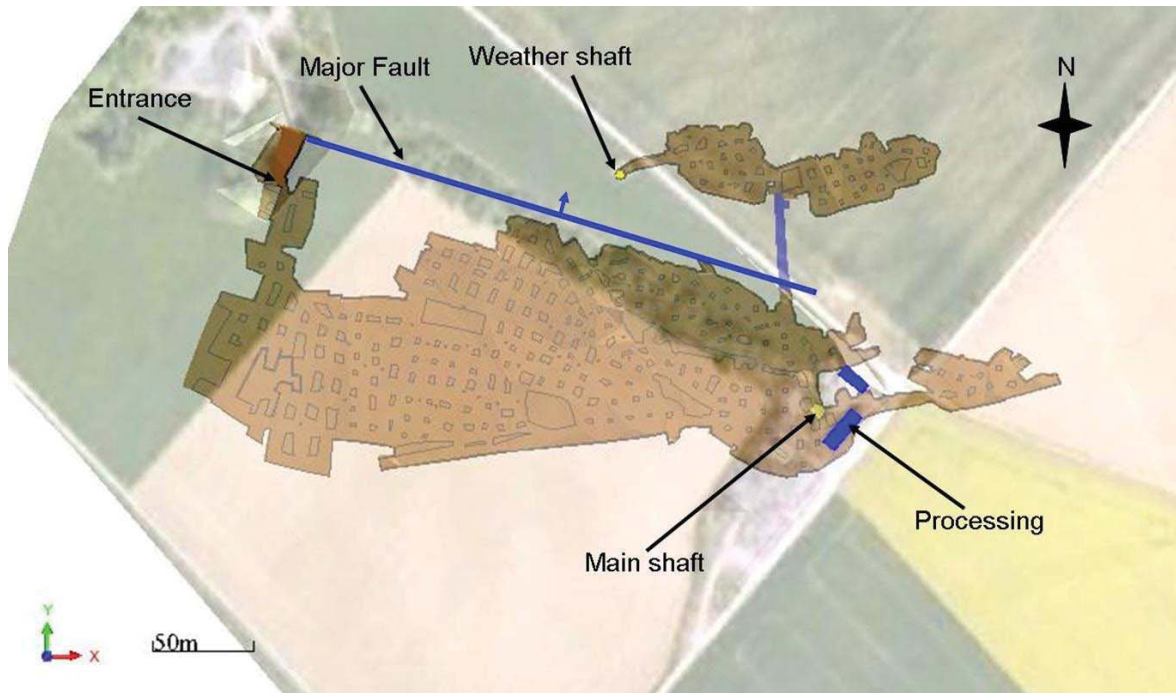


Figure 7: Location of the mine 4, plan view, Surpac

As in Figure 6, the main infrastructures are shown in Figure 7. The field north is shifted 17 [m] from the field south by a major fault, which is marked as blue line in Figure 7. Here the fault is simplified as a blue line to improve the visualization of the plan view of the mine. A detailed inspection of the fault and the shift is shown in chapter 4.2.2. The shift is apparent in Figure 8 at the side view (down, right).

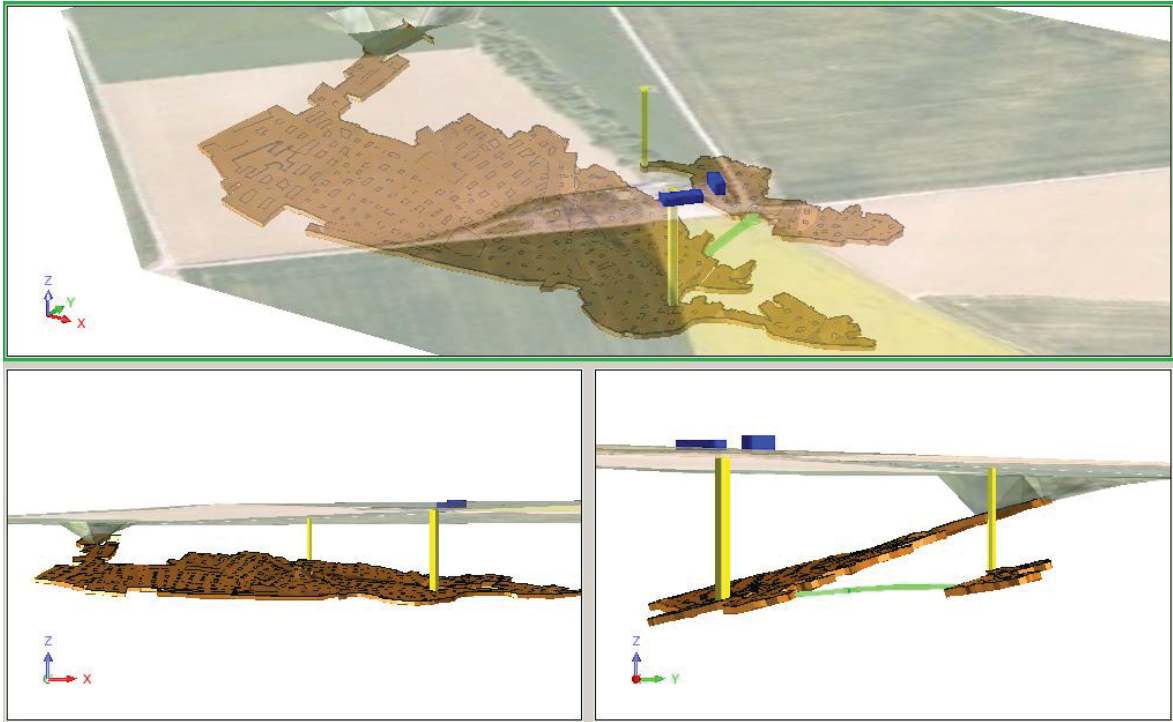


Figure 8: Location of the mine 5, Surpac

The major fault is faded out to improve the visualization of the 3D model.

4.2 Geology

The mine is a homogeneous, flat dipping stratified deposit with total thickness of 12 [m], based on the statement of the company concerning the quality and the saleability. 3,21 [m] are mined in the current operation (based on the survey of the fieldwork, see Annex, chapter 15.12)

The southern part of the deposit, based on the provided map of the company (see Annex, chapter 15.2), has a dipping between 10 [°] (in the east) and 17 [°] (in the center) into south direction. The northern part of the deposit has a dipping between 10 [°] (in the east) and 14,5 [°] (in the west) into south direction.

The thickness of the overburden, at the southern part of the mine, is between 67 [m] (south) and 35 [m] (north). Through the shift along a major fault the northern part has an overburden between 60 [m] and 49 [m]. This values are based on the spot heights marked in the from the company provided map (see Annex, chapter 15.2). The overburden consists of flat dipping stratified layers and a layer of soil. This conclusion was derived by the observation at the fieldwork at the entrance of the mine. A photography which was taken is shown in Figure 9.

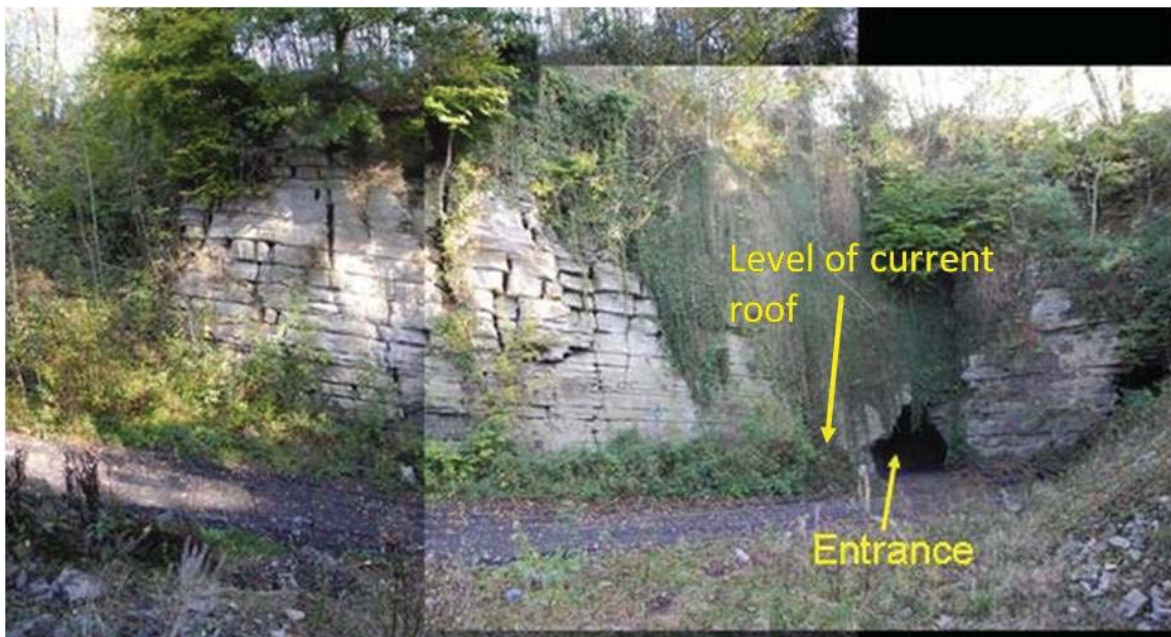


Figure 9: Overburden, Entrance

The south and the north field are connected by the connection passage. It cuts across a major fault, which shifts the north and the south field 17 [m] and has a dipping of ~ 2 [°]. At the connection passage the structure of the deposit is visible and is presented in chapter 4.2.1.

4.2.1 Structure of Deposit

The structure of the Deposit was recorded in the fieldwork (see Annex, chapter 15.12) at the connection passage as well as in the current mining operation by measuring the layer thickness of the pillars. Since the connection passage has a lower dipping as the layers of the deposit, the structure is visible by “cutting” through. In Figure 10 a sketch of the in the fieldwork done measurements is shown.

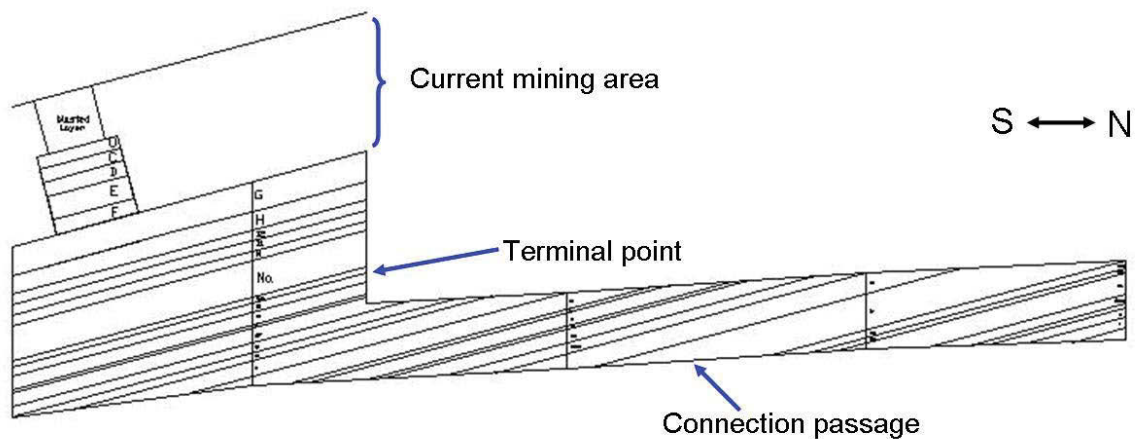


Figure 10: Sketch of recorded geological structure

The in Figure 10 shown sketch represents a cut through the southern part of the connection passage and the terminal point at the south field. Furthermore it shows the layers below the current mining area until the last layer (layer “T”) which is, according to the statement of the company, worth to mine. In Figure 11 a photo, which was taken of the terminal point, is shown (direction north).



Figure 11: Terminal point: south field – connection passage (north direction)

To gain the geological structure, the, from the company, marked layers along the connection passage and at the terminal point were measured. In Figure 12 an example is shown. The marked layers are located on the east wall (right side in Figure 11). The layers are separated by a thin layer of laminated black material, likewise schist. The thickness of the layers is not constant and reaches from 0 up to 1 [cm].



Figure 12: Layer Cr – T, connection passage (east wall)

Out of these measurements the geological structure of the deposit was developed. A sketch of the layers and their thickness are shown in Figure 13; where:

- The thickness of the deposit is presented by the layer “Layer Blasted” to layer “T”
- The value of the layer thickness is perpendicular to the layering and given in [cm], the total thickness of the deposit is 11,953 [m]
- The grey filled layers present a sketch of a pillar at the current mining area and therefore it represents the in the current mining operation extracted layers
- The “Layer Blasted” consists of several smaller layers, since there is no exact value of the thickness of the individual layers, it is designed as one
- The name and the thickness of the layers of the roof are taken from the company provided geological profile (“Coupe Veine inf+fotos.xls”; see attached data CD).

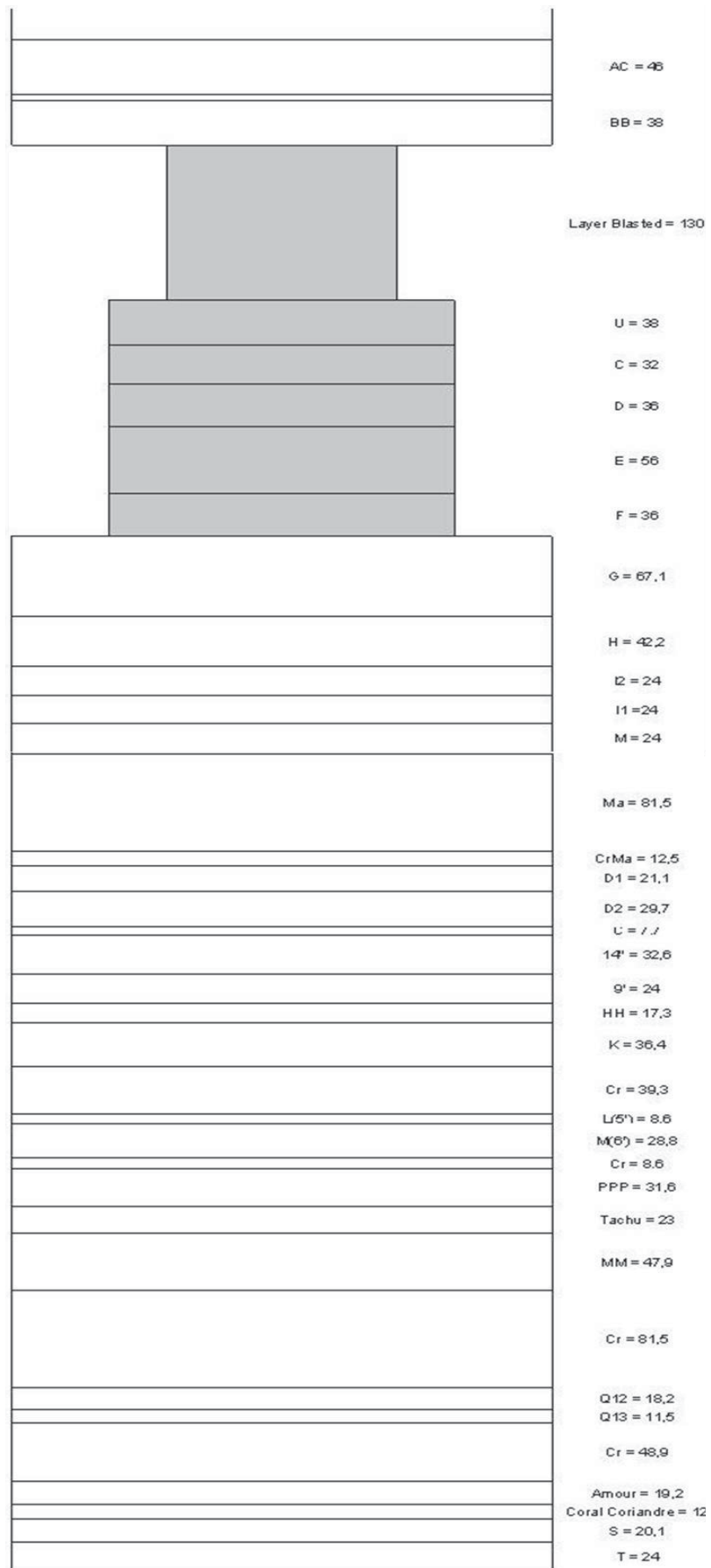


Figure 13: Geological structure, total deposit, sketch

4.2.2 Major Faults

In this chapter the major faults (shift of $\geq 0,5$ [m]) which were observed during the fieldwork will be presented. The first part of this chapter will deal with the faults “outside” of the borders of the current mining area and the second part will present the faults within the current mining area.

4.2.2.1 Major Faults “outside”

The first major fault could be found by outcrops during the fieldwork. The fault is designated as “17m”, since it shifts the north field from the south field of around 17 [m]. In Figure 14 the observed outcrops of the fault are shown (red circles).

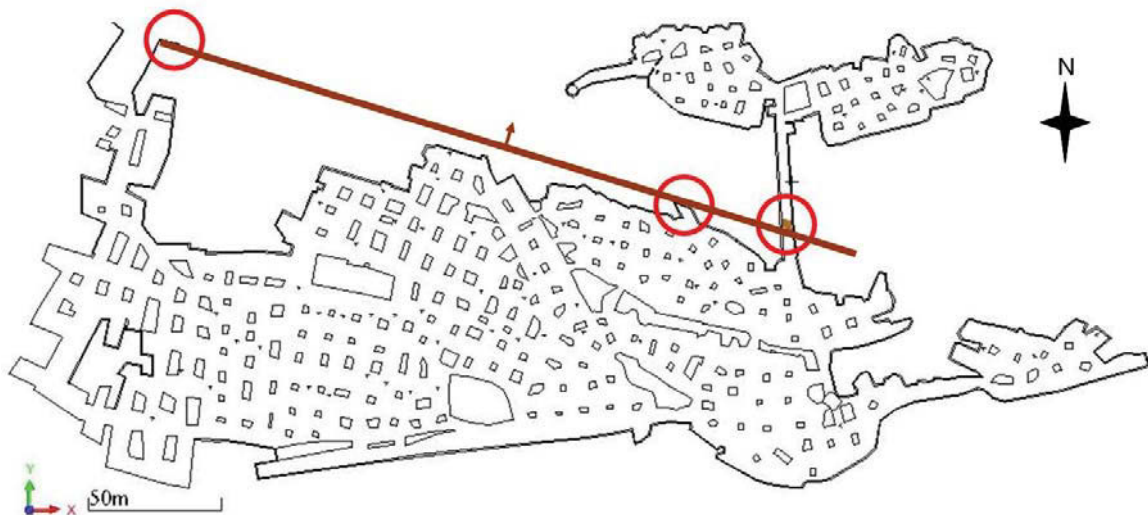


Figure 14: Major Fault „17m“, outcrops

The outcrop of the major fault “17m” at the connection passage is partly visible, since a support is installed. The support consists of concrete at the walls and straps at the roof (see Figure 15). Between the straps wooden planks are installed. The thickness of the fault can be estimated as 0,5 [m]. The discontinuity is filled with clayish material and is at the connection passage partly open.



Figure 15: Support major fault „17m“, connection passage

The major fault “17m” is dipping with an angle of $70 [^\circ]$ and has a dip direction of $34 [^\circ]$. These values could also be found in the 2nd outcrop (middle red circle, Figure 14). Furthermore these values were measured at the entrance of the mine (see Figure 16).



Figure 16: Outcrop entrance, Major fault „17m“

This leads to the conclusion and affirms the statement of the company, that the major fault “17m” is continuous. The alignment of the discontinuity is shown on hand of the 3D model (see Figure 17 and Figure 18). The discontinuity is simplified to a plane with no border through the topography.

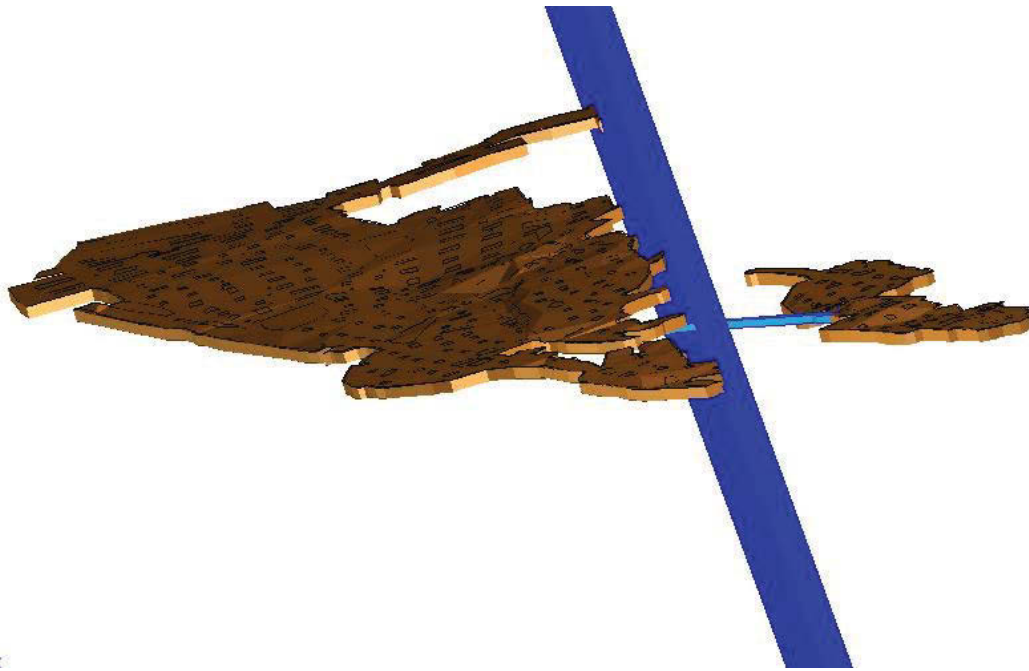


Figure 17: Major Fault „17m“, 3D, Surpac, 1

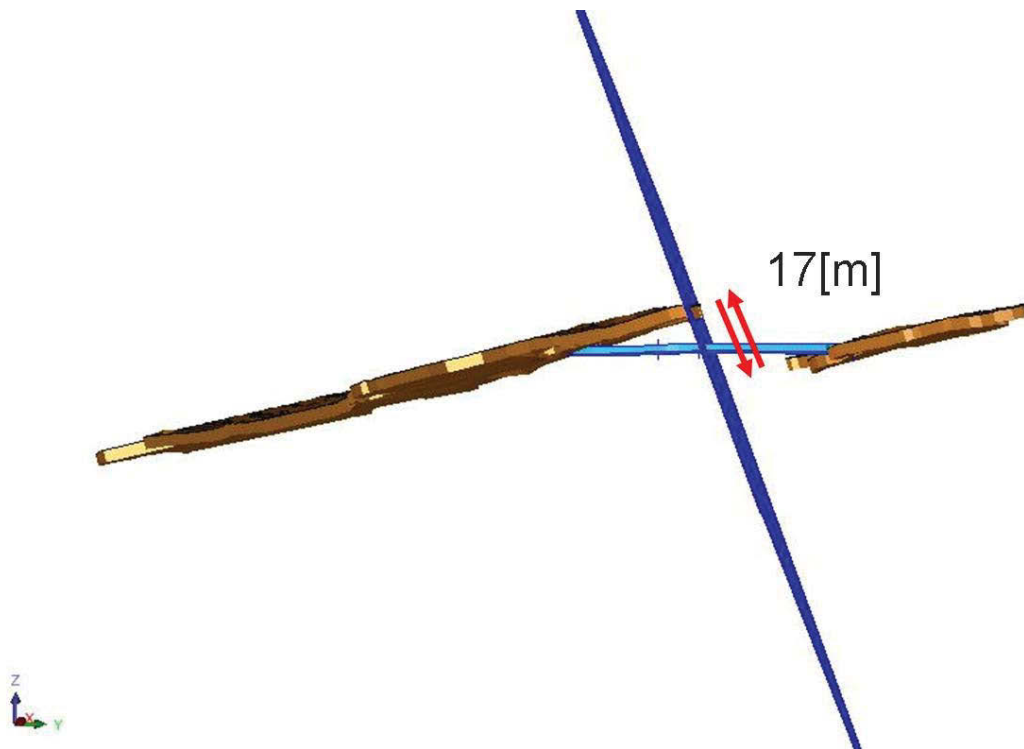


Figure 18: Major Fault „17m“, 3D, Surpac, 2

The second major fault is in the south of the mine. It is affirmed from company side that the fault is existent; however there is no proven data about the exact alignment, dip and dip direction as well as the value of possible shift. Therefore the alignment from the provided map of the company was taken to design the fault (see Figure 19). As dip value 90 [°] and as strike 100 [°] were taken to built it in Surpac. In the map the fault is named “d’Hermoye” and for the further discussion it is designated as major fault “south”.

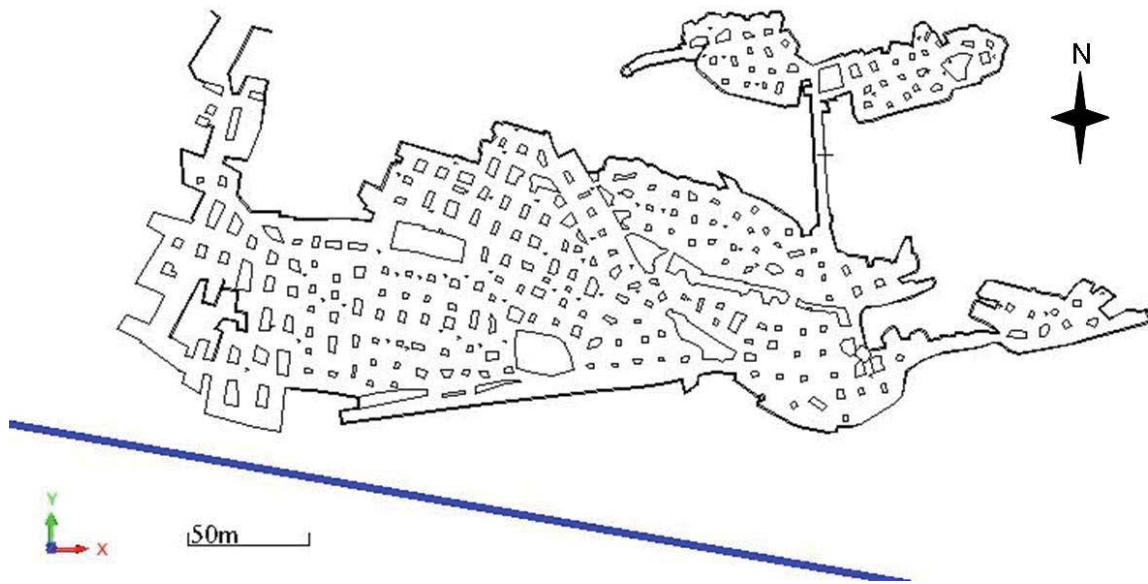


Figure 19: Major fault „south“, alignment, Surpac

Although the discontinuity is not important for the description of the current situation, it is presented here to unite the major faults outside the borders of the current mining area, which are discussed in this master thesis. The major fault “south” gets into consideration at the discussion of the future mining areas.

4.2.2.2 Major Faults “inside”

Within the mine following major faults (shift of $\geq 0,5$ [m]) were recorded. The location and the shift are shown on hand of the map (see Figure 20). The brown lines represent the in the fieldwork observed faults (shift). The blue line represents the in the map of the company marked faults.

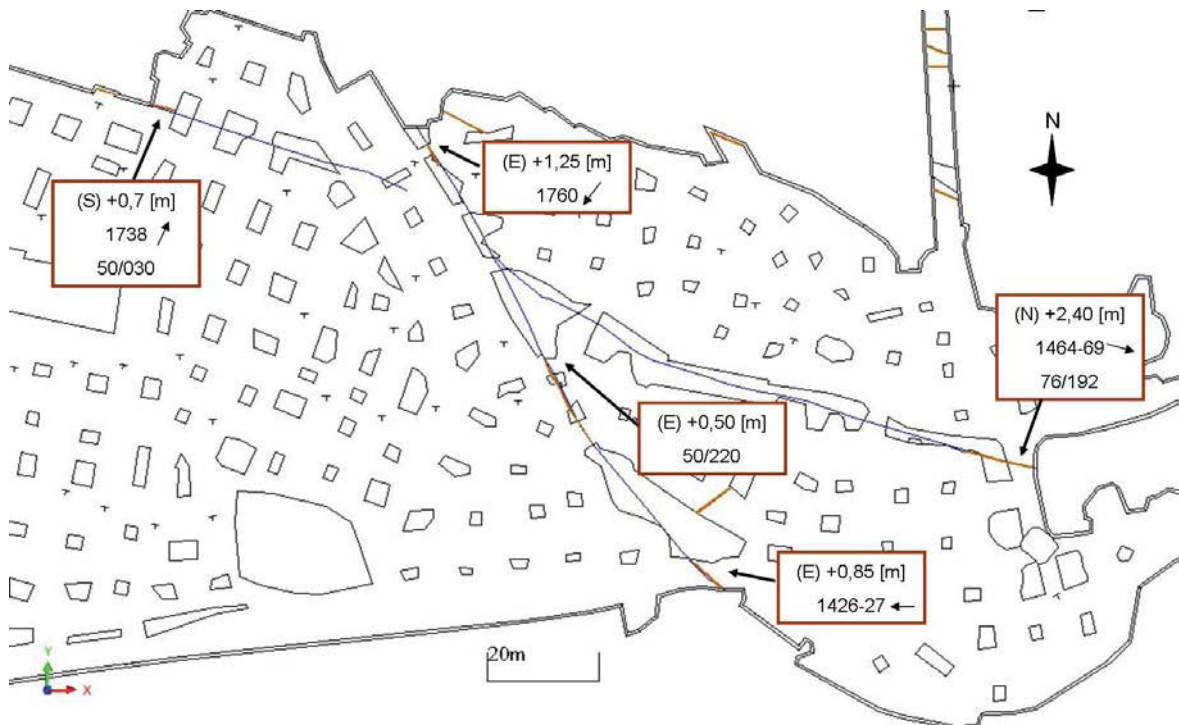


Figure 20: Major Faults „inside“

The in Figure 20 marked squares follow following system e.g.:

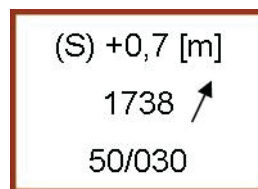


Figure 21: Major Faults „inside“ example

- “(S)” = South; viewed area according to the fault and compass point

- “+0,7 [m]” = amount of shift in [m] according to the roof/layer of the area opposite the fault
- “1738” = photo number; taken at the fieldwork
- “ ↗ ” = direction in which the photo has been take
- “50/030” = dip and dip direction of the fault

If, in example the photo number or the dip and dip direction is missing it was not possible to record the value/photo or it was not done. In the following, examples of the taken photos are presented (see Figure 22 - Figure 25)



Figure 22: Major fault „inside“; photo number: 1738



Figure 23: Major fault „inside“; photo number: 1760



Figure 24: Major fault „inside“; photo number: 1427



Figure 25: Major fault „inside“; photo number: 1464

All photos are available on the enclosed data CD.

4.2.3 Geophysics

The company ordered a geophysical study² (2003) to gain more information of the surrounding area concerning possible new mining areas. The in the study gained resistivity map was put over the 3D model in Surpac; once with the map out of the measurement with horizontal dipole (see Figure 26) and secondly with the vertical dipole (see Figure 27).

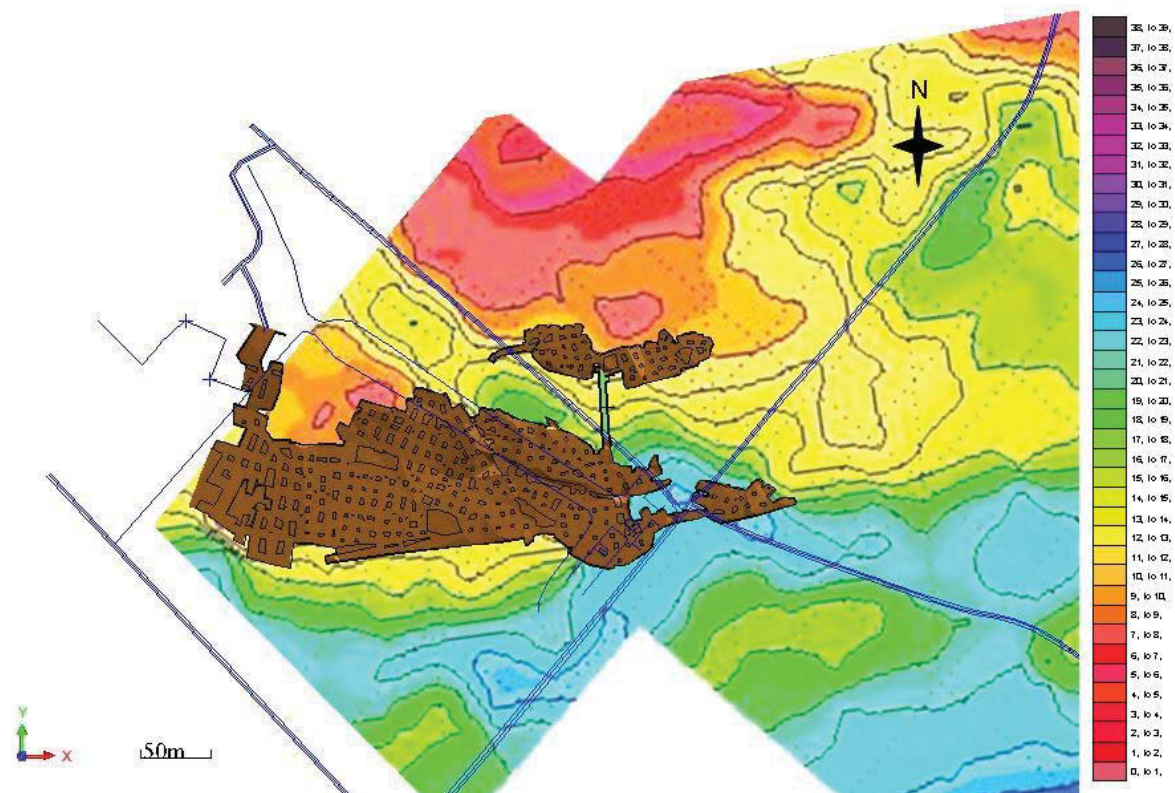


Figure 26: Geoelectric, Dipole H

² "Recherche de fracturation par méthode géophysique. Site de la mine de Marbre Noir de Golzinne en Belgique." (2003)

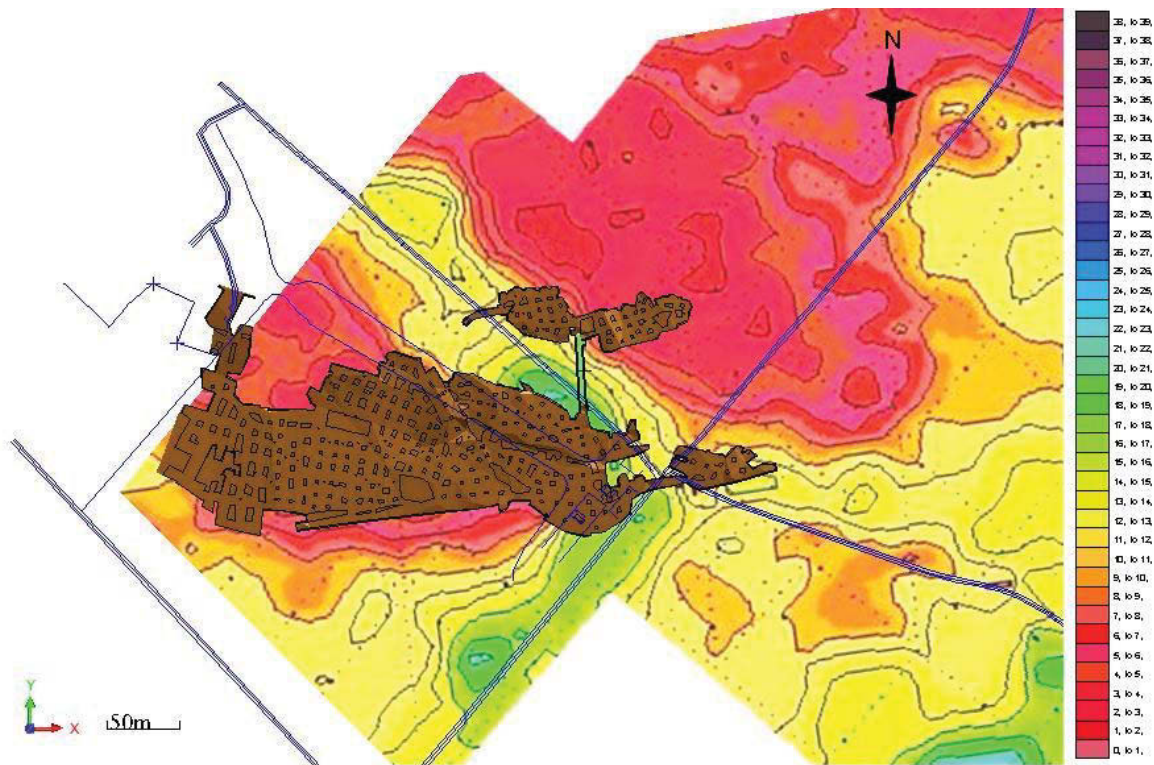


Figure 27: Geoelectric, Dipole V

According to the statement of the company the generated figures fit well with the assumed possible future mining areas (especially north). The red – orange areas mark possible deposits. Furthermore the major fault “17m” can be interpreted as the yellow area between the north and the south field. The “dislocation” concerning the geoelectrical map and the 3D model is, according to the company, normal, since the deposit shows a dipping and therefore a mismatch of the results.

The result underlines the assumption that the deposit, northern the major fault “17m”, continues the alignment of the current mining area and presents a possible new mining area.

For calibration and crosschecking these results, core drilling should be done, to gain greater geological certainty.

4.2.4 Geological discontinuities

During the fieldwork the geological discontinuities were recorded and marked in the from the company provided plan view of the mine. In Figure 28 the recorded joints (blue) and faults (brown) are shown.

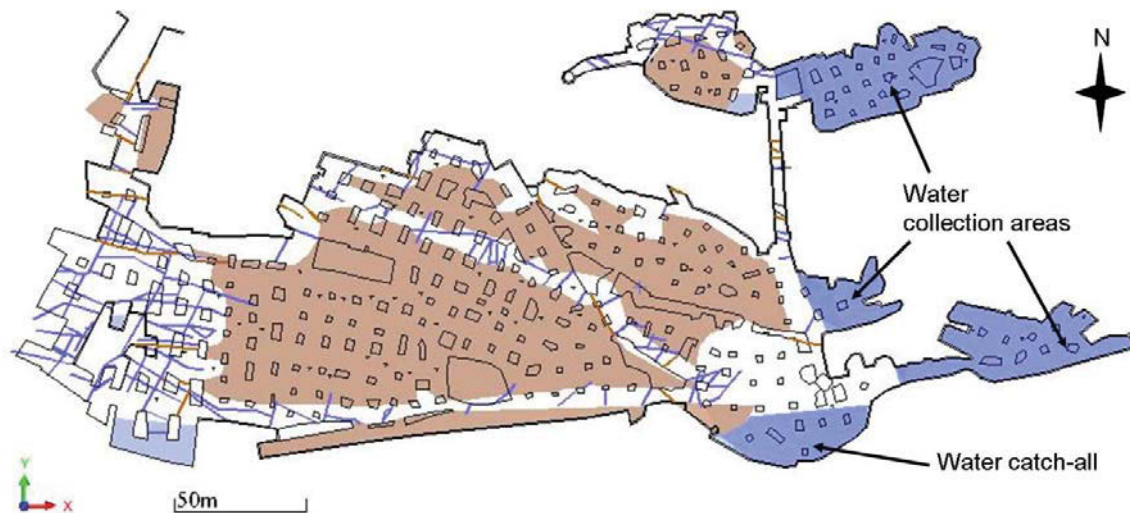


Figure 28: Geological discontinuities, overview

The brown areas present the backfilled areas where the accessibility was not given with the used equipment at the fieldwork. The backfill in these areas is up to the roof or nearly (~50 [cm]) up to it. The blue areas are water for the water collection and/or for the catching. At the catching a pump system is installed to pump up the water to the surface, through the main shaft, for agriculture usage. In these areas (backfill and water) no observation was done.

In the other areas, besides other data, the geological discontinuities were recorded. Aside from single outliers, 3 main systems of discontinuities were recorded:

1. Joint band 1 = Dip: 85 – 90 [°]; Strike: 180 – 215 [°]; (“ksys195”)
2. Joint band 2 = Dip: 85 – 90 [°]; Strike: 078 – 110 [°]; (“ksys95”)
3. Fault band = Dip: 50 – 70 [°]; Strike: 004 – 020 [°]; (“ssys10”)

The in the bracket shown names are the for further designation used ones. An enlargement of the single areas and the documentation at the fieldwork can be found at the Annex (see chapter 15.4 and 15.12). The thickness of the discontinuities reaches from 1 to 20 [cm]. The major part of it is filled with clayey and sandy material and is partly open.

To gain more knowledge of the frequency in which the discontinuities appear the distances between the faults and joints of each system were measured by putting a line through the recorded discontinuities (see Figure 29).

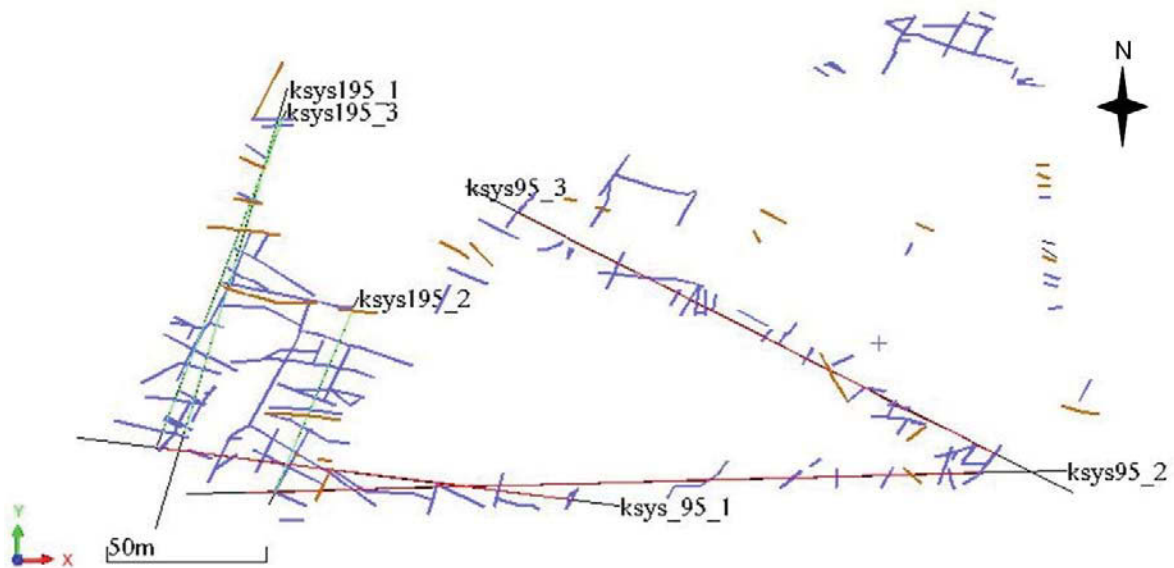


Figure 29: Distance distribution, discontinuities

The data (see Table 1) was sorted by classes and plotted into a diagram (see Figure 30 and Figure 31)

Taken distances	ksys195 1 Distance	ksys195 2 Distance	ksys195 3 Distance	ksys95 1 Distance	ksys95 2 Distance	ksys95 3 Distance	ssys10 Distance
[-]	[m]	[m]	[m]	[m]	[m]	[m]	[m]
1	2,29	11,27	2,29	19,02	9,56	35,87	11,57
2	10,76	8,19	11,14	12,81	50,31	20,66	9,05
3	13,64	7,97	13,48	9,14	20,15	4,41	19,77
4	16,19	2,86	15,90	46,47	25,16	1,91	
5	6,89	4,08	6,67	19,37	40,25	3,06	
6	4,22	5,91	5,16	23,08	26,06	20,88	
7	7,14	8,15	14,99		14,29	5,20	
8	6,43	5,18	7,80		15,97	9,80	
9	10,04	8,98	4,89		16,87	20,21	
10	4,21		8,46		2,53	10,98	
11	11,02		3,43		9,16	21,03	
12	7,77		6,08			7,57	
13	3,16		4,49			6,18	
Average		7,75			17,60		13,46
Variance		3,88			12,53		5,61

Table 1: Data distance distribution, discontinuities

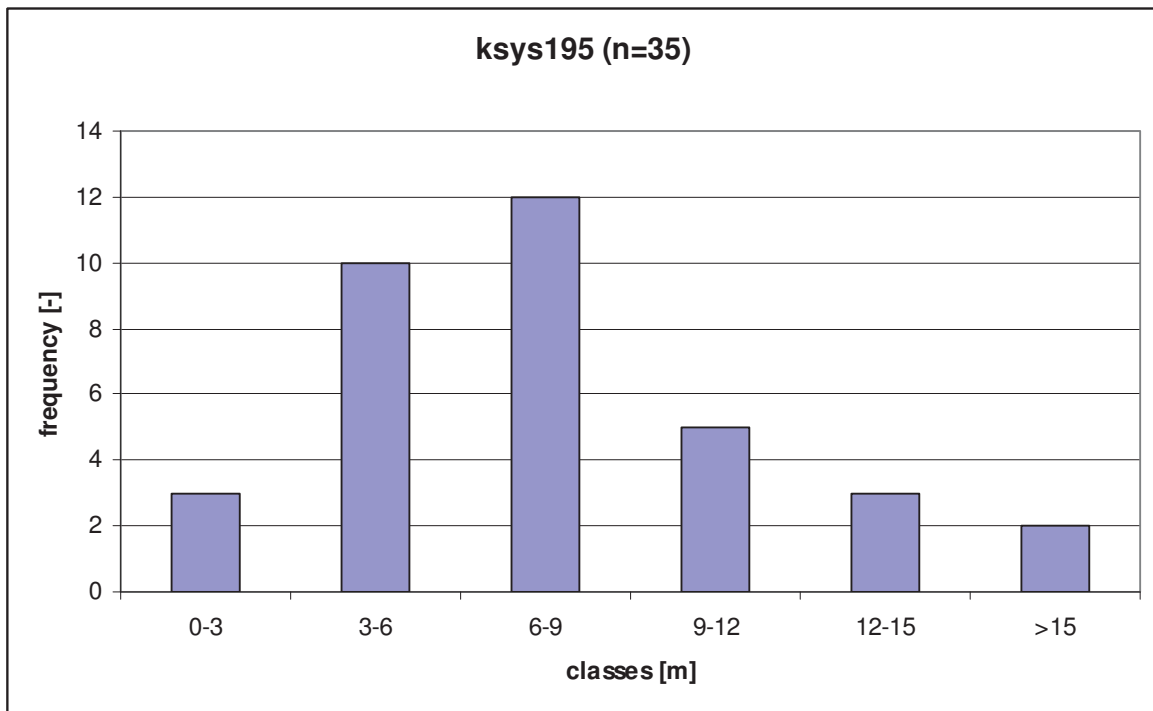


Figure 30: Data „ksys195“ sorted in classes

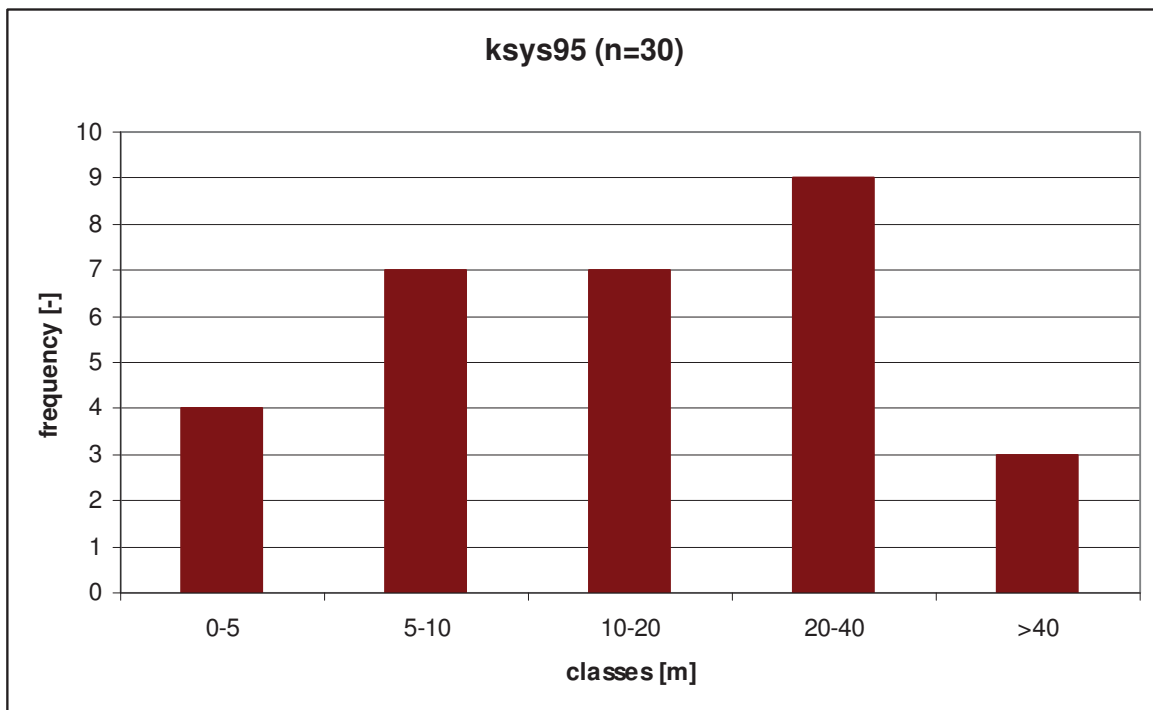


Figure 31: Data „ksys95“ sorted in classes

With the data of fault band “ssys10” no classification into classes were made, since the available data consists of 3 values.

4.3 Underground mine

In this chapter the general aspects (mining method, weathering, etc.) as well as the design of the 3D model are discussed. Furthermore the historical background and the external influences will be viewed.

4.3.1 General aspects

The mine is run by 5 workers who are working in one 8 hour shift 5 days per week. The underground operation is done with room and pillar mining. To gain the rooms the first layers, according to the roof, with a thickness of 1,3 [m] is blasted parallel to the layering. The drilling is done with an electric powered drilling machine with one boom, by percussion drilling (see Figure 32).



Figure 32: Mining method

Per blast, around 10 blast holes are drilled and filled with patronized explosives. For the initialization of the explosive a on a black powder cord mounted detonator is used. Detailed information of the used explosive could not be determined during the fieldwork.

The remaining layers with a thickness of 1,9 [m] are used for dimension stone. On the from the blasting achieved floor, the blocks are cut out with a saw. Before the saw was available the blocks where produced by drilling small distanced drill holes perpendicular to

the layering. In Figure 33, two taken photos at the fieldwork are shown which represent the current and the former “cutting”.



Figure 33: Cut vs. drilled remaining pillars

The blocks are transported with a diesel powered wheel loader through the main entrance to the processing where the final cutting is done (see Figure 7, chapter 4.1). Before the wheel loader was installed in the production cycle, the blocks were transported with a lorry to the main shaft and lifted to the surface to the processing.

The material which is produced through the blasting is used for backfilling. Today the backfill is placed with the wheel loader. In former times it was installed by hand. In the following Figure 34, a picture of two examples of backfill is shown.



Figure 34: Examples of backfill

The backfill reaches up to the roof or almost to the roof (~ 50 [cm]). The in the fieldwork mapped backfilled areas are shown in Figure 35 (brown areas).

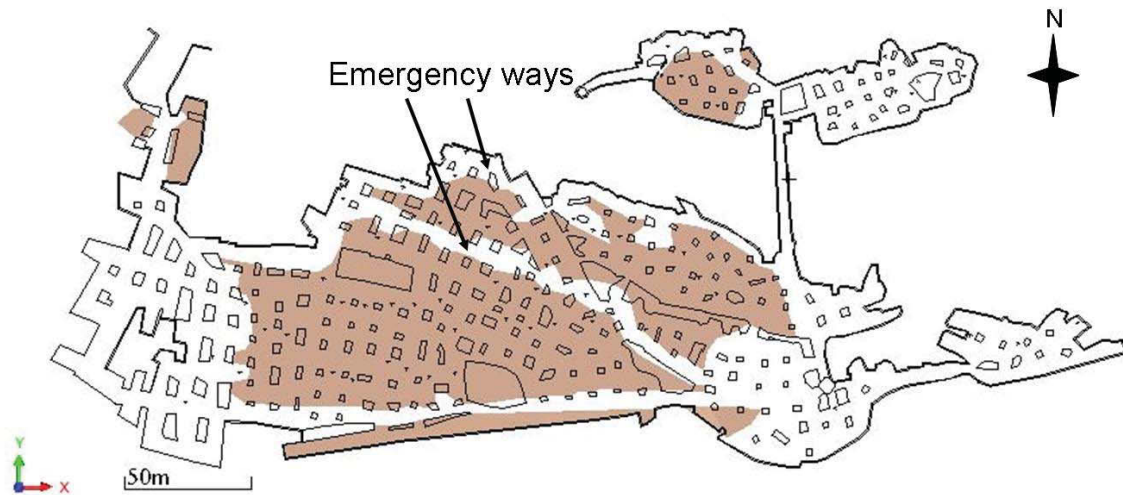


Figure 35: Backfilled areas

A small part of the backfill was tested during a project to use it as a construction material. Therefore the material was transported to the surface and was broken with crushers and sorted by sieves into constant particle sizes. However the project was stopped since the prize on the market did not exceed the production costs.

Additional in Figure 35 the emergency ways are marked. These assure the accessibility to the secondary exits (main shaft, weather shaft) in case of emergency. In the northern way a cord follows the alignment as guidepost. The northern emergency way ends at the top of the terminal point at the connection passage. The height difference is done by a ladder (see Figure 11, chapter 4.2.1). A more detailed discussion in terms of safety is presented at chapter 9.

The weathering of the mine is assured by a ventilator placed at the base of the weather shaft. The weather follows the sucking (under-pressure) principle. The blasting is done at the end of the 8 hour shift. Until the next day the ventilation dilutes the bad weathers. During the fieldwork (Oct. 2011) no natural ventilation of the mine could be detected. A picture of the ventilator at the base of the weather shaft is presented in Figure 36.



Figure 36: Ventilator, at weather shaft

The dimension stone is cut at the processing into the wished final shape for the customers. In Figure 37 a picture, of the processing is shown. It was taken into northern direction. In the white hut the cutting takes place. The two brick buildings in the background are the shelter for personnel rooms, for equipment and for maintenance.



Figure 37: Processing

The total yearly extraction rate is around 900 [m³], whereof around 200 [m³] dimension stone are produced.

4.3.2 3D Model

To gain a 3D model of the current mine following data was used:

1. The AutoCAD file provided by the company of the year 2007 (“golzinne.dwg”; see Annex, chapter 15.2, or data CD)
2. The survey which was done at the fieldwork 2011 (see Annex, chapter 15.2)

The “.dwg” file with the mine plan was transferred into a “.dxf” file and loaded into Surpac, which was used to visualize the mine into a 3D model and further, to plan and visualize the development of possible future mining areas.

Therefore the mine plan in the left part of the AutoCAD file was taken into consideration (see Figure 38).

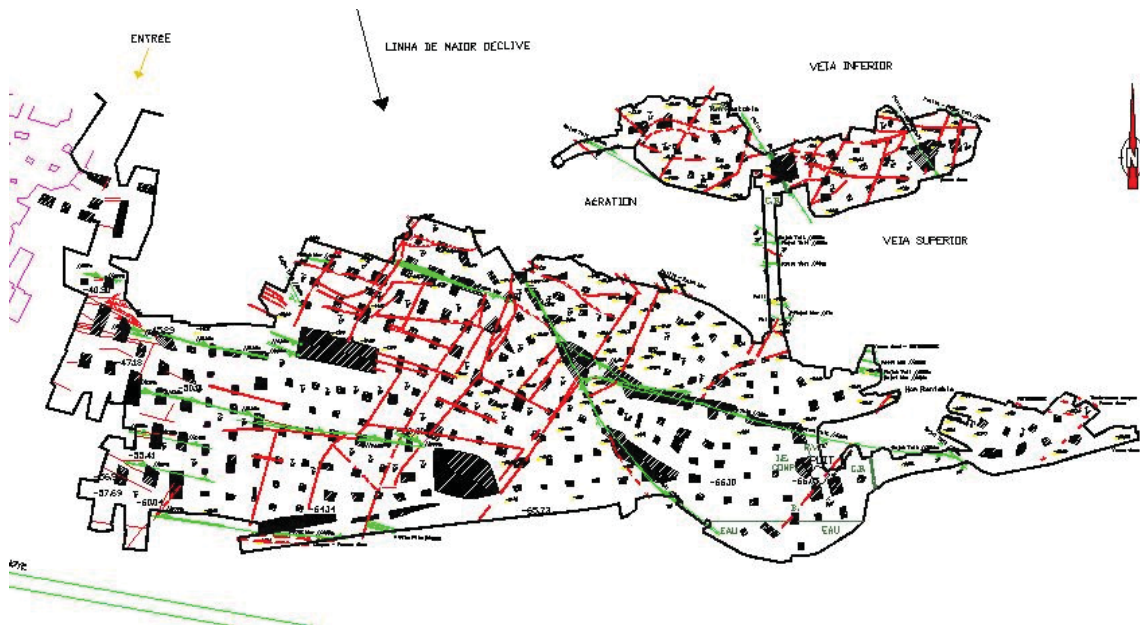


Figure 38: Mine Plan 2007, AutoCAD

NOTE: The 3D model serves as visualization of the mine. A high accuracy is not given since less data was available and an interpretation of the few data was necessary to be able to create the model. This is valid for the whole, during the master thesis, derived 3D models and the derived values.

4.3.2.1 Current mine

The plan, presented in chapter 4.3.2, Figure 38, was simplified to gain the clear boundaries of the mine itself and the pillars. At this stage the faults (green lines) and the joints (red lines) as well as the lettering was left aside. This resulted in the raw layout of the mine (see Figure 39).

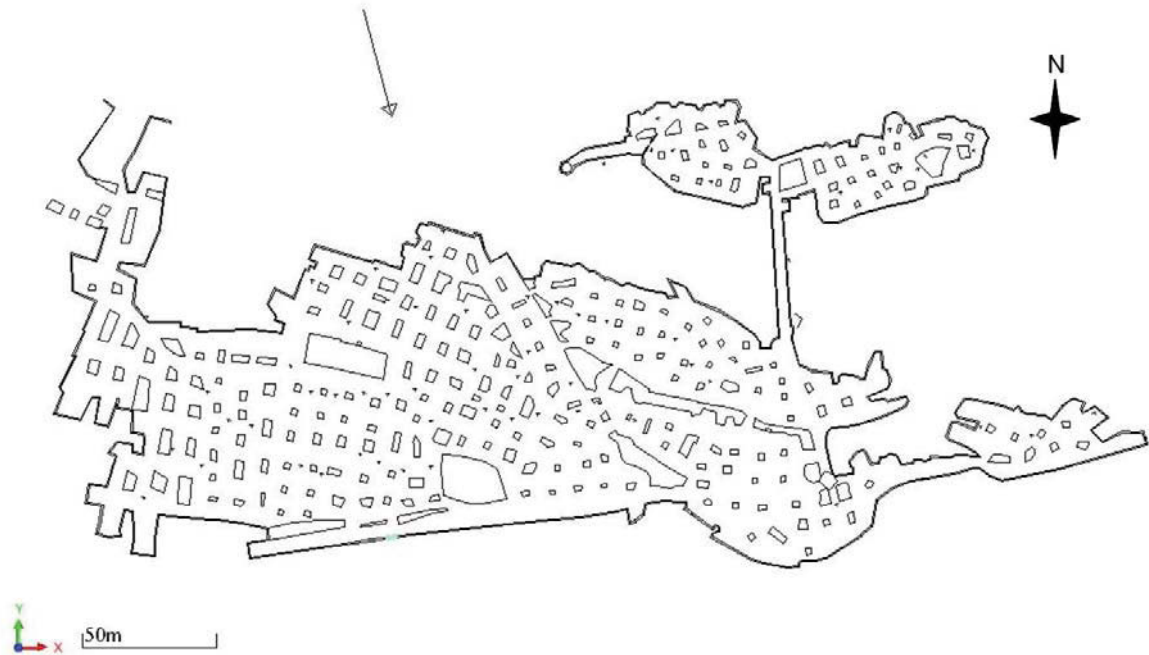


Figure 39: Mine Plan 2007, Surpac

With the data from the survey at the fieldwork the mine plan (2007) was updated which is shown in Figure 40.

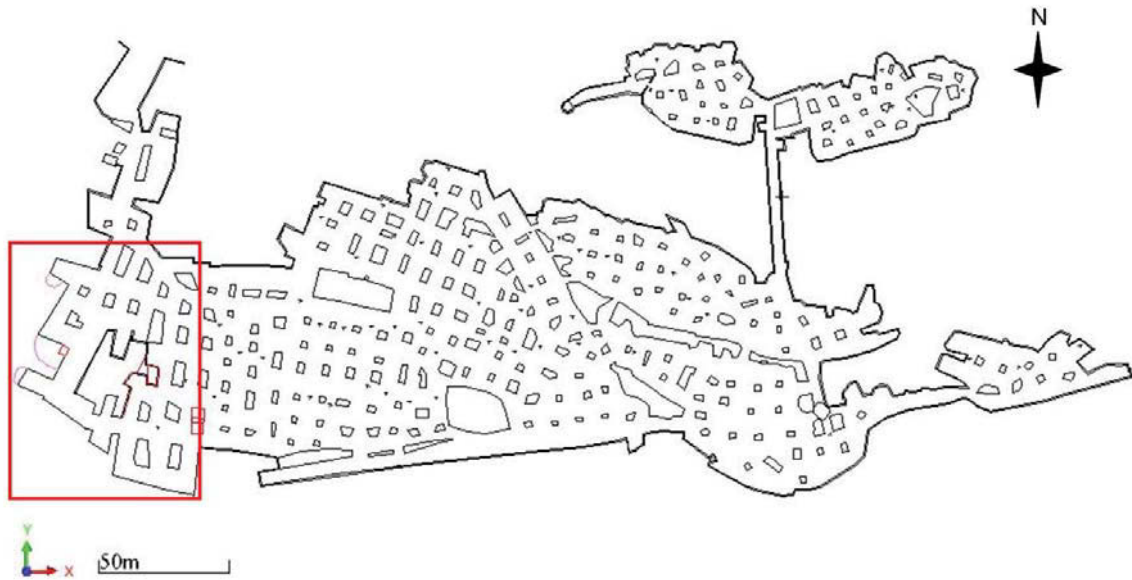


Figure 40: Mine Plan 2011, Surpac

As seen in Figure 40 the current mining activities and the mine development in the past years are situated in the South-West of the mine (red square). An enlargement of this area is shown in Figure 41

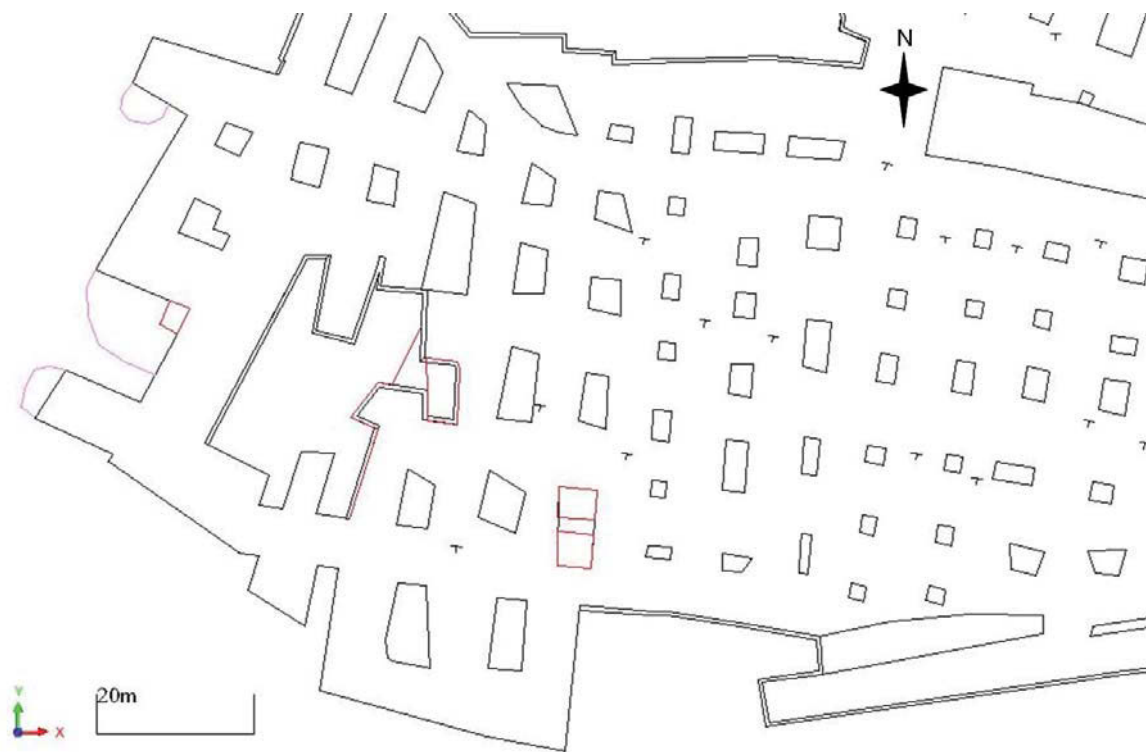


Figure 41: Enlargement of current mining area

The pink lines in Figure 41 mark the level of development according to the blasted layer, which is related to the height of mining the first 1,3 [m] pertain to the roof. The red line marks the alignment of the pillars of the first 1,3 [m].

The plan is according to the z – coordinate (perpendicular to the plan view) in the 0 – horizon. The next step is to bring the plan view of the mine into the 3D position.

Therefore the in the plan marked points with the spot heights are used. As an example see Figure 42.

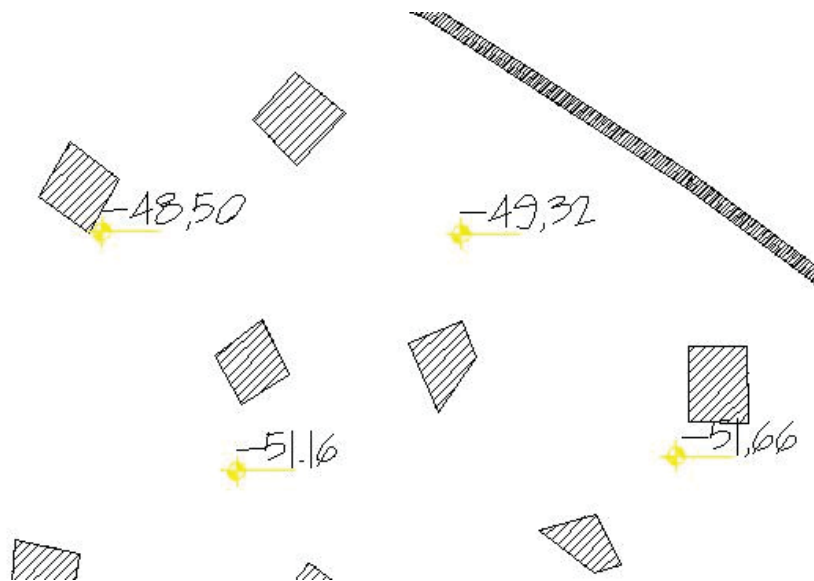


Figure 42: Example spot heights, AutoCAD 2007

It is assumed that the values of the spot heights are related to the 0 – Point, the main shaft. Furthermore it is assumed that the values are related to the roof. Therefore the points were filtered out of the rest of the mine plan and by editing the z – coordinate, the points were shifted from the 0 – horizon to the in the plan marked spot height. Out of this step a point cloud was build. Additionally a border was drawn around the point cloud by hand, following the position in the room and the dipping of the point cloud. With this database a surface was made. With the borderline of the mine, this surface was cut, so that the remaining object is a projection of the roof area of the mine. To work out the shift of the two main faults within the mine, south, the alignment of the faults was shifted into the model (see Figure 43, red line).

Note: 3 spot heights were outliers and not taken into consideration in the 3D model of the mine areas south and north. They belong to the spot heights of the connection passage.

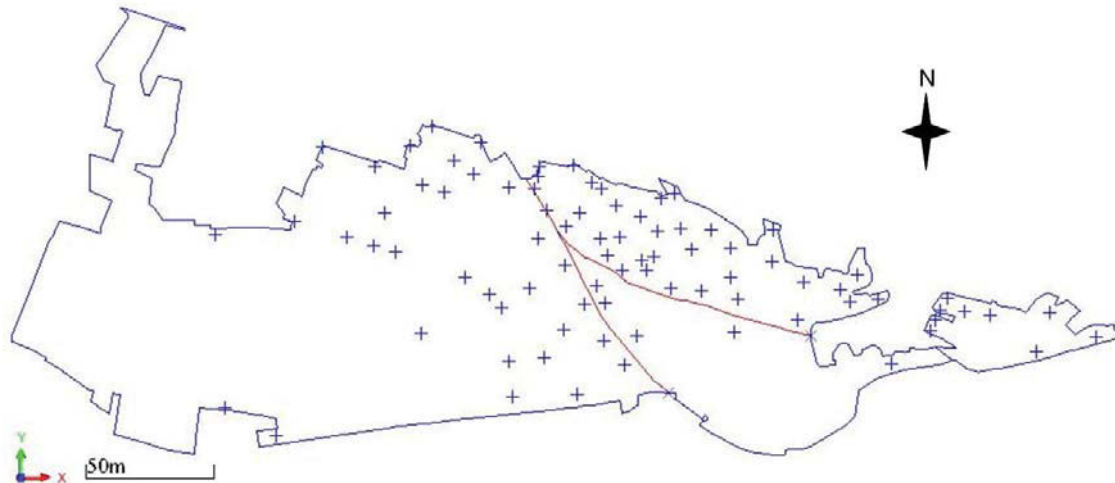


Figure 43: Basis for roof area mine south

The in Figure 43 shown database was used to build the 3D Model for field south. To gain the floor area, the roof area was shifted $-3,08$ [m] into the z – coordinate and $+0,91$ [m] into the y – coordinate. This results of the fact that the dipping is nearly in north south direction on the basis of the provided map. The dipping has been simplified as an average value of $16,5$ [°]. With the, during the fieldwork, measured average mining height of $3,21$ [m] the above represented values of the shifting can be calculated.

The same procedures were done to get the model for field north. Except that the average dipping, on basis of the provided map, is $14,25$ [°]. Therefore the shift of the roof area to gain the floor area amounted in z – direction is $-3,11$ [m] and in y – direction $+0,79$ [m].

To gain the connection passage between field south and north the 3 spot heights, which didn't fit to the rest of the heights were taken to put the passage into position. As an illustration a sketch of the area south – connection passage from the provided map is shown in Figure 44.

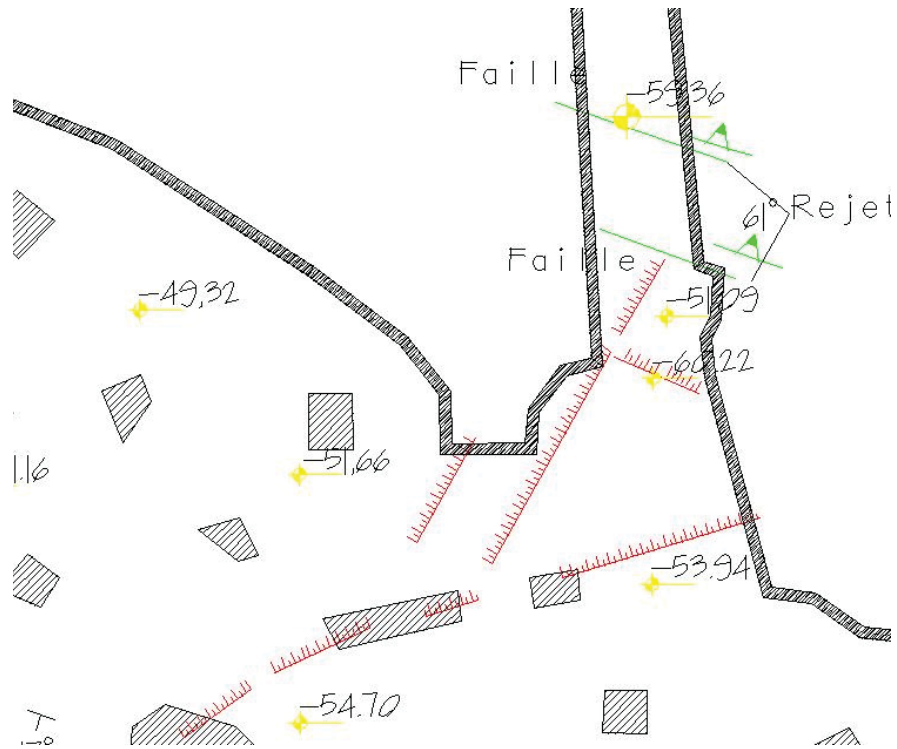


Figure 44: Spot heights field south – connection passage, AutoCAD 2007

As shown in Figure 44 the spot heights “-59,36” and “-60,22” don’t fit into the other ones. The heights are directed to the connection passage. With these 2 spot heights and the one at the field north the connection passage was built with the same procedure as shown above. Since the height of the connection passage is over the most parts in average 2 [m], which was determined at the fieldwork, the 3D model was designed with this value.

The resulting 3D model is shown in Figure 45. It shows a 3D view, the top view and the side view.

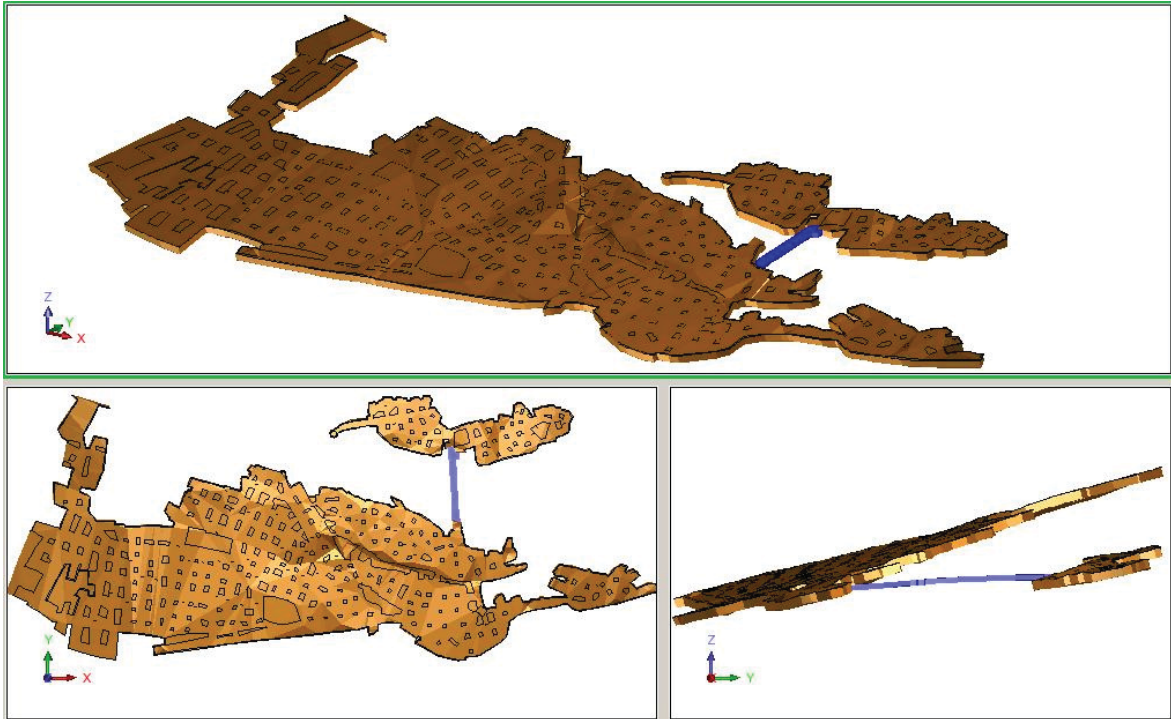


Figure 45: 3D model, current status, Surpac, 2011

Note: The design of the major fault “17m”, which shifts field north from field south, is faded out. The alignment of the major fault is discussed at chapter 4.2.2.

4.3.2.2 Topography

The topography was designed on basis of the right plan of the AutoCAD file, provided by the company. Out of this part of the plan the surveyed streets and buildings (blue lines) where used to build up the topography (see Figure 46; enlarged: see Annex, chapter 15.3).

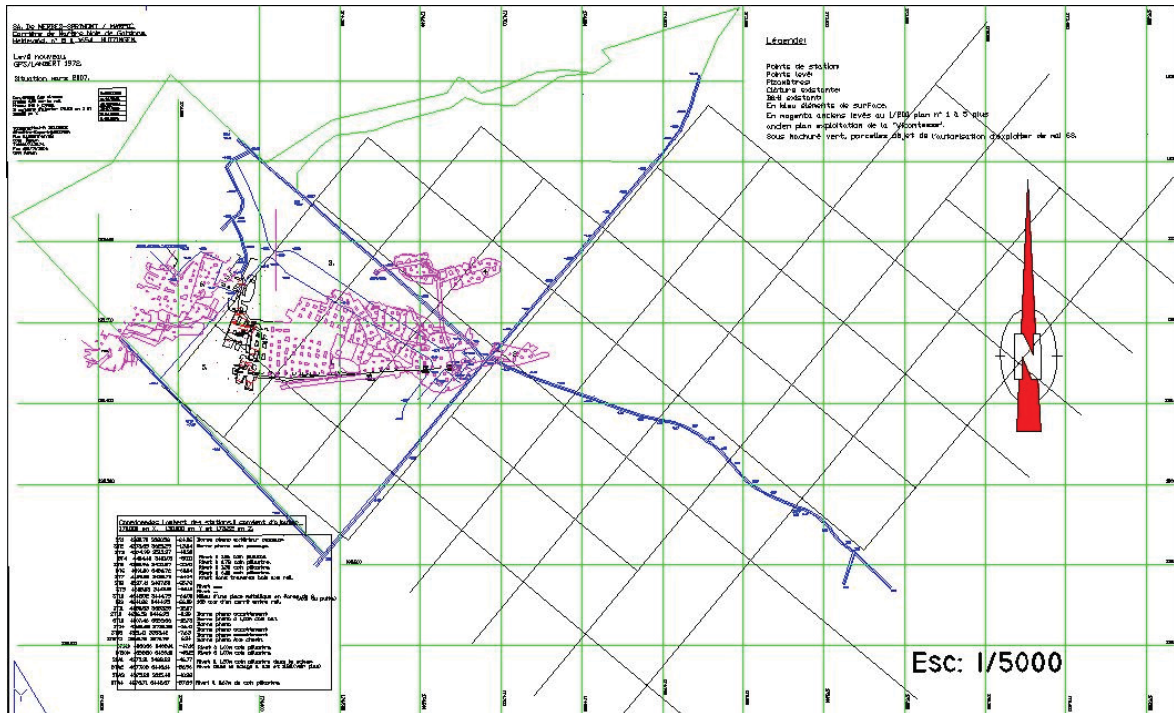


Figure 46: Mine Plan 2007 incl. streets and buildings, AutoCAD

To gain the blue lines the rest of the present drawings were extinguished. The 0-horizon, according to the z-coordinate, is based at the main shaft. The rest of the surveyed points are displaced according to this 0-point. So the system is correct in itself but not in the global survey system, because then the main shaft would be at sea level, which is not the case (~167 [m] according to the sea level of the north sea).

The data of the topography (streets, buildings) is connected to the survey system of the area, in comparison, the taken data of the mine plane not. To lap those two data the data for the topography was shifted manually in the z-horizon over the mine plan data. As basing point the ventilation shaft was used. This implement that the whole 3D model in Surpac is correct in itself but not connected to the local survey system. The mine plan shown in Figure 46 was not used, since the drawings are incomplete. An exemplary comparison is shown in Figure 47



Figure 47: Comparison incomplete (left, from Figure 46) and complete and used one (right, from Figure 40, chapter 4.3.2.1) mine plan 2007, AutoCAD

With the shifted base data of the topography the 3D model in Surpac could be created. To increase the realism an ortho – photo by Google Earth was superimposed over the created topography in Surpac. (See Figure 48, Figure 49)

Note: the following two figures are not in plan view.

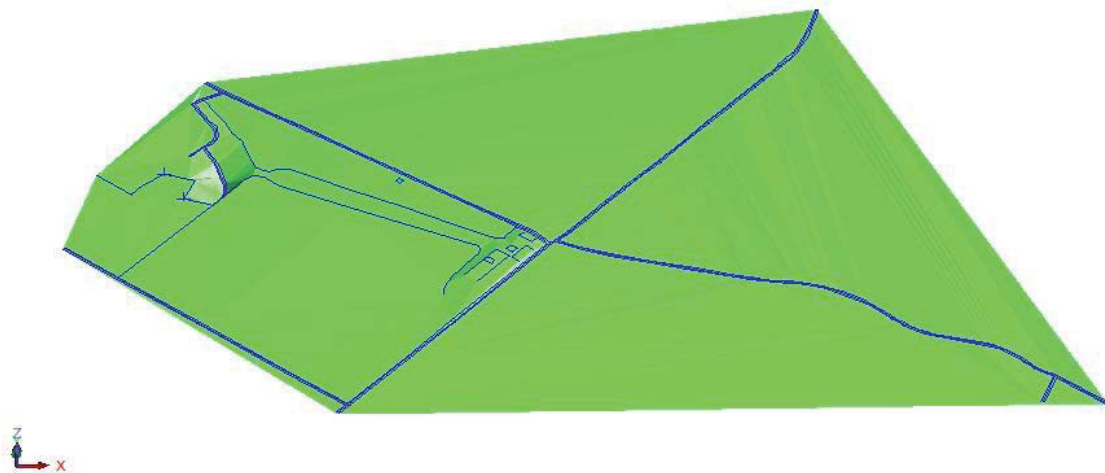


Figure 48: Topography, Surpac

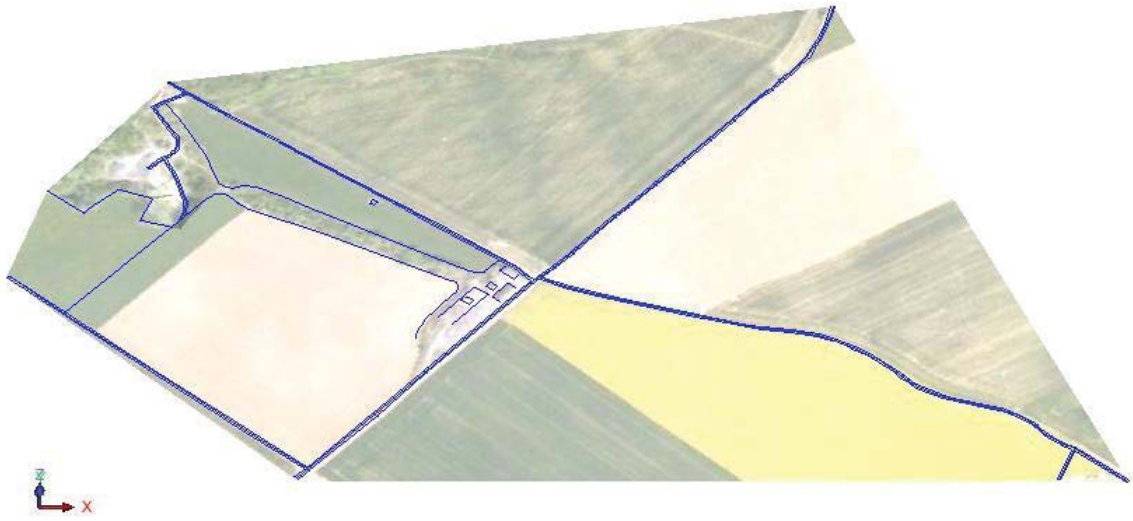


Figure 49: Topography incl. ortho – photo, Surpac

4.3.3 Historical development of the mine

The underground operation started around 80 years ago. The first access point to the deposit was achieved through the main shaft, where the first exploitation and extraction was done. In the 1970's the today's weather shaft was sank and the mining of the today's north field was carried on simultaneously to the south field. To connect these two mining operation the connection passage was developed. Through the connection passage the shift along the major fault "17m" was manifested. The further mining activities were concentrated on the south field and the mine was developed into the western direction until to present day.

In the north field the mining activities and the yearly development reaches from 1970 – 1975; as seen in Figure 50, which is a picture from a map, taken at the fieldwork.

NOTE: The following pictures are in the negative of the original due to increase the contrast and the visibility of the numbers. At the reference the picture number is added so that it can be looked up at the enclosed data CD.



Figure 50: Historical development, north field, photo number: 1489

The first mining activities in the north field are situated in circular form around the main shaft. The development into the east is dated with 1970 and 1972. The extraction fields and the development in the west, besides the pervious mined area around the shaft, start with 1969 – 2012. The area around the shaft and the development to the east are shown in Figure 51. The development into the west, associated to the area around the main shaft, is shown in Figure 52.

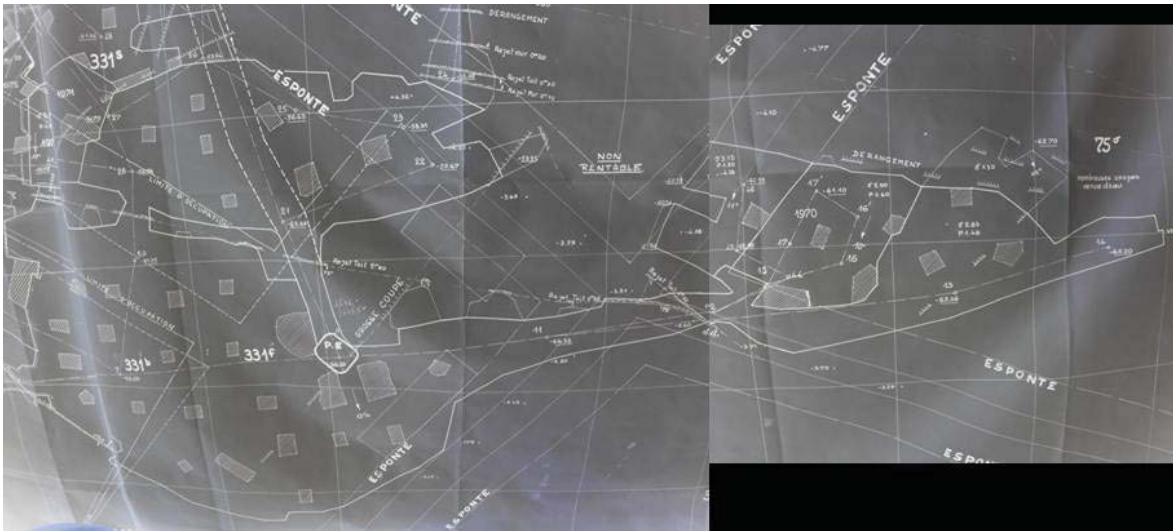


Figure 51: Historical dev., south field, shaft and east, photo Nr.: 1494, 1495

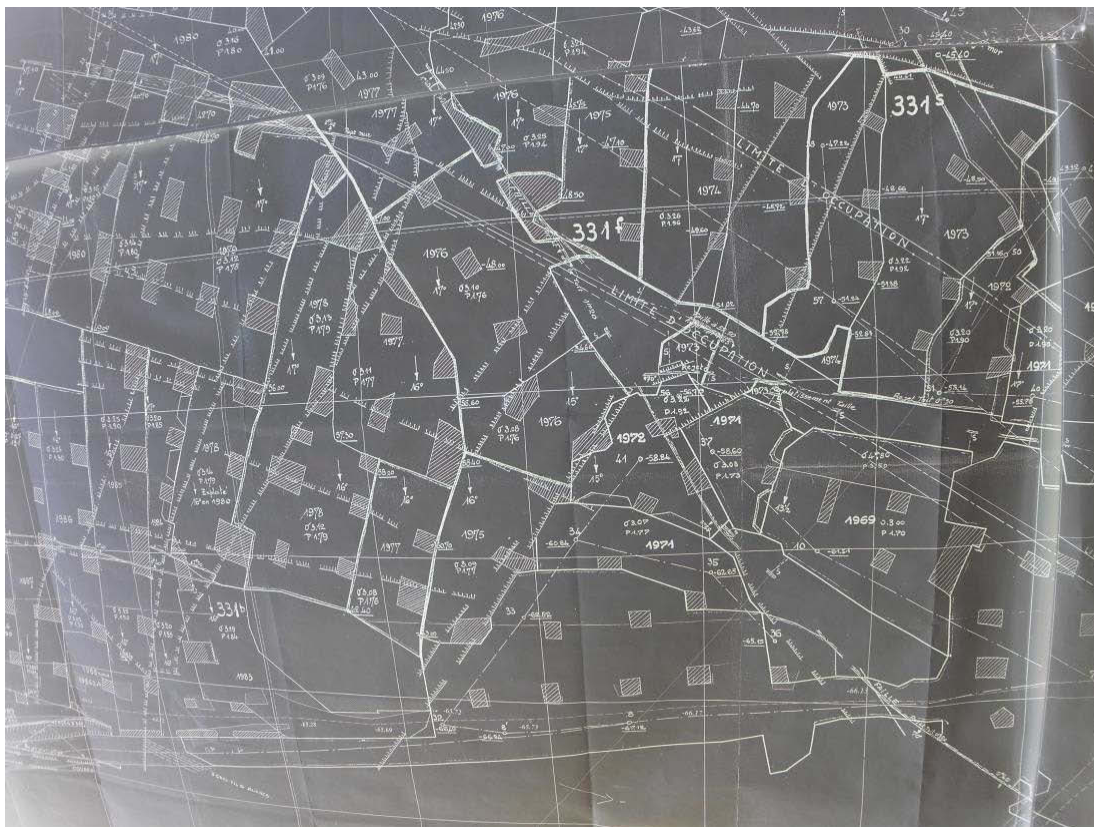


Figure 52: Historical dev., south field, west, photo number: 1496

The possible main reason for the stop of further development into the eastern direction could be the increasing water inflow. Today these areas are used for water collection (see Figure 28, chapter 4.2.4).

The historical development influenced besides the geological discontinuities, the arrangement of the pillars. Heading away from the main shaft into western direction, the

pillars get arranged in a more regular way, since the dimensions of the mine increased as well as the knowledge of the deposit. Furthermore it has to be mentioned at this point, that often the arrangements of the pillars are placed at geological discontinuities to support the roof – for instance the barrier pillars along the major faults within the mine.

4.3.4 External influences

The development of the mine as well as the existing mine are influenced by several external influences, which will be explained in this chapter.

4.3.4.1 Water

The water collection areas and the water catch have an economical importance, since the caught water is pumped up to the surface through the main shaft and used and sold for agricultural usage. To terminate this income is no option. This is one reason that the development into the east direction cannot be pursued at the moment. Another reason is, that through the increase of the water income the mining itself would get aggravated. The water collection areas and the water catch are presented in Figure 53.

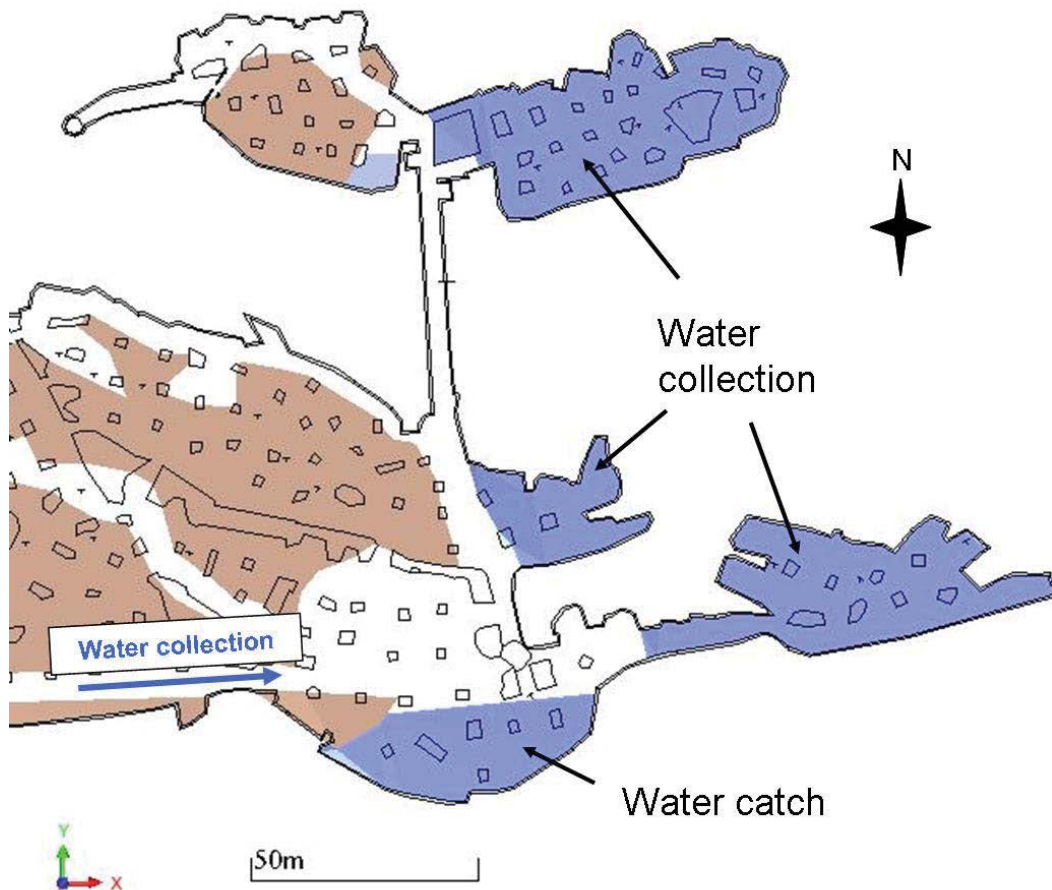


Figure 53: Water collection and catch areas

The in Figure 53 plotted blue arrow symbolizes the water collection direction of the rest of the mine. It is guaranteed by refilling partly the floor and installing water trenches.

4.3.4.2 Abandoned mine

The development into the west is blockaded through an abandoned mine, which mined marble in the lower layers, according to the floor of mine Mazy. The old mine is shut down and due to safety and stability issues prohibited to enter. The existing maps of the old mine, which were provided by the company, are uncertain in terms of position. In Figure 54 the location of the abandoned mine to Mazy is presented.

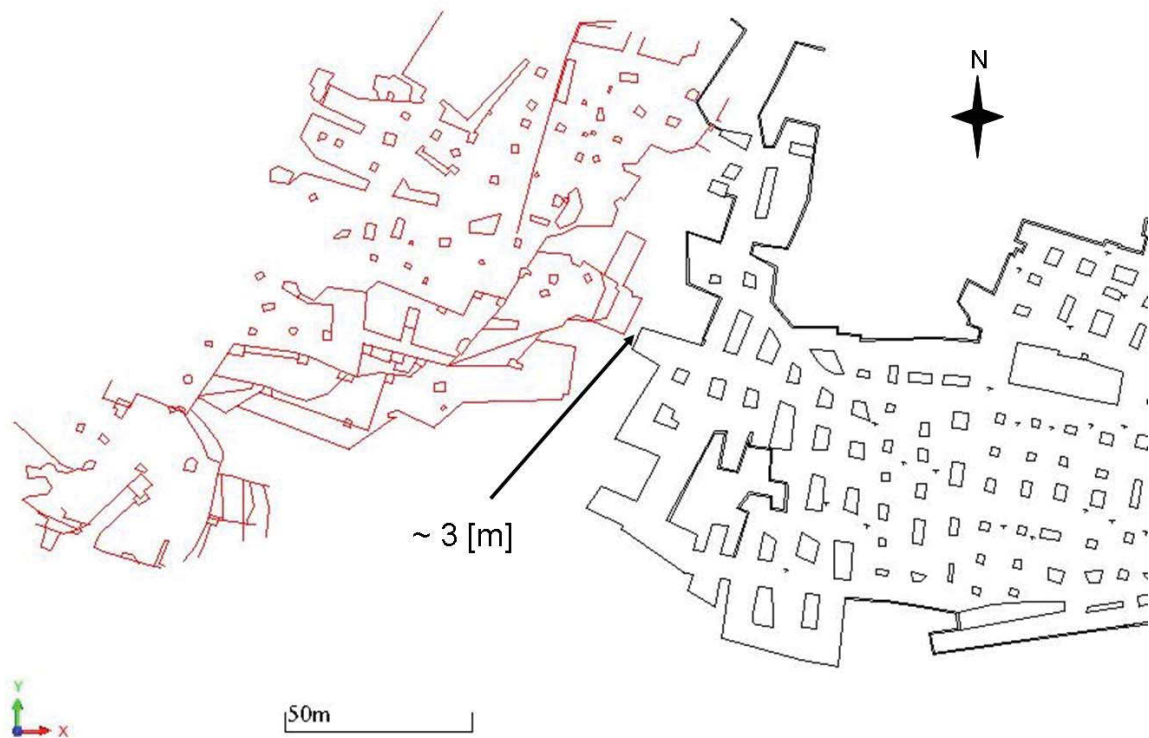


Figure 54: Position abandoned mine to Mazy

As shown in Figure 54 the distance between the border of the current mine and the old mine is around 3 [m] (horizontal), according to Surpac. The fact that the position of the mine is uncertain underlines that a development into the west is not suggested. Furthermore the possibility is given, that the old mine, which extracted the layers below the floor of Mazy, is already overlapping. To gain certainty, a drilling program should be realized to define the real position of the abandoned mine to the underground mine of Mazy.

4.3.4.3 Major faults

Another external influence are the major faults “outside” the borders of the current mining area. The position and the description of the major faults “17m” and “south” are discussed in chapter 4.2.2.1. A repetition is given in Figure 55.

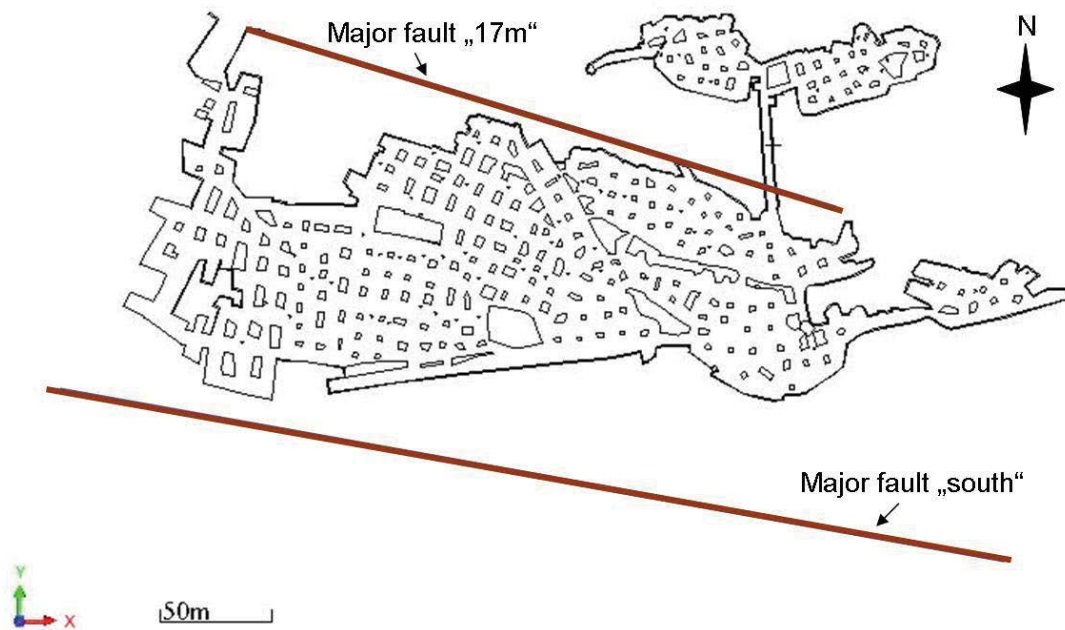


Figure 55: Major faults „17m“ and „south“

The faults limit the extension of the mine into the north and south direction. In every further development the faults have to have a special consideration. Especially the geological discontinuity “south”, since the position of it is uncertain or unknown.

5 Geotechnical investigations

In this chapter the geotechnical investigations will be presented. The investigations are necessary to describe the current state and the stability of the current mine. Furthermore the gained results are important input factors for the future mining areas.

The geotechnical investigations are based on the gained information at the fieldwork as well as the provided data from the company. The fieldwork was done between the 24th and the 28th of October 2011. The report and the results of the fieldwork are added in the Annex (see chapter 15.12).

The first impression of the mine is that it is situated in compact layered rock. During the mine visit a special focus was on the observation of the pillars and if pressure syndromes are visible. Occasional pressure syndromes at the near roof edges of the pillars (blasted layer) were detected. The pressure syndromes manifested in slight spalling. In Figure 56 the detected syndromes (red dots) are shown on basis of the plan view of the map.

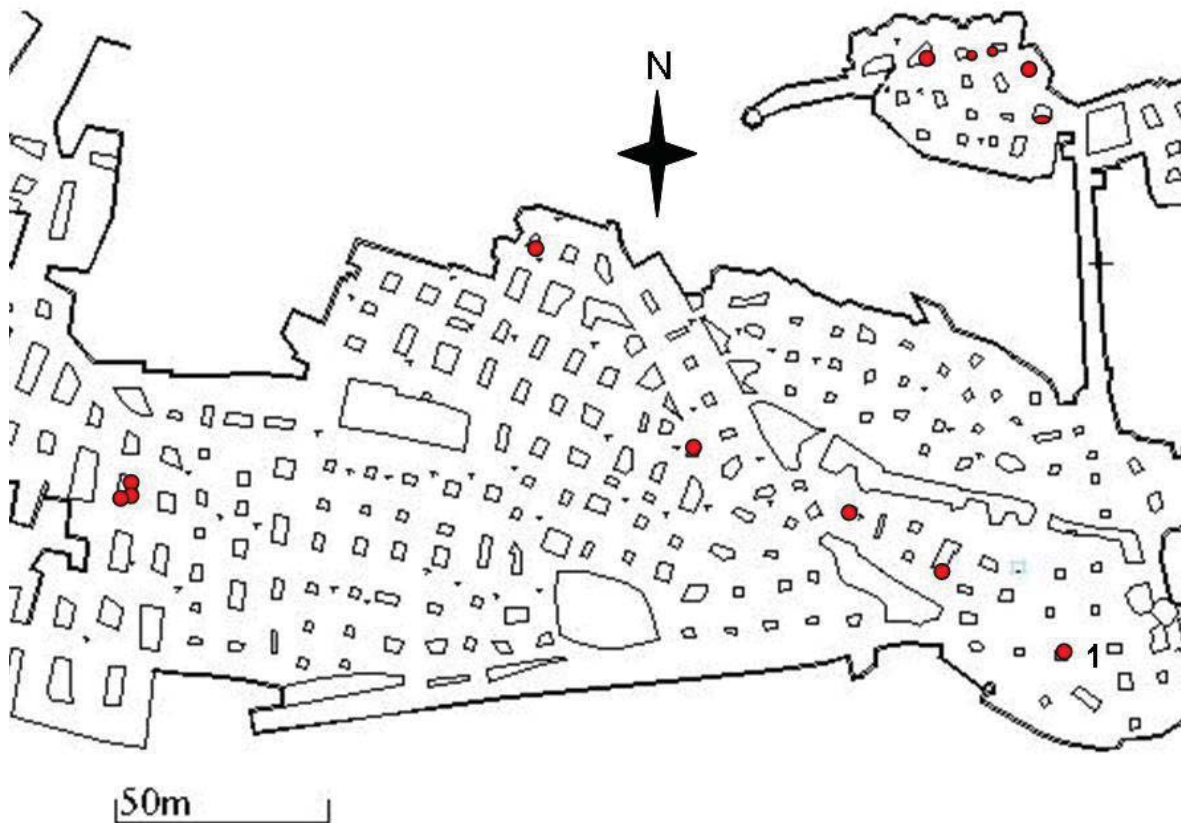


Figure 56: Pressure syndromes, overview

In Figure 57 an example of a pressure syndrome from the in Figure 56 marked pillar (1) in the south east is shown.



Figure 57: Example pressure syndrome, photo nr.: 1431

The pillars within the backfill could not be observed. Except from the occasional slight pressure syndromes the pillars gave no indication that a too high load is acting on it, except at the entrance of the mine.

At the right area of the entrance clear pressure syndromes are visible. A joint with an opening of ~ 10 [cm] separates the left abutment and the remaining pillar experiences an unfavourable position. Through spalling the typical shape of an overstressed pillar occurs which is shown in Figure 58.



Figure 58: Pressure syndrome, entrance, photo nr.: 1394

The company is aware of this issue and charged an external company to deal with the problem and will not be further discussed in this thesis. As part of the planned future mining operation the entrance will be enlarged and reinforcement.

The lower part of the pillars, which consists out of the layers which are used for dimension stone production, have, dependent on the extraction method (drilling or cutting), a trapezoid to cubic form. The layering is clearly visible. The upper part of the pillar (blasted layer) has a cubic to sand glass shape form, with rough surface, which arises through blasting. The layering is not detectable. Out of the mining method the area parallel to the layering decreases or tapers concerning the floor area compared to the roof area. An impression is given with Figure 33, chapter 4.3.1.

The water income occurs mainly through the geological discontinuities. The amount is depending on the precipitation and was not measured during the fieldwork. The subjective impression is that the amount is low in the west (current mining area), since the floor shows dry areas. In the east the water income is significant more. This is underlined by the fact that at the east the water collection areas and the water catch are placed. There is no complication for the production cycle through the water income within the current mining area.

One possible “main local failure mechanism” is the failure of single pillars influenced by geological discontinuities. Especially the filled and/or partly open joints and faults decrease the stability of the pillar. Although no significant sign of overloading was detected during the fieldwork, it represents a safety issue which has to be considered. An

example of a pillar which is cut through by a fault (brown line) and additional a joint (blue line) is shown in Figure 59.

(Note: The definition of “joint” and “fault” is annexed in chapter 14)



Figure 59: Pillar cut though by fault and joint

The quality of the roof depends on the appearance of geological discontinuities.

The second possible “main local failure mechanism” is the roof in combination with joints and faults. Where discontinuities with clayey filling are present the cohesive, shear and clamping force can be estimated with almost 0. Especially plates within the roof which are exposed by faults/joints represent a hazard. Examples are shown in Figure 60 (red circles).



Figure 60: Exposed roof plates

As shown in the figure above an anchoring is suggested in those cases. A basic calculation of the support of preventing plates of falling down will be discussed in chapter 7.6.

5.1 Rock strength parameter

To determine parameters for the rock mass strength, specimens were taken at the fieldwork and tested for the uniaxial compressive strength (UCS, σ_c) and the bending tension strength (BTS, σ_b). The procedure and the results are presented in this chapter (see chapter 5.1.1.1 and 5.1.1.2).

5.1.1 Uniaxial compressive strength (UCS)

To gain the UCS, the layers were tested in the laboratory of the Montanuniversität Leoben, department Mining. The material consisted of 7 specimens where 5 specimens were from the layers of the pillars which are used for gaining the dimension stones (Layer U, C, D, E, and F; see Figure 13, chapter 4.2.1). One specimen was from the roof layer (Layer BB). Additionally a specimen out of the blasted material was tested. The blasted layer consists of several layers and the assignment of the taken specimen to a layer is not possible because the specimen was taken after the blasting.

5.1.1.1 Preparation of the specimen

To secure the traceability the specimens were assimilated into the internal documentation system of the university. Each base specimen is allocated to a unique number, weighed and a photo is taken. An exemplary photo documentation is viewable in the annex (see chapter 15.5); the whole photo documentation is attached at the data CD. A summary of the assimilated base material is shown in Table 2.

Layer	rough Dimensions	Identification Number
	[cm]	[-]
Layer BB	15*15*15	BBK 79
Layer blasted		BBK 80
Layer U	20*20*20	BBK 81
Layer C	20*20*20	BBK 82
Layer D	20*20*20	BBK 83
Layer E	20*20*20	BBK 84
Layer F	20*20*20	BBK 85

Table 2: Base Material

For each specimen which was drilled out of the base material this number is foregoing (example: Layer U → BBK 81; First core out of Layer U: → BBK 81 – 1). The production

of the specimen out of the base material was done accordingly to the Austrian norm (ÖNORM B 3124-1). A special focus was the height to diameter ratio of 2:1. To use the material sustainable for possible further testing, the diameter of the specimen was set to 45 [mm].

To gain the UCS the Layers “blasted”, U, C, D, E and F were used. Layer BB is reserved for further tests. Generally, out of each base material samples perpendicular and parallel to the layering were drilled to gain a comparison of the influence of the layering. With the material out of Layer U and C, each 8 samples were drilled out (4 perpendicular, 4 parallel). Out of the Layers D, E and F each 4 samples were drilled (2 perpendicular, 2 parallel). The amount of samples was reduced to reserve the material and the necessity was not given because the results of the first samples of layer U and C showed that within one layer, the scattering of test results is minimal. Out of the Layer “blasted” 3 samples were drilled. 2 were perpendicular and 1 was parallel to the layering.

5.1.1.2 Results

The results of the UCS are shown in Table 3.

Doc. Number	diameter	height	UCS	Direction	Layer
[-]	[mm]	[mm]	[MPa]	[-]	[-]
BBK-80-1	45,3	92,9	189	perpendicular to layering	Blasted Material
BBK-80-2	45,3	92,0	210	perpendicular to layering	
BBK-80-3	45,4	91,7	218	parallel to layering	
BBK-81-1	45,4	94,0	142	perpendicular to layering	Layer U
BBK-81-2	45,2	91,5	141	perpendicular to layering	
BBK-81-3	45,3	93,2	235	perpendicular to layering	
BBK-81-4	45,3	94,1	263	perpendicular to layering	
BBK-81-5	45,3	91,2	174	parallel to layering	
BBK-81-6	45,2	92,5	186	parallel to layering	
BBK-81-7	45,3	93,1	278	parallel to layering	
BBK-81-8	45,3	93,7	190	parallel to layering	
BBK-82-1	45,3	92,9	259	perpendicular to layering	Layer C
BBK-82-2	45,2	92,4	271	perpendicular to layering	
BBK-82-3	45,2	91,6	272	perpendicular to layering	
BBK-82-4	45,3	91,1	265	perpendicular to layering	
BBK-82-5	45,3	90,6	268	parallel to layering	
BBK-82-6	45,2	91,4	271	parallel to layering	
BBK-82-7	45,2	92,0	263	parallel to layering	
BBK-82-8	45,2	94,1	258	parallel to layering	
BBK-83-1	45,2	92,6	283	perpendicular to layering *	Layer D
BBK-83-2	45,3	93,1	274	perpendicular to layering *	
BBK-83-3	45,3	91,0	285	parallel to layering *	
BBK-83-4	45,4	91,9	288	parallel to layering *	
BBK-84-1	45,2	92,1	240	perpendicular to layering *	Layer E
BBK-84-2	45,2	90,6	272	perpendicular to layering *	
BBK-84-3	45,3	90,9	273	parallel to layering *	
BBK-84-4	45,3	91,1	247	parallel to layering *	
BBK-85-1	45,3	90,0	269	perpendicular to layering	Layer F
BBK-85-2	45,3	90,1	277	perpendicular to layering	
BBK-85-3	45,3	91,2	284	parallel to layering	
BBK-85-4	45,2	84,7	286	parallel to layering	

Table 3: Results UCS

In the following special observations will be discussed separated by the layers.

Layer blasted

The results, compared to the other layers (except layer U) are lower. This can be interpreted that due to the energy release of the blasting the material is pre-weakened. The use of the blasted material for the laboratory test is justifiable due to the fact that the remaining material in the pillar experiences similar energy input.

Layer U

The results of this layer vary within the samples the most. It seems that the white layer (probably calcite (CaCO_3)) within the marble reduces the strength. This is validated by the comparison of the optical viewing before testing and the result of the UCS test and it will be shown at direct comparison of the specimen BBK 81 – 2 and BBK 81 – 3.

BBK 81 – 2 has an UCS of 141 [MPa] and the calcite layer is distinctive – see Figure 61.



Figure 61: BBK 81 – 2, before testing

In comparison BBK 81 – 3 has an UCS of 234 [MPa] and although it has a separating layer it isn't filled with calcite (see Figure 62).



Figure 62: BBK 81 – 3, before testing

Furthermore an influence of the energy input by the blasting is possible, since the blasted layer is above of layer U.

Layer D, Layer E

The main problem with these layers was to determine the direction of the layering. Up to now an exact statement of the layering within the samples is not possible. Even after the drilling no layering could be determined. Therefore the orientation has been assumed on the basis of the marking on the base material, which was done from company side. At the base material of Layer U, C and F the tag of the layer name was on the upper layer parallel to the layering.

5.1.1.3 Interpretation of the results

To gain the for the safety calculations necessary strength (σ_c), the results of the UCS are compared to each other. In Table 4 the average values of the UCS are shown. The blue marked column and the average result at the bottom of the column represent the average value without differentiations of the layering or the layers itself. The green column represents the layers which may have been influenced by the blasting. The yellow column gives the average value of the layers which might not be influenced by the blasting. The adjoining column represents the average results of each layer. The last two white columns represent the average results differentiated by orientation.

The numbers next to the UCS represent the amount of samples.

Doc. Number	No layering respected					Layering respected				
	UCS	influenced by blasting			UCS	perpendicular		parallel		
		Layer	UCS			UCS	UCS	UCS		
[-]	[MPa]	[-]	[MPa]		[MPa]	[MPa]	[MPa]	[MPa]		
BBK-80-1	189	1		189	1		189	1		
BBK-80-2	210	1	blasted	210	1		210	1		
BBK-80-3	218	1		218	1				218	
	0	0		0	0	0	sum	617	3	sum
	0	0		0	0	average	206		average	
						average	200		218	
BBK-81-1	142	1	Layer U	142	1		142	1		
BBK-81-2	141	1		141	1		141	1		
BBK-81-3	235	1		235	1		235	1		
BBK-81-4	263	1		263	1		263	1		
BBK-81-5	174	1		174	1				174	
BBK-81-6	186	1		186	1				186	
BBK-81-7	278	1		278	1				278	
BBK-81-8	190	1		190	1				190	
	0	0		sum	2228	11	sum	1611	8	sum
	0	0	average	203		average	201		average	
						average	195		830	
						average	207		4	
BBK-82-1	259	1	Layer C	259	1		259	1		
BBK-82-2	271	1		271	1		271	1		
BBK-82-3	272	1		272	1		272	1		
BBK-82-4	265	1		265	1		265	1		
BBK-82-5	268	1		268	1				268	
BBK-82-6	271	1		271	1				271	
BBK-82-7	263	1		263	1				263	
BBK-82-8	258	1		258	1				258	
	0	0		sum	2127	8	sum	1067	4	1059
	0	0	average	266		average	267		265	
BBK-83-1	283	1	Layer D	283	1		283	1		
BBK-83-2	274	1		274	1		274	1		
BBK-83-3	285	1		285	1				285	
BBK-83-4	288	1		288	1				288	
	0	0		sum	1130	4	sum	557	2	573
	0	0	average	282		average	278		286	
BBK-84-1	240	1	Layer E	240	1		240	1		
BBK-84-2	272	1		272	1		272	1		
BBK-84-3	273	1		273	1				273	
BBK-84-4	247	1		247	1				247	
	0	0		sum	1033	4	sum	512	2	521
	0	0	average	258		average	256		260	
BBK-85-1	269	1	Layer F	269	1		269	1		
BBK-85-2	277	1		277	1		277	1		
BBK-85-3	284	1		284	1				284	
BBK-85-4	286	1		286	1				286	
	sum	7634		31	sum	5406	20	sum	1117	4
	average	246		average	270		average	279		
							average	273		
							average	285		

Table 4: Average results of UCS

The average results, differentiated by the layers and the orientation, are visualized in Figure 63.

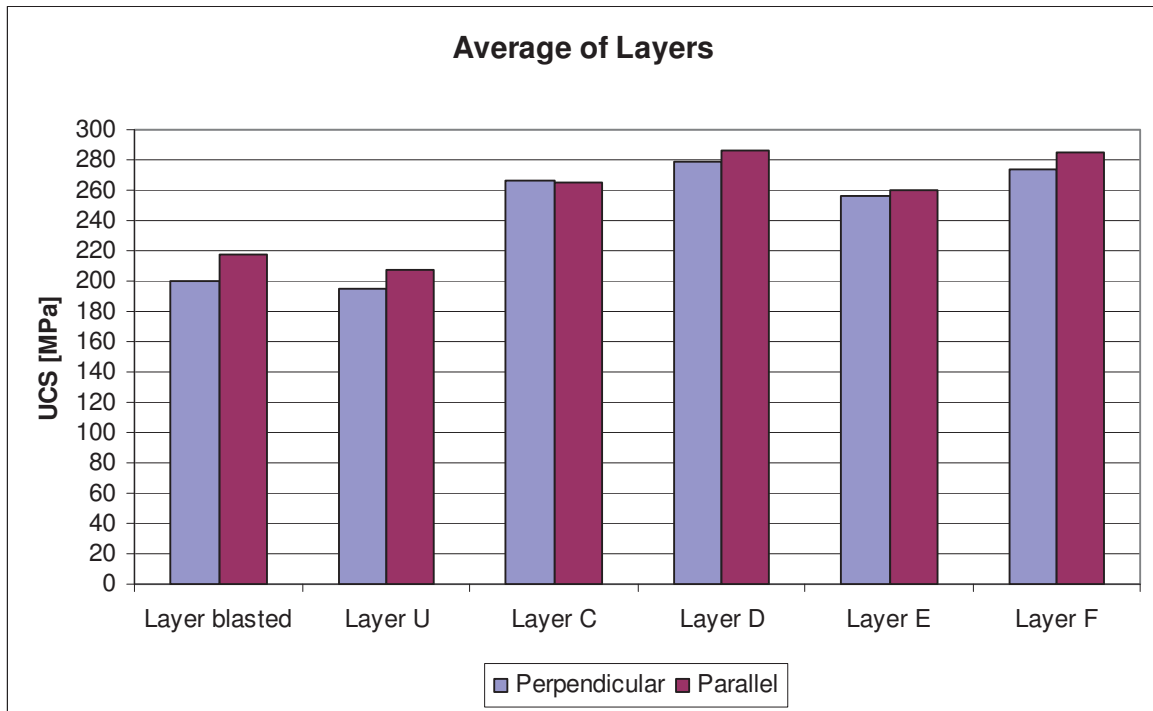


Figure 63: Average results UCS of layers

Furthermore a diagram of the average results for the layers, without respect on the layering, is shown below (see Figure 64).

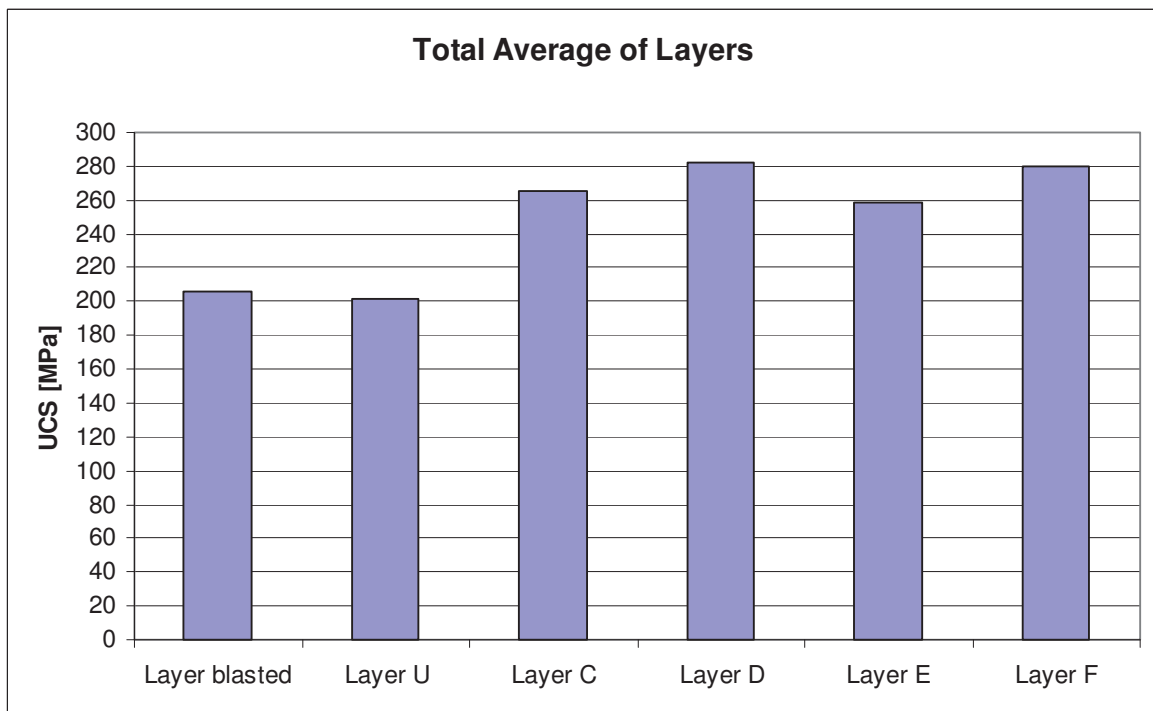


Figure 64: Total average results UCS of layers

As shown in figure 3 and 4 the limiting layer of the uniaxial compressive strength (σ_c) is layer U. Since the average value perpendicular and parallel to the layering differs with 3,43 [%], the total average value of layer U is acceptable.

Therefore the UCS (σ_c) is:

$$\sigma_c = 200 \text{ [MPa]}$$

This gained value will be taken for the further calculations.

5.1.2 Bending tension strength (BTS)

The bending tension strength (BTS) is used for getting an impression of the tension strength of the rock and to get an idea about the maximum width of the unsupported roof length (see chapter 5.3.5). To gain the BTS the preserved material of the layers D (BBK 83), E (BBK 84) and F (BBK 85) were taken as testing material.

5.1.2.1 Preparation of the specimen

The specimen were produced and tested according to the Austrian ÖNORM B 3124-5. As with the specimen for the UCS, the specimen where assimilated into the internal documentation system of the university, to gain a secure traceability. The experimental setup was third point load (see Figure 65, red square).

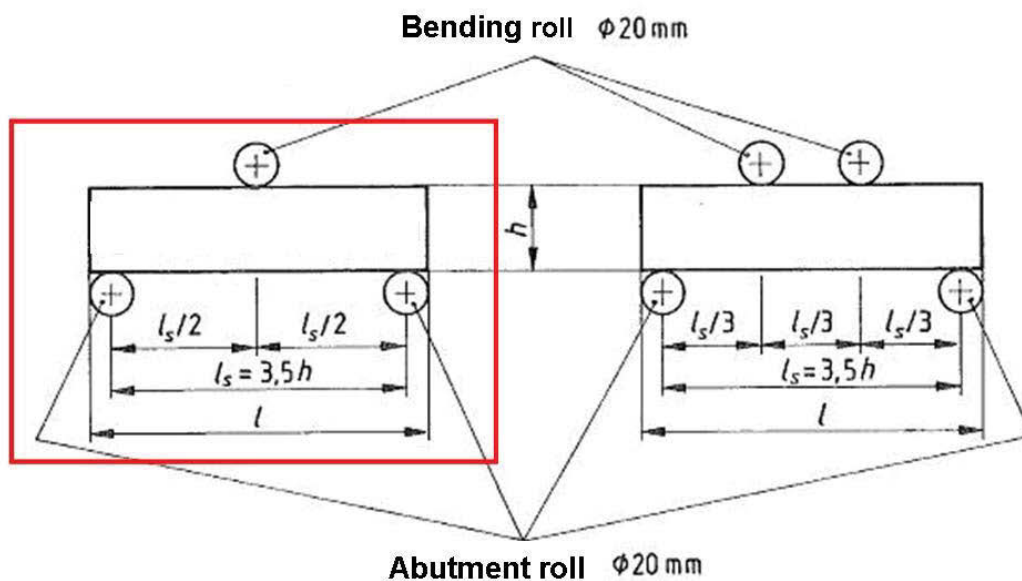


Figure 65: Experimental setup (cp. ÖNORM B 3124-5, p 3)

5.1.2.2 Results

The results are presented in Table 5.

Sample	Height	Width	Length	BTS (σ_b)	Note
[-]	[mm]	[mm]	[mm]	[MPa]	[-]
BBK-83-5	41	38	162	36	
BBK-83-6	40	42	161	22	
BBK-83-7	40	41	161	33	
BBK-83-8	42	40	159	33	
BBK-83-9	42	40	158	32	
BBK-83-10	41	40	161	33	
BBK-83-11	41	37	160	33	
BBK-83-12	37	41	161	26	
BBK-84-5	39	39	162	34	
BBK-84-6	39	40	161	28	
BBK-84-7	40	39	161	31	
BBK-84-8	40	39	162	26	1
BBK-84-9	40	39	160	32	
BBK-84-10	40	40	160	28	
BBK-84-11	40	40	161	30	
BBK-85-5	41	41	160	30	
BBK-85-6	39	41	160	25	2
BBK-85-7	41	41	161	29	2
BBK-85-8	41	38	161	14	1
BBK-85-9	38	40	161	17	1
BBK-85-10	37	41	161	34	

1= Test not guilty. Abutmentarea not prallel. Spalling at the abutment.

2 = Test not guilty. Abutmentarea not prallel. Fracture similar to torsion fracture.

Table 5: Results bending tension strength

The in Table 5 shown results are visualized in Figure 66. The “missing” columns are those where the test was not guilty.



Figure 66: Bending tension strength, entire

5.1.2.3 Interpretation of the results

A separation of the gained values concerning the layering was not taken into consideration since within the sample of layer D and E (BBK 83, 84) no layering could be detected. Furthermore the results of layer F (BBK 85) consist of 2 values.

The average value for the bending tension strength (σ_b) is:

$$\sigma_b = 31 \text{ [MPa]}$$

5.2 Pillar strength

To calibrate the current status in terms of the strength and the safety of the pillars, the classic approach of the factor of safety was used. A detailed presentation is done in the chapters below. After that, the concept of the factor of safety will be applied to the pillars of the mine. Furthermore the arching effect will be taken into consideration.

5.2.1 Factor of safety (FOS) – theory

To determine the stability of the pillars the classical approach of the factor of safety is used. The factor of safety is defined by:

$$FOS = \frac{S_p}{\sigma_p} \quad \text{(Formula 1)}$$

FOS...	Factor of safety	[-]
S _p ...	Strength of pillar	[MPa]
σ _p ...	Load acting on pillar	[MPa]

The Strength of the Pillar (S_p) is calculated by the empirical formulas for hard rock pillars as shown in Table 6.

Author	Equations	S_o	σ_c	Año
Hedley	$S_p = S_o \cdot \frac{a_p^{0.5}}{H_p^{0.75}}$	0.578 σ_c	230 MPa	1972
Kimmelmann	$S_p = S_o \cdot \frac{a_p^{0.46}}{H_p^{0.66}}$	0.691 σ_c	94 MPa	1984
Potvin	$S_p = S_o \cdot \frac{a_p}{H_p}$	0.420 σ_c	–	1989
Krauland	$S_p = S_o \cdot \left(0.778 + 0.222 \cdot \frac{H_p}{a_p}\right)$	0.354 σ_c	100 MPa	1987
Sjöberg	$S_p = S_o \cdot \left(0.778 + 0.222 \cdot \frac{H_p}{a_p}\right)$	0.308 σ_c	240 MPa	1992
Lunder-Pakalnis	$S_p = S_o \cdot \left(0.680 + 0.520 \cdot \frac{H_p}{a_p}\right)$	0.440 σ_c	–	1997
CMRI	$S_p = S_o \cdot \left(\frac{1}{H_p}\right)^{0.36} + \left(\frac{H_p}{250} + 1\right) \cdot \left(\frac{a_p}{H_p} - 1\right)$	0.270 σ_c	–	2000
Hardy-Agapito	$S_p = S_o \cdot \left(\frac{V_p}{V_s}\right)^{-0.118} \cdot \left(\frac{a_p}{H_p} \cdot \frac{a_s}{H_s}\right)^{0.833}$	σ_c	–	1982

Table 6: Sp, pillar design formulae for hard rock (cp. González-Nicieza et al 2006, p. 424)

As shown in Table 6 the formula of the strength of the pillar compiles of the uniaxial compressive strength and the ratio of the width of the pillar (a_p) and the height of the pillar (H_p) – except Hardy-Agapito. The formula of Hardy-Agapito takes the additionally the volume of the tested specimen (V_s), the volume of the pillar (V_p) and the specimen width to height ratio (a_s / H_s) into consideration.

The factors which are used were found in different rock types and were determined empirically.

The load acting on the pillar (σ_p) is calculated by using the Tributary Area Theory (TAT). The basic concept of the TAT is that every pillar carries an equal share of the overburden.

The TAT is valid for:

- Constant mining layout (constant depth, pillar area, room width and pillar height)
- Panel width > 1,3 * depth of mining

(cp. González-Nicieza et al. 2006, p. 428)

Although not all of these requirements are fulfilled, a first impression of the stress situation is gained with the TAT.

The load acting on the pillar is basically the primary in situ stress ($\rho \cdot g \cdot H$, see Formula 2) times the ratio of the tributary area (A_{RC}) to the area of the pillar (A_p) and is defined by:

$$\sigma_p = \rho * g * H * \frac{A_{RC}}{A_p} \quad \text{(Formula 2)}$$

σ_p ...	Load acting on pillar	[Pa]
ρ ...	Density of overburden	[kg/m ³]
g ...	Acceleration of gravity	[m/s ²]
H ...	Thickness of overburden	[m]
A_{RC} ...	Area of rock column (Tributary area)	[m ²]
A_p ...	Area of pillar	[m ²]

(cp. Hoek E. and Brown E.T. 1980, p. 114)

In the formula above the shape of the area is not taken into consideration however it is applicable for irregular pillars (see Figure 67).

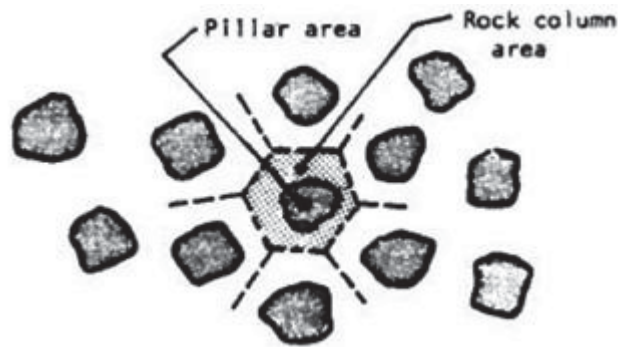


Figure 67: TAT irregular pillar sketch (cp. Hoek E. and Brown E.T. 1980, p. 114)

The load acting on the pillar is hinged by the ratio of the area of the rock column and the area of the pillar. For square or rectangular pillars the dimensions of the side lengths of the rooms and the pillars are taken into consideration (see Figure 68 and Figure 69).

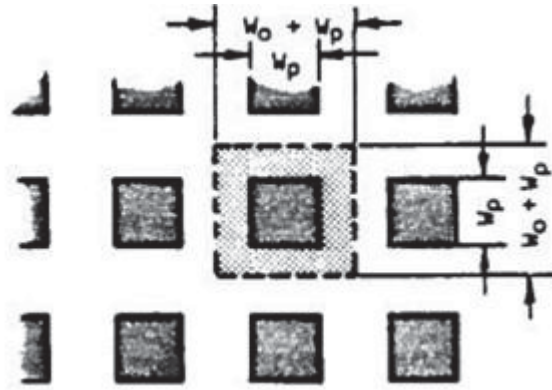


Figure 68: TAT square pillar sketch (cp. Hoek and Brown 1980, p. 114)

The basic formula is applicable on square pillars. However, the formula can be rewritten with more detail.

$$\sigma_p = \rho * g * H * \frac{(W_p + W_0)^2}{(W_p)^2} \quad \text{(Formula 3)}$$

σ_p ...	Load acting on pillar	[Pa]
ρ ...	Density of overburden	[kg/m ³]
g ...	Acceleration of gravity	[m/s ²]
H ...	Thickness of overburden	[m]
W_p ...	Width of pillar	[m]
W_0 ...	Width of room	[m]

Furthermore the formula for square pillars are expressed with the area extraction ratio (e), since the term

$$\frac{(W_p + W_0)^2}{(W_p)^2} \quad \text{(Formula 4)}$$

is the reciprocal value of (1 – e). The area extraction ratio is defined as the tributary area decreased by the area of the pillar divided by the tributary area.

$$e = \frac{((W_p + W_0)^2 - W_p^2)}{(W_p + W_0)^2} \quad \text{(Formula 5)}$$

e...	Extraction ratio	[-]
W _p ...	Width of pillar	[m]
W ₀ ...	Width of room	[m]

So the load on the pillar can be defined as:

$$\sigma_p = \rho * g * H * \frac{1}{(1 - e)} \quad \text{(Formula 6)}$$

σ _p ...	Load acting on pillar	[Pa]
ρ...	Density of overburden	[kg/m ³]
g...	Acceleration of gravity	[m/s ²]
H...	Thickness of overburden	[m]
e...	Extraction ratio	[-]

For calculating the load acting on rectangular pillars the definition of the area extraction ratio is enlarged by the length of the pillar and the length of the room. A sketch is shown in Figure 69.

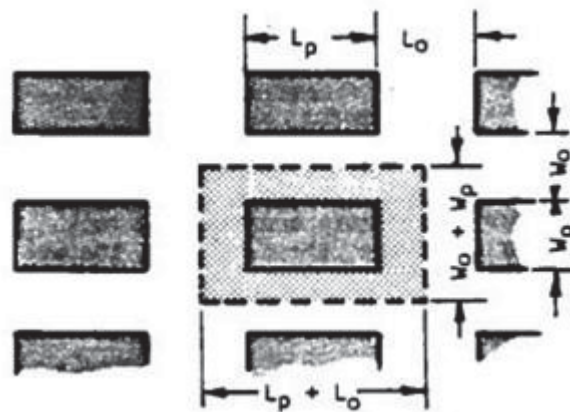


Figure 69: TAT rectangular pillar sketch (cp. Hoek and Brown 1980, p. 114)

The area extraction ratio of rectangular pillars is defined by:

$$e = \frac{((W_p + W_0) * (L_p + L_0)) - (W_p * L_p)}{((W_p + W_0) * (L_p + L_0))} \quad \text{(Formula 7)}$$

e...	Extraction ratio	[-]
W _p ...	Width of pillar	[m]
W ₀ ...	Width of room	[m]
L _p ...	Length of pillar	[m]
L ₀ ...	Length of room	[m]

The formula for a strip pillar takes into consideration that the pillar has an “infinite” expansion. Therefore the point of view changes from a 2 dimensional into an 1 dimensional view with the consideration of a unit length. The load acting on the pillar is calculated by the width of the room between the strip pillars and the appending width of the pillar itself per unit length (see Figure 70).

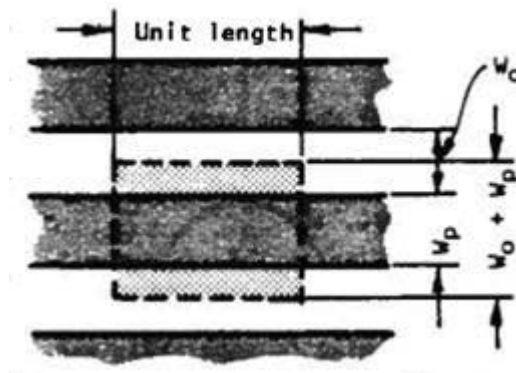


Figure 70: TAT strip pillar sketch (cp. Hoek and Brown 1980, p. 114)

Expressed by the area extraction ratio:

$$e = \frac{((W_p + W_0) - W_p)}{(W_p + W_0)} \quad \text{(Formula 8)}$$

e...	Extraction ratio	[-]
W _p ...	Width of pillar	[m]
W ₀ ...	Width of room	[m]

5.2.2 Factor of safety (FOS) – applied to the mine

The theory described in chapter 5.2.1 is now applied to the mine. The determination of each parameter is described in the following.

Note: To achieve the description, the whole calculation of pillar 10 is presented. The location of pillar 10 is shown in Figure 71. The total gained data, results and maps are added in the Annex (see chapter 15.6 and 15.7).

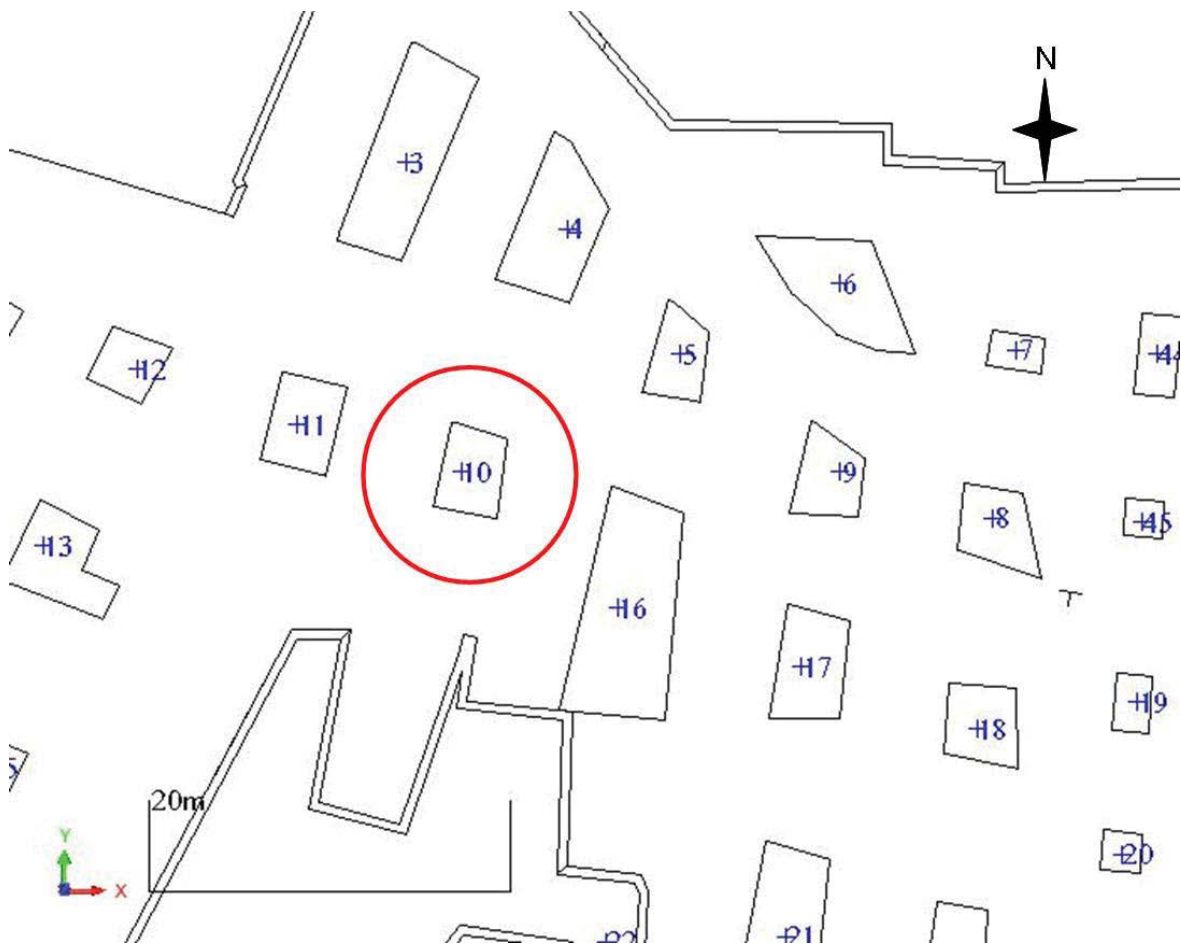


Figure 71: Location Pillar 10, Surpac

5.2.2.1 Strength of the pillar (S_p)

To calculate the strength of the pillars (S_p), the empirical hard rock design concept of Hedley is taken, with:

$$S_p = S_0 * \frac{a_p^{0.5}}{H_p^{0.75}} \quad \text{(Formula 9)}$$

S_p ...	Strength of pillar	[MPa]
S_0 ...	Reduced USC	[MPa]
a_p ...	Width of pillar	[m]
H_p ...	Height of pillar	[m]

(cp. González-Nicieza et al 2006, p. 424)

Where:

$$S_0 = 0,578 * \sigma_c \quad \text{(Formula 10)}$$

S_0 ...	Reduced USC	[MPa]
σ_c ...	USC	[MPa]

(cp. González-Nicieza et al 2006, p. 424)

The empirical pillar strength formula from Hedley was taken, because on the one hand the at Hedley used UCS is similar to the determined one from the laboratory tests, and on the other hand the concept of Hedley is in the midfield of the approaches (see Figure 72).

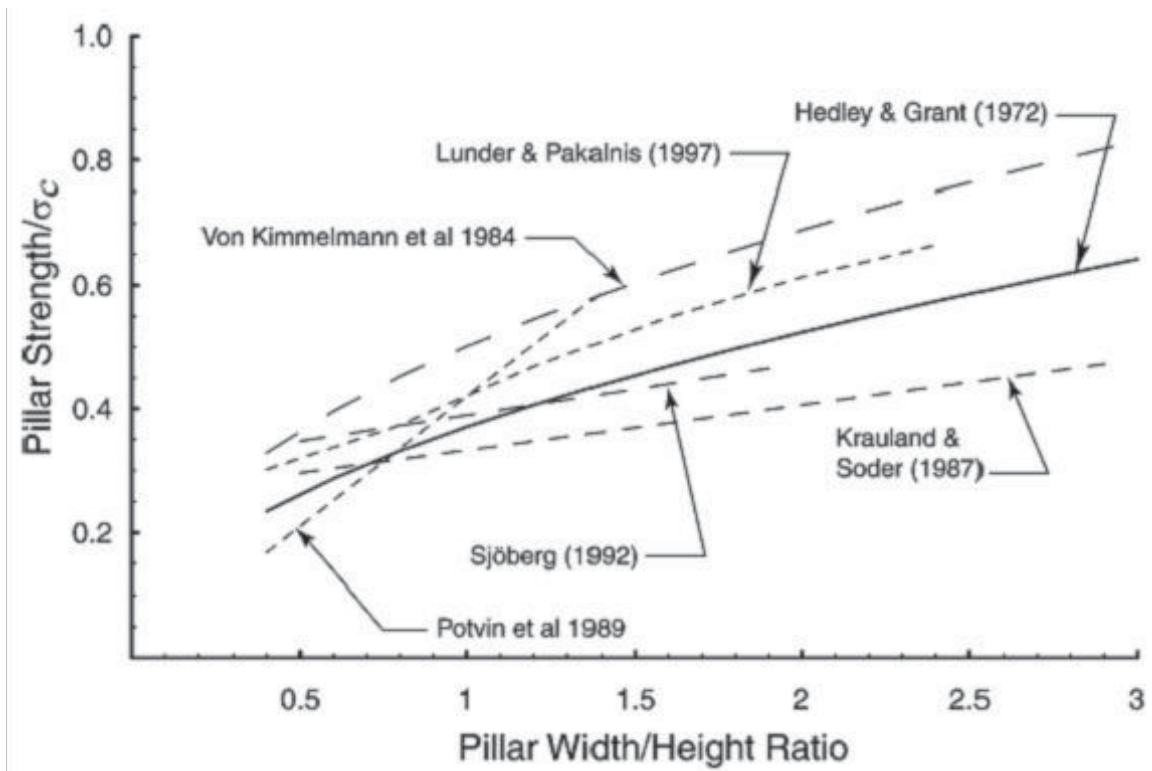


Figure 72: Pillar strength formulas, comparison of different approaches (cp. Martin and Maybee 2000, p. 1240)

5.2.2.2 S_p – width of the pillar (a_p)

To gain the width of the pillar the data from the fieldwork done survey concerning the pillar shape as well as the data from the company provided map are taken into consideration. The shape of the pillar, concerning the top view, mainly is not regular. Therefore the following equation for the effective width (w_e) is used (cp. Salamon 1983, p. 181).

$$w_e = 4 * \frac{A_p}{R} \quad \text{(Formula 11)}$$

w_e ...	Effective width	[m]
A_p ...	Area of pillar	[m ²]
R ...	Circumference of pillar	[m]

Although this equation is based on the approach for rectangular pillars, it is used here for irregular pillars.

To gain the area of the pillar (A_p) 3 data bases were used:

1. Once, the during the fieldwork taken side lengths of the pillar (floor-, mid- and roof-distance), which were measured mainly at the current mining area with a laser guided distance meter (Leica DISTO D5) are used. Out of the distances the area was calculated. Where the pillar shape, based on the top view of the provided map, is roughly rectangular or square like, the opposite measured lengths were summed up and divided by 2. With this 2 gained values the area was calculated. If the shape is not like the before described ones, the shape was divided into best fitting calculateable geometrical figures, calculated and summed up. A contrast of the database is shown on hand of pillar 10 in Table 7 below.

Where to less measurements were available to calculate sensible values for the area or this approach seemed not to be reasonable, the area was calculated by the third database.

2. The second used data base is the, during the fieldwork measured surveying with a theodolite, Trimble S6. The gained point cloud was converted into Surpac and the points were connected to each other to gain the areas (floor, midfloor, midroof and roof). The surveying was concentrated on the entrance and the first pillars near the entrance. The value of the area was read out with Surpac. A contrast of the database is shown on hand of pillar 10 in Table 7 below.
3. The third used data base is the in the provided map marked plan view of the pillars. The areas were read out with Surpac. Besides the area, the first and second data base was used to determine the related area marked in the map. The surveying confirmed that the marked pillar shapes/areas are obtained to the floor area of the pillar. Due to the fact that the first database describes mainly the current mining area and the second database describes the first pillars at the current mining area near the entrance, the surveyed data was used to gain values for the roof areas of the not surveyed pillars. Therefore the percentage of the reduction of the floor area to the roof area was calculated and multiplied with the floor area of the provided map. The calculated reduction is 42 [%]. With the reduction factor it is possible to gain values for the roof area in the not surveyed parts of the mine (e.g.: backfilled). A contrast of the database is shown on hand of pillar 10 in Table 7 below.

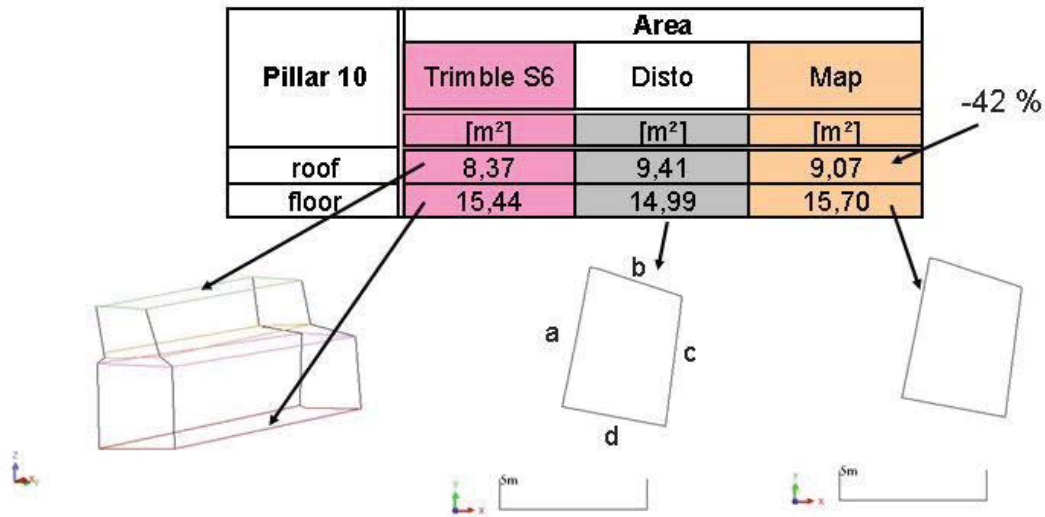


Table 7: Contrast of the area of the pillar results, pillar 10

The circumference (R) was determined similar to the calculation of the area (A_p). To gain values for the first database the measured side lengths were summed up. The values of database two and three were read out with Surpac.

With these two gained results the effective width (w_e) was calculated. Table 8 presents the results for the example of pillar 10.

Pillar 10	w_e		
	Trimble S6	Disto	Map
	[m]	[m]	[m]
roof	2,85	3,03	3,01
floor	3,88	3,82	3,90

Table 8: Contrast of results, effective width pillar 10

(Note: The entire recorded measurements and data is attached in the Annex, see chapter 15.6)

5.2.2.3 S_p – height of the pillar (H_p)

The height of the pillar is defined by the average of the during the fieldwork measured heights of the pillars. The measurements apply mainly on the current mining area. During the fieldwork at the emergency routes, areas were detected, where a 6th layer was mined. This observation was not taken into consideration, since the increased mining height,

compared to the current mining area, was only detectable at occasional pillars at the emergency routes where no backfill was present. At the north field the mining height was decreased through settlement of probably calcite, which is transported by the water income.

The above described observations were not taken into consideration of the calculation of the mining height. The mining height is:

$$H_p = 3,21 \text{ [m]}$$

With the in chapter 5.2.2.2 and at this chapter determined results, the strength of the pillar can be calculated according to Formula 9, chapter 5.2.2.1.

5.2.2.4 Load acting on pillars (σ_p)

To calculate the load acting on the pillar (σ_p) the formula for irregular pillars is used (see Formula 2, chapter 5.2.1). Since the deposit is dipping with an average value of $16,5^\circ$, concerning the marked dip values in the provided map, the vertical load, or primary in situ stress ($\sigma_v = \rho \cdot g \cdot H$), has to be adapted to the dipping of the deposit. Therefore the result of σ_v was decreased by the factor of " $\cos^*(16,5^\circ)$ " to gain the normal load (σ_n) acting on the pillars. The principle is shown a sketch below (see Figure 73).

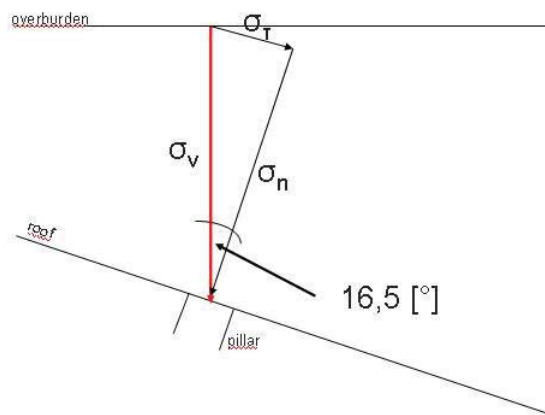


Figure 73: Sketch vertical-normal load, σ_p

$\sigma_v \dots$	Primary in situ stress	[MPa]
$\sigma_n \dots$	Normal stress or „Load acting on Pillar“	[MPa]
$\sigma_T \dots$	Shear stress	[MPa]

The determination of the area of the pillar (A_p) is described at chapter 5.2.2.2. The other necessary parameters are described below.

5.2.2.5 σ_p - Density (ρ)

The density was determined during the laboratory tests of the uniaxial compressive strength (UCS). The average value for the density is:

$$\rho = 2,69 \text{ [t/m}^3\text{]}$$

5.2.2.6 σ_p – Thickness overburden (H)

To determine the values for the overburden of each pillar the 3D model of Surpac was used. In each pillar area a centre point was drawn. This gained point cloud was mirrored on to the surface of the topography as well as on the roof surface of the developed 3D model of the mine. The result was that at each pillar 2 points were created with the same coordinates concerning the x-y-level but with different z-coordinate. The distance between the points represents the thickness of the overburden. Figure 74 shows skeletal structure of the roof of the mine and the topography of the surface including the mirrored points. As an example the distance of 2 thicknesses of the overburden are marked (red line) in the figure.

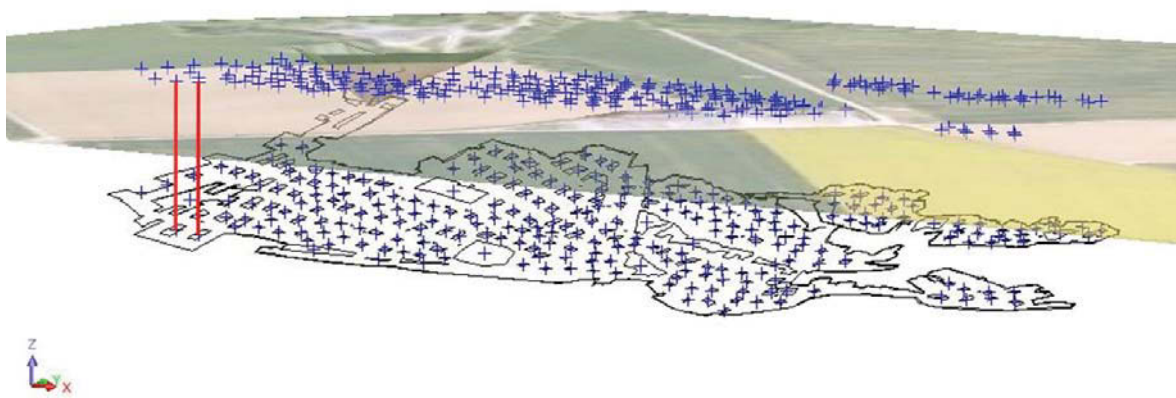


Figure 74: Thickness overburden

$$(H_{\text{Pillar10}} = 39,77 \text{ [m]})$$

5.2.2.7 σ_p – Area rock column – Tributary Area (A_{RC})

The area for the associated rock column or tributary area (A_{RC}) was determined by drawing it into the plan view (Surpac) of the mine. For each pillar the area of the gained database was read out for the calculation. In Figure 75 the plan view and the rock column or tributary area (red squares) is shown.

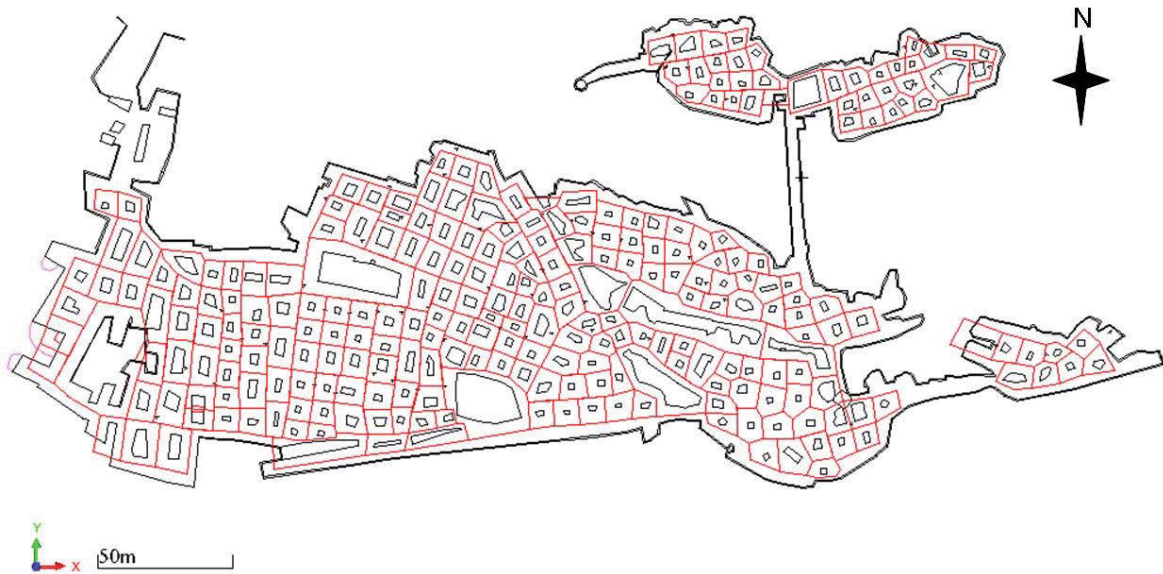


Figure 75: Rock column areas

$$(A_{RC, Pillar10} = 112,83 [m^2])$$

With the above acquired values the factor of safety can be calculated (Formula 1, chapter 5.2.1). As an example the results of the strength of the pillar (S_p), load acting on the pillar (σ_p) and the whence following factor of safety (FOS) are presented on hand of the example of pillar 10 (see Table 9).

Pillar 10			Trimble S6	Disto	Map
σ_p	[MPa]	roof	13,56	12,07	12,52
		floor	7,35	7,57	7,23
S_p	[MPa]	roof	81,33	83,97	83,65
		floor	95,00	94,20	95,23
FOS	[-]	roof	6,00	6,96	6,68
		floor	12,92	12,44	13,17

Table 9: Results of pillar 10, stability calculation

The gained results of the factor of safety (Trimble S6, Disto, Map) for the roof and floor areas are used for the further analysis of the effect of the panel width (see chapter 5.2.3).

5.2.3 Effect on the panel width

The basic idea of the effect on the panel width is the analogous to a beam which is supported at three points. The ends of the beam are fixed and in the centre an elastic spring supports the beam (see Figure 76). Through a rigid distributed load (p) a reaction force is induced at the centre. The deflection is dependent on the deformation characteristics of the beam and the spring. When now instead of one spring, several springs are employed, the conclusion will be the same. The deflection will depend on the characteristics of the spring and the beam, although the load on one spring will be influenced by the stiffness of the others. (cp. Salamon 1983, p. 176 f)



Figure 76: Deformation of beam and spring (cp. Salamon 1983, p176)

This analogy can be transferred to pillars (springs) and the surrounding rock (beam). If the panel width increases and the pillars are arranged in a uniform pattern, each pillar will experience the same load or said in another way, the weight of the overburden is carried by the pillars in equal proportions. This is represented by the tributary area theory, where the upper limit for the load on the pillar is calculated. An error exists in the vicinity of the edges, however in large mining areas this error is insignificant since the main focus is on the central region. If the panel width decreases, the abutments (rib side rock) are gaining more influence and the pillars will experience fewer loads (viewed from the centre to the edges of the mining area). The concept or analogy follows the approach shown in Figure 77. (cp. Salamon 1983, p. 177 ff)

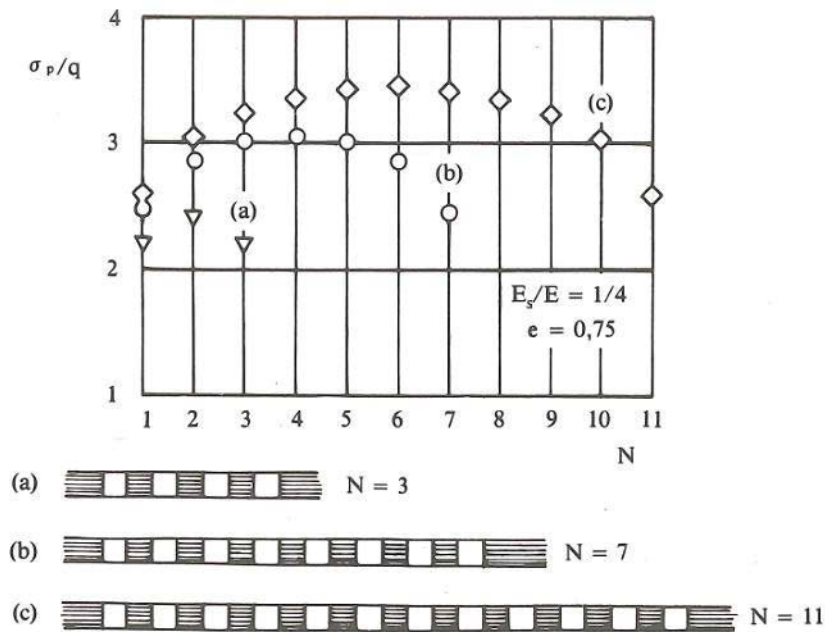


Figure 77: Effect on the panel width (cp. Salamon 1983, p178)

$\sigma_p...$	Load acting on pillar	[MPa]
$q...$	Virgin vertical stress	[MPa]
$E_s...$	Young's module (Rock)	[MPa]
$E...$	Young's module (Pillar)	[MPa]
$e...$	Extraction rate	[-]

Figure 77 shows the effect on the panel width. The tributary area theory is approaching to $\sigma_p/q = 4$ since the area extraction rate (e) is 0,75 [-] (cp. Salamon 1983, p. 179). Even though the constraints (E, e, \dots) of the above shown figure is not similar to the mine Mazy, it is used to determine the reduction through the effect on the panel width, since the size of the mine is applicable to this approach. Furthermore it should highlight that a further mining activity which increases the panel width at the existing mining panel, is increasing as well the load acting on the pillars.

To gain the alignment of the effect on the panel width as well as the value of reduction of this analogy, following constraints were set:

1. The "shortest" alignment which is possible is determining the reduction factor. Since the abutment with the smallest panel width has the biggest influence.
2. Barrier pillars have the same approach as the ribside of the mining area.
3. In circular area around the barrier pillar the reduction factor is at least $\leq 2,5$ in the first row and at least $\leq 3,1$ at the second row.

Examples of the above listed constraints will be explained and shown on hand of a section of the map of the alignments of the effect on the panel width (see Figure 78).

NOTE: The entire map with the alignment of the panel width is attached in the Annex (see chapter 15.7) as well as at the Data CD.

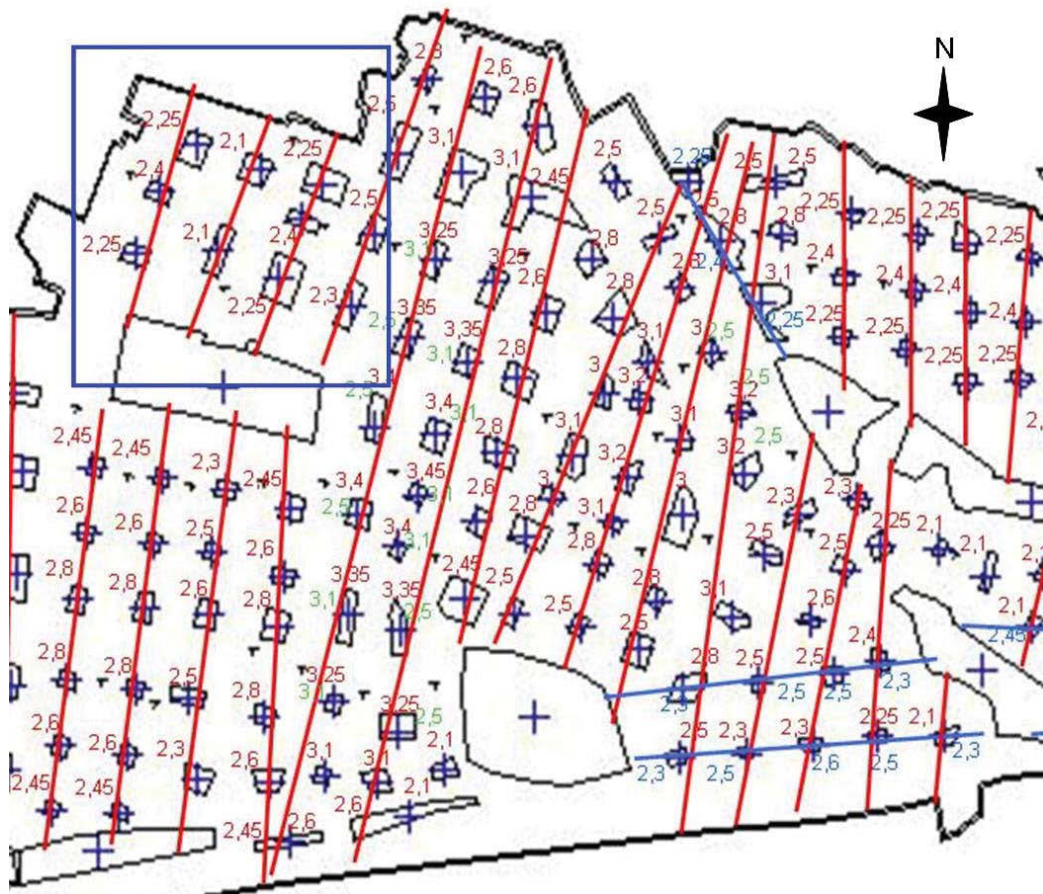


Figure 78: Effect on panel width, section of alignment map

The red lines represent the alignments to determine the effect on the panel width. The numbers near the pillars are values which were determined by Figure 77, based on the amount of pillars which are on the alignment. The blue square in Figure 78 represents an example to constraint 1. The alignment from the barrier pillar to the ribside has a greater influence or higher reduction than if the alignment would be warped at 90 [°]. The green values represent constraint 3. The blue alignments are additional viewed alignments of the effect on the panel width. The value near a pillar with the highest reduction factor (or lower value) was taken into consideration.

As example the calculation at pillar 10 is shown. Two pillars span the alignment and therefore the value after Figure 77 is 2,1. With this value the reduction (0,53 %) is calculated (see Formula 12) and therefore the load on the pillar (σ_p) is reduced.

$$\sigma_p' = \frac{RF}{4} * \sigma_p \quad \text{(Formula 12)}$$

σ_e' ... Reduced load acting on the pillar [MPa]
 RF... Reduction factor [-]
 σ_p ... Load acting on pillar after TAT [MPa]

Pillar 10			Trimble S6	Disto	Map
σ_p'	[Mpa]	roof	7,12	6,34	6,57
		floor	3,86	3,98	3,80
σ_p	[Mpa]	roof	13,56	12,07	12,52
		floor	7,35	7,57	7,23
S_p	[Mpa]	roof	81,33	83,97	83,65
		floor	95,00	94,20	95,23
FOS'	[-]	roof	11,42	13,25	12,73
		floor	24,61	23,69	25,08

Table 10: Results with reduced σ_p , pillar 10

As shown in the table above, the factor of safety for pillar 10 increases. The result of the analysis of the whole pillars is presented in chapter 5.2.4.

5.2.4 Result of the stability of the pillars

The calculations which are presented in chapter 5.2.2 and 5.2.3 was done for each pillar. The results and calculation tables are attached at the Annex (see chapter 15.6). Five out of the 265 recalculated pillars drop below a factor of safety of $1,6^3$ [-]. The location and the calculated factor of safety (FOS), including the reduction through the effect on the panel width, is shown in Figure 79.



Figure 79: Results incl. reduction

The in Figure 79 shown results mean not that there is an urge hazard in terms of safety, since during the fieldwork no pressure syndromes were detected at these pillars. All results are related to the calculated roof area, which was determined by using the floor area, marked in the provided map, and multiplied with the computed reduction factor of 42 [%]. No actual measurement was done at these pillars. The possibility that the reduction factor is too high is given. A resurveying of these pillars combined with a recalculation would be necessary to gain certainty.

However the results represent that in the shown area a weakness zone is given and a further change in the geometry of the pillar as well as the surrounding should not be done (e.g. increasing the pillar height by extracting the floor layers). Furthermore an expansion

³ Factor of safety for panel pillar layout, based on RSA experience

of the panel width, especially in south direction, by extraction, would lead, as explained above, to an increase of the load acting on the pillars by the effect on the panel width (see chapter 5.2.3). If a further expansion is considered a barrier pillar would be necessary.

To gain certainty if these pillars are overloaded and tend to spalling and therefore a major safety issue is possible, a surveying of these pillars is suggested. To recognize any spalling a coloring of the pillars for instance with white color is possible. If a part spalls, it is easier to detect the spalling through the contrast. Furthermore a photo documentary is useful, so the long term movement is possible to detect. A possible interval is half-yearly where a photo from each side from roughly the same position is made.

5.3 Stability of the roof

To analyze the stability of the roof, classification systems and the concept of a cantilever beam were used. Since the at the fieldwork gained information consists mainly of optical observations and judgments, several classification systems are used, to minimize the probability of failure or miss-interpretation and to describe the stability of the roof. With the from the samples determined bending tension strength (BTS, chapter 5.1.2) the span width of roof plates, which are cut through a geological discontinuity and remain with one abutment, is calculated by using the classical cantilever beam approach. This is done to gain a value how far a plate can overhang before anchoring is necessary to prevent a safety hazard. Furthermore the gained information is used to get a basis of comparison for the outlay of future mining areas.

Following classification systems were taken into consideration, whereof each will be described in detail in this chapter:

- Hangingwall Stability Rating (HSR)
- Bieniawski (Rock Mass Rating (RMR)) → Laubscher (Mining Rock Mass Rating (MRMR))
- Barton (Q-System) → Mathew (N – Stability Number)

(Note: “→” means that the system is based or built up on the previous one)

General, each classification system is an empirical determined approach, which is based on observations of existing mines. The basic concept is to describe the viewed area or rock mass (e.g. roof) with parameters of influence and contrast it with geometrical properties of the viewed area. Through the collected data of observed mines, which is plotted in diagrams, a statement concerning the stability can be given by entering the determined values of the current viewed area. The description of the rock mass is done for example by geological mapping and/or core logging.

Three areas are determined concerning the stability of the roof within the current mining area (see Figure 80).

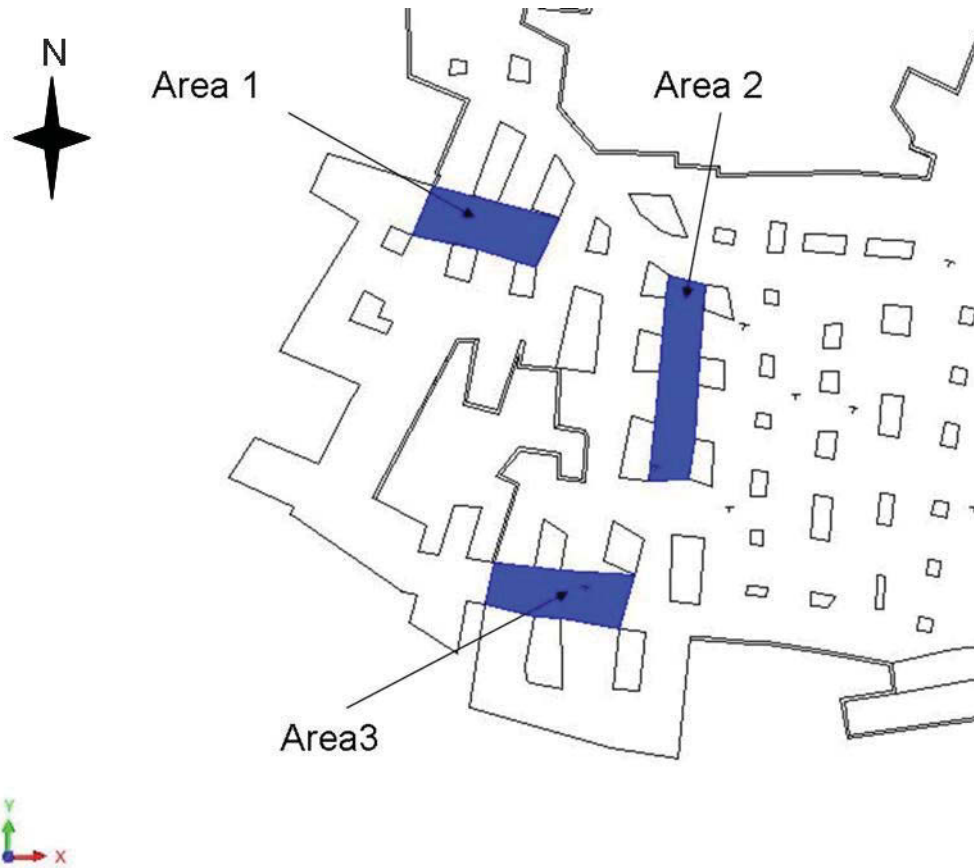


Figure 80: Viewed areas for geomechanical classification system, current situation, current mining area south

The dimensions are presented in Table 11.

	Length	Width
	[m]	[m]
Area 1	20	8
Area 2	30	6,1
Area 3	20	7,2

Table 11: Dimensions of viewed areas, classification system, current situation

5.3.1 Hangingwall stability rating (HSR)

The hangingwall stability rating was developed by E. Villaescusa et al at the Mount Isa Mine (AUS), where copper, silver, lead and zinc are mined with sublevel bench stoping with backfill. The deposit is closely spaced, narrow, steeply dipping (65°, west) and the rock mass can be described as highly jointed and steeply dipping bedded rock. Although the HSR method is to be considered to be applicable for steeply dipping deposits (> 55°) it is used as one classification system to determine the stability of the roof. (cp. Villaescusa 1997, p 171 – 176)

The rating uses following factors:

1. Bedding plane brake frequency (50 [%])
2. Number of joint sets and continuity (20 [%])
3. Mining induced stresses (15 [%])
4. Blast damage (15 [%])

(Note: The value in the brackets is the valuation in which amount the figure is considered in the rating)

To gain the rating for the bedding plane breaks per meter the first 3 [m] of the roof layers and their bedding planes are observed. (cp. Villaescusa 1997, p 172 f) Therefore the from the company provided data⁴ of the geological profile from the roof layers. Out if this data the first 3 [m] were taken into consideration. The listing of the layers or bedding planes are shown in Table 12.

⁴ See attached data CD: „Coupes veine inf+fotos.xls“

	Layer thickness	Planes
	[cm]	[-]
Croutes et Raches	7	1
	20	1
Croutes	10	1
-	0	0
Croutes	10	1
Mâle	33	1
Croutes	3	1
Croutes	2	1
A	48	1
-	0	0
R	61	1
AB	22	1
Nouveau banc	0	0
AC	46	1
BB	5	1
	38	1
Sum	305	13
plane breakes/metre =		4

Table 12: Calculation of bedding plane breaks / meter

*) = no values known/mentioned, not taken into consideration

With the gained value the HSR component can be read out from the chart (see Figure 81).
The rating value = 23 [-].

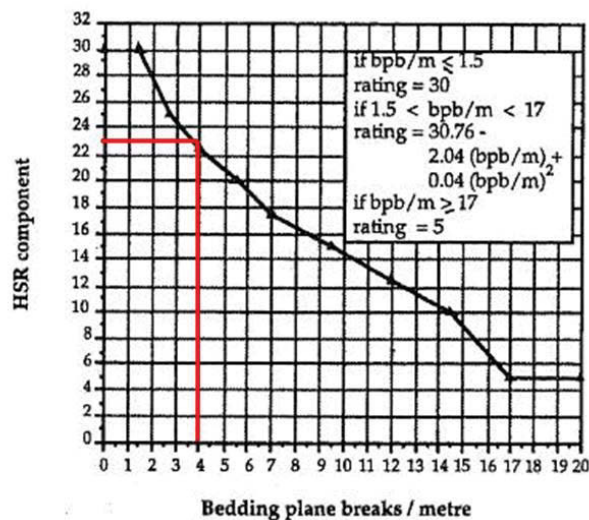


Figure 81: Bedding plane break frequency, HSR (cp. Villaescusa 1997, p 173)

For the rating for the joint set which influence the roof was set to 10 (1-2 joint set; 1 intersecting; see Figure 82)

Joint set number	Joint sets transecting	HSR component
>5	>3	2
3-5	3	4
2-4	2	6
1-3	1	8
1-2	1	10
1-2	0	12

Figure 82: Number of joint set and continuity, HSR (cp. Villaescusa 1997, p 173)

Since the current mine has maximum overburden, according to the Surpac model of around 60 [m] the normal induced stress the rating is set to 4 (< 20 [MPa]; see Figure 83)

Normal stress (MPa)	HSR component
>90	1
80-90	2
70-80	3
60-70	5
50-60	6
40-50	8
30-40	9
20-30	7
< 20	4

Figure 83: Normal induced stresses, HSR (cp. Villaescusa 1997, p 174)

The rating of the blasting is set to 9, since the blasting holes are parallel to the bedding of the layers and, compared with the uniaxial compressive strength, situated in strong rock (see Figure 84).

Rock type	Hangingwall hole orientation to bedding	HSR component
Weak	Across	1.5
(13/80, 13, 11 orebodies)	parallel	3
Medium	Across	4.5
(5/110, 12, 14 orebodies)	parallel	6
Strong	Across	7.5
(5/60, 5,7, 8 orebodies)	parallel	9

Figure 84: Table for Blast damage, HSR (cp. Villaescusa 1997, p 174)

In Table 13 the rating is summarized and the final HSR value summed up.

		HSR	
Geological discontinuities (70%)	Bedding plane break frequency (50%) 1)	23	(4 per m)
	Number of joint sets and continuity (20%)	10	(1-2 joint set; 1 intersecting)
Mining induced stresses (15%)		4	(< 20 Mpa)
Blast damage (15%)		9	(Strong, parallel)
HSR		46	

Table 13: Summary, HSR rating, current situation

To plot the HSR the hydraulic radius or shape factor is used (see Formula 13).

$$S = \frac{A}{U} \quad \text{(Formula 13)}$$

S...	Hydraulic radius	[m]
A...	Area of viewed region	[m ²]
U...	Circumference of viewed region	[m]

In Table 14 the after Formula 13 calculated hydraulic radius for the viewed areas or regions (see Figure 80, chapter 5.3) is presented.

	Area 1	Area 2	Area 3
Length (L)	20	30	20
Width (W)	8	6,1	7,2
Hydr. Radius (S)	2,86	2,53	2,65

Table 14: Hydraulic radius, HSR, current situation

With the above determined values the HSR chart is entered (see Figure 85)

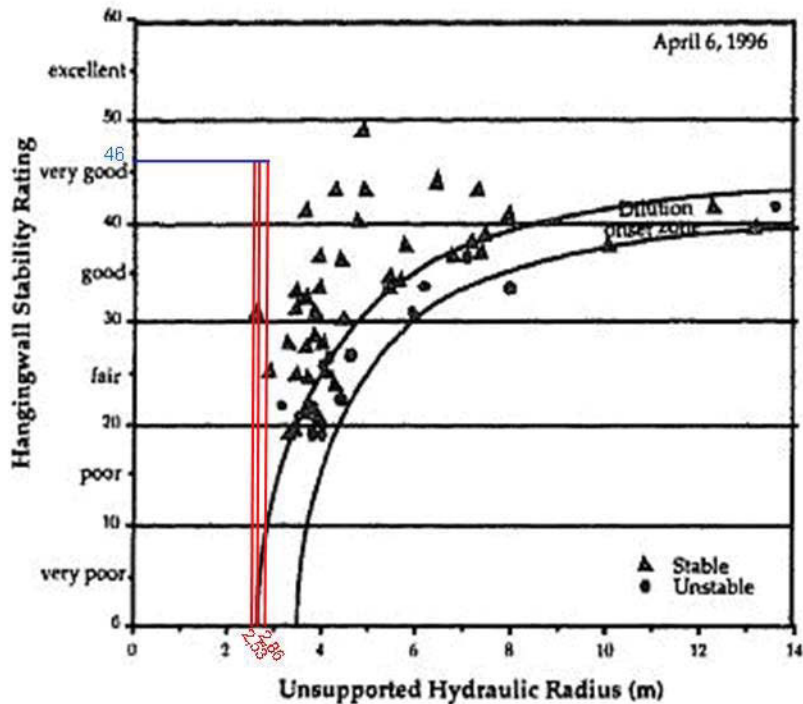


Figure 85: Bench stope stability chart, HSR, current situation (cp. Villaescusa 1997, p 176)

The chart above is described in 3 zones:

1. Stable (above the curve)
2. Transitional area (between the curves)
3. Unstable or failure zone (below the curve)

(cp. Villaescusa 1997, p 175 f)

According to the previous shown chart the stability of the roof is classified as stable after the HSR method.

It has to be noted again that this classification system is based on the experience of one mine and is considered to be applicable to steeply dipping deposits (cp. Villaescusa 1997, p 171 – 176).

5.3.2 Bieniawski (Rock Mass Rating (RMR)) & Laubscher (Mining Rock Mass Rating (MRMR))

5.3.2.1 Bieniawski (Rock Mass Rating (RMR))

The geomechanical classification by Bieniawski takes following parameters into account to describe the rock mass along a tunnel (mine):

1. Strength of intact rock (UCS, σ_c)
2. Rock quality designation (RQD)

The RQD is a core – recovery technique and is defined as (cp. Laubscher 1990, p. 259):

$$RQD = \frac{100 * \sum x_i}{L} \quad \text{(Formula 14)}$$

RQD...	Rock quality designation	[%]
x_i ...	Parts of the drill core > 10 [cm]	[cm]
L...	Length of the bore hole	[cm]

3. Spacing of discontinuities
4. Condition of discontinuities
5. Groundwater conditions
6. Orientation of discontinuities

(cp. Bieniawski 1984, p. 112 ff)

The RQD value was derived by using the from the company provided data⁵ of the geological profile from the roof layers. Out if this data all layers which are > 10 [cm] are summed up and divided through the total thickness of the viewed layers. The gained RQD value = 92 [%]. The calculation and the listening of the layers is attached in the Annex (see chapter 15.8).

The classification is done after the following table (see Figure 86).

⁵ See attached data CD: „Coupes veine inf+fotos.xls“

A. CLASSIFICATION PARAMETERS AND THEIR RATINGS									
Parameter		Range of values							
1	Strength of intact rock material	Point-load strength index	>10 MPa	4 - 10 MPa	2 - 4 MPa	1 - 2 MPa	For this low range - uniaxial compressive test is preferred		
		Uniaxial comp. strength	>250 MPa	100 - 250 MPa	50 - 100 MPa	25 - 50 MPa	5 - 25 MPa	1 - 5 MPa	< 1 MPa
	Rating		15	12	7	4	2	1	0
2	Drill core Quality RQD		90% - 100%	75% - 90%	50% - 75%	25% - 50%	< 25%		
		Rating		20	17	13	8	3	
3	Spacing of discontinuities		> 2 m	0.5 - 2 . m	200 - 600 mm	60 - 200 mm	< 60 mm		
		Rating		20	15	10	6	5	
4	Condition of discontinuities (See E)		Very rough surfaces Not continuous No separation Unweathered wall rock	Slightly rough surfaces Separation < 1 mm Slightly weathered walls	Slightly rough surfaces Separation < 1 mm Highly weathered walls	Slickensided surfaces or Gouge < 5 mm thick or Separation 1-5 mm Continuous	Soft gouge >5 mm thick or Separation > 5 mm Continuous		
		Rating		30	25	20	10	0	
5	Ground water	Inflow per 10 m tunnel length (l/m)	None	< 10	10 - 25	25 - 125	> 125		
		(Joint water pressure) (Major principal σ)	0	< 0.1	0.1 - 0.2	0.2 - 0.5	> 0.5		
		General conditions	Completely dry	Damp	Wet	Dripping	Flowing		
		Rating		15	10	7	4	0	
B. RATING ADJUSTMENT FOR DISCONTINUITY ORIENTATIONS (See F)									
Strike and dip orientations			Very favourable	Favourable	Fair	Unfavourable	Very Unfavourable		
Ratings	Tunnels & mines		0	-2	-5	-10	-12		
	Foundations		0	-2	-7	-15	-25		
	Slopes		0		-5	-50			
C. ROCK MASS CLASSES DETERMINED FROM TOTAL RATINGS									
Rating			100 ← 81	80 ← 61	60 ← 41	40 ← 21	< 21		
Class number			I	II	III	IV	V		
Description			Very good rock	Good rock	Fair rock	Poor rock	Very poor rock		
D. MEANING OF ROCK CLASSES									
Class number			I	II	III	IV	V		
Average stand-up time			20 yrs for 15 m span	1 year for 10 m span	1 week for 5 m span	10 hrs for 2.5 m span	30 min for 1 m span		
Cohesion of rock mass (kPa)			> 400	300 - 400	200 - 300	100 - 200	< 100		
Friction angle of rock mass (deg)			> 45	35 - 45	25 - 35	15 - 25	< 15		
E. GUIDELINES FOR CLASSIFICATION OF DISCONTINUITY conditions									
Discontinuity length (persistence)			< 1 m	1 - 3 m	3 - 10 m	10 - 20 m	> 20 m		
Rating			6	4	2	1	0		
Separation (aperture)			None	< 0.1 mm	0.1 - 1.0 mm	1 - 5 mm	> 5 mm		
Rating			6	5	4	1	0		
Roughness			Very rough	Rough	Slightly rough	Smooth	Slickensided		
Rating			6	5	3	1	0		
Infilling (gouge)			None	Hard filling < 5 mm	Hard filling > 5 mm	Soft filling < 5 mm	Soft filling > 5 mm		
Rating			6	4	2	2	0		
Weathering			Unweathered	Slightly weathered	Moderately weathered	Highly weathered	Decomposed		
Rating			6	5	3	1	0		
F. EFFECT OF DISCONTINUITY STRIKE AND DIP ORIENTATION IN TUNNELLING**									
Strike perpendicular to tunnel axis				Strike parallel to tunnel axis					
Drive with dip - Dip 45 - 90°		Drive with dip - Dip 20 - 45°		Dip 45 - 90°		Dip 20 - 45°			
Very favourable		Favourable		Very unfavourable		Fair			
Drive against dip - Dip 45-90°				Drive against dip - Dip 20-45°					
Fair				Unfavourable					
Dip 0-20 - Irrespective of strike°									
Fair									

Figure 86: Classification table, Bieniawski (cp. Hoek 2007, chapter 3, p. 9)

With the table, shown in Figure 86, following results were determined and summed up in Table 15.

influencing factors	rating	Information
Strength	13	100 - 250 Mpa (200 Mpa)
RQD	20	90 - 100 % (92 %)
Spacing of discontinuities	10	200 - 600 mm (see geolog. Profile)
Conditions discontinuities	19	see 1)
Ground water	15	complete dry
Raiting of discont. Orient.	-5	strike parallel to tunnel, Dip 0-20° - Fair
RMR	72	GOOD ROCK

1) classification of disc. Conditions		
Persistence	0	> 20m
Aperture	4	0,1 - 1 mm
Roughness	6	very rough
Infilling	4	hard filling < 5mm
Weathering	5	slightly weathered
	19	

Table 15: Results RMR, current situation

The gained value for the RMR is used to get a statement concerning the stability of the roof, by entering in to the stability chart of Brady.

Brady's determination of the stability graph was done on the basis of 292 case histories from mines mainly in Canada. The investigations correlate to weak rock quality and opening design. He plots the RMR against critical span, which is defined as the largest circle that can be drawn within the boundaries of the viewed area. 3 categories are used:

1. Stable excavation (No uncontrolled falls of ground, no extraordinary support measures have been employed,...(below curve))
2. Potentially unstable excavation (Extra ground support has been installed to prevent potential falls of ground,...(between curves))
3. Unstable excavation (Area has collapse,...(above curve))

(cp. Brady, p. 2 f)

The critical spans of the viewed areas in the current mining area (see Figure 80, chapter 5.3) are shown in Table 16.

design span (circle)		
Area 1	9,32	[m]
Area 2	9,44	[m]
Area 3	12,08	[m]

Table 16: Critical span or design span, Brady, current situation

With the determined values it is possible to enter the design chart of Brady (see Figure 87). (Note: The smallest and the largest values of the design span are marked in the chart.)

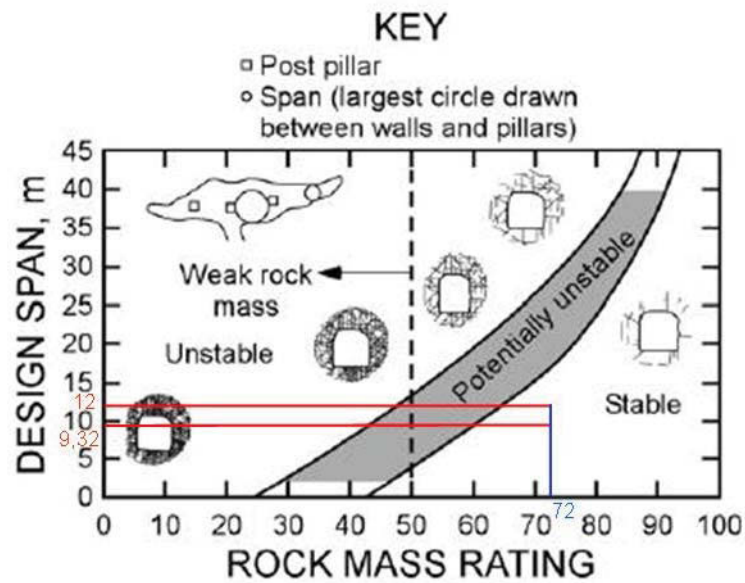


Figure 87: Design span curve, Brady, RMR, current situation (cp. Brady, p. 2)

After the stability graph after Brady the viewed areas of the current mining operation are in the stable area.

5.3.2.2 Laubscher (Mining Rock Mass Rating (MRMR))

Based on the geomechanical classification system after Bieniawski (see chapter 5.3.2.1), Laubscher's system uses the determined classification and extends it with adjustments to make it more applicable for mining situations. (cp. Laubscher 1990, p. 257)

The basic exposition of the system and the adjustment is shown in Figure 88.

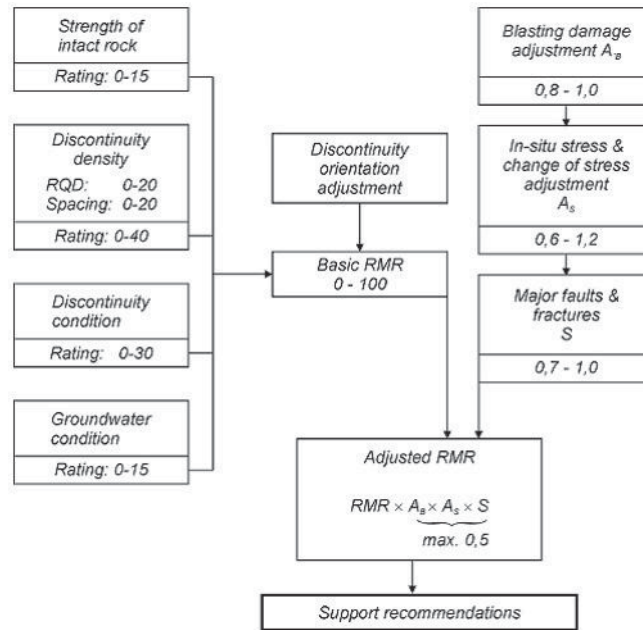


Figure 88: Adjustment for mining applications, Laubscher, current situation (cp. Bieniawski 1984, p. 119)

In detail Laubscher extends the classification system from Bieniawski with following adjustments:

1. Weathering
2. Joint orientation
3. Mining-induced stresses
4. Blasting effects

(cp. Laubscher 1990, p. 263 – 266)

The adjustment of the weathering was set after Table 17, which shows the adjustment percentages related to the degree of weathering after a period of exposure (cp. Laubscher 1990, p. 264).

Degree of weathering	Potential weathering and adjustments, %				
	½ y	1 y	2 y	3 y	4 + y
Fresh	100	100	100	100	100
Slight	88	90	92	94	96
Moderate	82	84	86	88	90
High	70	72	74	76	78
Complete	54	56	58	60	62
Residual soil	30	32	34	36	38

Table 17: Adjustment of weathering, Laubscher, current situation (cp. Laubscher 1990, p. 264)

The adjustment of the joint orientation is set one time with no influence (no reduction through adjustment), 100 [%], and one time with 80 [%], where the bedding of the layers and two joints inclined away from the vertical are taken into consideration (see Table 18).

No. of joints defining the block	No. of faces inclined away from the vertical				
	70%	75%	80%	85%	90%
3	3		2		
4	4	3		2	
5	5	4	3	2	1
6	6	5	4	3	2,1

Table 18: Adjustment of joint orientation, Laubscher, current situation (cp. Laubscher 1990, p. 265)

The mining induced stress adjustment is set to 90 [%] (range 60 – 120 [%]) and the adjustment on the blasting effect is set to 80 [%] (see Table 19).

<i>Technique</i>	<i>Adjustment, %</i>
Boring	100
Smooth-wall blasting	97
Good conventional blasting	94
Poor blasting	80.

Table 19: Adjustment of blasting, Laubscher, current situation (cp. Laubscher 1990, p. 266)

A summary (Table 20) and the calculation (Formula 15) of the MRMR is shown below.

$$MRMR = RMR * A_W * A_{JO} * A_{MS} * A_B \quad (\text{Formula 15})$$

MRMR...	Mining rock mass rating	[-]
RMR...	Rock mass rating	[-]
A _W ...	Adjustment weathering	[-]
A _{JO} ...	Adjustment joint-orientation	[-]
A _{MS} ...	Adjustment mining induced stress	[-]
A _B ...	Adjustment blasting effects	[-]

RMR	72	GOOD ROCK, Bieniawski
weathering	0,90	moderate (1y)
joint orientation	0,80	3 No.of joints defining block/2 away from vertical
mining induced stress	0,90	
blasting	0,80	poor blasting
Adjustment total	0,52	cp. Formula 15
MRMR (incl. Discont)	37,32	

weathering	0,90	moderate (1y)
joint orientation	1,00	No joints
mining induced stress	0,90	
blasting	0,80	poor blasting
Adjustment total	0,65	cp. Formula 15
MRMR (no Discont.)	46,66	

Table 20: Summary, MRMR, Laubscher, current situation

Since the adjustment for the joint orientation is set one time with no influence (no reduction through adjustment), 100 [%], and one time with 80 [%], – where the bedding of the layers and two joints inclined away from the vertical are taken into consideration – two different values for the MRMR are resulting (see Table 20).

The MRMR values after Laubscher are plotted against the Hydraulic radius (S; see Formula 13 and Table 14, chapter 5.3.1) in the stability diagram. With the determined values the diagram is entered (see Figure 89). Three areas are used to describe the stability of the viewed area:

1. Stable (local support, above curve)
2. Transition zone (between curves)
3. Caving/unstable (below curve)

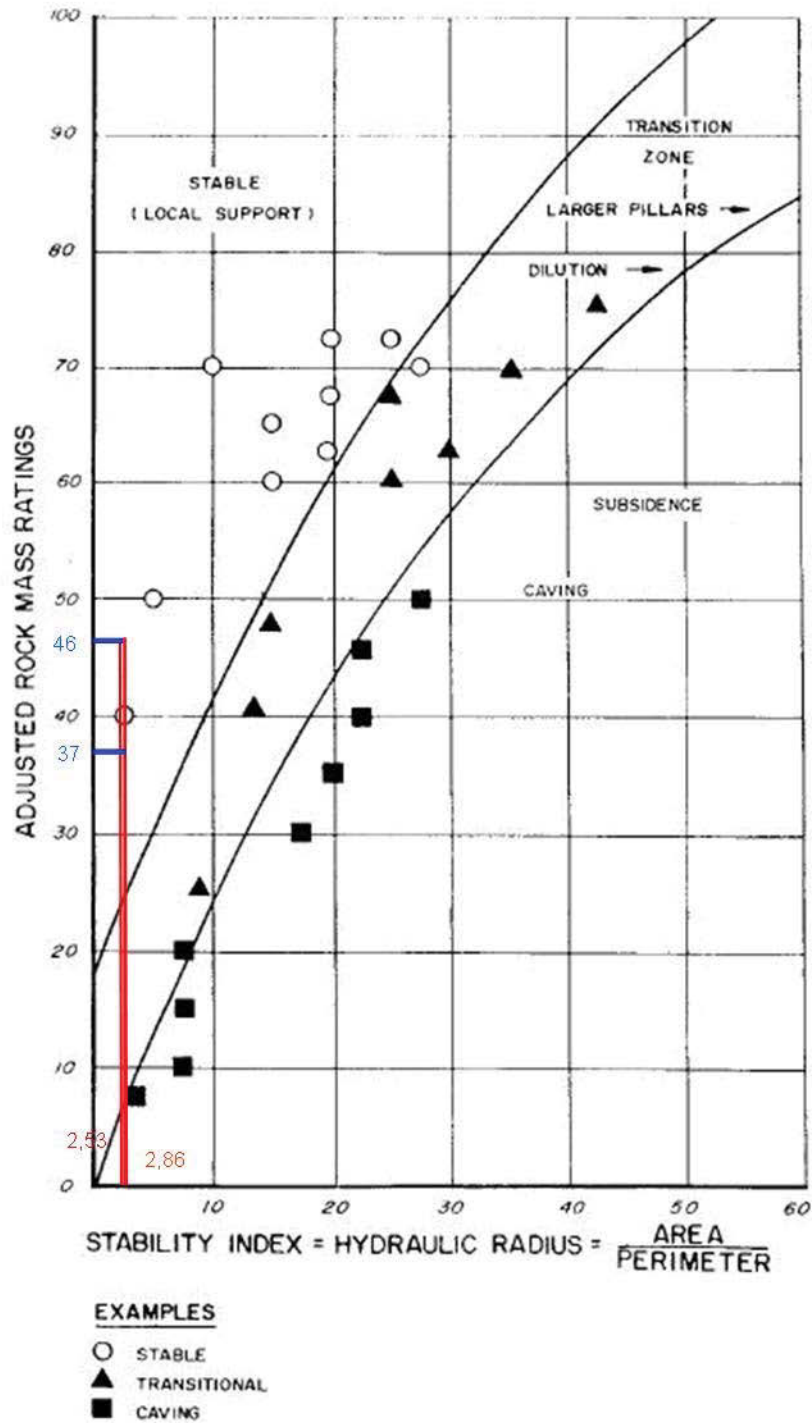


Figure 89: Stability diagram, Laubscher, current mining situation (cp. Laubscher 1990, p. 270)

The stability diagram shows that after the classification system after Laubscher, the viewed areas in the current mining area are in the stable area.

5.3.3 Barton (Q-System) → Mathew (N – Stability Number)

5.3.3.1 Barton (Q-System)

The Q-system of Barton is a system for the classification of rock masses, regarding to the stability in tunnels and caverns and was developed between 1971 and 1974. The system is based on a database of more than 1000 examples of existing caverns and tunnels and their needs for support (cp. Løset 1997, p. 26).

The classification of the rock mass is influenced by three major factors which are assembled by two factors. The factors are:

1. Degree of jointing
 - a. Rock Quality Designation (RQD)
 - b. Joint set number (J_n)
2. Joint friction
 - a. Joint roughness number (J_r)
 - b. Joint alteration number (J_a)
3. Stress
 - a. Joint water reduction factor (J_w)
 - b. Stress Reduction Factor (SRF)

With these 6 parameters the Q-value for the classification is calculated after:

$$Q = \frac{RQD}{J_n} * \frac{J_r}{J_a} * \frac{J_w}{SRF} \quad \text{(Formula 16)}$$

Q...	Q-value	[-]
RQD...	Rock Quality Designation	[-]
J_n ...	Joint set number	[-]
J_r ...	Joint roughness number	[-]
J_a ...	Joint alteration number	[-]
J_w	Joint water reduction factor	[-]
SRF	Stress Reduction Factor	[-]

(cp. Løset 1997, p. 2 ff)

To improve the readability and since the determination of the parameters follows the similar procedure as for Bieniawski (see chapter 5.3.2.1), the tables for assigning the values for each parameter are attached in the Annex (see chapter 15.9). In Table 21 the summary of the assessment of the Q-system is shown.

Degree of jointing (or block size)	RQD =	92,30	[%]	1)
	J_n =	3,00	[-]	C = One joint set plus random joints
Joint friction (inter- block shear strength)	J_r =	1,50	[-]	E = rough, irregular, planar
	J_a =	2,70	[-]	D = silty or sandy clay coatings, small clay friction
Active stress	J_w =	0,66	[-]	B = Medium inflow or pressure, occasional outwash of joint fillings
	SRF =	1,00	[-]	J = Medium stress, favourable stress conditions ($\sigma_c / \sigma_1 = 100$; $\sigma_3 / \sigma_c = 0,01$)
Q =		11,28	[-]	B = GOOD

Table 21: Summary, Q-System, current situation

1) For the determination and the result of the RQD, see chapter 5.3.2.1, Formula 14

Ad) SRF

To determine the Stress Reduction Factor (SRF) the principal stresses were estimated with $\sigma_1 = \sigma_2 = \sigma_3 = 2$ [MPa], (k (ratio of σ_3/σ_1) = 1), based on the rounded normal strength acting on the viewed area and for the uniaxial compressive strength (UCS, σ_c), the in the laboratory tests found value was taken ($\sigma_c = 200$ [MPa] (see chapter 5.1.1)).

The Q-value is plotted against two other factors. Once the span width and second the Excavation Support Ratio (ESR). The ESR was set to 1,6 [-], according to Table 22.

Type of Excavation	ESR
A Temporary mine openings, <i>etc.</i>	ca. 3-5
B Vertical shafts: i) circular sections ii) rectangular/square section	ca. 2.5 ca. 2.0
C Permanent mine openings, water tunnels for hydro power (exclude high pressure penstocks), pilot tunnels, drifts and headings for large openings	1.6
D Storage rooms, water treatment plants, minor road and railway tunnels, surge chambers, access tunnels, <i>etc.</i>	1.3
E Power stations, major road and railway tunnels, civil defence chambers, portals, intersections, <i>etc.</i>	1.0
F Underground nuclear power stations, railways stations, sports and public facilities, factories, <i>etc.</i>	0.8
G Very important caverns and tunnels with a long lifetime, tunnels for gas pipe lines.	0.5

Table 22: Excavation Support Ratio (ESR), Barton, current situation (cp. Løset 1997, p. 26)

These two factors are set into relation after (cp. Løset 1997, p. 27):

$$y = \frac{\text{Span width}}{\text{ESR}} \quad (\text{Formula 17})$$

y...	Equivalent dimension	[m]
Span...	Span width	[m]
ESR...	Excavation Support Ratio	[m]

The results for the equivalent dimensions (y) for the viewed areas are presented in Table 23.

ESR =	1,60	[-]
-------	------	-----

AREA 1		
Span =	8,00	[m]
y =	5,00	[m]

AREA 2		
Span =	6,10	[m]
y =	3,81	[m]

AREA 3		
Span =	7,20	[m]
y =	4,50	[m]

Table 23: Results equivalent dimension (y), Barton, current situation

With the above defined values the from Barton proposed diagram for tunnel/cavern support can be entered (see Figure 90).

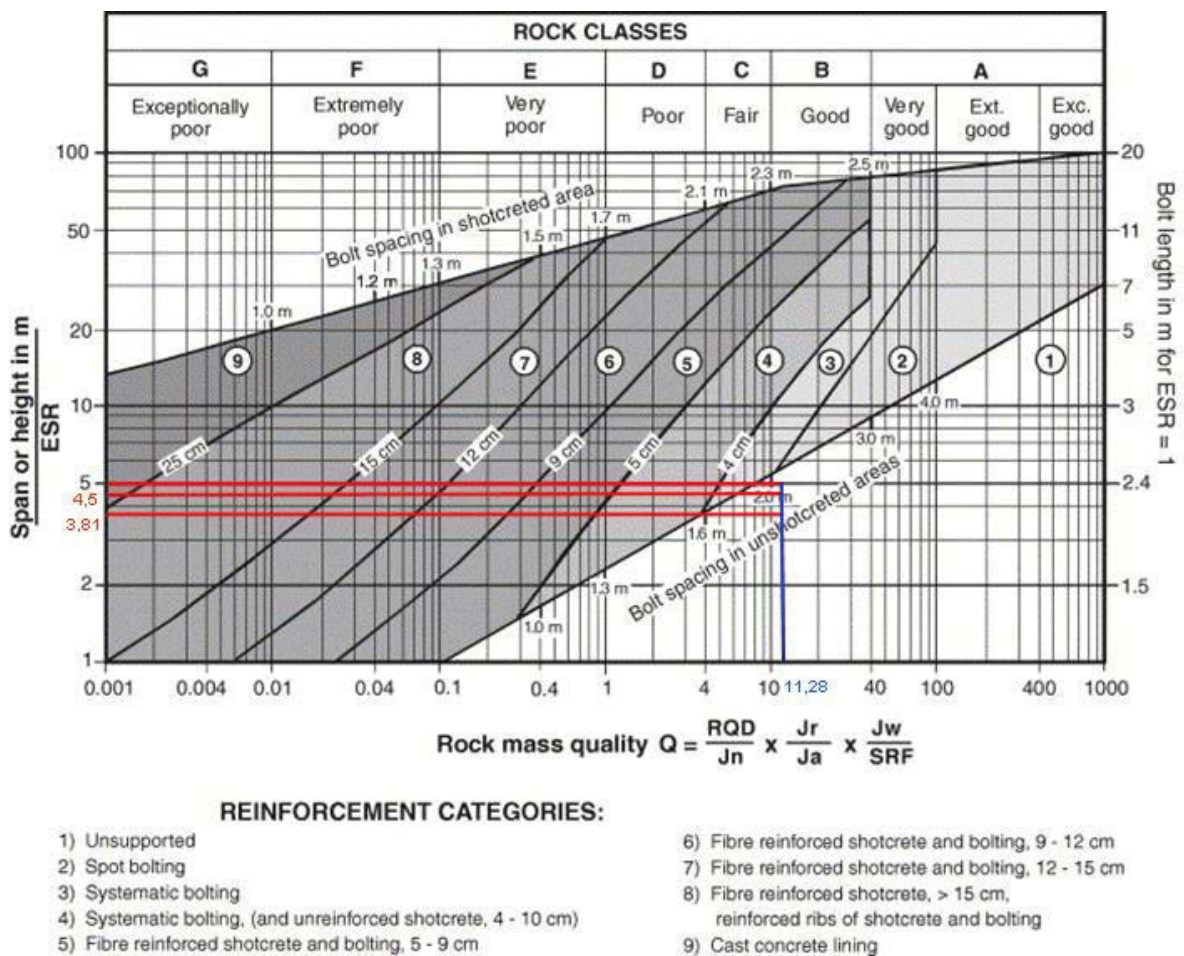


Figure 90: Diagram for support, Barton, current situation (cp. Løset 1997, p. 28)

Otherwise as the previous presented classification systems (see chapter 5.3.1 and 5.3.2), Barton classifies the results into classes of suggested support and not into classes of stability. As shown in Figure 90, the representative viewed areas for the current mining area are in the “unsupported” class.

5.3.3.2 Mathew (N – Stability Number)

Mathew's classification system uses Barton's Q-value (see chapter 5.3.3.1) as basis, modifies it and extends it with further parameter. Mathew's system describes the rock mass by:

$$N = Q' * A * B * C \quad \text{(Formula 18)}$$

N...	Stability number	[-]
Q'...	Modified NGI* rock mass rating	[-]
A	Rock stress factor	[-]
B...	Rock defect orientation factor	[-]
C	Design surface orientation factor	[-]

* NGI = Norwegian Geotechnical Institute

The modified NGI rock mass rating (Q') is determined by setting the stress reduction factor (SRF, see chapter 5.3.3.1) to 1. Since the SRF is set to one at the calculation of the original Q-value after Barton, it follows that $Q = Q'$

To assign the rock stress factor (A), the first step is put to planes of view into the inspected area. As an example a sketch for area 1 is shown in Figure 91.

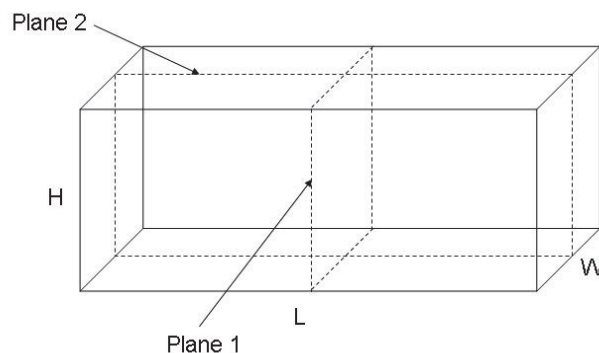


Figure 91: Planes for the rock stress factor (A), sketch, area 1

The second step is to determine the induced stresses (σ_i) parallel to the planes. In this case only the roof area is inspected. To gain the value for the induced stress (σ_i) the proposed diagram to estimate the induced stresses in hangingwalls is used (see Figure 92, cp. Stewart and Forsyth 1995, p 52)

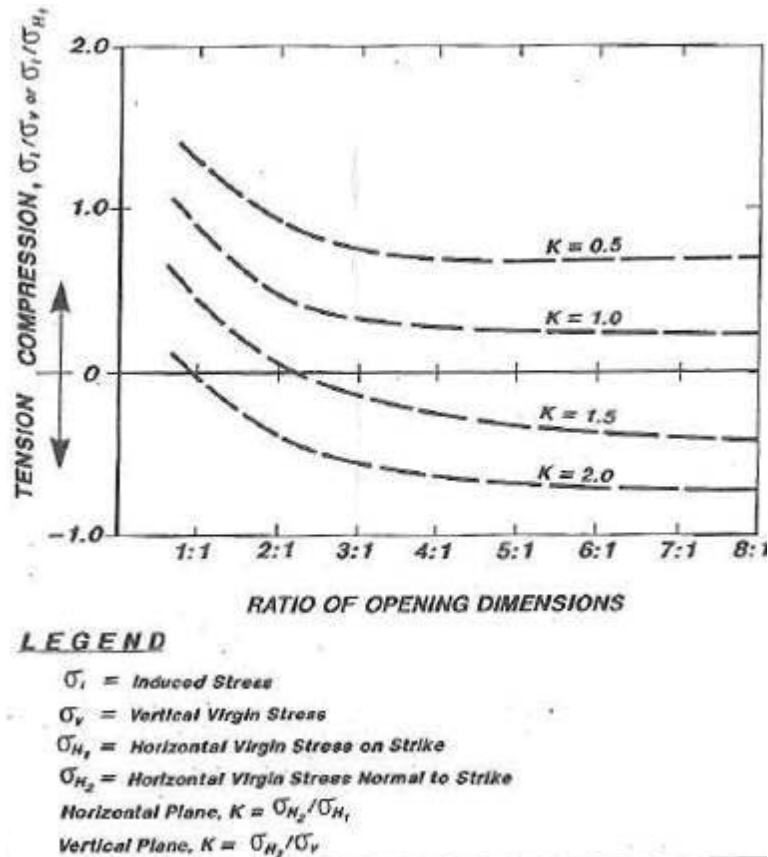


Figure 92: Diagram to estimate induced stresses in hangingwalls (cp. Stewart and Forsyth 1995, p 52)

To be able to use the in Figure 92 shown diagram the vertical and the horizontal stress, which are acting in the planes, have to be determined. Since there were no measurements concerning the virgin stress, it has to be estimated. The vertical stress (σ_v) is estimated with $\sim 1,2$ [MPa], which results for example for area 1 with an overburden of 45 [m] and a density of 2690 [kg/m³] (see Formula 19)

$$\sigma_v = g * \rho * H \quad (\text{Formula 19})$$

σ_v ...	Vertical stress	[Pa]
g ...	Gravitational acceleration	[m/s ²]
ρ ...	Density	[kg/m ³]
H ...	Thickness overburden	[m]

The ratio (K) of the average horizontal stress (σ_H) to the vertical stress (σ_v) is estimated as 1. Therefore the horizontal stress is equal to the vertical stress and is $\sigma_H = 1,2$ [MPa].

The ratio of opening dimension is the ratio of the side lengths of the set planes of views. From this it follows that for area 1, the ratio for plane 1 is the width of the viewed area (8

[m]) to the mining height (3,2 [m]) and results in 2,5 [-]. For plane 2 the length of the viewed area (20 [m]) and the mining height is determining the ratio of opening dimensions and results in 6,25 [-].

With this gained values the diagram for estimating the induced stress in the hangingwalls can be entered. A value for the term " σ_i / σ_v or σ_i / σ_H " of 0,4 (plane 1) and 0,25 (plane 2) is read out. With this value the estimated induced stress (σ_i) is calculated by transforming the ratio and the read out value for each plane. The calculated induced stress for plane 1 is $\sigma_{i,plane1} = 0,48$ [MPa] and for $\sigma_{i,plane2} = 0,30$.

To determine the value of the rock stress factor (A) the above found induced stresses are used and entered into Figure 93 (cp Stewart and Forsyth 1995, p 50)

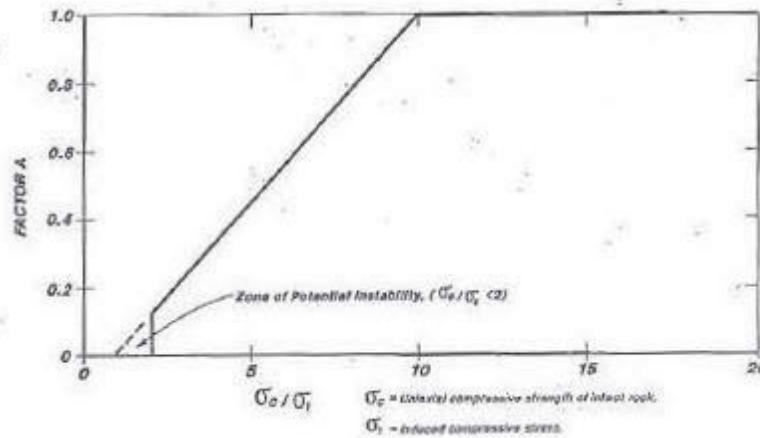


Figure 93: Rock stress factor (A), (cp. Stewart and Forsyth 1995, p 50)

On the x-axis the ratio of the uniaxial compressive strength (σ_c) to the induced stress is applied. The values for (A) for each plane are compared and the one with the greatest influence is taken into consideration. Since $\sigma_c = 200$ [MPa], the rock stress factor (A) is for each plane 1. An induced stress of > 20 [MPa] would be necessary to gain a decrease of factor (A).

To determine the rock defect orientation factor (B), Figure 94 is used (cp. Stewart and Forsyth 1995, p 50)

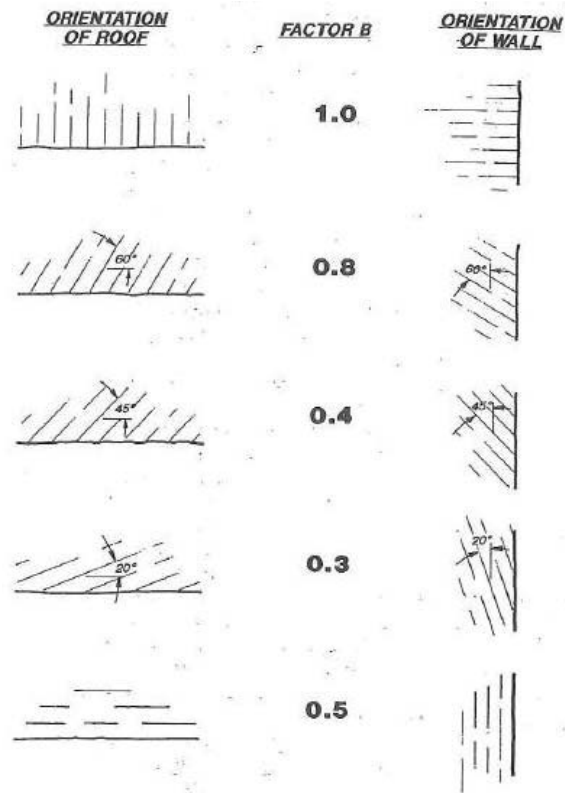


Figure 94: Rock defect orientation factor (B), (cp. Stewart and Forsyth 1995, p 50)

Since the layering is parallel to the viewed areas the factor (B) is set to 0,5.

For gaining the value for the design surface orientation factor (C) the in Figure 95 shown chart is used (cp. Stewart and Forsyth 1995, p 51).

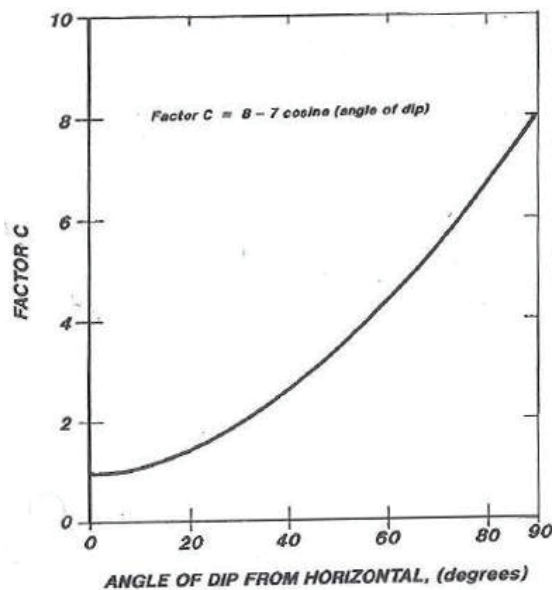


Figure 95: Design surface orientation factor (C), (cp. Stewart and Forsyth 1995, p 51)

The average dipping of the deposit is 16,5 [°] into approximately south direction, according to the from the company provided map. Therefore, value (C) is set to 1,3 [-] after Figure 95.

With this above determined values the stability number (N) is calculated. A summary with each area is shown in Table 25. For the calculation used constants are shown in Table 24.

ρ	density	2,69	[t/m ³]
g	grav. Acc.	9,81	[m/s ²]
K	ratio σ_H/σ_V	1,00	[-]

Table 24: Used constants for calculating the stability number (N)

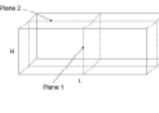

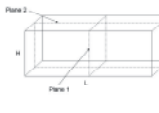
		Area 1		Area 2		Area 3		
								
H	thickness overburden	45		50		60		[m]
σ_V	vertical stress	1,19		1,32		1,58		[MPa]
$\sigma_{H1} = \sigma_{H2} = \sigma_H$	horizontal stress	1,19		1,32		1,58		[MPa]
W	width	8		6,1		7,2		[m]
L	length	20		30		20		[m]
H	height	3,2		3,2		3,2		[m]
		Plane 1	Plane 2	Plane 1	Plane 2	Plane 1	Plane 2	
L/H		-	6,25	9,38	-	-	6,25	[-]
W/H		2,5	-	-	1,91	2,25	-	[-]
σ_i/σ_V or σ_i/σ_H		0,4	0,25	0,25	0,6	0,5	0,25	[-]
σ_i	induced stress	0,48	0,33	0,33	0,79	0,79	0,4	[MPa]
σ_c/σ_i		421,05	673,68	606,32	252,63	252,63	505,26	[-]
A	rock stress factor	1	1	1	1	1	1	[-]
B	defect orient. factor	0,5	0,5	0,5	0,5	0,5	0,5	[-]
C	surface orient. factor	1,3	1,3	1,3	1,3	1,3	1,3	[-]
Q'	mod. rock mass rating	11,28	11,28	11,28	11,28	11,28	11,28	[-]
N	stability number	7,33		7,33		7,33		[-]

Table 25: Stability number, summary, current situation

With the determined stability numbers (N) and the hydraulic radius or shape factor of the viewed areas, the stability diagram of Mathew's can be entered. The diagram describes 4 zones which area also marked in Figure 96:

1. Potentially stable – surface should be essentially self supporting; local support or spot bolting may be required
2. Potentially unstable – surface should require some form of pattern support
3. Potential major collapse/failure – surface will require extensive and heavy support
4. Potential caving – surface probably unsupportable; will fail a continue to fail until the void is completely filled

(cp. Stewart and Forsyth 1995, p 48 f)

In Figure 96 the stability diagram by Mathew's is shown with the entered results.

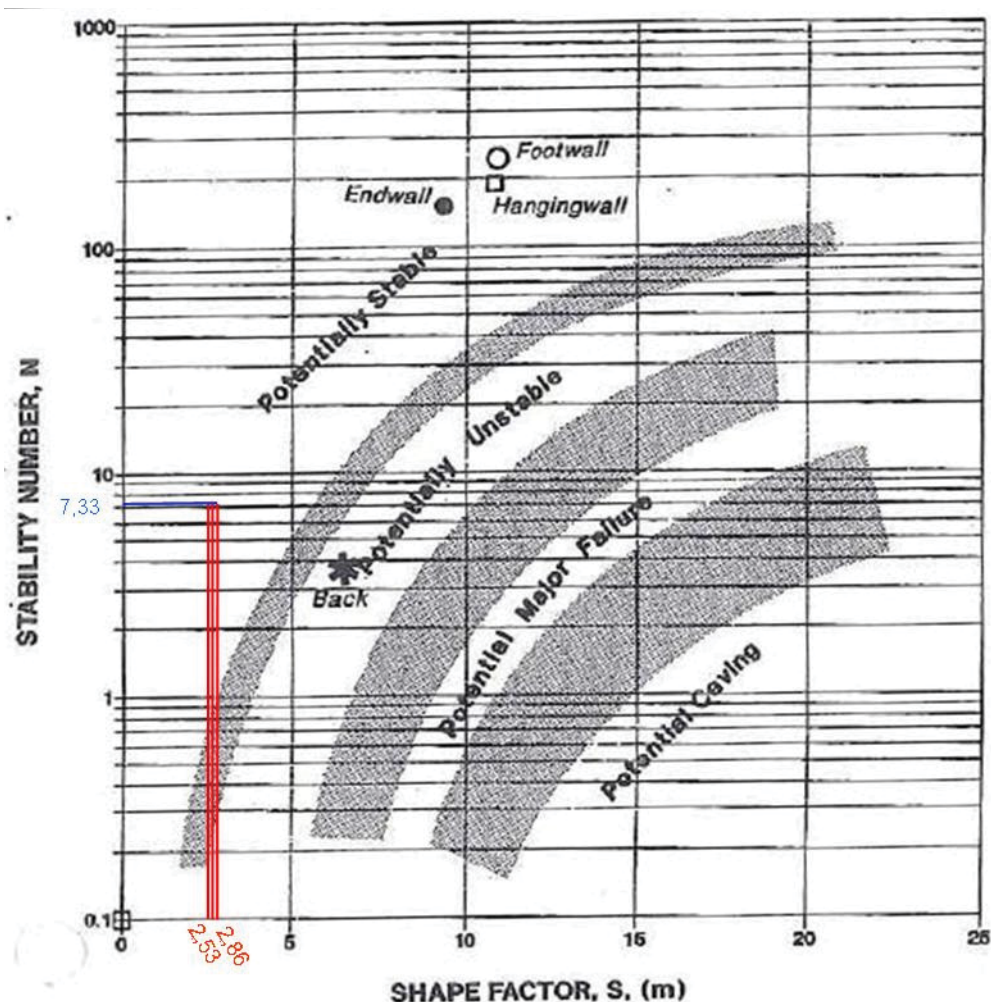


Figure 96: Stability diagram Mathew's, current situation (cp. Stewart and Forsyth 1995, p 49)

As shown in Figure 96 the viewed areas are, concerning the classification system after Mathew's, in the potentially stable area.

It has to be noted that the curves are derived of a set of data, which was mainly collected from open stoping mines and typically represents experience in steeply dipping ore bodies in strong rocks of medium to good quality. (cp. Stewart and Forsyth 1995, p 49)

5.3.4 Summary of the geomechanical classification systems

The results of the used classification systems on the viewed areas of the current mining situation are presented in Table 26. The viewed areas and their dimensions are shown in chapter 5.3.

Classification System	HSR	Stable
	Bienawski (RMR)	Stable
	Laubscher (MRMR)	Stable (local supported)
	Barton (Q-System)	Unstupported (Stable)
	Mathew's (N)	Potentially Stable

Table 26: Summary of classification systems

The in Table 26 presented results leads to the inference that the viewed areas are stable. However it has to be pointed out that the used classification systems are not fitting perfectly to the deposit of Mazy. Although with the use of the several classification systems the confidence of reaching a first statement concerning the stability of the roof increases. With further observations and measurements the confidence can be increased. Also remarkable is that except of Barton's Q-System the results show a margin concerning the unstable zones of the stability diagrams (e.g. see Figure 96, chapter 5.3.3.2).

5.3.5 Width of roof plate

According to the observation at the fieldwork, the limiting factor of the stability of the roof layers is the span width in combination with geological discontinuity, which cut through the roof plates and allow through the spacing, which are mainly filled with clayey material and/or are partly open, no transfer of forces. It follows that the only remaining abutment is responsible for the stability of roof plate.

Furthermore, tabular strata seems to separate under deflection of the other layers and each laminated beam transfers its own weight to the abutments (cp. Diederichs and Kaiser 1999, p.97).

Therefore the simplification to a cantilever beam with a uniformly distributed load (own weight, $q(x) = q_0 = \text{const.}$, see Figure 97) is used to gain a value how far a roof plate can overhang before anchoring is necessary to prevent a safety hazard.

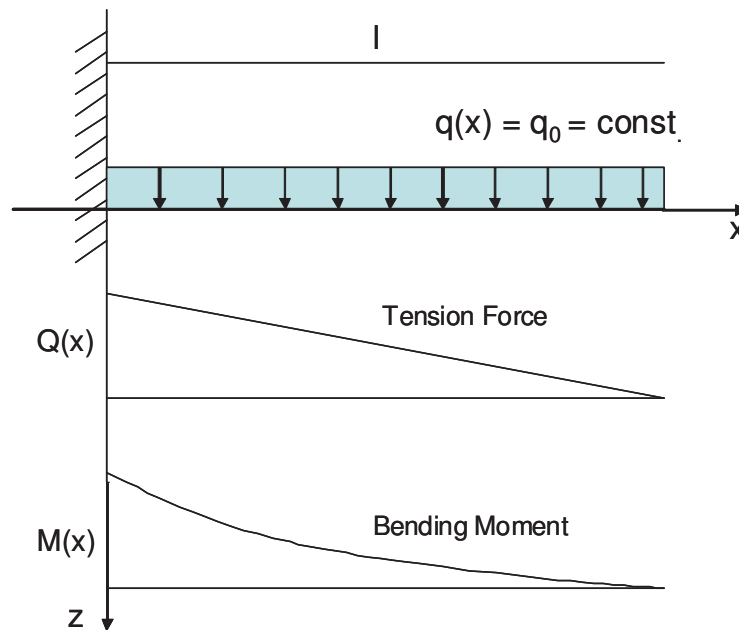


Figure 97: Cantilever beam, sketch

To determine a “maximum” width, the basic equation of the bending tension stress is used (see Formula 19).

$$\sigma_b = \frac{|M_y|}{W_y} \quad \text{(Formula 19)}$$

σ_b ...	Bending tension stress	[Pa]
$ M_y $...	Absolute bending moment	[Nm]
W_y ...	Moment of resistance	[m ³]

The beam is seen as double symmetric whereby following profile results (see Figure 98)

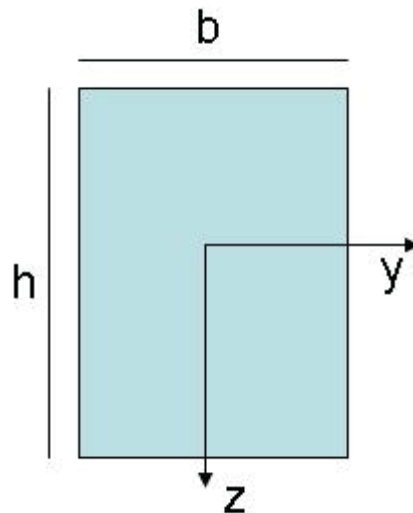


Figure 98: Cantilever profile, sketch

With the above shown profile (see Figure 98) in z-y-plane following moment of resistance (W_y) is defined:

$$W_y = \frac{b * h^2}{6} \quad \text{(Formula 20)}$$

W_y ...	Moment of resistance	[m ³]
b ...	Width of profile	[m]
h ...	Height of profile	[m]

The bending moment (M_y) is calculated by integrating the abutment force:

$$M(x) = \int Q(x) dx \quad (\text{Formula 21})$$

$M(x) \dots$	Bending Moment	[Nm]
$Q(x) \dots$	Abutment force	[N]

The abutment force is defined by:

$$Q(x) = -\int q(x) * dx \quad (\text{Formula 22})$$

$Q(x) \dots$	Abutment force	[N]
$q(x) \dots$	Line load	[N]

With the constraints that the abutment force and the bending moment is 0 at the end of the beam ($x=l$) the integration constants can be calculated and results in the final equation for the bending moment (see Formula 23)

$$M(x) = -q_0 * \left[\frac{x^2}{2} - l * x + \frac{l^2}{2} \right] \quad (\text{Formula 23})$$

$M(x) \dots$	Bending moment	[Nm]
$q_0 \dots$	Uniformly distributed load	[N/m]
$l \dots$	Width of beam	[m]

The maximum bending moment is at the abutment of the cantilever beam ($x=0$, see Figure 97) and it follows that the absolute maximum bending moment is:

$$|M(x=0)_{\max}| = q_0 * \left[\frac{l^2}{2} \right] \quad (\text{Formula 24})$$

$ M(x) \dots$	Absolute bending moment	[Nm]
$q_0 \dots$	Uniformly distributed load	[N/m]
$l \dots$	Width of beam	[m]

The above defined elements (Formula 20 and 24) are applied to the bending tension stress (Formula 19) and transformed to the length (l_{\max}) of the beam (see Formula 25).

$$l_{\max} = \sqrt{\frac{\sigma_b * b * h^2}{3 * q_0}} \quad (\text{Formula 25})$$

$l_{\max}...$	Maximum width of beam	[m]
$\sigma_b...$	Bending stress	[Pa]
$b...$	Width of profile	[m]
$h...$	Height of profile	[m]
$q_0...$	Uniformly distributed load	[N/m]

To gain the maximum span width the uniformity distributed load (q_0) is calculated after:

$$q_0 = \frac{V * \rho * g}{l} \quad (\text{Formula 26})$$

$q_0...$	Uniformly distributed load	[N/m]
$V...$	Volume	[m ³]
$\rho...$	Density	[kg/m ³]
$g...$	Gravitational acceleration	[m/s ²]
$l...$	Length	[m]

For calculation a beam with a width of 1 [m] is taken. The height is the thickness of the roof layer, which is stated at the geological profile, provided from the company side, with an value of 0,38 [m]. The density (ρ) is 2690 [kg/m³] which was determined at the laboratory tests for the uniaxial compressive strength (see chapter 5.1.1). Therefore an uniformity distributed load (q_0) is calculated by setting the values into Formula 26:

$$q_0 = \frac{1 * 0,38 * 1 * 2690 * 9,81}{1} \quad [\text{N/m}]$$

$$q_0 = 10027,8 \quad [\text{N/m}]$$

The by the laboratory tests determined value for the bending tension strength (σ_b) = 30,89 [MPa] (see chapter 5.1.2). This figure is reduced by a global factor of safety (γ) of 2. This is done since the geometrical arrangement (e.g. sharp edges) has not been taken into consideration. Furthermore the laboratory tests were determined from the material of the extracted layers. The assumption has been taken that, based on the observation of the fieldwork, the material properties of the roof layer (BB) is similar to the extracted layers (F, E, D, C, U and blasted layer). In addition, the provided basis sample of the roof layer had not the dimensions, in volume and side lengths, to receive valid results of the bending tension strength tests. The laboratory tests describe only a small sector of the rock, compared to the dimensions of the roof layer in the mine. The bigger the viewed sector, the bigger is the probability that an element of weakness (e.g. inclusion) is lowering the strength. These uncertainties are encountered with the global factor of safety. Therefore the for the valid length (l_{valid}) used bending tension strength is:

$$\sigma_{b,valid} = \frac{\sigma_b}{\gamma} = 15,4 \quad [MPa] \quad \text{(Formula 27)}$$

$\sigma_{b,valid}...$	Reduced bending tension strength	[MPa]
$\sigma_b...$	Bending tension strength	[MPa]
$\gamma...$	Global factor of safety	[-]

With the above determined values, the valid length is calculated and results in:

$$l_{valid} = \sqrt{\frac{\sigma_{b,valid} * b * h^2}{3 * q_0}} = 8,6 \quad [m] \quad \text{(Formula 28)}$$

$l_{valid}...$	Valid width of beam	[m]
$\sigma_{b,valid}...$	Reduced bending tension strength	[Pa]
$b...$	Width of profile	[m]
$h...$	Height of profile	[m]
$q_0...$	Uniformly distributed load	[N/m]

The calculation above shows that, after the approach of the simplification of a cantilever beam, the maximum length of a roof plate, applied to the first roof layer (BB), is roughly 8 [m] and therefore gives a first estimation for the unsupported span width. If the span width exceeds, the probability is given that through appearance of discontinuities near the 2nd abutment (pillar), a one side fixed roof plate arises (similar to a cantilever beam) with

greater length than 8 [m]. This results, that the factor of safety is smaller 1 [-] and the probability of failure increases.

At this stage it has to be noted that the gained result is based on a simplification. No clamping through horizontal or induced stresses was taken into consideration. Furthermore the influence of the above mentioned uncertainties, which are encountered with the global factor of safety, is undefined. However this value presents a first estimation and a further parameter for defining the span width of the future mining areas. With detailed stress measurements and case studies the value could be recalculated and occupied with greater significance.

With the above presented calculation the effect of increasing the stability by connecting a second roof layer (AC) to the first one (BB) can be shown, for example by anchoring. The addition of the thickness of the first two layers give 0,89 [m] (BB = 0,38 [m]; AC = 0,46 [m] as well as a bedding layer between of 0,05 [m]). If this value is entered (Formula 28) a valid length of 13,2 [m] results. If the bending tension strength (see Formula 19) with the valid length of the first roof layer (BB) is compared to the bending tension strength with the valid length of the combined first two roof layers (BB+AC) by the classical approach of the factor of safety (see Formula 29), an additional factor of safety of 4,7 [-] is achieved.

$$FOS = \frac{\sigma_{b,valid}(13,2)}{\sigma_{b,valid}(8,6)} = 4,7 \quad [-] \quad \text{(Formula 29)}$$

5.4 Strength of the geological discontinuities

The geological discontinuities, which are filled with clayey and sandy material and are partly open, have the greatest influence on the stability of the roof and the pillars. The thickness of the joints and faults are between 1 and up to 20 [cm]. An example is shown in Figure 99.



Figure 99: Example partly open and filled joint, pillar 3, photo nr.: 1413

According to literature, the residual cohesion (c') of clayey material is 0 – 0,003 [MPa] and the residual friction angle (φ) is between 10,5 to 16 [°] (cp. Hoek 2007, chapter 4, p.11).

The above mentioned values lead to the conclusion that the geological discontinuities, which are filled, lead to a significant decrease of the stability, since no forces or stresses can be assimilated or transferred.

6 Possible future mining areas

The second major topic, besides describing the geomechanical status of the current mining operation (chapter 4 - 5), is the search and the outlay of possible future mining areas.

Besides the type of deposit (see chapter 4.1, Figure 8 and chapter 4.2) and the external influences (see chapter 4.3.4) new possible mining areas arise near the current mining operation. Therefore each possibility will be shown and described. All 4 cardinal points are reviewed as well as the lower levels of the current mining area (see chapter 6.2 - 6.6). According to the company the yearly amount of extraction should be increased. This shall be achieved by changing the extraction method from blasting and cutting to exclusive cutting. Therefore a chain saw cutting machine, in combination with a bigger wheel loader, should be acquired. The planned machinery is presented and discussed in chapter 6.1.

6.1 Planned deployed machinery

To achieve an increase of production a chain saw cutting machine should be acquired. The company provided plans for two models offered by the company “fantini sud”. The first model is declared as “GU70-3-R” and the second as “GU50 SC”. In the following figures (see Figure 100 - Figure 102) the AutoCAD plans of the first model are presented. An enlargement and additional plans are added on the data CD.

All mining layouts for the future mining area are respecting the presented and from the company preferred machines (“GU70-3-R” and exemplary “Volvo L220 F”).

The in Figure 100 presented sketch of the cutting machine GU70-3-R shows the machine at the folded up configuration and the dimensions while driving.

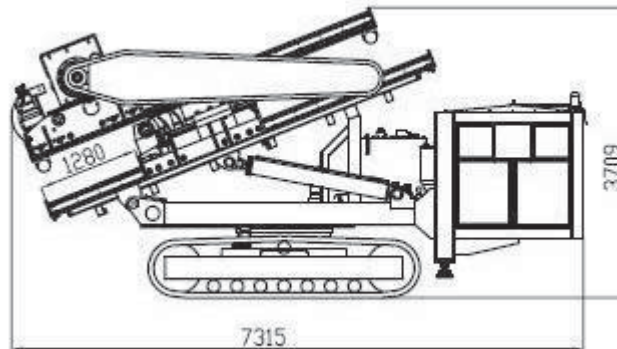


Figure 100: GU70-3-R, sketch at driving position

In Figure 101 the dimensions and the configuration of the machine before cutting is presented.

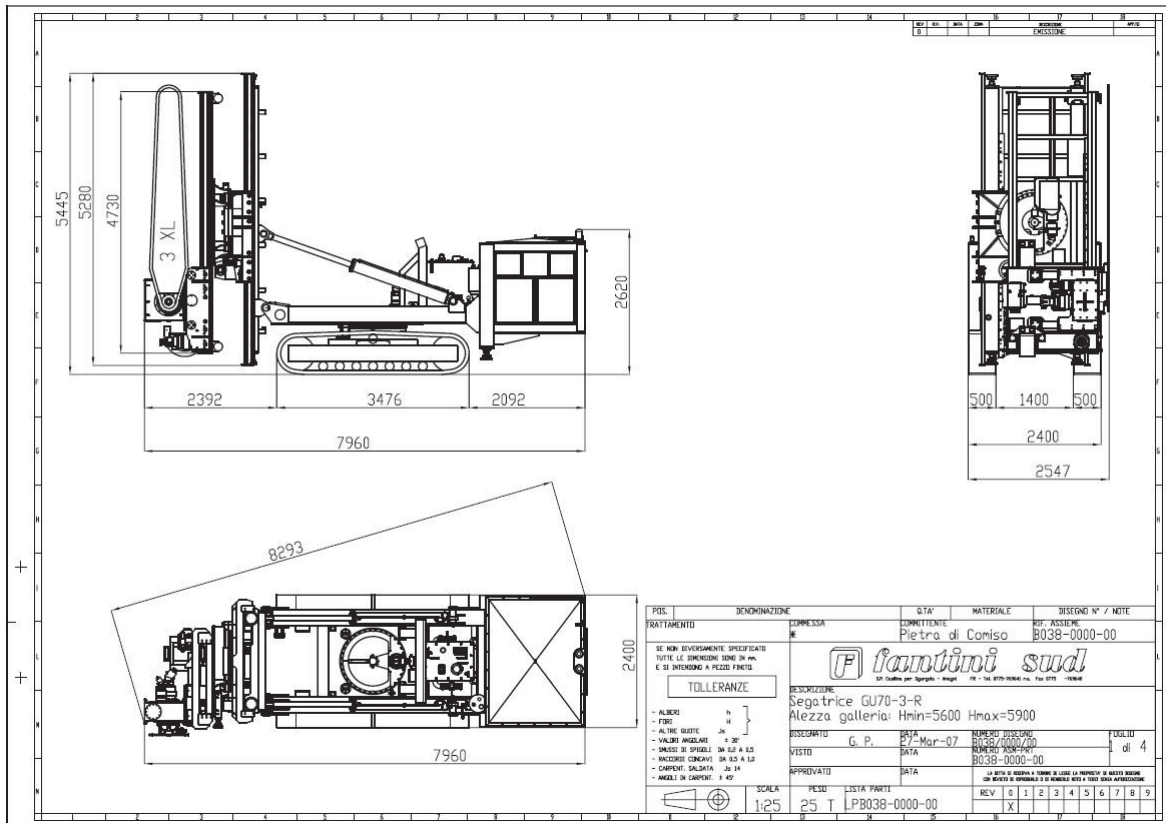


Figure 101: GU70-3-R, sketch at cutting position

Figure 102 presents the basic phases of cutting.

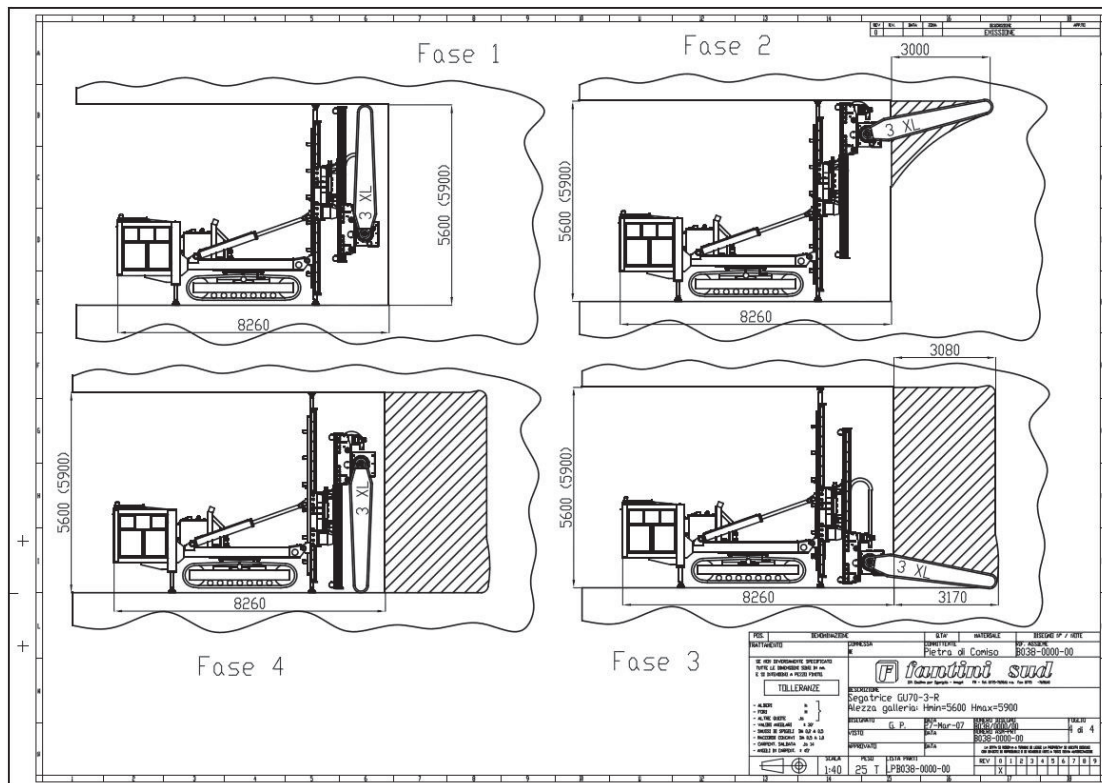


Figure 102: GU70-3-R, sketch of cutting phases

To achieve stability while cutting, the machine is clamped with hydraulic props, mounted at the booms, between the roof and the floor. Therefore it follows that a minimum room height of 5,6 [m] is necessary before the machine can start to cut. The first stage of the working cycle is the vertical cut as shown in Figure 102. Subsequent the horizontal cut is done. When the first extraction/cutting on a new face is done and no sideways area is available for undercutting, the cut blocks are removed from the ribside by using a diamond rope saw. The accruing dimension stone blocks are removed with the wheel loader.

As shown in the figures above following constraints and dimensions occur for the planning of the new mining areas:

- Cutting depth: 3,17 [m]
- Moving configuration:
 - Length = 7,3 [m]
 - Width = 2,6 [m]
 - Height = 3,7 [m]
- Cutting configuration:
 - Length = 8,3 [m]
 - Width = 2,6 [m]
 - Height = 5,6 – 5,9 [m]

The maximum working angle of the cutting machine is according to the company 17 [°] (see Figure 103). Although the working angle is presented by the model “GU70 R-XC” the results are applicable for the “GU70-3-R”, which is the basis for the defining dimensions.

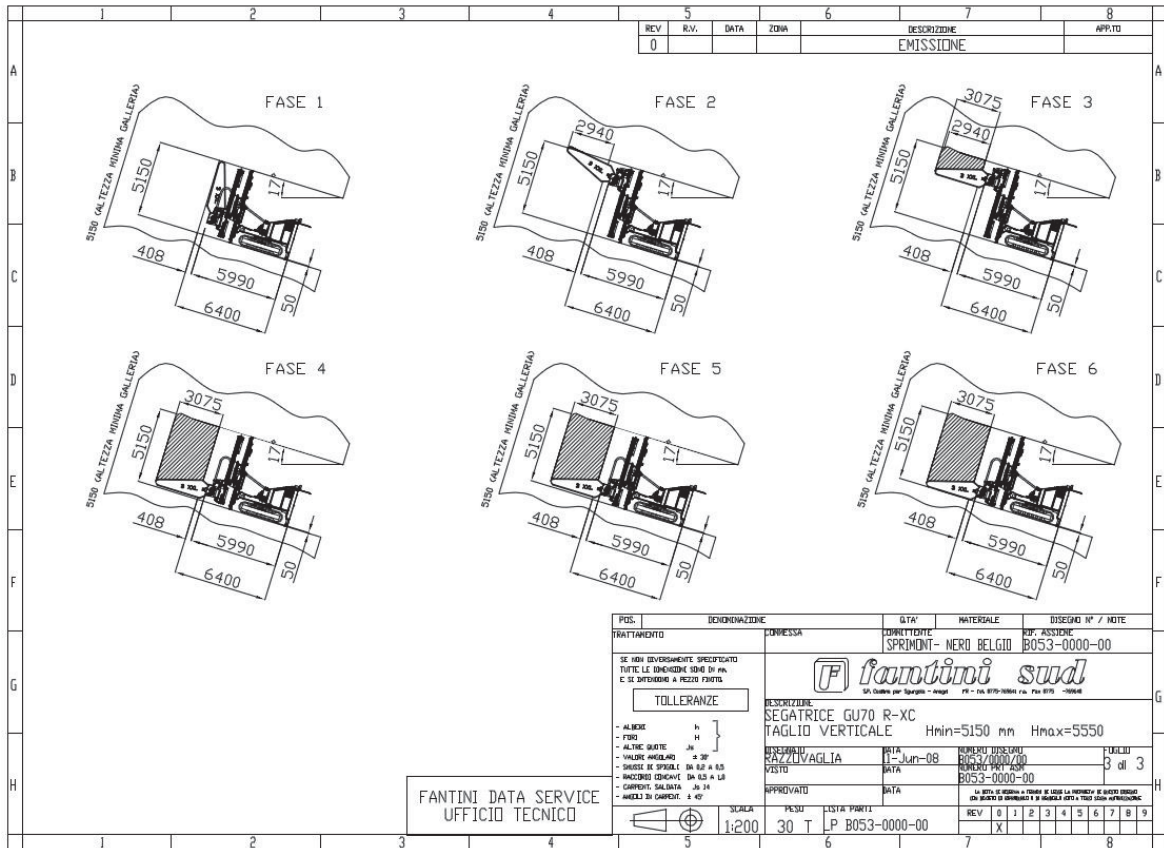


Figure 103: GU70 R-XC, working angle

After the statement of the company a wheel loader similar to the size of a Volvo L220 F is a possible option of acquisition for the extraction after cutting and for transportation of the material to the processing. According to the data sheet from Volvo, the wheel loader has following dimensions and constraints with a standard boom and a rock bucket (see Table 27, cp. Figure 104):

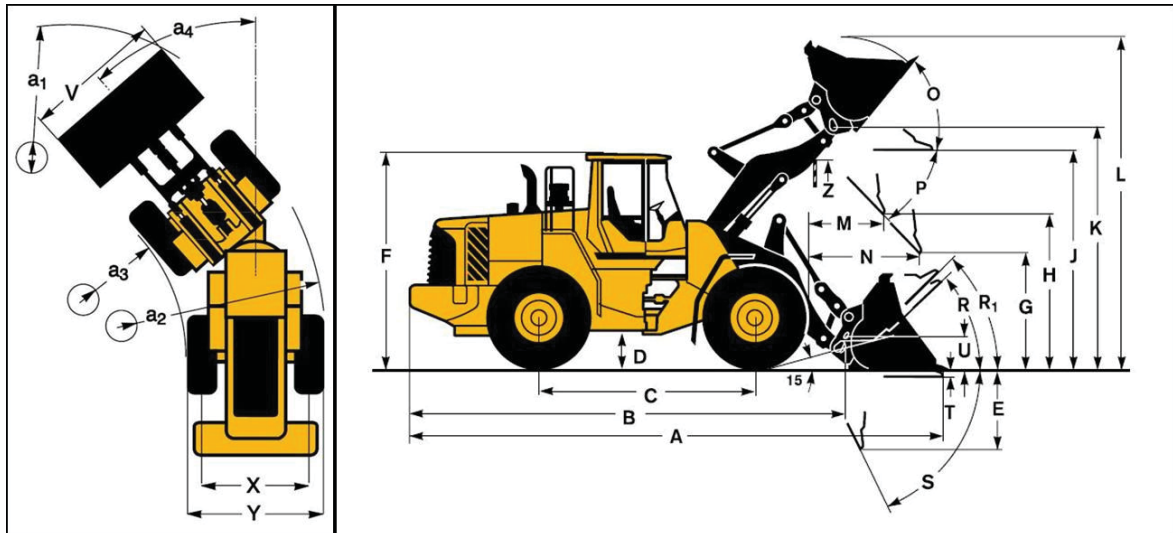


Figure 104: Volvo L220 F, sketch and naming of dimensions (cp. Volvo 2007, p. 30)

Length (A)	9,6	[m]
Width (Y)	3,2	[m]
Bucket width (V)	3,4	[m]
Height (F)	3,7	[m]
Clearance cycle (a1)	15,8	[m]
Interior radius (a3)	3,9	[m]
Static tipping load	23,4	[t]
Tipping load at full turn (37°)	20,5	[t]
Operating weight	32	[t]
Installed machine power	355	[HP]

Table 27: Volvo L220 F, dimensions (cp. Volvo 2007, p 24 – 33)

The presented and planned machinery are a guideline from the company and are considered in the further layout of the possible future mining areas.

At this point it has to be mentioned that the maximum height which the bucket can enter the cut blocks parallel to the floor of this machine is $J = 4,26$ [m] (cp. Volvo 2007, p. 30). If the maximum possible height is mined which the cutting machine can achieve (5,9 [m]), a height of the first block to lift results in 1,64 [m]. With a cutting depth of 3 [m], a width of the bucket of 3,4 [m] and a density of 2,69 [m³], a weight for the first block, according to

the roof, of around 45 [t] has to be lifted. The maximum load which “should” be lifted (nominal load) is defined as:

$$Load_{nominal} = \frac{Load_{Tipping(37^\circ)}}{2} \quad \text{(Formula 30)}$$

Load_{nominal} Nominal load [t]

Load_{Tipping(37°)} Tipping load at full turn [t]

(cp. Eymer 2006, p.66)

The nominal load results in ~ 10 [t]. One solution is to lower the width of the cut blocks and using instead of a bucket, a fork. Another option is to mount a winch onto the boom and pull the first blocks, according to the roof, onto the fork. Furthermore a rapid change system for changing between the bucket and fork would be useful.

Furthermore it is uncertain if the wheel loader is suitable for the inclinations. A request directed to Volvo to solve this question, remains unanswered. In any case these two above mentioned questions/tasks have to be solved e.g. by testing, before an acquisition is done.

With the above presented machinery, following maximum dimensions or constraints results, which are influencing the outlay of possible future mining areas (see Table 28).

Turnradius	inside	R _i	4	[m]
	outside	R _o	8	[m]
Width maximum		W _{max}	3,2	[m]
Height maximum machinery		H _{mmax}	3,7	[m]
Heigth cutting	minimum	H _{cut,min}	5,6	[m]
	maximum	H _{cut,max}	5,9	[m]

Table 28: Final dimensions, planned machinery

In consultation with the company a planed extraction height of 5,9 [m] was defined.

Additionally a sketch of the second model of the cutting machine (GU50 SC) and its dimensions is attached at this point (see Figure 105). This model is not taken into further consideration but has been added to round up the presentation of the possible planned machinery.

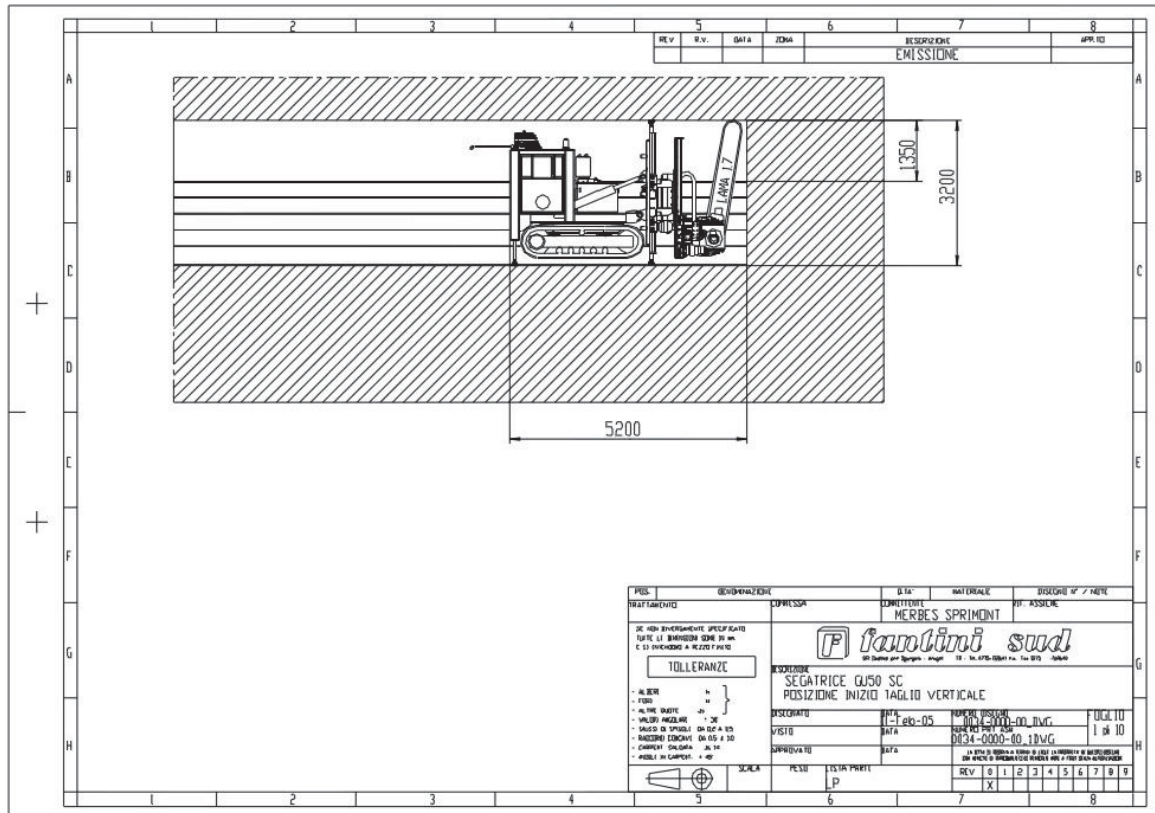


Figure 105: GU50 SC, sketch at working configuration

6.2 Lower Levels

The first area which is pointed out as a possible future mining area is the lower levels of the current mining area. The deposit is structured from layer “blasted” to layer “T” and results in ~ 12 [m] thickness. A detailed listing of the layers and their thickness is described in chapter 4.2.1. To gain accessibility of the planned machinery (see chapter 6.1), floor layers have to be removed. In consultation with the company a resulting roof height of 5 [m] is the target to ensure a safe accessibility of the machinery. Therefore the layers “G” to “M” have to be removed to get the declared height. The sketch of the alignment of the access is shown in Figure 106.

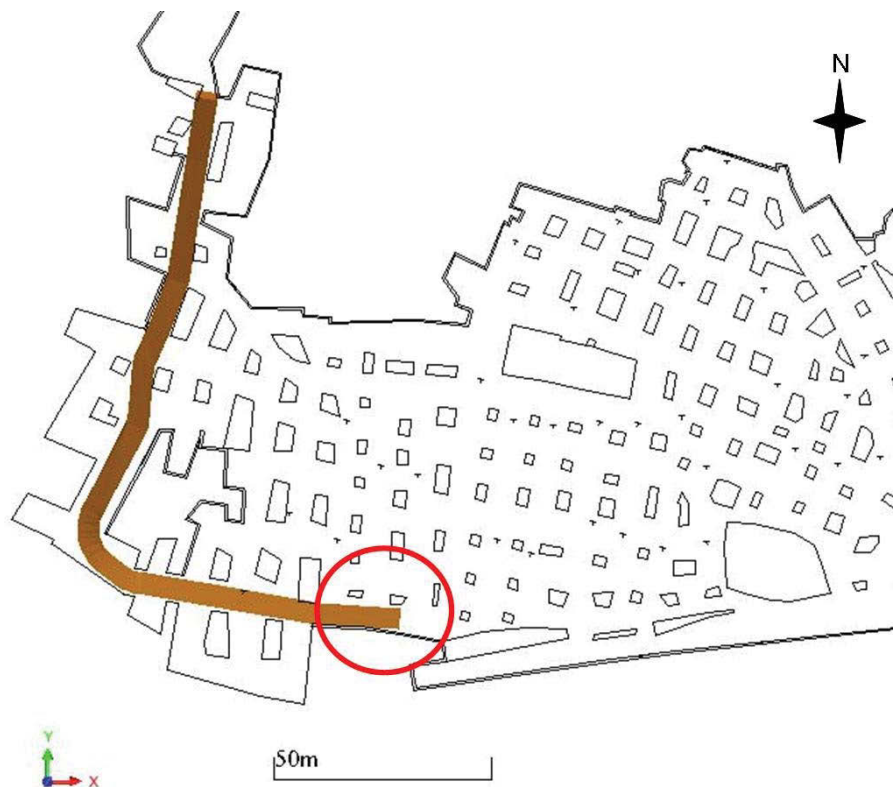


Figure 106: Alignment of the access (brown) to the lower levels within the existing mining area, sketch, Surpac

The in Figure 106 marked red circle presents a possibility, where the access plunge into the lower levels to gain access to it and mine the lower ~ 6 [m] of the deposit. This would lead to a residual rib pillar of 2,6 [m] between the current mining area and the lower levels. The undermining of the access must not be done, since with the removed layers of the access and the mining height, the layer “Ma”, with a thickness of 0,8 [m], would remain. Furthermore a barrier pillar should remain in the lower levels, between the access and the mining front. In consultation with the company a detailed investigation of the alignment,

the outlay and the possible amount was canceled, since the company wants to preserve the material for future investigations.

It has to be noted at that point, that if in future, an extraction of the lower levels is considered, a special focus has to be put on the alignment of the stopes in the lower levels. Since the arrangement of the pillars in the current mining area are irregular and uncertain in the backfilled areas at the center, the danger of undermining a pillar of the current mining area is high. This would create a hazard concerning the stability of the mine. The named risk has to be evaluated with a detailed investigation.

6.3 Area East

The possible future mining area in the east is locked since the water collection and catch is situated there. The location of the areas is shown in chapter 4.3.4.1, Figure 53. The water collection has an economical importance for the company and therefore it is no option to terminate or disturb it. The possibility of a redirection of the water flow through discontinuities, by mining the lower levels, leads to the conclusion that a further investigation into the east for possible future mining areas is not to be done within this master thesis.

6.4 Area West

As described in chapter 4.3.4.2 a development into the west of the current mining area, by extracting the lower levels (as well as for the current mining area), must not be done, since the location of the abandoned mine is uncertain. Before any investigations for an extend into the west is useful, certainty of the location and position of the old mine has to be given by, for example, core drilling. The fact that the old mining area is closed and a visit is not possible, underlines the need of further investigations into this direction.

6.5 Area South

Area South is, at the current point of few, a possible option for a future mining area. The assumption has been taken that the deposit is homogeneous expanding into the south. The border of the expansion is given by the major fault “south” (see chapter 4.2.2.1). The existence is affirmed by the company, however there is no proven data about the exact alignment, dip and dip direction. The alignment of the southern fault has been taken from the provided map and 90 [°] has been assumed as dip. The thickness of the deposit has been derived by the geological profile, which has been measured in the current mining area and the connection passage (see chapter 4.2.1) and results in a thickness of ~ 12 [m]. The basis of the deposit of the future mining area south has been designed in Surpac (see Figure 107).

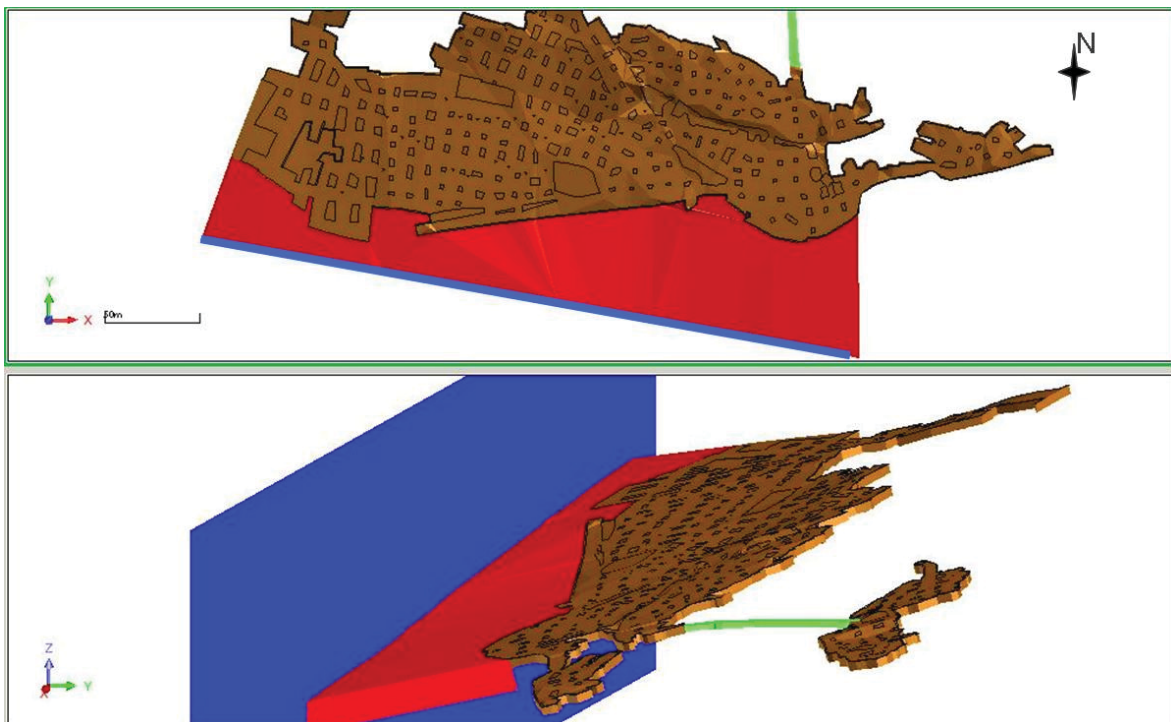


Figure 107: Future mining area south, basis, Surpac

In Figure 107 the expansion (red body) of the current mining area (brown body) into the south is presented. The expansion has a thickness of 12 [m] and is cut by the major fault south (blue line/area).

The expansion has been designed by following the alignment of the roof area of the designed current mine (see chapter 4.3.2). This receipt area was copied down by a y – value of +3,38 [m] and z – value of -11,45 [m]. This results by using the total thickness of 11,95 [m] and the average dipping of 16,5 [°] into south.

The gained areas are cut by the designed fault and joined. The overburden has a thickness (roof of deposit – surface) from 62 to ~88 [m], based on the above presented basis of the deposit.

This basis is used for the further investigations and designing the detailed outlay of the future mining area south (see chapter 7).

6.6 Area North

The first area into the northern direction, which was viewed as a possible new mining area, is presented in Figure 108 (green area).

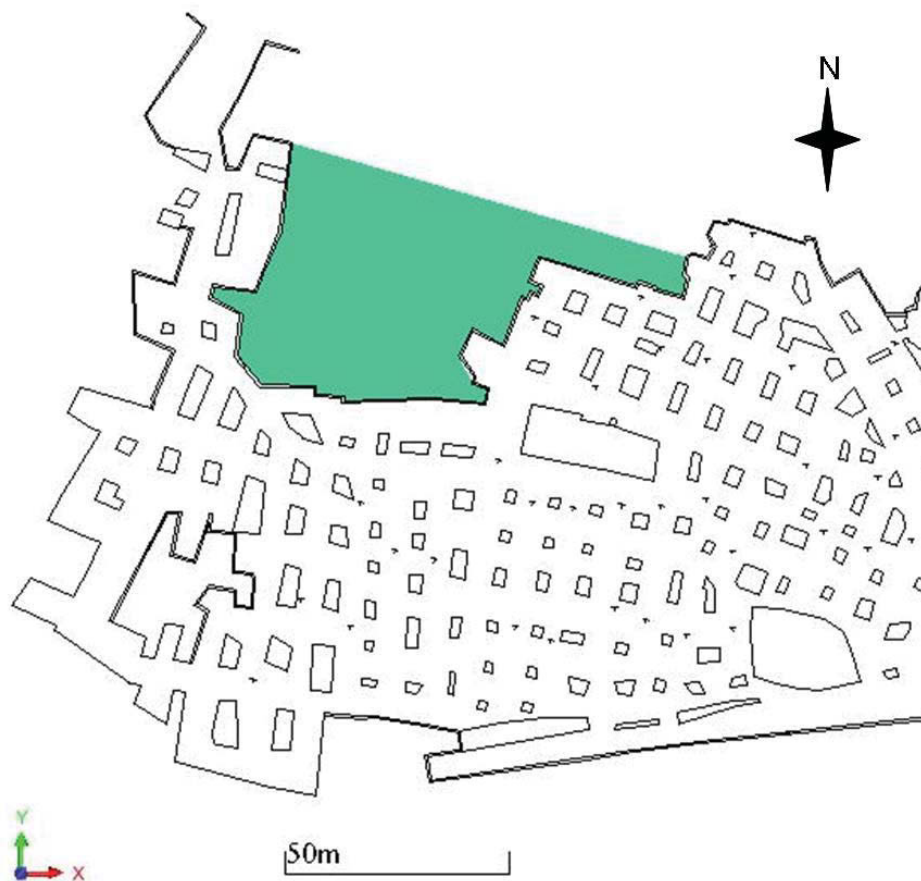


Figure 108: Future mining area north, current situation, Surpac

The in Figure 108 presented area was considered as expansion of the current mining level and mining method. According to the statement of the company the quality of the material is low and not worth to mine. Therefore a further investigation in the outlay and most notably, in the effect on the current mining area by increasing the panel width (see chapter 5.2.3) was not done.

The second possible future mining area into the north is beyond the major fault “17m”. It is assumed, as in the south, that the deposit follows the alignment of the north field of the current mining area and is limited by the major fault “17m”. A further fault, which influences the expansion of the north field, is not known at the moment. A confirmation of the northern deposit is given by the geophysical investigations (see chapter 4.2.3). In

Figure 109 the position of the basis of the northern possible future mining area, beyond the major fault “17m”, is presented.

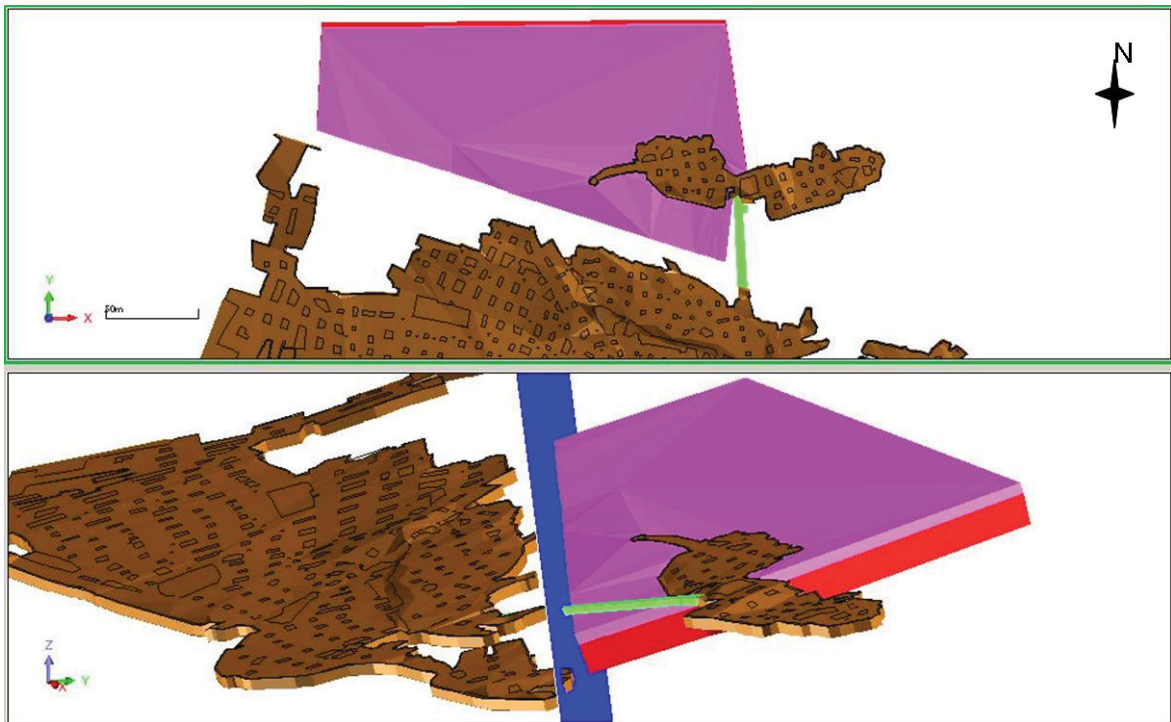


Figure 109: Future mining area north, basis, Surpac

The in Figure 109 presented expansion is separated in two layers. The first layer (pink) represents the current mined thickness (3,2 [m]) and the second layer (red) represents the difference to the total thickness of the deposit of ~ 12 [m]. The thickness of the deposit has been derived by the geological profile, which has been measured in the current mining area and the connection passage (see chapter 4.2.1). The procedure to gain the basis is similar to the one at the south field (see chapter 6.5), except that the alignment is based on the roof of the field north of the current mining area and the average dipping is 14,5 [°]. The overburden has a thickness (roof of deposit – surface) between 16,5 and 61,4 [m] based on the above presented basis of the future mining area.

This above mentioned future mining area is the basis for further investigations, concerning outlay. The detailed view of the future mining area north is presented in chapter 8.

6.7 Basic access

The basic alignment of the access to the future mining area south (and north) was defined during the first intermediate presentation with the company. To ensure safe working conditions the height and the width of the moving routes of the machinery was set to 5 [m]. This height should be achieved by removing the floor layers. Removing the roof layers is no option since a weakening of the whole roof would occur. In Figure 110 the basic alignment is presented.

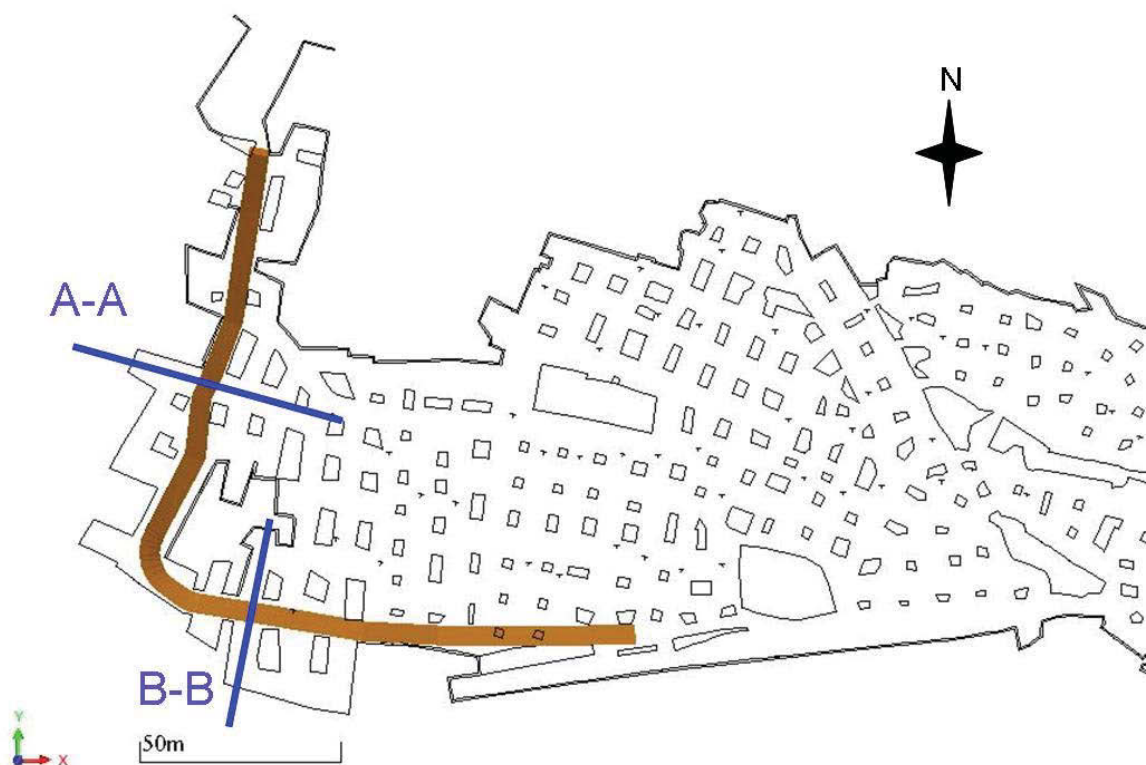


Figure 110: Basic alignment of access, Surpac

The in the figure above blue marked cuts (A-A and B-B) will be presented below. The access is achieved by the current entrance. The enlargement and the support at the entrance are done by an external company. The height of the entrance will be 5 [m].

As already mentioned, the height of the rest of the access will be achieved by removing the floor layers which are, according to the geological profile (see chapter 4.2.1), layer “G” to layer “M” and result in 5,09 [m]. In Figure 111 below, the cut of the access which follows nearly the north – south direction is presented by a sketch.

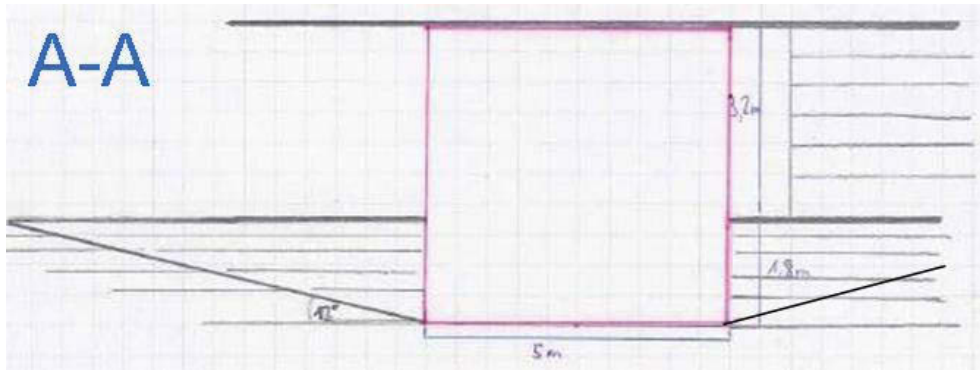


Figure 111: Cut A-A, access, sketch

Additional to the removal of the layers ramps have to be made to ensure the accessibility to the higher levels of the current mining area.

The curve radius where the access turns from north – south to east – west is 10 [m] related to the center line of the access.

In Figure 112 the cut B-B is shown, which represents a sketch of the profile along the east – west direction.

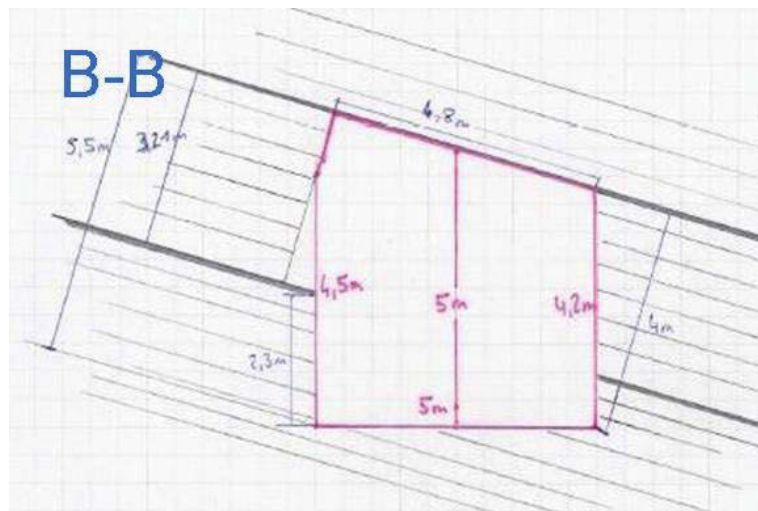


Figure 112: Cut B-B, access, sketch

The floor of the access into the west direction should remain horizontal, to reduce forces acting on the machinery caused by the inclination. Furthermore the safe transportation of the blocks is improved. The reduction of the height of the profile at the sides is to decrease the necessary span width of the roof to implement the profile. At this point it has to be mentioned that this profile is theoretical. The final exact geometry is depending on the real room width at the current mining area. According to the distances of the room widths, read out in Surpac, the smallest horizontal distance between pillar and ribsides is 5 [m] and therefore the above presented profile (see Figure 112) is applicable.

7 South field

In this chapter the detailed investigations concerning the stability and the outlay of the possible future mining area south is presented. The basis of the deposit south is presented in chapter 6.5. The company stated that the outlay should be done for the whole thickness of the deposit (~12 [m]). The general mining method should remain as room and pillar mining where the rooms are done exclusive with the cutting machine, presented in chapter 6.1.

In the following the alignment of the access to the future mining area will be shown. Furthermore the dimensioning of the roof, global and local (support), will be presented. With these information's the size of the pillars is set up. Additional to the final outlay, different variants with changing mining heights will be compared by the extraction rate and the possible volume.

It has to be noted at this place that the position of the major fault "south" is uncertain and therefore the whole outlay of the south field is based on the assumption that the alignment of the fault is situated as shown in the provided maps with a dip of 90 [°]. However if the position of the major fault south is assigned a recalibration is necessary to ensure an increase of certainty of the assumed outlay.

Before the detailed investigations and outlay are presented in the chapters below, a plan view out of Surpac, which represents the results is shown in Figure 113. This anticipation is done to improve the understanding within the following chapters.

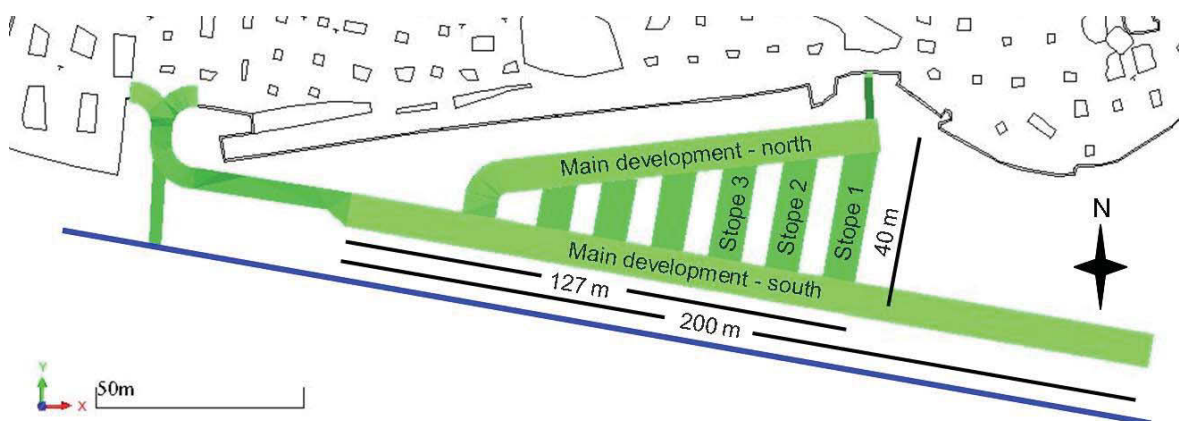


Figure 113: Anticipated result, south field, plan view, Surpac

The marked blue line in the figure above represents the major fault south. Additional to the plan view the side view of the theoretical profile is shown in Figure 114.

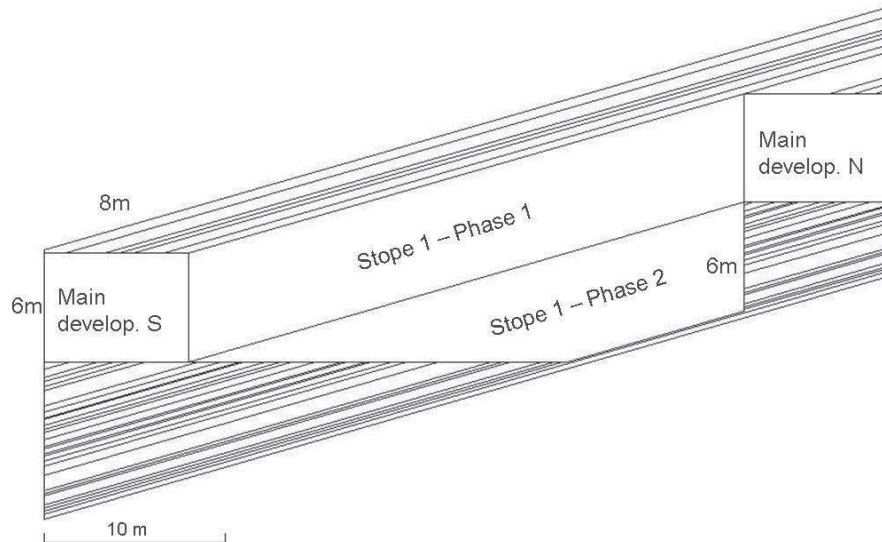


Figure 114: Profile, side view, south

The profile and the super ordinate mining sequence were derived during the intermediate presentations. After mining the main developments in the first step, the first 6 [m] are mined of the deposit and in a second step the remaining material is extracted in the above presented manner. This profile results of following reasons:

1. To prevent a room height of 12 [m] within the main developments north and south (long term safety)
2. To have the opportunity for selective extraction, since the saleable amount of the lower 6 [m] (Phase 2) is uncertain
3. To achieve a “upwards” mining direction within the stopes (from main development south to main development north)
4. The duration of working in 12 [m] high rooms is reduced
5. To increase the reach ability of the roof at the main developments to control the support
6. To ensure a natural water outflow at stope 1, phase 2 (into the main development south)

At this point, the other checked and discussed mining methods and basic outlays are mentioned. Once, overhand cut and fill, which was excluded after emergence of the above mentioned point 2. Secondly, mining the whole height at the main developments and the stopes by using either the planned machinery or the in chapter 6.1 mentioned smaller cutting machine. This option was eliminated by the above mentioned point 2 and due safety reasons concerning the long term stability (point 1). Furthermore a significant increase of the necessary weathering would occur. Third, a single main development with

a similar position to main development north with stopes heading to the major fault south was suggested. The benefit of this version would have been that a kind of independence would result concerning the fault, since the only main development would align nearly parallel to the current mining area separated by a barrier pillar. Additionally each single stope could be forwarded into the dip direction until the quality of the host rock and the deposit gets weakened by the influence of the fault within a safety margin. This option was excluded after the above mentioned point 2 and mainly point 3. Additionally the water handling and the weathering would have become a major influence.

7.1 Access to South field

From the basic access within the current mining area (see chapter 6.7) the access to the possible future mining area is designed. The profile is 5x5 [m]. The basic alignment is shown in Figure 115.

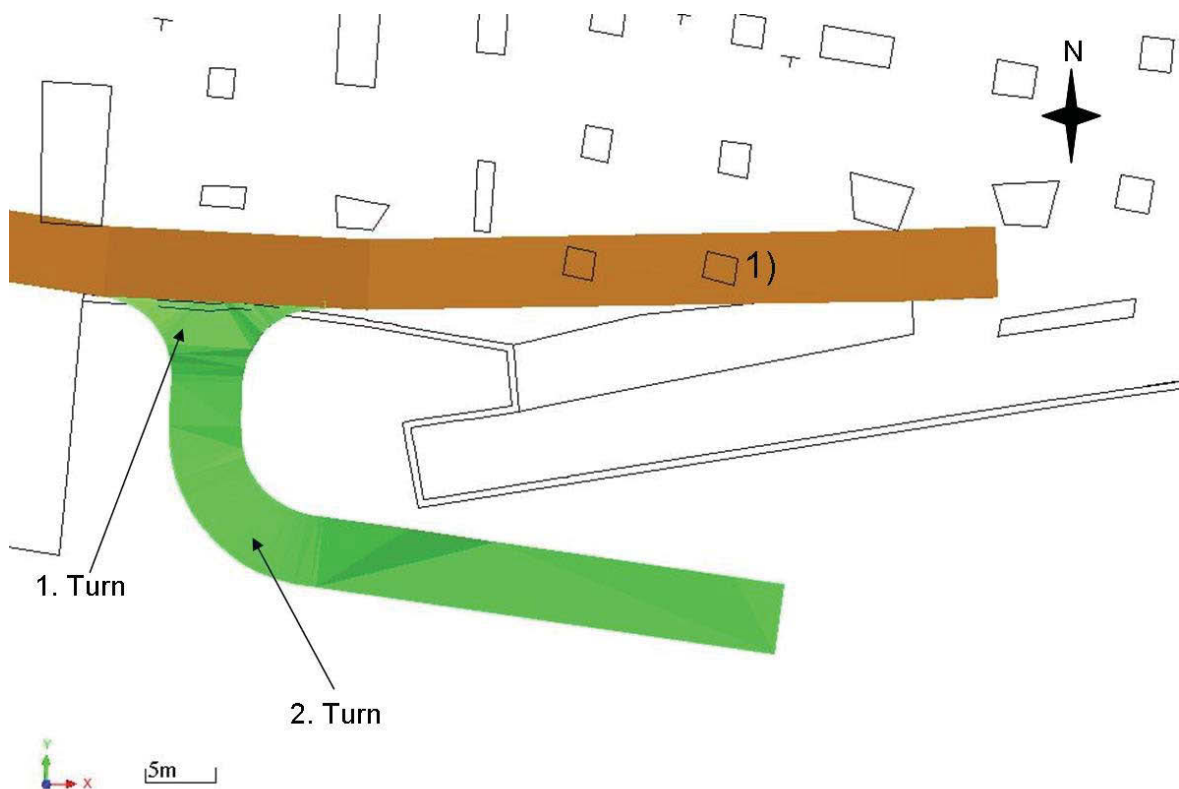


Figure 115: Access to south field, Surpac

(1) = These 2 Pillars are marked wrong in the provided map. The position is shifted ~ 4 [m] into the north, according to the observations at the fieldwork.)

The access is entering in that manner because at this position no backfill has to be removed and the access is cutting through maiden ribside. It has to be noted that the 1st turn, from the basic access to the access to the south field, represents a key point. Since the southern side of the profile of the basic access within the current mining area (see Figure 112, chapter 6.7) has a height of 4,2 [m]. Two options are possible to regain the aimed height of 5 [m] in the access to the south field. One possibility is to remove at this point further layers to reach a height of 5 [m] at the southern ribside, before turning into the south. The other option is that the height of 4,2 [m] is applicable to the machinery for this key point and the height is increased by increasing the dipping/inclination of the

access in that manner so that the floor layers are cut through until the aimed height is reached. In every case the leading layer is the current roof layer.

A central curve radius of 8 [m] is set for the design of the access to the south field.

Before reaching the 2nd turn of the access to the south field, a drilling program should be done to ensure the position of major fault south. Furthermore this position provides the possibility to install an exploration stope to determine the quality of the rock mass when getting closer to the fault. If the exploration stope is realized, special attention concerning the stability of the roof has to be done. The profile of the stope has to be downsized and to be built by conventional drilling and blasting. In Figure 116 the suggested excavation stope is presented with an assumed profile of 3x3 [m].

(Note: The profile is dependent on the necessary space for working and the quality of the rock mass)

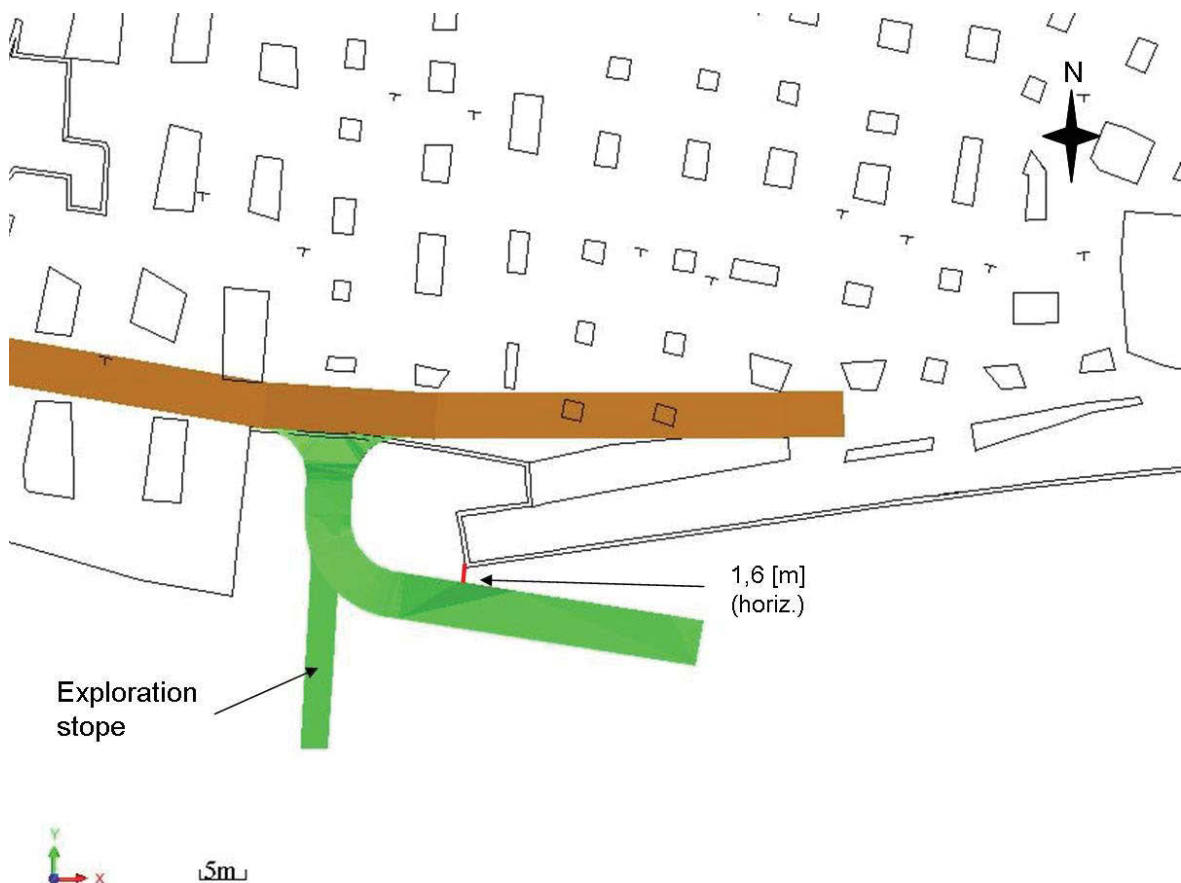


Figure 116: Exploration stope

The access after the 2nd turn to the south field runs close to the current mining area. A distance of 1,6 [m] (horizontal) remains. The “small” distance represent no hazard since the remaining pillar in the east of the access to the south field (between 1st and 2nd turn) has a factor of safety of 35 [-] and can be seen as barrier pillar. The calculation is done

after the presented procedure in chapter 5.2. The values and results are presented in Table 29.

Strength of pillar (Hedley)				
UCS	Uniaxial compressive strength	200	[MPa]	see chapter 5.1.1
S_0	Reduced UCS	116	[MPa]	Formula 10, chapter 5.2.2.1
a_p	Width of pillar/effective width	13	[m]	Formula 11, chapter 5.2.2.2
A_p	Area pillar	192	[m ²]	Determined with Surpac
U_p	Circumference pillar	60	[m]	Determined with Surpac
H_p	Height of pillar	5	[m]	Height of access
S_p	Strength of pillar	124	[MPa]	Formula 9, chapter 5.2.2.1

Load acting on pillar (irregular)				
P	Density	2,69	[t/m ³]	
G	Grav. acceleration	9,81	[m/s ²]	
H_b	Height overburden	60	[m]	Determined with Surpac
A_{RC}	Area rock column	423	[m ²]	Determined with Surpac
A_p	Area pillar	192	[m ²]	Determined with Surpac
σ_p	Load acting on pillar	3	[MPa]	Formula 2, chapter 5.2.1

FOS	Factor of safety	35	[-]	Formula 1, chapter 5.2.1
------------	-------------------------	-----------	------------	--------------------------

Table 29: Calculation of FOS of the pillar at the south access (east)

The area for the pillar (A_p , green line) and the rock column area (A_{RC} , red line) were derived by taken the in Figure 117 presented areas into consideration.

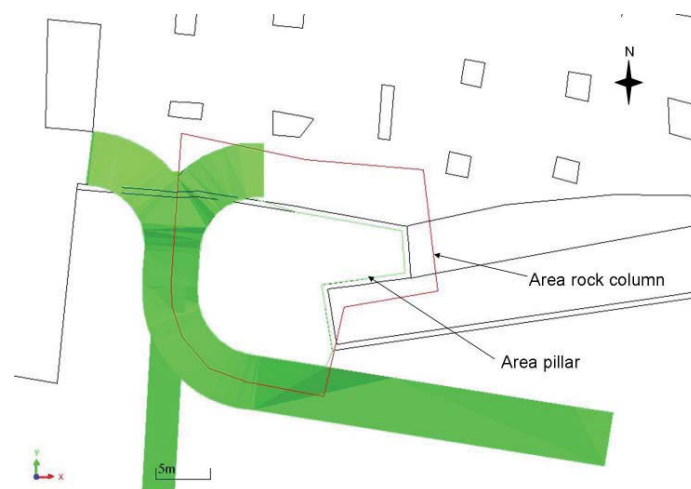


Figure 117: Barrier pillar, access south, viewed areas

7.2 Dimensioning roof

To gain a statement concerning the dimension and the stability of the roof, 2 viewed areas are assessed with the geomechanical classification systems and compared to the found results of the current mining area. This procedure is describing the global stability of the roof. Additionally the calculation of the cantilever beam will be taken into consideration. The global goal is to find a width of the room which basically is, as in the current mining area, stable without any support (global).

The local reviewing of the dimensioning of the room width and the possible influence of the geological discontinuities and outlay is done within the chapter 7.6 – support. This is done to join the hazards or possible failure mechanism with the supposed counter measurements.

7.2.1 Geomechanical classification systems - Global stability of the roof

The goal of the use of the classification systems is, to gain a width of the room, based on fixed viewed areas, where the results are in the same area (e.g. “potentially stable”) as the found results within the current mining area (see chapter 5.3). Additionally the main developments and the stopes should have the same room width. The classification system was applied to the in Figure 118 presented roof (and room, Mathew’s) areas of the main development south and the first stope.

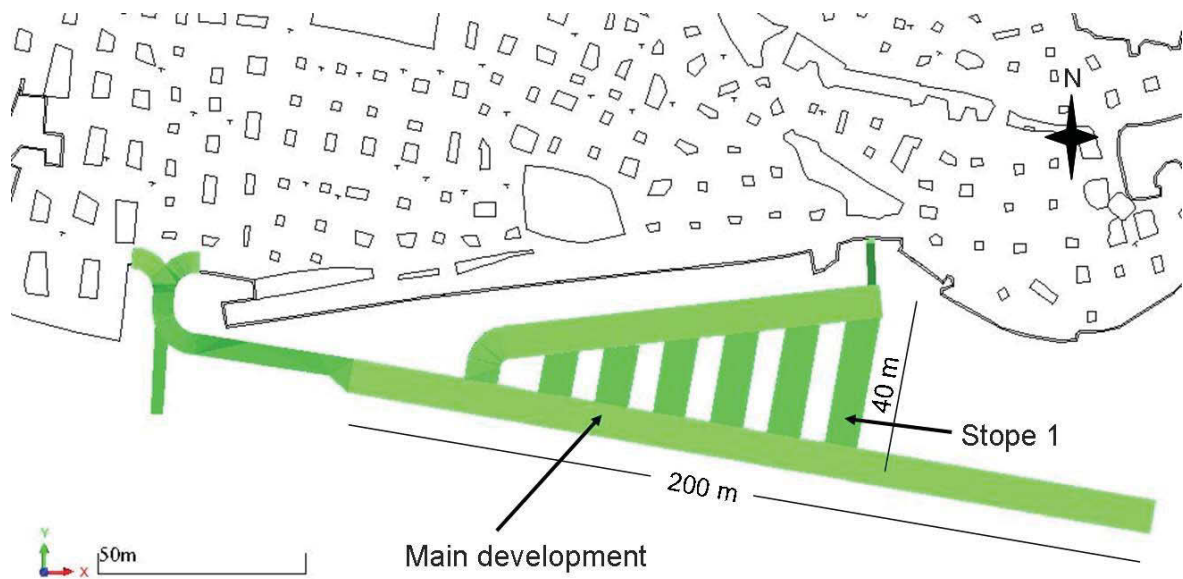


Figure 118: Viewed areas, classification systems, future mining area south

As shown in the figure above the viewed areas, for determining a statement concerning the stability and the room width by using the classification systems, have a length of 200 and 40 [m]. The width of the room was once set to 8 [m] and once to 10 [m] and applied to the classification systems.

In the following the results and the entered values are shown for each classification system. Same values (e.g. RQD) are mentioned but not derived in the following. Changing values will be described. The detailed approach of the classification systems and the results of the current mining area are presented in chapter 5.3.

7.2.1.1 Hangingwall stability rating (HSR) – Future mining area south

The basic values of the Hangingwall stability rating (HSR) are the same as at the current mining area (see chapter 5.3.1). The summary of the derived HSR-value is presented in Table 30.

		HSR	
Geological discontinuities (70%)	Bedding plane break frequency (50%) 1)	23	(4 per m)
	Number of joint sets and continuity (20%)	10	(1-2 joint set; 1 intersecting)
Mining induced stresses (15%)		4	(< 20 Mpa)
Blast damage (15%)		9	(Strong, parallel)
HSR		46	

Table 30: HSR rating, future mining area south

Note: The in the table above used value of the “Blast damage” is the highest possible value (= 9) and therefore used, although no blasting is done within the future mining areas.

The shape factor or hydraulic radius (S) of the 2 viewed areas of the future mining area south are calculated after Formula 13 (see chapter 5.3.1) and are presented for once with 8 [m] and once with 10 [m] room width in Table 31.

8 [m]			10 [m]		
S (Main development)	3,85	[-]	S (Main development)	4,76	[-]
L =	200	[m]	L =	200	[m]
W =	8	[m]	W =	10	[m]
S (Stope 1)	3,33	[-]	S (Stope 1)	4,00	[-]
L =	40	[m]	L =	40	[m]
W =	8	[m]	W =	10	[m]

Table 31: Hydraulic radius, HSR, future mining area south

With the above determined values the stability chart of the HSR method is entered (see Figure 119).

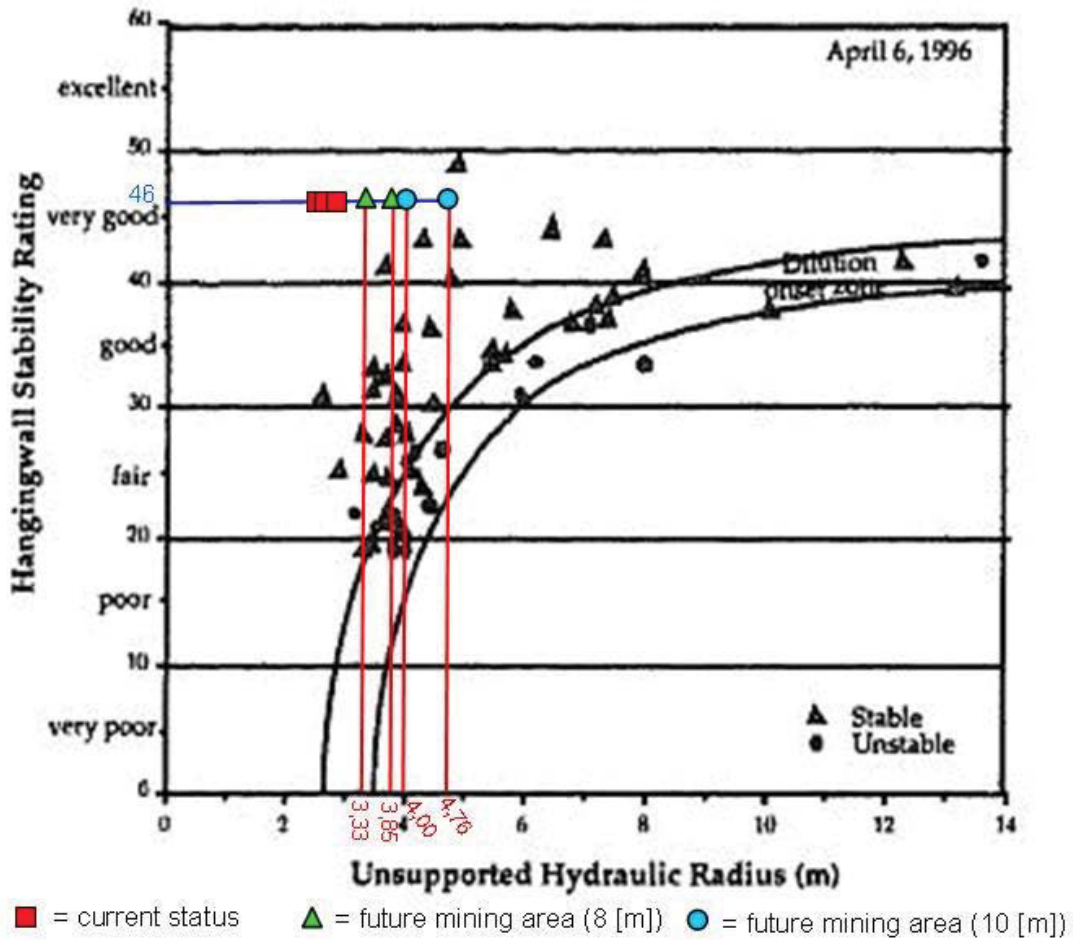


Figure 119: Bench stope stability chart, HSR, future mining area south (cp. Villaescusa 1997, p 176)

As seen in the figure above, the viewed areas with both room widths are in the stable area.

7.2.1.2 Bieniawski (Rock Mass Rating (RMR)) → Laubscher (Mining Rock Mass Rating (MRMR))

7.2.1.2.1 Bieniawski (Rock Mass Rating (RMR))

The value for the Rock Mass Rating (RMR) after Bieniawski for the future mining areas is the same as for the current mining area (see chapter 5.3.2.1). A summary of the used values to determine the RMR is presented in Table 32.

influencing factors	rating	Information
Strength	13	100 - 250 Mpa (200 Mpa)
RQD	20	90 - 100 % (92 %)
Spacing of discontinuities	10	200 - 600 mm (see geolog. Profile)
Conditions discontinuities	19	see 1)
Ground water	15	complete dry
Rating of discont. Orient.	-5	strike parallel to tunnel, Dip 0-20° - Fair
RMR	72	GOOD ROCK

1) classification of disc. Conditions		
Persistence	0	> 20m
Aperture	4	0,1 - 1 mm
Roughness	6	very rough
Infilling	4	hard filling < 5mm
Weathering	5	slightly weathered
	19	

Table 32: RMR, future mining area south

As geometrical parameter the design span is used to enter with the RMR the design span curve after Brady. The design span is the largest circle that can be drawn within the boundaries of the viewed area. (cp. Brady, p.2 f)

The design span for 8 and 10 [m] room width are presented in Table 33.

design span (circle)		
with 10m span	14,14	[m]
with 8m span	11,31	[m]

Table 33: Critical span or design span, Brady, future mining area south

With the determined values above the design span curve after Brady can be entered (see Figure 120).

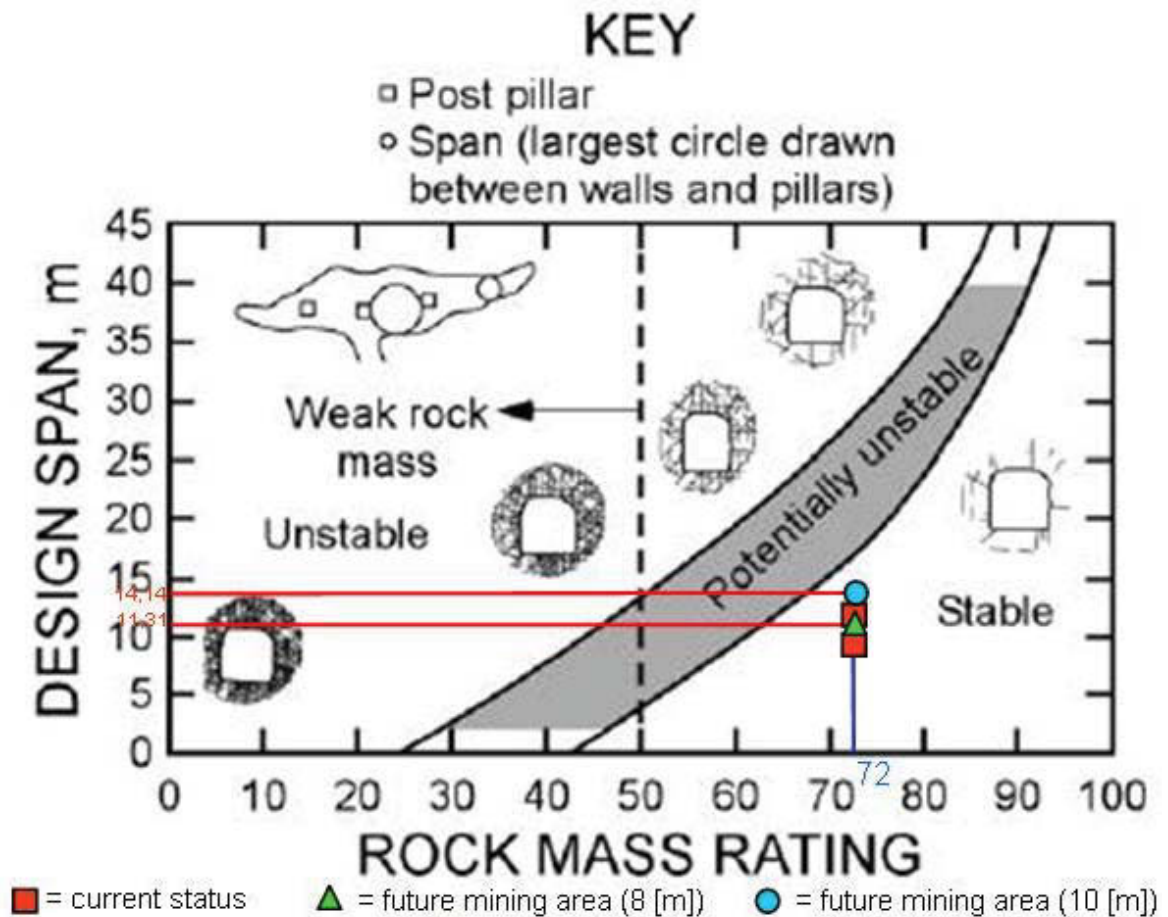


Figure 120: Design span curve, Brady, RMR, future mining area south (cp. Brady, p. 2)

As seen in the figure above, the viewed areas with both room widths are in the stable area, although the result for a room width of 10 [m] is close to the potentially unstable area.

7.2.1.2.2 Laubscher (Mining Rock Mass Rating (MRMR))

The basis of the Adjusted rock mass rating (MRMR) is the with Bieniawski determined rock mass rating (RMR, see chapter 5.3.2.1). As for the current mining area the classification system is applied once for the joint orientation with no influence (no reduction through adjustment), 100 [%]) and once with 80 [%], where the bedding of the layers and two joints inclined away from the vertical are taken into consideration (see chapter 5.3.2.2).

By changing the mining method from blasting and cutting to exclusive cutting, the value of the adjustment “Blasting” increases from “poor blasting” (= 0,8) to “boring” or “no blasting” (= 1) (cp. Laubscher 1990, p. 266).

With this change following values for the MRMR arise (see Table 34).

RMR	72	GOOD ROCK
weathering	0,9	moderate (1y)
joint orientation	0,8	3 No.of joints defining block/2 away from vertical
mining induced stress	0,9	
blasting	1	no blasting
Adjustment	0,6	
MRMR (incl. Discont)	46,7	

weathering	0,9	moderate (1y)
joint orientation	1	No joints
mining induced stress	0,9	
blasting	1	no blasting
Adjustment	0,8	
MRMR (no Discont.)	58,3	

Table 34: MRMR, Laubscher, future mining area south

With the hydraulic radius or shape factor, which is presented at the HSR classification system (see chapter 7.2.1.1, Table 31), the stability diagram after Laubscher can be entered (see Figure 121).

figure above, the 2 viewed areas with both room widths and different MRMR are in the stable area.

7.2.1.3 Barton (Q-System) → Mathew (N – Stability Number)

7.2.1.3.1 Barton (Q-System)

The value of the Q-System by Barton for the future mining area south is the same as for the viewed areas within the current mining area (see chapter 5.3.3.1). The determined values and the final Q-value is presented in Table 35.

Degree of jointing (or block size)	RQD =	92,30	[%]	1)
	J_n =	3,00	[-]	C = One joint set plus random joints
Joint friction (inter- block shear strength)	J_r =	1,50	[-]	E = rough, irregular, planar
	J_a =	2,70	[-]	D = silty or sandy clay coatings, small clay friction
Active stress	J_w =	0,66	[-]	B = Medium inflow or pressure, occasional outwash of joint fillings
	SRF =	1,00	[-]	J = Medium stress, favourable stress conditions ($\sigma_c / \sigma_1 = 100$; $\sigma_3 / \sigma_c = 0,01$)
Q =		11,28	[-]	B = GOOD

Table 35: Q-Value, Barton, future mining area south

The Q-value is plotted against the equivalent dimension (y) which is the ratio of the span width and the excavation support ratio (ESR) (see Formula 17, chapter 5.3.3.1). The equivalent dimension is shown in Table 36.

ESR =	1,60	[-]
Span =	8,00	[m]
y =	5,00	[-]
Span =	10,00	[m]
y =	6,25	[-]

Table 36: Equivalent dimension (y), Barton, future mining area south

With the above gained values, Barton's diagram for support can be entered (see Figure 122).

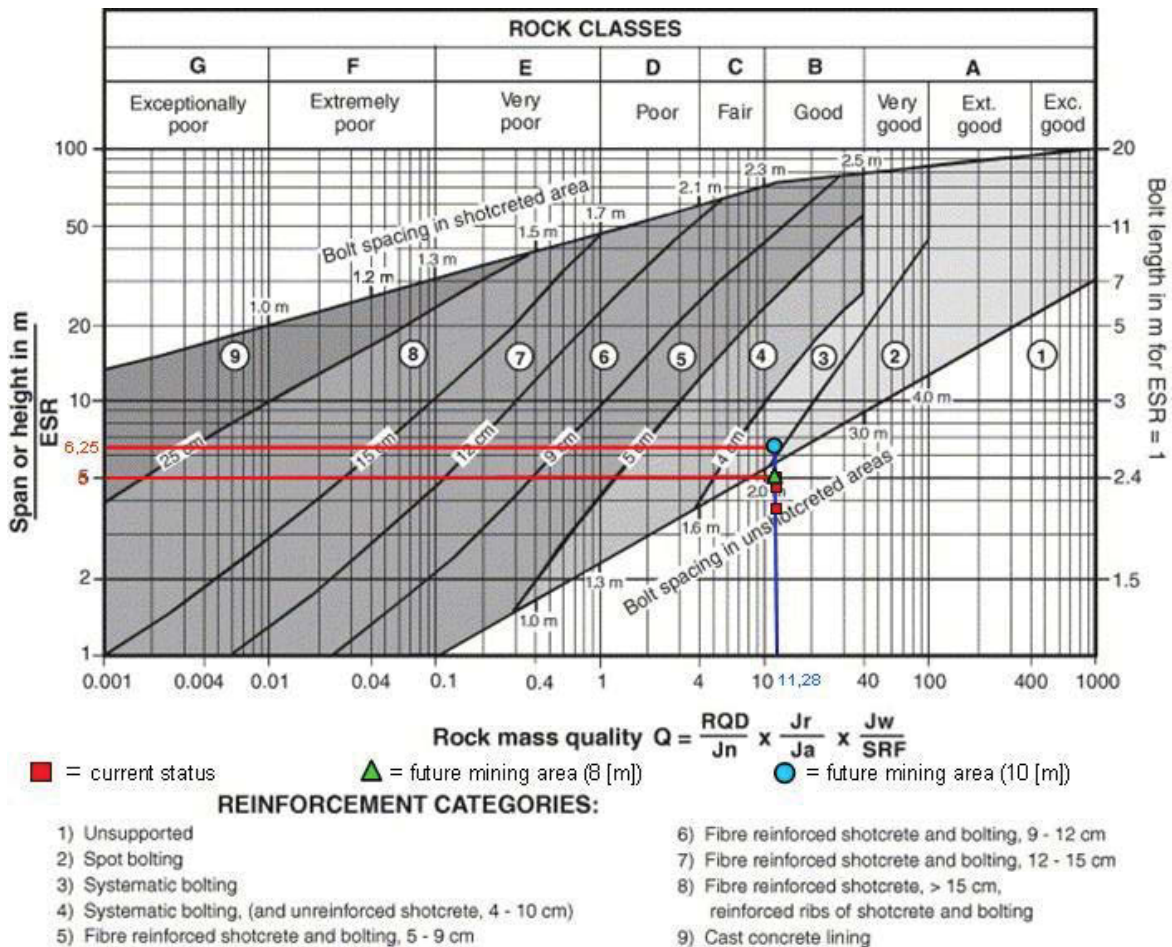


Figure 122: Diagram for support, Barton, future mining area south (cp. Løset 1997, p. 28)

As seen in the figure above the span width of 8 [m] is similar to the span width of Area 1 of the viewed areas of the current mining operation and therefore at the border of “Unsupported” and “Spot bolting” / “Systematic bolting”. The span width of 10 [m] is in the area of the “Systematic bolting”, what means that with that span width the goal of being in the same area as with the viewed area at the current mining operation has failed.

7.2.1.3.2 Mathew (N – Stability Number)

Mathew's classification system uses Barton's Q-value as basis, which is the same for the future mining area south and the current mining area (see chapter 7.2.1.3.1). The values of Mathew's system are influenced by the changing geometry of the viewed areas, the changing profile of extraction and the mining depth or thickness of overburden. Therefore following changes occur:

1. The overburden increases from 45, 50 and 60 [m] (Area 1, 2 and 3) to 71 and 81 [m] (slope 1 and main development south)
2. Therefore the vertical stresses increase from 1,19; 1,32 and 1,58 [MPa] (Area 1, 2 and 3) to 1,87 and 2,14 [MPa] (slope 1 and main development south)
3. With the changing geometry (width, height and length) of the viewed areas/rooms, the ration of the viewed planes change

The above mentioned changes influence mainly the rock stress factor (A). The change of the mining profile influences the rock defect orientation factor (B) for the main development (see Figure 123)

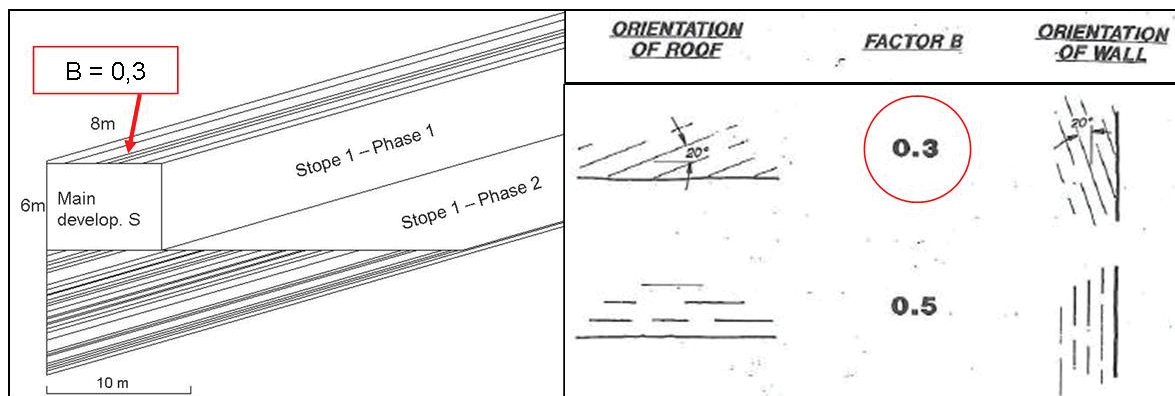


Figure 123: Change Factor B, Mathew's, future mining area south (cp. Stewart and Forsyth 1995, p 50)

As seen in the figure above the rock defect orientation factor (B) is decreased at the main development to 0,3 [-]. At the stope the factor remains the same as at the viewed areas of the current mining area (0,5 [-]).

With these above mentioned changes the stability number (N) can be determined (see Table 37).

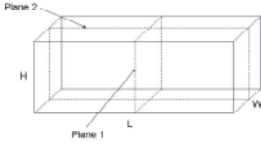
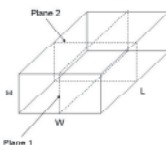
		Main develop. S				Stope 1				
										
H	thickness overburden	81,0	81,0	71,0	71,0	[m]				
σ_V	vertical stress	2,14	2,14	1,87	1,87	[MPa]				
$\sigma_{H1} = \sigma_{H2} = \sigma_H$	horizontal stress	2,14	2,14	1,87	1,87	[MPa]				
W	width	8,0	10,0	8,0	10,0	[m]				
L	length	200,0	200,0	40,0	40,0	[m]				
H	height	6,0	6,0	12,0	12,0	[m]				
		Plane 1	Plane 2	Plane 1	Plane 2	Plane 1	Plane 2	Plane 1	Plane 2	
L/H		-	33,33	-	33,33	-	1,50	-	-	[-]
W/H		1,33	-	1,67	-	3,33	-	3,33	1,20	[-]
σ_i/σ_V or σ_i/σ_H		0,75	0,25	0,60	0,25	0,30	0,70	0,30	0,80	[-]
σ_i	induced stress	1,60	0,53	1,28	0,53	0,56	1,31	0,56	1,50	[MPa]
σ_c/σ_i		124,8	374,3	156,0	374,3	355,8	152,5	355,8	133,4	[-]
A	rock stress factor	1,0	1,0	1,0	1,0	1,0	1,0	1,0	1,0	[-]
B	defect orient. factor	0,3	0,3	0,3	0,3	0,5	0,5	0,5	0,5	[-]
C	surface orient. factor	1,3	1,3	1,3	1,3	1,3	1,3	1,3	1,3	[-]
Q'	mod. rock mass rating	11,3	11,3	11,3	11,3	11,3	11,3	11,3	11,3	[-]
N	stability number	4,4	4,4	7,3	7,3	7,3	7,3	7,3	7,3	[-]

Table 37: Stability Number (N), Mathew's, future mining area south

As seen in the table above the change of the mining profile and the geometry as well as the mining depth does no influence the stability number (N) in this case. This is caused by the fact that the uniaxial compressive strength (σ_c , UCS) is high and the vertical stress is low, subjected to the vicinity of the surface.

The stability number (N) is plotted against the shape factor of hydraulic radius (S), which is presented at the HSR classification system (see chapter 7.2.1.1, Table 31). With the determined values above, Mathew's graph can be entered (see Figure 124).

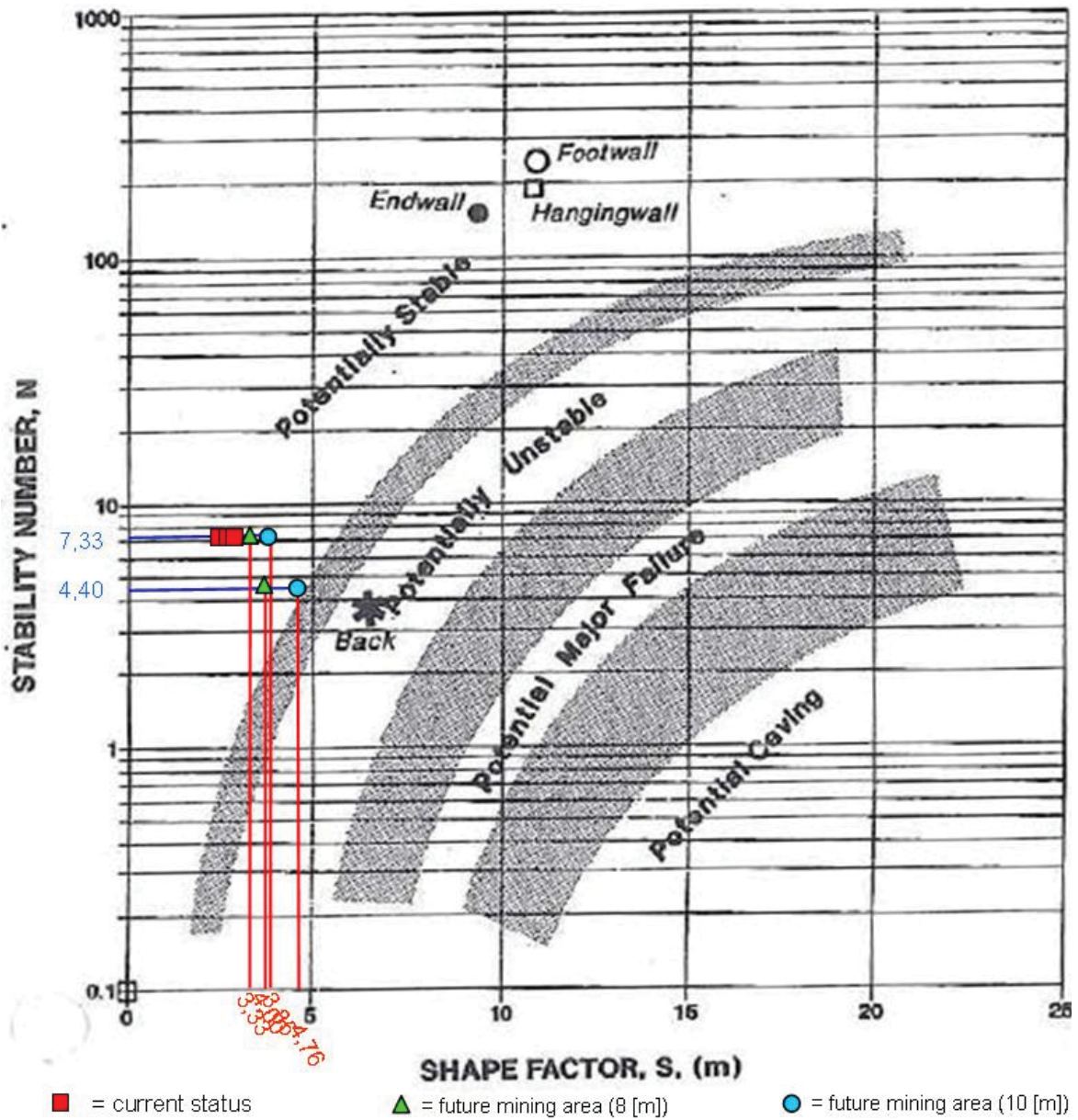


Figure 124: Stability diagram Mathew's, future mining area south (cp. Stewart and Forsyth 1995, p 49)

As shown at the figure above the span width of 8 [m] is as the viewed areas of the current mining operation in the stable area. The results of the span width of 10 [m] is near the border to the transitional area to the "potentially unstable" area, what means that with that span width the goal of being in the same area as with the viewed area at the current mining operation has failed.

7.2.2 Cantilever beam calculation

Additionally to the classification systems (see chapter 7.2.1) the simplification of the cantilever beam calculation (see chapter 5.3.5) of the first roof layer is taken into consideration. This approach brings a further criterion for the determination of the room width for the future mining areas. After the calculation (Formula 28, chapter 5.3.5) the valid length of the first roof plate of 8,6 [m] results. With a room width of 10 [m] and the assumption that the geological discontinuity systems are similar in the future mining areas as in the current ones, the possibility is given that a joint of fault cuts near a pillar and a roof plate arises which exceeds the calculated roof plate. This would cause a failure of the global goal, that the room width is dimensioned as stable and with basically no support. Therefore a room width of 8 [m] is applicable.

7.2.3 Summary of the global dimensioning of the room width

With the gained results of the geomechanical classification systems (see chapter 7.2.1) and the consideration of the simplified cantilever approach (see chapter 7.2.2) following summary can be established (see Table 38).

		<u>Result</u>		
		Current	8m	10m
Classification System	HSR	Stable	Stable	Stable
	Bienawski (RMR)	Stable	Stable	Stable
	Laubscher (MRMR)	Stable (local supported)	Stable (local supported)	Stable (local supported)
	Barton (Q-System)	Unstupported (Stable)	Unstupported (Stable)	Systematic bolting
	Mathew's (N)	Potentially Stable	Potentially Stable	Border to potential unstable

Cantilever calculation	Calculation	8m	10m
		8,6	

Table 38: Summary of the global dimensioning of the room width

As seen in the table above a room width of 10 [m] fails with the goal to gain a global room width which is basically stable without support in 3 out of 6 points. This leads to the conclusion that for the further dimensioning a room width of 8 [m] is used. This conclusion is underlined by the fact that by observing the plan view of the current mine, which can be seen as stable, only in few situations the width of the room between pillars exceed the room width of 8 [m]. Typically the room width is below 8 [m].

7.3 Dimensioning Pillar

With the defined room width (see chapter 7.2), the dimensions of the pillars can be determined. The determination of the type of pillar and the dimension is done within this chapter in this manner, that first the result is presented and, in the following, the method of solution is explained on hand of examples.

It has to be mentioned at this point, that the basic calculation and the formulas which are used to determine the factor of safety (FOS), the strength of the pillar (S_p) and the load on the pillar (σ_p) are explained and mentioned at chapter 5.2.

The suggested type of the pillar is a strip pillar nearly into the dip direction of the deposit. The basic input parameters are shown in Table 39.

USC	σ_c	200	[MPa]
Height pillar	H_p	12,00	[m]
Height overburden	H_{overb}	75,00	[m]
Density	ρ	2690	[kg/m ³]
Grav. acc.	g	9,81	[m/s ²]
Normal stress	σ_n	1,90	[MPa]

Table 39: Input parameters, pillar design, future mining area south

The height of the overburden was taken at the southern end of the first pillar at stope 1. With the height of the overburden the normal stress or the stress acting on the pillar is calculated (see chapter 5.2.2.4). As height of the pillar the total height is taken (12 [m]).

As width of the pillar 6 [m] is defined. With the input parameters, the width of the pillar and the in chapter 7.2 defined room width, the extraction rate (e) and the load on the pillar (σ_p ; by the Tributary Area Theory (TAT)) is calculated. To gain the strength of the pillar (S_p) the approach of Hedley has been used. With these values the factor of safety (FOS), which is the ratio of the strength of the pillar (S_p) divided by the load (σ_p) on the pillar, has been calculated (see Table 40):

Description	Symbol	Formula	Value	Unit
Width room	W_0	-	8,00	[m]
Width pillar	W_p	-	6,00	[m]
Extraction rate	e (strip)	$((W_p+W_0)-W_p)/(W_p+W_0)$	0,57	[-]
Load pillar	σ_p (strip)	$\sigma_n/(1-e)$	4,43	[MPa]
Strength pillar (Hedley)	S_p	$0,578*UCS*(W_p^{0,5})/(H_p^{0,75})$	43,92	[MPa]
Factor of Safety	FOS	-	9,91	[-]

Table 40: Result strip pillar 1, future mining area south

¹⁾ = cp. González-Nicieza et al 2006, p. 424

Since the pillar height increases from 3,2 [m] to 12 [m] the influence of the geological discontinuities is increasing as well. The assumption has been taken that the in the current mine observed fault and joint systems are also appearing in the future mining areas. The most influencing joint system is the joint band 2, where of a dip of 85 [°] and a dip direction of 110 [°] was assumed (see Figure 125).

Note: A detailed investigation in the joint and fault systems of the current mine was done in chapter 4.2.4.

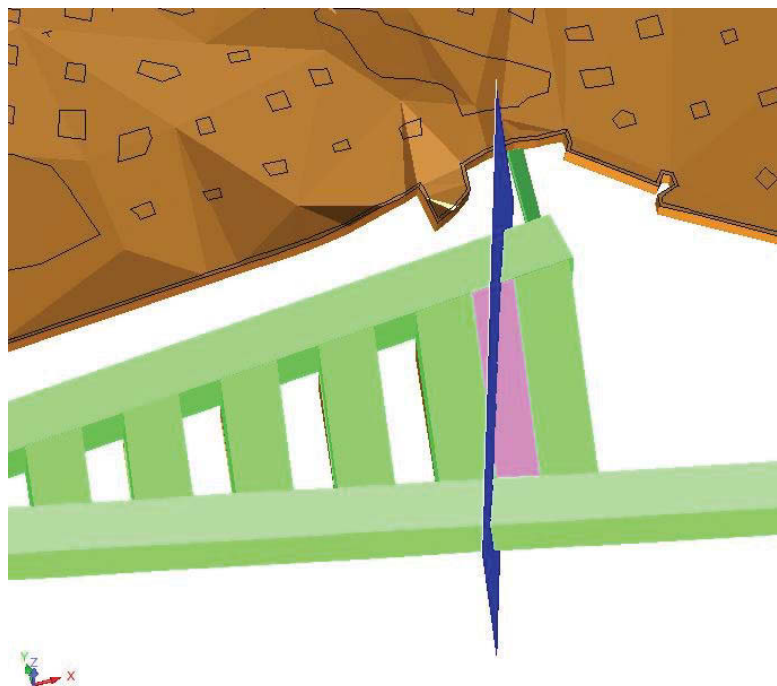


Figure 125: Pillar 1 incl. joint, future mining area south, Surpac

In Figure 125 the joint is marked as blue area, which cuts through pillar 1 (pink). In green the future mining area and in brown the current mine is shown.

To describe the influence of the joint on the stability of the pillar the investigations after Esterhuizen (2011) are taken into consideration (see Figure 126).

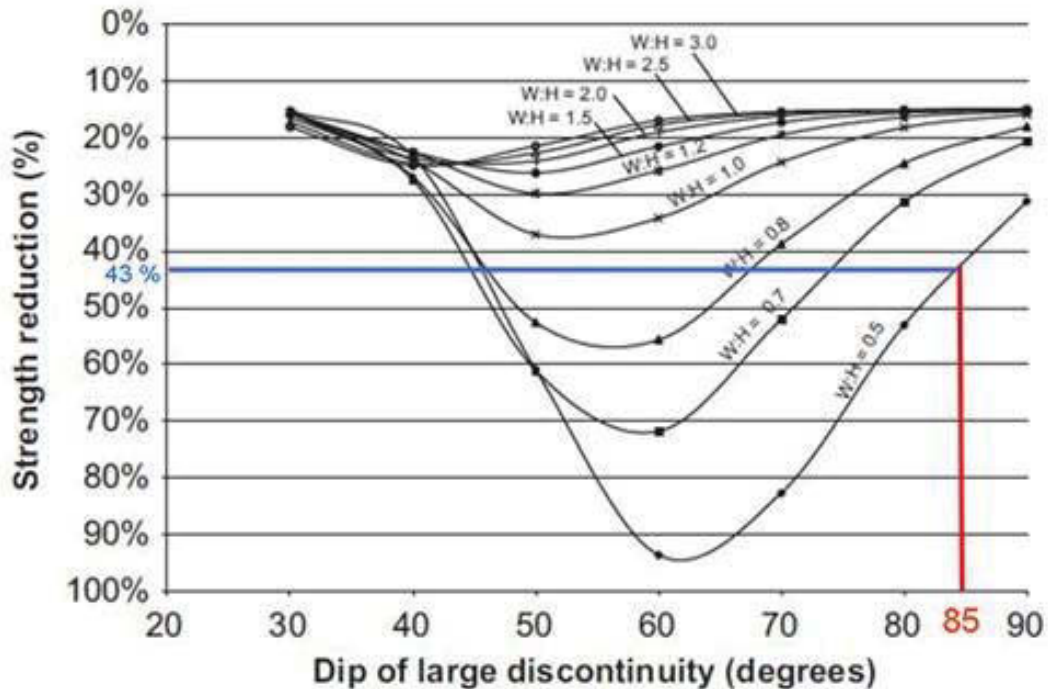


Figure 126: Mitigation of the pillar strength through discontinuities, strip pillar 1 (cp. Esterhuizen 2011, p. 47)

As shown in the figure above, the reduction of the strength of the pillar is 43 [%], with a width to height ratio (pillar) of 0,5 [-] and a dipping of the joint with 85 [°]. With the decrease of the strength of the pillar the factor of safety is decreasing. The mitigation and the result are shown in Table 41.

Load pillar	σ_p (strip)	$\sigma_n/(1-e)$	4,43	[MPa]
Strength pillar (Hedley)	S_p	$0,578*UCS*(W_p^{0,5})/(H_p^{0,75})$	43,92	[MPa] ¹⁾
Width/Height ratio	W_p/H_p	-	0,50	[-]
Mitigation after Esterhuizen		at 85°	43,00	[%]
Mitigated Strength	S_p^*	S_p^* mitigation	25,03	[MPa]
Factor of Safety	FOS	-	5,65	[-]

Table 41: Result strip pillar 1 incl. mitigation after Esterhuizen, future mining area south

¹⁾ = cp. González-Nicieza et al 2006, p. 424

The high factor of safety is chosen since after Esterhuizen a width to height ratio of 0,8 [-] is suggested for designing a stable pillar layout (cp. Esterhuizen 2011, p.49). With the outlay of the strip pillar a width to height ratio of 0,5 [-] is resulting. In combination with the high factor of safety the pillar design remains back in the stable area, although less data exists for these dimensions (see Figure 127).

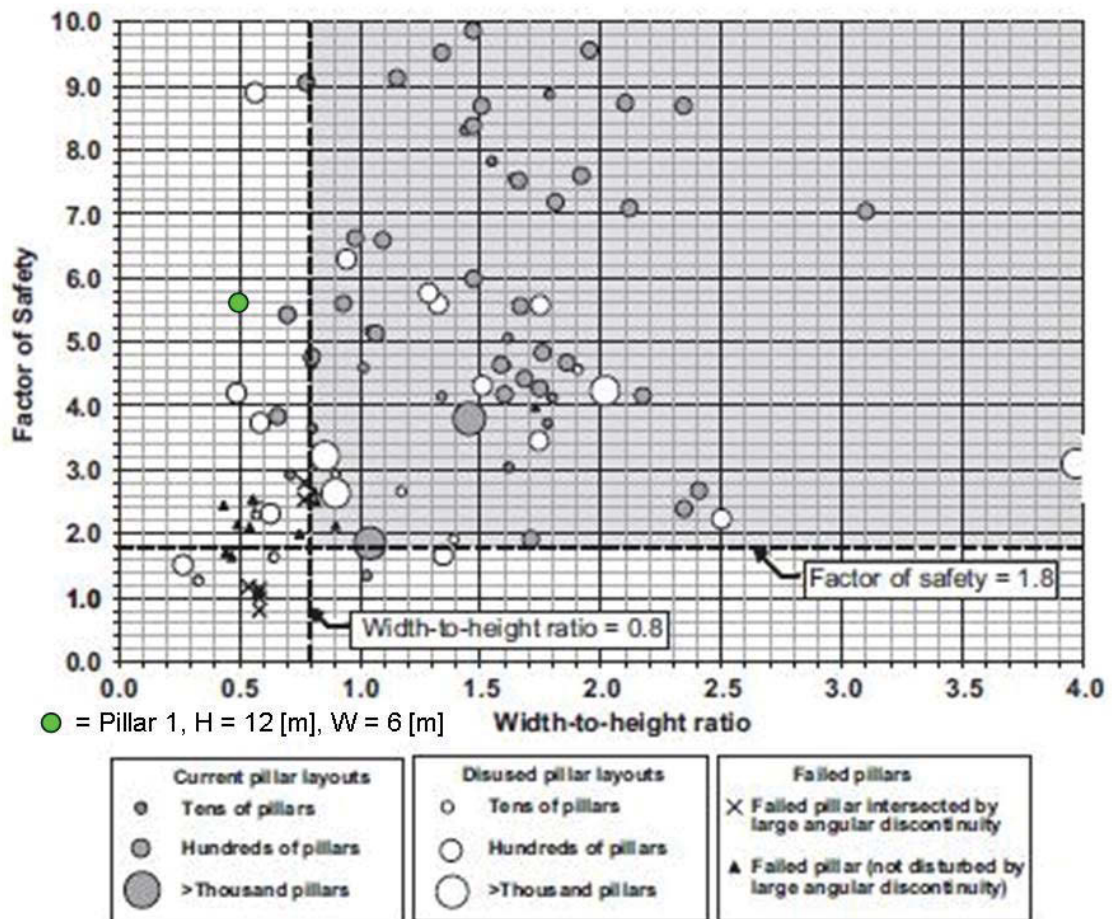


Figure 127: Result strip pillar 1 incl. mitigation, chart Esterhuizen, future mining area south (cp. Esterhuizen 2011, p. 49)

The width of the pillar of 6 [m] has been chosen, since an increase of the width would decrease the output of the future mining area and a decrease of the width would decrease the stability of it, as shown in the following example.

If for instance as width of the pillar 5 [m] is taken instead of 6 [m], the load on the pillar increases from 4,43 [MPa] to 4,93 [MPa]. Furthermore the strength of the pillar decreases from 43,92 [MPa] to 40,09 [MPa] and the width to height ratio decreases to 0,42 [-]. This would result, after Esterhuizen, a mitigation of ~73 [%] (see Figure 128).

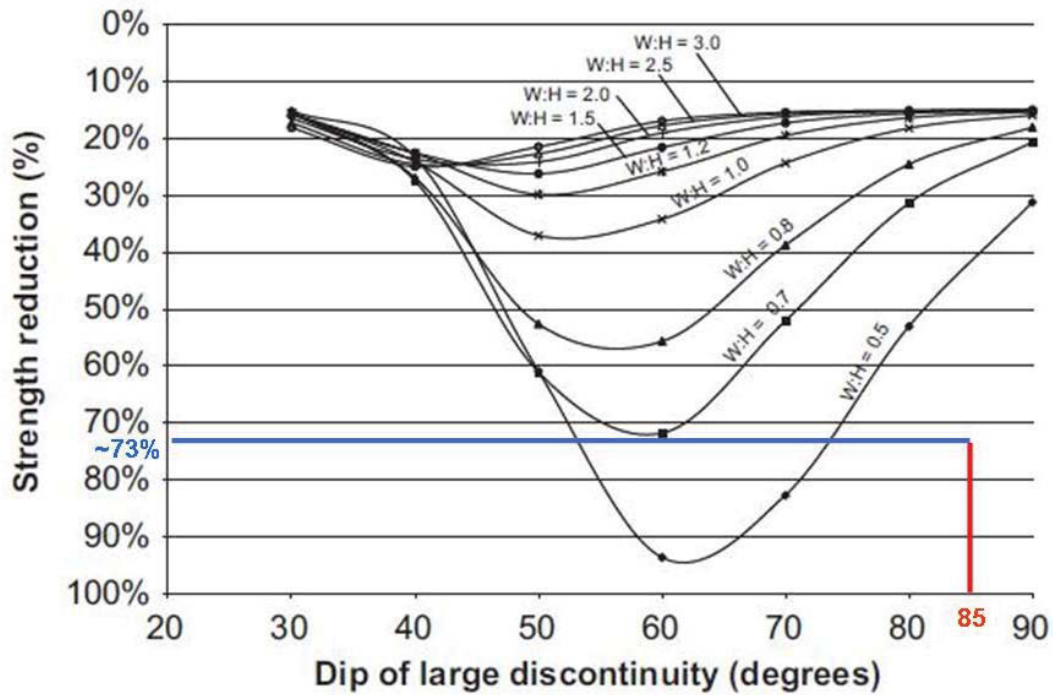


Figure 128: Mitigation of the pillar strength through discontinuities, strip pillar 1; 5 [m] width (cp. Esterhuizen 2011, p. 47)

The derivation of the factor of safety including the mitigation and the above mentioned values is shown in Table 42.

Description	Symbol	Formula	Value	Unit
Width room	W_0	-	8,00	[m]
Width pillar	W_p	-	5,00	[m]
Extraction rate	e (strip)	$((W_p+W_0)-W_p)/(W_p+W_0)$	0,62	[-]
Load pillar	σ_p (strip)	$\sigma_n/(1-e)$	4,93	[MPa]
Strength pillar (Hedley)	S_p	$0,578*UCS*(W_p^{0,5})/(H_p^{0,75})$	40,09	[MPa] ¹⁾
Width/Height ratio	W_p/H_p	-	0,42	[-]
Mitigation after Esterhuizen		at 85°	73,00	[%]
Mitigated Strength	S_p^*	S_p^* mitigation	10,82	[MPa]
Factor of Safety	FOS	-	2,20	[-]

Table 42: Result strip pillar 1; 5 [m] width, incl. mitigation after Esterhuizen, future mining area south

¹⁾ = cp. González-Nicieza et al 2006, p. 424

With the above calculated values of the factor of safety and the width to height ratio, the graph after Esterhuizen can be entered (see Figure 129).

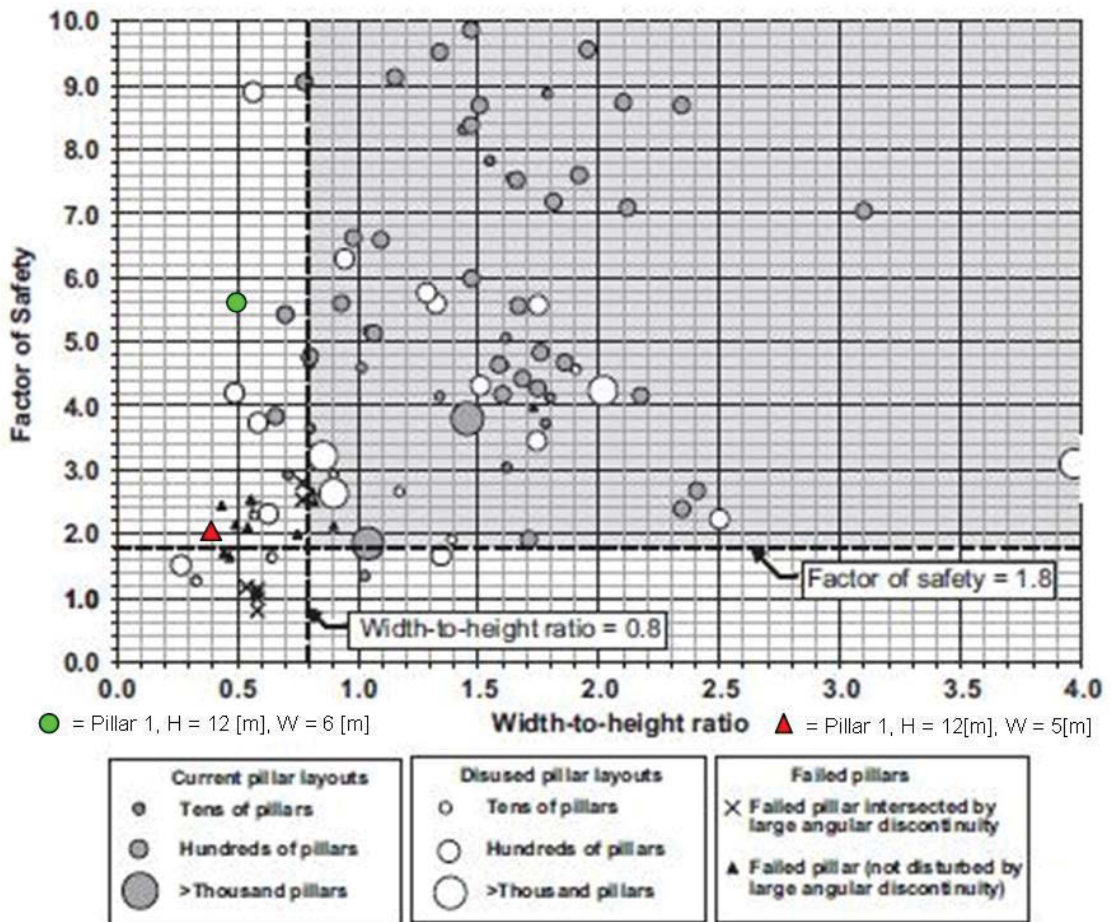


Figure 129: Result strip pillar 1, 5 [m] width, incl. mitigation, chart Esterhuizen, future mining area south (cp. Esterhuizen 2011, p. 49)

As seen in the figure above the factor of safety of a pillar with a width of 5 [m], including the approach of the mitigation after Esterhuizen, would result in an area where failed pillars were recorded. Therefore a pillar width of 5 [m] is not applicable.

The chosen type of pillar (strip pillar) is explained with the next example. If the type of pillars would be changed from strip pillar with a pillar width of 6 [m] to a square pillar with the equal side lengths, the area extraction rate would increase from 0,57 to 0,82 [-]. Through this change the fault system with a dipping of 60 [°] is getting the most influencing one. A sketch is shown in Figure 130.

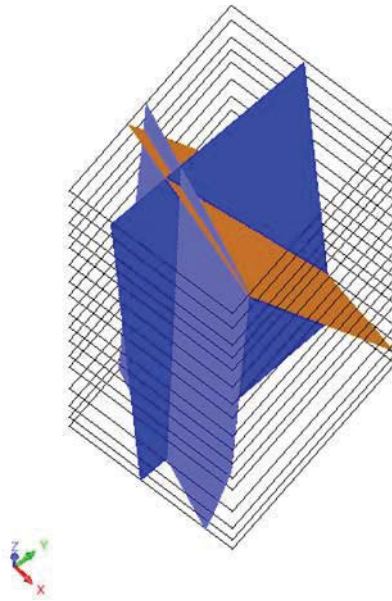


Figure 130: Square pillar 6x6x12m incl. geological discontinuity systems

This fact increases the mitigation after Esterhuizen (see Figure 131).

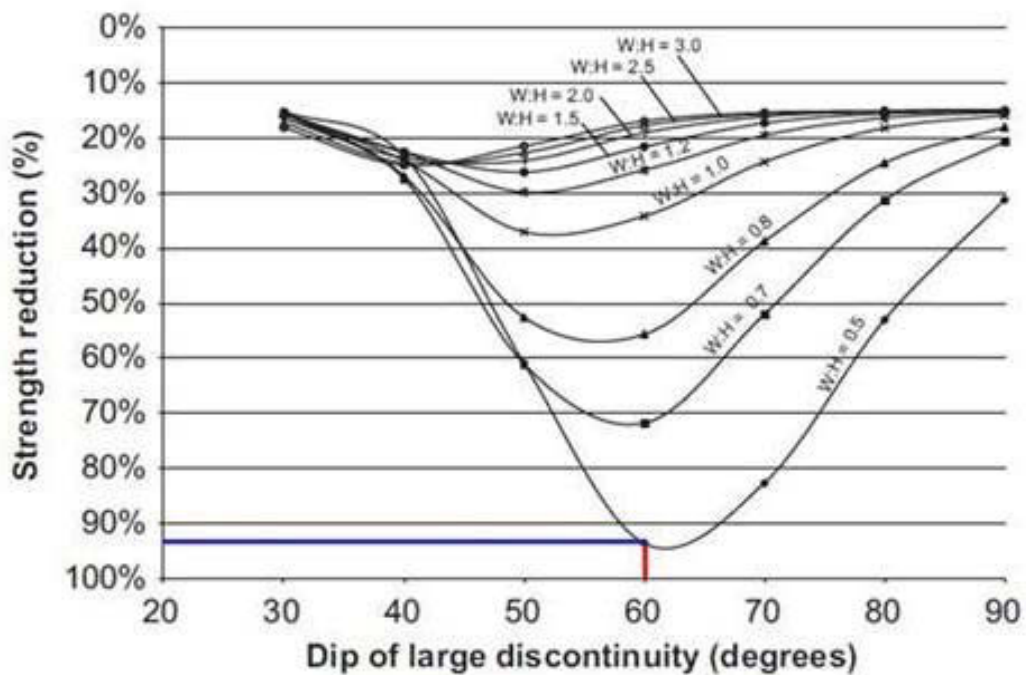


Figure 131: Mitigation of the pillar strength through discontinuities, square pillar, 6x6 [m] (cp. Esterhuizen 2011, p. 47)

With this above mentioned changing constraints the calculation and the resulting factor of safety changes (see Table 43).

Description	Symbol	Formula	Value	Unit
Width room	W_0	-	8,00	[m]
Width pillar	W_p	-	6,00	[m]
Extraction rate	e (strip)	$((W_p+W_0)^2-W_p^2)/(W_p+W_0)^2$	0,82	[-]
Load pillar	σ_p (strip)	$\sigma_n/(1-e)$	10,33	[MPa]
Strength pillar (Hedley)	S_p	$0,578*UCS*(W_p^{0,5})/(H_p^{0,75})$	43,92	[MPa] ¹⁾
Width/Heigth ratio	W_p/H_p	-	0,50	[-]
Mitigation after Esterhuizen		at 85°	94,00	[%]
Mitigated Strength	S_p^*	S_p^* mitigation	2,64	[MPa]
Factor of Safety	FOS	-	0,26	[-]

Table 43: Result square pillar; 6x6 [m] area, incl. mitigation after Esterhuizen, future mining area south

¹⁾ = cp. González-Nicieza et al 2006, p. 424

The in the table above shown result of the factor of safety drops below < 1 [-] and therefore a safety for stability is not given.

The two shown examples above underline the final outlay and design of the strip pillars with a width of 6 [m]. These dimensions are used for the further investigations and the outlay of the future mining area south (see chapter 7.4). Nevertheless a geological mapping is inevitable to react on possible unfavorable constellations of faults and joints. After the mapping the performed dimensioning has to be evaluated and, with regard of the mapping gained intelligence, has to be complemented.

7.4 Outlay of field south

The in chapter 7.2 and 7.3 gained dimensions are used to design the outlay for the possible future mining area south. A plan view of the 3D model is shown in Figure 132.

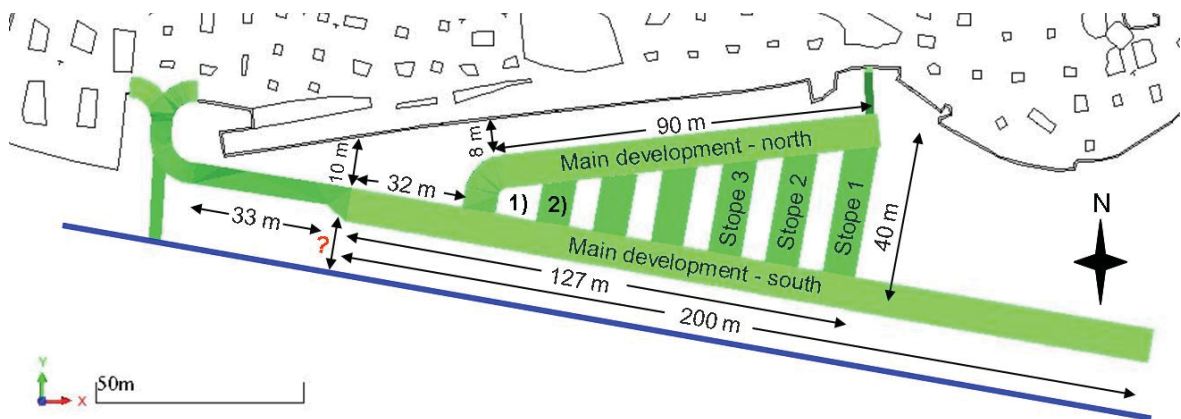


Figure 132: Outlay future mining area south, plan view, Surpac

As shown in Figure 132, after around 33 [m] after the 2nd turn of the access the profile changes from 5x5 [m] to 8x6 [m]. At this point the planned cutting machine can be used and the main production is initiated. After 32 [m] the connection point for the main development north is reached. To ensure the stability of the connection point a pillar with a factor of safety of 11 [-] is left (see Figure 132, 1)). A sketch with the dimensions of this pillar is shown in Figure 133 and the calculation is attached in the Annex (see chapter 15.10).

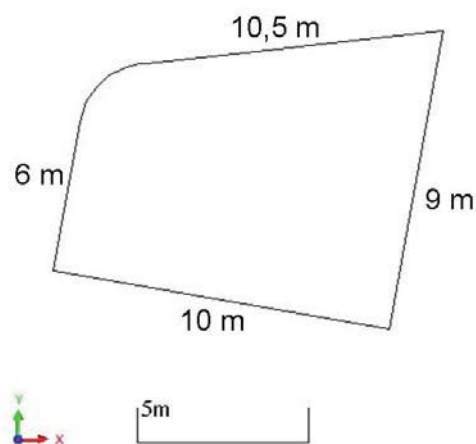


Figure 133: Pillar connection point, south, sketch

The height of the pillar is 6 [m] and therefore it follows that at the 6th stope (see Figure 132, 2)) only the upper layers are mined. The resulting loss of material, 80 [m³], of the lower levels is marginal, since the reachable thickness at the end of the main development north is between 1,7 and 2,2 [m]. It is suggested that a barrier pillar between the current mine and the main development north is left with a thickness of 8 [m] (horizontal).

After mining the main development north an emergency exit from the end of the main development to the current mine is produced. A suggested profile is 2x2 [m]. According to Surpac the secondary exit has a length of 13 [m] and a gradient of 34 [°]. The installation of a ladder would be useful, so that in case of an emergency a safe pass is guaranteed.

The in Figure 132 shown main development south represents the long term future and the used dimension for calibration of the roof stability. It shows the possibility that the main development can be advanced further the 127 [m] after mining the future mining area south is extracted, although with the new gained experiences a recalibration of the total situation should be done. For the first step the 127 [m] length should be applied.

After mining the main development south and north the first stope (Stope 1, see Figure 132) is extracted and in the following the other stopes are mined in retreat. Each stope is mined in two phases. First, the upper first 6 [m] are mined and secondly the lower levels are extracted. This results in a theoretical profile shown in Figure 134.

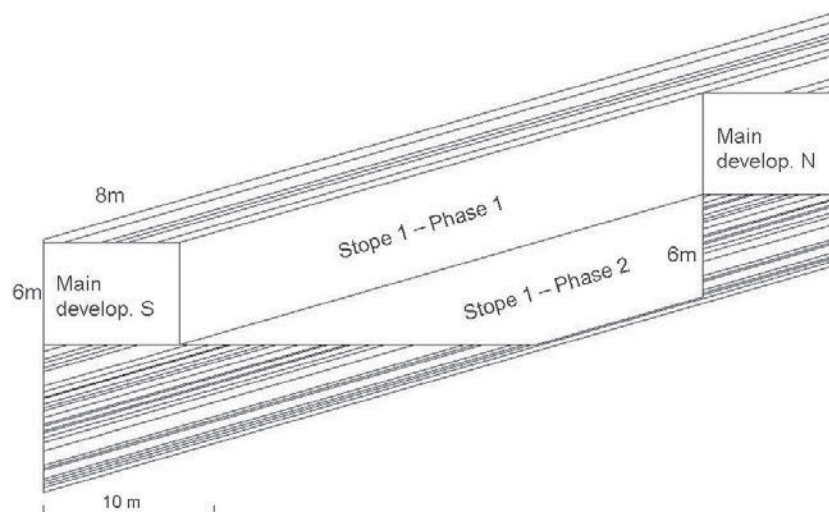


Figure 134: Profile, side view, south

The profile and the super ordinate mining sequence were derived during the intermediate presentations. This profile results of following reasons:

1. To prevent a room height of 12 [m] within the main developments north and south (long term safety)

2. To have the opportunity for selective extraction, since the saleable amount of the lower 6 [m] (Phase 2) is uncertain
3. To achieve an “upwards” mining direction within the stopes (from main development south to main development north)
4. To reduce the duration of working in 12 [m] high rooms
5. To increase the reach ability of the roof at the main developments to control the support
6. To ensure a natural water outflow at stope 1, phase 2 (into the main development south)

The inclinations of the main developments and the stopes, according to Surpac, are listed in Table 44.

	Inclination	Direction
	[°]	[-]
Main development north	1	East
Main development south	3	East
Stope 1 - 6 (Phase 1)	11	South
Stope 1 - 6 (Phase 2)	1	South

Table 44: Inclinations, future mining area south

These in the table above presented inclinations are chosen in that manner, that the possible incoming water is guided by nature to the south-east of the future mining area, to the main development south. A water catch can be installed at the cross point Stope 1 and main development south. With an installed pump the water can be evacuated through the emergency exit to the main water catch at the current mining area and used for additional saleable water for agricultural usage.

Around the main water catch in the current mining area an 8 [m] (horiz.) thick safety belt to the future mining area south, in form of a barrier pillar, is suggested to be installed, where no mining must be done. This is to ensure the tightness of the catch at the current mining area and to separate the current and the future mining area.

The main question of the presented outlay is the position of the major fault south as well as the conditions of the rock. Since in this area the alignment of the main development south is running parallel to the fault, which represents an unfavorable position concerning the stress distribution, the importance of the determination of the position and quality of the fault and the surrounding rock is underlined. To define the exact position, a core drilling program is suggested, before any mining activity is done into the south field. Out of the cores a statement concerning the quality of the rock near the fault can be taken. With these new gained data a validation of the presented outlay can be obtained. Furthermore

a recalibration has to be done to improve the accuracy and the certainty of the existing outlay and calibration, which was done within the master thesis. A basic calculation for the thickness of the barrier pillar between the major fault “south” and the main development south is presented in chapter 7.5. This approach is based on the existing data and has to be recalibrated after the definition of the position of the fault.

In Figure 135 the possible future mining area south is presented on hand of different views of the 3D model from Surpac.

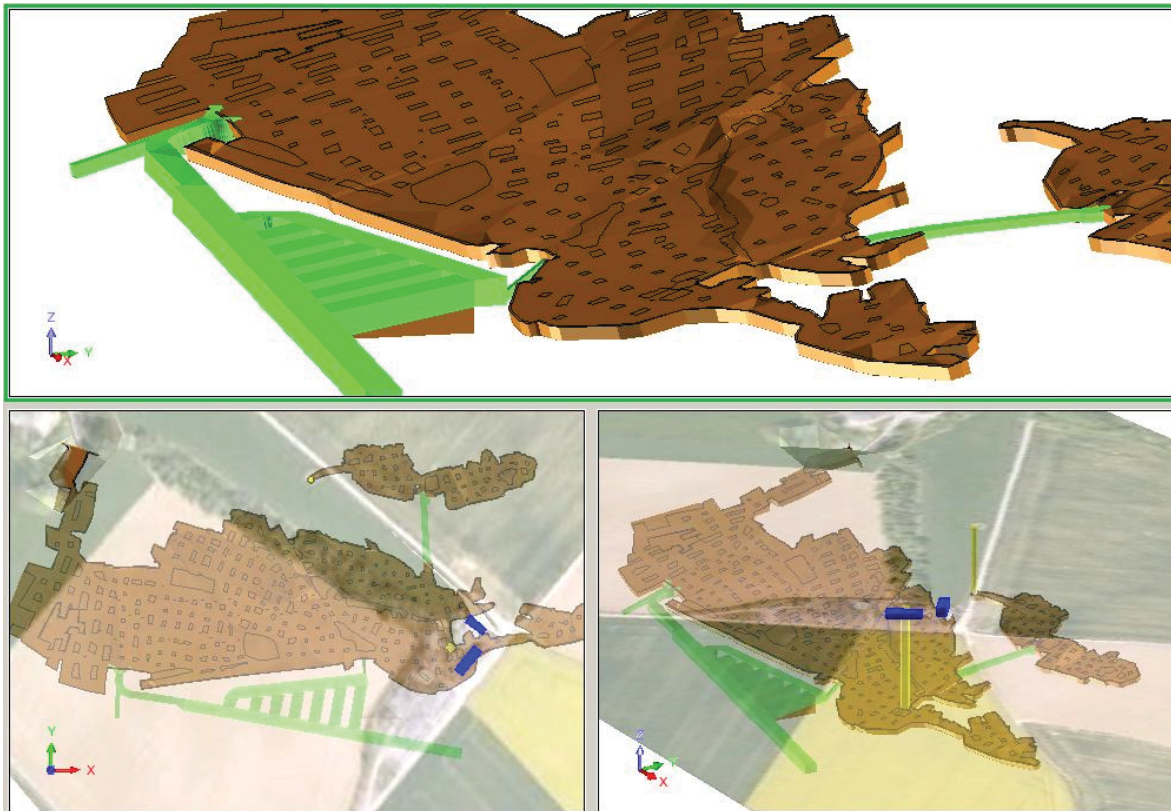


Figure 135: Future mining area south, 3D views, Surpac

The in the figure above shown views represent the future mining area south and the current mining area. In the lower part of the figure the topography, the shafts and the processing is included. The lower left part represents a plan view.

As seen in the upper part of Figure 135 the in Figure 134 presented theoretical profile cannot be applied completely, since the distance of the main development south and north is too low so that the 1 [°] into south inclined Phase 2 has the complete height to mine parallel related to the layering of the deposit. In Figure 136 a cut (North-South) of Stope 1 is presented according to Surpac.

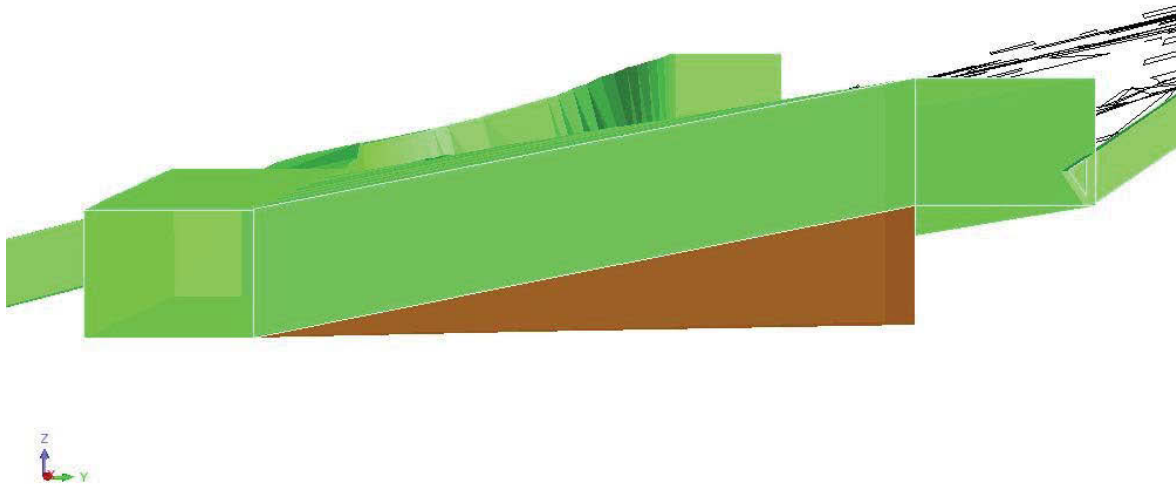


Figure 136: Cut N-S, Stope 1, profile, Surpac

As shown in the figure above the width of the deposit, based on the current database and the done outlay, is to low so that phase 2 can be fully applied.

The possible amount of resources from the in Figure 137 presented viewed sector (red square) is shown in Table 45.

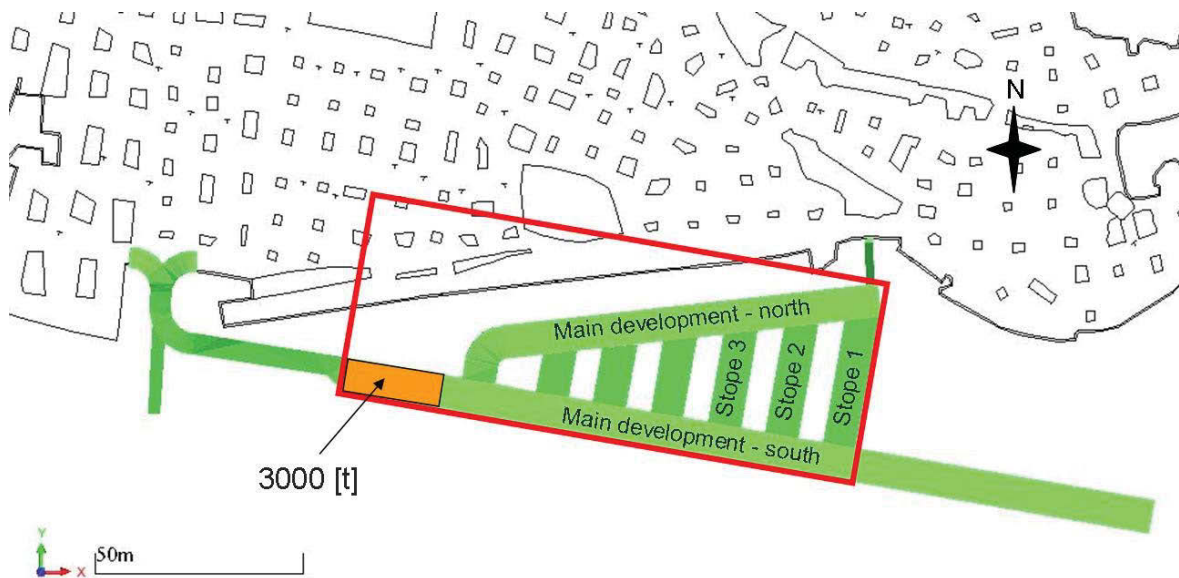


Figure 137: Determination of possible minable volume

	Phase 1	Phase 2	
Maindevel - South	6085	0	[m ³]
Main devel - North	4939	0	[m ³]
Stope 1	1472	672	[m ³]
Stope 2	1276	506	[m ³]
Stope 3	1078	358	[m ³]
Stope 4	880	238	[m ³]
Stope 5	682	141	[m ³]
Stope 6	485	0	[m ³]
Sum	16897	1915	[m ³]
	45453	5151	[t]

Table 45: Possible resources, future mining area south, Surpac

As shown in the table above, the possible resources are 45.453 [t] for phase 1 including the main developments and 5.151 [t] for phase 2. The total is 50.604 [t]. This figure represents the theoretical value with no loss included (100 [%]). For the conversion from [m³] to [t] the in the laboratory tests gained density of 2,69 [t/m³] is used.

At the current mining operation ~ 60 [%] loss occurs, related to the complete mining height of 3,2 [m] (incl. the blasted "layer"). Since the mining method is changing from blasting and cutting to exclusive cutting a figure for the loss is not known at this moment and therefore the total possible extractable material is quoted.

As previous mentioned, the width of the future mining area south of the current design is too low so that phase 2 takes a complete effect. A comparison of the viewed sector with the outlay of a mining height of 12 [m] is done to a version with 6 and 3,2 [m] mining height to check if, based on the expansion of the above presented future mining area south, a reduction of the mining height and the attending change of reduction of the pillar width and the changing extraction ratio, more material can be mined. The outlay, the dimensioning and the comparison is done in the following subchapter 7.4.1.

7.4.1 Comparison to other variants

In this subchapter the outlay of the in chapter 7 presented future mining area south is compared to reduced mining heights and therefore changing volumes. The following values for the amount of mineable volume represent the total volume with no loss taken into consideration. Two mining heights are used and compared to the variant with the 12 [m] mining height. Once a variant with 6 [m] and once a variant with 3,2 [m]. The 6 [m] mining height was chosen that the difference of mining the hole thickness of the deposit is compared to the outcome of mining “only” the first upper layers of the deposit, mined with the cutting machine. The variant with a height of 3,2 [m] is used to gain a value what happens if the future mining area south is mined with the mining height as at the current mining area.

Following constraints have been taken to ensure comparability:

1. The viewed area whereof the volume is calculated remains the same as the one which was viewed for the variant with the mining height of 12 [m] (see chapter 7.4)
2. The alignment of the main developments and the lengths are equal
3. The room width is fixed to 8 [m] (after the assessment at chapter 7.2)

Note: In the following the nomenclature for the different variants will be put under quotation mark (e.g.: Variant with a mining height of 6 [m] → Variant “6 [m]”).

As seen at the above mentioned constraints the change happens at the width of the pillar which occur by reducing the mining height and therefore the amount of stopes and cross cuts (variant “3,2 [m]”) increase.

As type for the pillar for variant “6 [m]” strip pillars and for variant “3,2 [m]” rectangular pillars are suggested. This results that for variant “3,2 [m]” cross cuts are possible (see Figure 141). Variant “6 [m]” is separated into variant “6 [m] A” (see Figure 139), which has nearly the same factor of safety as variant “12 [m]” and variant “6 [m] B” (see Figure 140) where the width to height ratio (W/H) is the same as for variant “12 [m]”.

In Table 46 the fixed input parameters are presented.

USC	σ_c	200	[Mpa]
Height overburden	H_{overb}	75,00	[m]
Density	ρ	2690	[kg/m ³]
Grav. acc.	g	9,81	[m/s ²]
Normal stress	σ_n	1,90	[Mpa]

Table 46: Input parameters, pillar design, comparison to other variants

The basic calculation and the including changes with reference to the mitigation after Esterhuizen (2011) is shown in Table 47.

Description / Symbol	Var "12 [m]"	Var "6 [m] A"	Var "6 [m] B"	Var "3,2 [m]"	Unit
Width room W_0	8	8	8	8	[m]
Width pillar W_p	6	3,5	3	3	[m]
Height pillar H_p	12	6	6	3,2	[m]
Lenght pillar L_p	-	-	-	6	[m]
Extraction rate e	0,6	0,7	0,7	0,9	[-] 1)
Load pillar σ_p	4,4	6,2	7,0	16,3	[MPa] 2)
Strength pillar (Hedley) S_p	43,9	56,4	52,2	83,7	[MPa] 3)
Width/Heigth ratio W_p/H_p	0,5	0,6	0,5	0,9	[-]
Mitigation after Esterhuizen	43 (at 85 [°])	38 (at 85 [°])	43 (at 85 [°])	35 (at 60 [°])	[%] 4)
Mitigated Strength S_p^*	25,0	35,0	29,8	54,4	[MPa]
Factor of Safety FOS	5,6	5,6	4,3	3,3	[-]

Table 47: Comparison dimensions variant „12[m]”; “6 [m] A”; “6 [m] B”; “3,2 [m]”

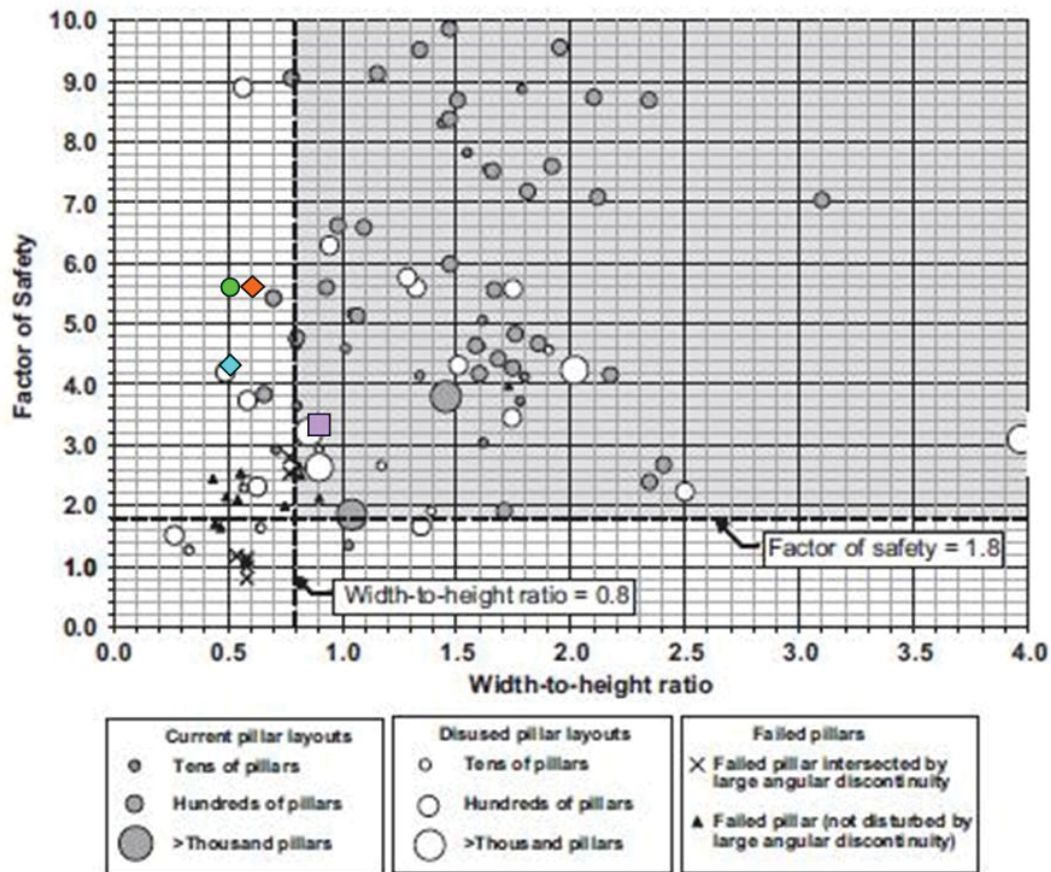
1) Formulas see chapter 5.2.1

2) Formula see chapter 5.2.1

3) See chapter 5.2.2.1; cp. González-Nicieza et al 2006, p. 424

4) See chapter 7.3; cp. Esterhuizen 2011, p. 47

In Figure 138 the in Table 47 presented calculations are entered in the chart by Esterhuizen (2011).



- = Var „12 [m]“; $H_p = 12$ [m], $W_p = 6$ [m]
- ◆ = Var „6 [m] B“; $H_p = 6$ [m], $W_p = 3$ [m]
- ◇ = Var „6 [m] A“; $H_p = 6$ [m], $W_p = 3,5$ [m]
- = Var „3,2 [m]“; $H_p = 3,2$ [m], $W_p = 3$ [m], $L_p = 6$ [m]

Figure 138: Results comparison, incl. mitigation, chart Esterhuizen, future mining area south (cp. Esterhuizen 2011, p. 49)

As seen in the figure above the results of the dimensioning of the pillars are in the stable areas after Esterhuizen.

The in Table 47 calculated values are used to design the layout within the in chapter 7.4 presented viewed sector for the determination of the volume. In the following figures the designed outlay is presented for the different variants on hand of the plan view by Surpac (see Figure 139, Figure 140 and Figure 141).

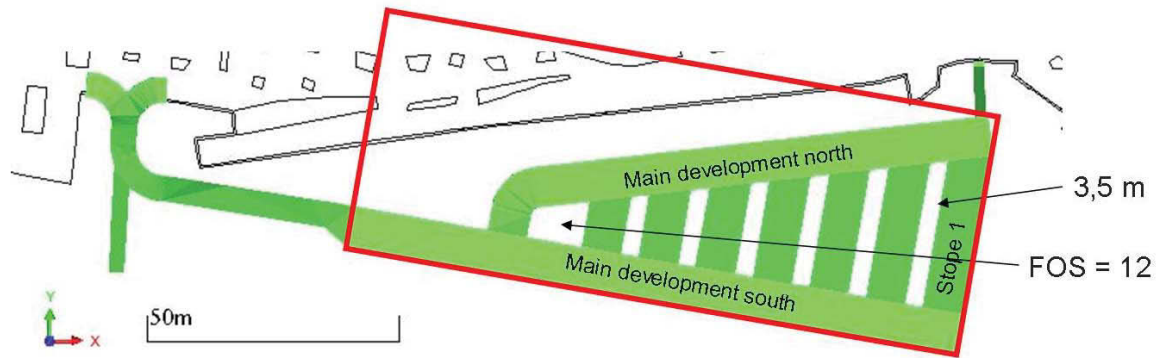


Figure 139: Variant „6 [m] A“, plan view, Surpac

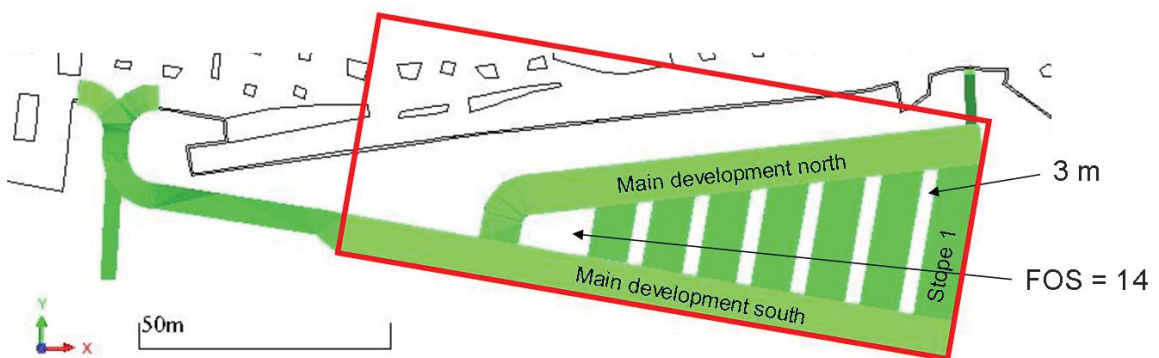


Figure 140: Variant „6 [m] B“, plan view, Surpac

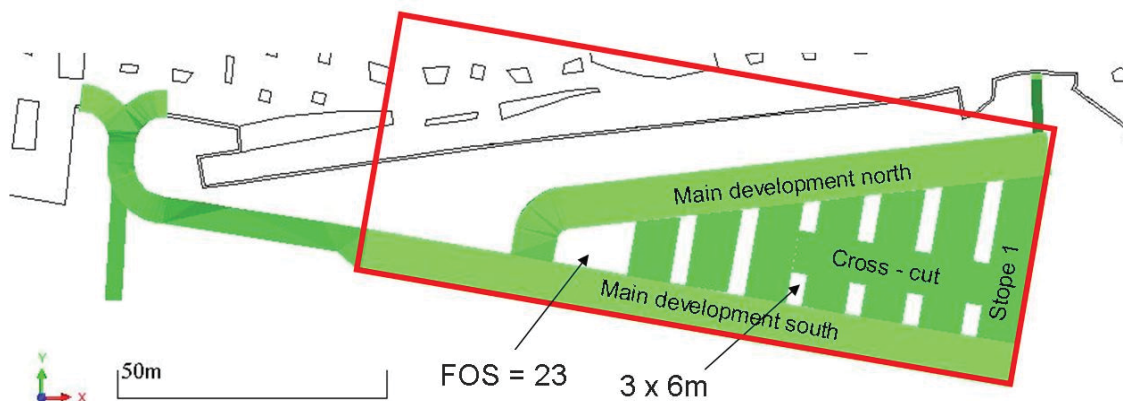


Figure 141: Variant „3,2 [m]“, plan view, Surpac

The above presented figures of the plan view of different variants, which are compared to the variant “12 [m]”, are designed in that way, that Slope 1 is in the same position as variant “12 [m]”. With the in Table 47 shown calculations the amount of stopes varies and therefore the dimension of the pillar where the main development north and south connects differs. This leads to a different factor of safety (FOS), marked in the figures. The red square represents the viewed area where the volume is calculated. The contrast is shown in Table 48.

	Var "12 [m]"		Var "6 [m] A"	Var "6 [m] B"	Var "3,2 [m]"	Unit
	Phase 1	Phase 2	Phase 1	Phase 1	Phase 1	
Maindevel - South	6085	0	6085	6085	3258	[m ³]
Main devel - North	4939	0	4939	4939	2636	[m ³]
Stope 1	1472	672	1472	1472	785	[m ³]
Stope 2	1276	506	1311	1318	703	[m ³]
Stope 3	1078	358	1149	1163	620	[m ³]
Stope 4	880	238	986	1007	537	[m ³]
Stope 5	682	141	824	852	454	[m ³]
Stope 6	485	0	661	697	372	[m ³]
Stope 7	0	0	499	541	289	[m ³]
Cross - Cut	0	0	0	0	300	[m ³]
Sum	16897	1915	17926	18074	9954	[m ³]
	18812					
	50604		48221	48619	26776	[t]

Area extraction ratio e	0,57	0,70	0,73	0,88	[-]
--------------------------------	-------------	-------------	-------------	-------------	------------

Table 48: Contrast of different variants by volume

Note: The in Table 48 presented figures represent the total amount/volume. No loss was taken into consideration.

As presented in the table above, the difference of the total extractable material between variant "12 [m]" and variant "6 [m]" is between 3,9 [%] (B) and 4, 7 [%] (A). The difference between variant "12 [m]" and variant "3,2 [m]" is 47 [%] less total extractable material. The main reason why variant "12 [m]" and variant "6 [m]" differ only in ~ 4 [%] is because the width of the future mining area south is too low so that Phase 2 of variant "12 [m]" comes not into full height and the complete thickness of the lower layers (6 [m]) cannot be mined. The in Table 48 presented area extraction ratio (e) is only partially comparable since it is related to the area and the height is not taken into consideration. The contrast of the theoretical profile and the profile of Surpac, which is presented in Figure 142, visualizes this fact.

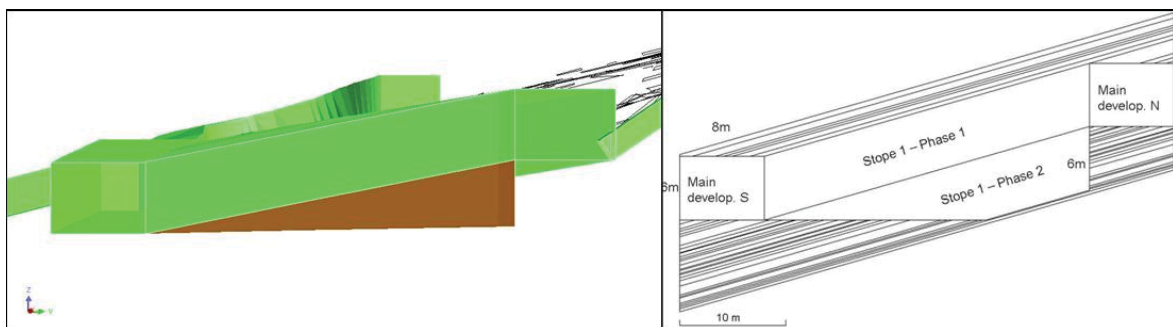


Figure 142: Contrast profile Surpac (left) against profile theoretical (right)

The presented volumes (see Table 48) underline the necessity to determine the position of the major fault “south” (see chapter 4.3.4.3). The full height of the lower levels can only be mined if the width of the deposit increases. If the position of it is similar as the assumed one and the further investigation of the surrounding rock results that the distance of the main development south and the fault is valid (and therefore the width of the future mining area south is as designed), the marginal difference between variant “12 [m]” and variant “6 [m]” becomes negligible - especially, when the argument of safety is taken into consideration.

The effect of increasing the width is presented on hand of a simplified example presented in the following. A deposit with a fixed length of 200 [m], a thickness of the deposit, as shown by the geological profile (see chapter 4.2.1), of 12 [m] and a variable width is used to compare the different variants and how the total amount of material is developing. To simplify this example the deposit is turned 16 [°] into the horizontal. A sketch of variant “12 [m]” is shown in Figure 143. The example does not consider the main developments.

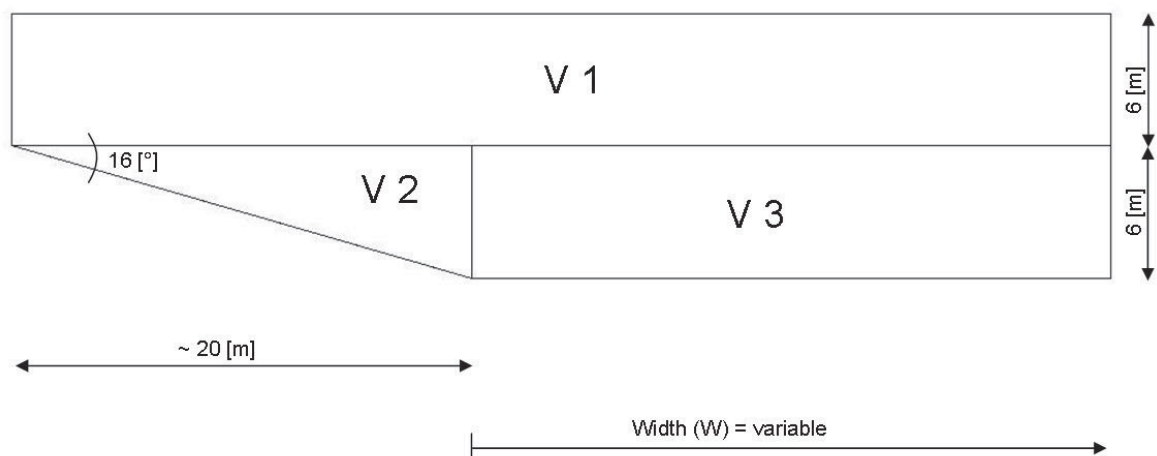


Figure 143: Sketch for volume comparison, variant „12 [m]“

To explain the procedure of calculating the volume, the steps of the calculation of variant “12 [m]” is presented. As seen in the figures above the full height of the lower levels, or lower 6 [m] of the deposit, can be mined after ~ 20 [m] (Volume “V3”). Therefore the minimum width of the exemplary deposit is 20 [m]. To gain a value of the volume the first step is to define, how often the sequence pillar and stope is applicable in 200 [m] length (e.g. variant “12 [m]”: 8 [m] (stope) + 6 [m] (pillar) → 14 times (n) in 200 [m]; 4 [m] rest).

The basic formula of calculating the volume is presented below (see Formula 31 – 33).

$$V("12[m]") = N * (V1 + V2 + V3) + V' \quad (\text{Formula 31})$$

V("12[m])...)	Volume variant "12 [m]"	[m ³]
N...	N-times of full length of pillar and stope in 200 [m]	[-]
V1...	Volume 1 (see Figure 143)	[m ³]
V2...	Volume 2 (see Figure 143)	[m ³]
V3...	Volume 3 (see Figure 143)	[m ³]
V'...	Remaining volume to 200 [m]	[m ³]

The basic formula transformed with more detail:

$$V("12[m]") = N * [(\frac{H_p}{2} * W_0 * W) + (\frac{H_p}{2} * W_0 * \frac{20}{2}) + (\frac{H_p}{2} * W_0 * (W - 20))] + V'$$

(Formula 32)

N...	N-times of full length of pillar and stope in 200 [m]	[-]
H _p ...	Height pillar/room	[m]
W ₀ ...	Width room	[m]
W...	Width deposit (variable, minimum 20 [m])	[m]
V'...	Remaining volume to 200 [m]	[m ³]

The remaining volume (V'), which occurs of the non complete stope at the end of the 200 [m], is defined by:

$$V' = (\frac{H_p}{2} * X * W) + (\frac{H_p}{2} * X * \frac{20}{2}) + (\frac{H_p}{2} * X * (W - 20)) \quad (\text{Formula 33})$$

V'...	Remaining volume to 200 [m]	[m ³]
H _p ...	Height pillar/room	[m]
X...	Remaining length of deposit	[m]
W...	Width deposit (variable, minimum 20 [m])	[m]

The volume of variant "6 [m] A" and "6 [m] B" is calculated after the same principle with the difference that only the upper layers are mined/calculated (Volume 1 ("V1"), see Figure 143).

The volume of variant “3,2 [m]” is calculated by using the area extraction ratio (e) times the area of the exemplary deposit times the mining height of 3,2 [m]. This simplification is valid, since the basic volume within the deposit is the same and the marginal differences at the border areas/volumes are negligibly for this purpose of this example.

The basic input parameters for the calculation of the volume are presented in Table 49.

	"Var 12"	"Var 6m A"	"Var 6m B"	"Var 3,2m"	Unit
L_{deposit}	200	200	200	200	[m]
W_0	8	8	8	8	[m]
W_p	6	3,5	3	3	[m]
H_p	12	6	6	3,2	[m]
N times in 200m	14	17	18	18	[-]
remaining (X)	4	4,5	2	2	[m]
Area extracion ratio (e)	0,57	0,7	0,73	0,88	[-]

Table 49: Input parameters for the volume calculation, comparison of variants

With the above presented input parameters and the described procedure of calculation, the results of the total volume are presented in Figure 144. The main development was not taken into consideration. The calculated values are attached in the Annex (see chapter 15.11).

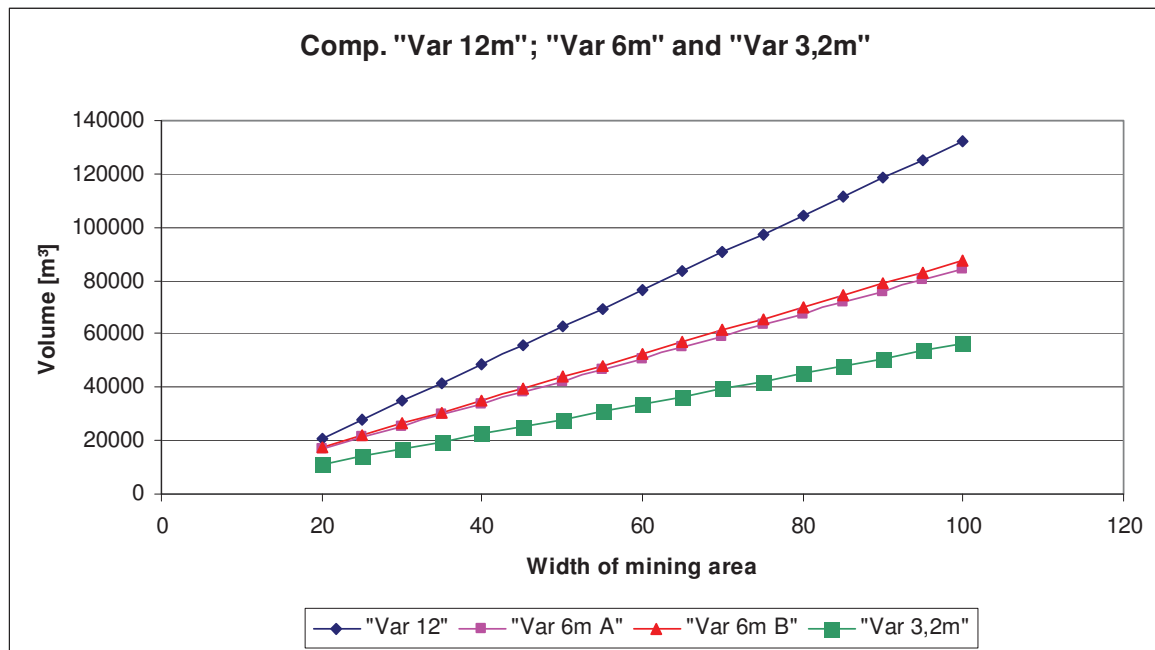


Figure 144: Results of comparison/contrast of volumes by different variants

As seen in Figure 144, with an increasing width of the deposit, the most extractable volume is possible with variant “12 [m]”. Furthermore it underlines the importance of

determining the position of the major fault “south” and the valid and safe distance (basic approach; see chapter 7.5) to the main development south, since these two constraints will define the width of the possible future mining area south.

At this point the basic formula for determining the length of the stope, where the full height of the lower layers (Phase 2) can be extracted is quoted. The influencing value is the dip of the stope (α). The mineable thickness (T) of the mineable lower layers is fixed (at this outlay: ~ 6 [m]). Therefore the horizontal length is calculated by:

$$L = \frac{T}{\sin(\alpha)} \quad \text{(Formula 34)}$$

L...	Necessary horizontal length	[m]
T...	Mineable thickness of lower layers	[m]
α ...	Dip of stope	[°]

In Figure 145 a sketch to Formula 34 is presented on hand of the theoretical profile of variant “12 [m]”.

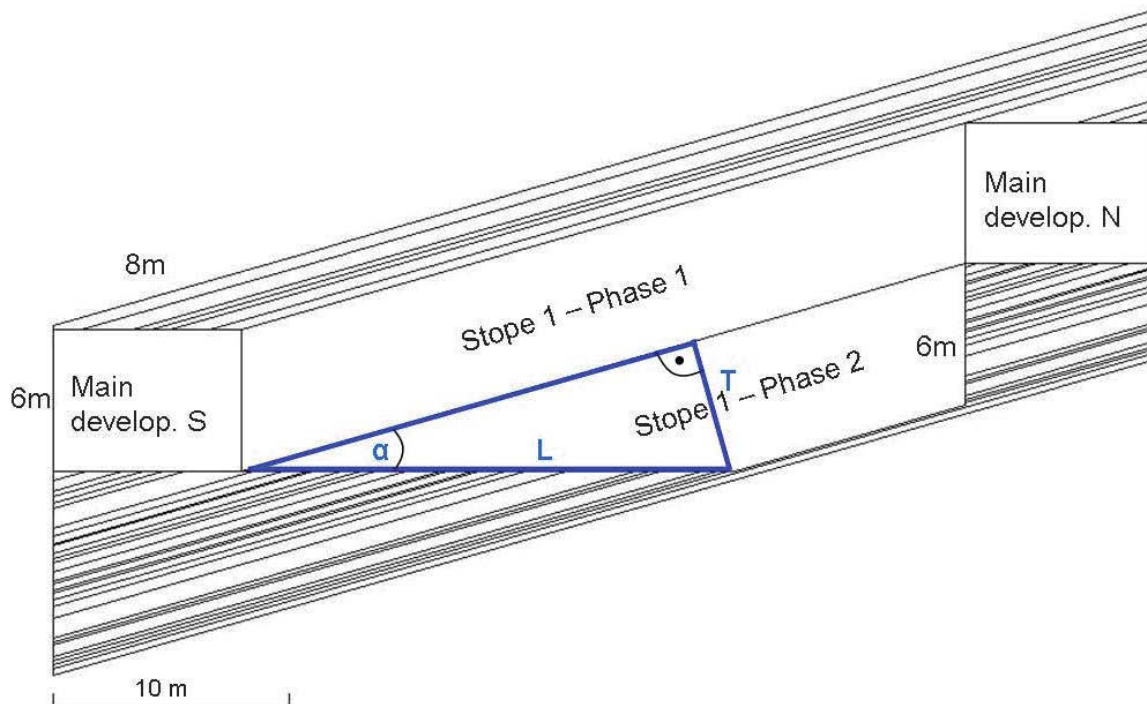


Figure 145: Sketch for necessary length to reach total possible height of lower layers

7.5 Width barrier pillar major fault “south” – main development “south”

In this chapter a simplified model is used to determine the width of the barrier pillar between the (uncertain) major fault “south” and the main development south. It has to be mentioned that the following calculation is a simplification and only presenting a first approach. After determining the exact position of the major fault “south” with a core drill program (dip, dip direction, thickness and quality of the surrounding rock strata), a recalibration has to be done. The result of barrier pillar south is not implemented into the 3D model of Surpac, to prevent a false conclusion in terms of the final outlay. Additionally a numerical investigation is suggested after the definition of the position of the major fault “south”.

To gain a first idea of the width of the barrier pillar, the extreme case has been used, that no intact pillar within the mine exists and the block of overburden, which is cut by the 2 major faults “17m” and “south”, is carried by the barrier pillars parallel to the faults. This simplification is a conservative approach.

To determine the force acting on the barrier pillars a block with 1 [m] width is used. The height and the length of the block are determined by the average values of the block designed in Surpac. The model is shown in Figure 146.

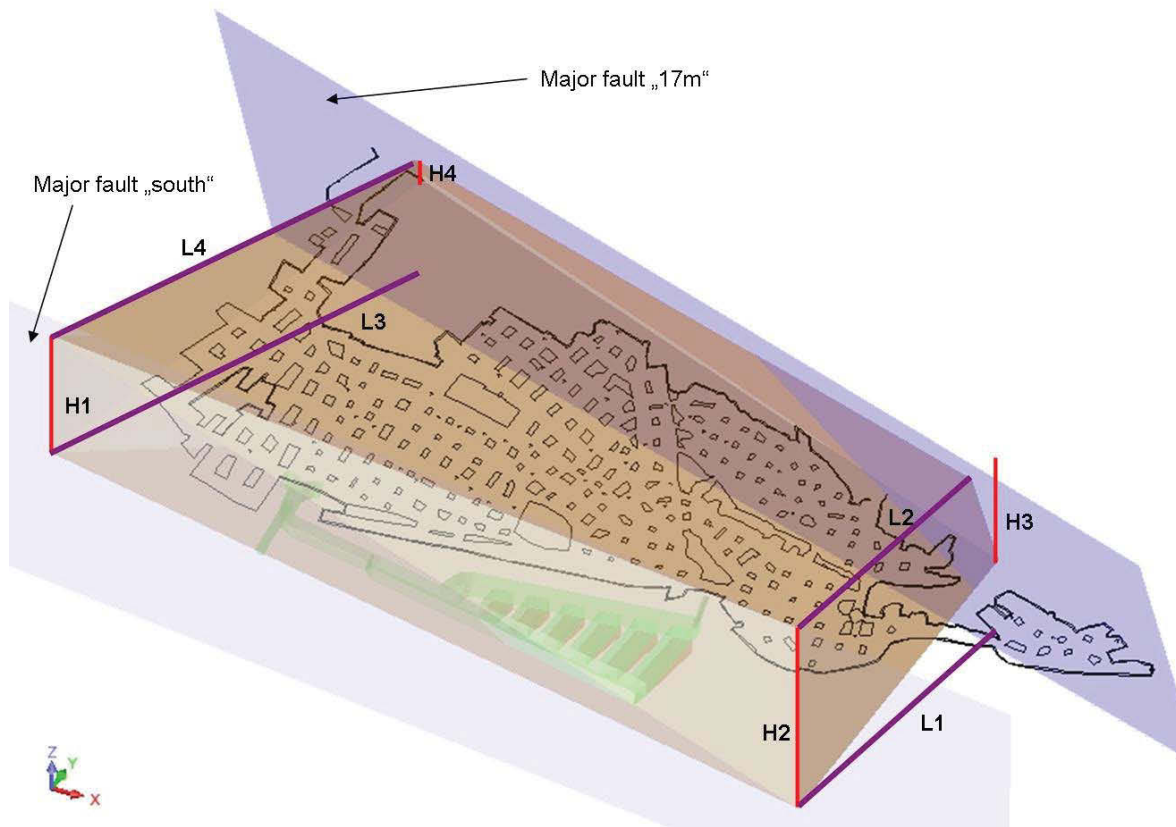


Figure 146: Mass on southern mine, sketch, Surpac

In Figure 146 the mass of overburden on the main part of the mine is presented. To gain values for the length and the height of the mass which acts on the barrier pillars the average of the in the figure shown heights and lengths are used. It has to be noted that these values are determined by the vertical and the horizontal values. The values and the average results are listed in Table 50.

Length (L)		
Length East (L1)	139	[m]
Length East (L2)	120	[m]
Length West (L3)	185	[m]
Length West (L4)	181	[m]
L_{average}	156	[m]

Overburden (H)		
Thickness south (H1)	57	[m]
Thickness south (H2)	88	[m]
Thickness north (H3)	51	[m]
Thickness north (H4)	12	[m]
H_{average}	52	[m]

Table 50: Values and the average result of the height and the length of the mass, mining area south

With the in the tables above shown average length of 156 [m] and height of 52 [m], the force applied by the mass can be calculated. With a width of 1 [m], a gravitational acceleration of 9,81 [m/s²] and a density of 2,69 [t/m³], a force of ~ 214 [MN] results. Since the deposit is inclined with a dip of ~ 16 [°] into south and the surface can be seen as horizontal, the force is split with a ratio of 2:1 on the barrier pillar south and north.

Therefore the barrier pillar north has to be capable to “carry” a force of ~71 [MN] and the barrier pillar in the south of 143 [MN]. A sketch for a better imagination is shown in Figure 147.

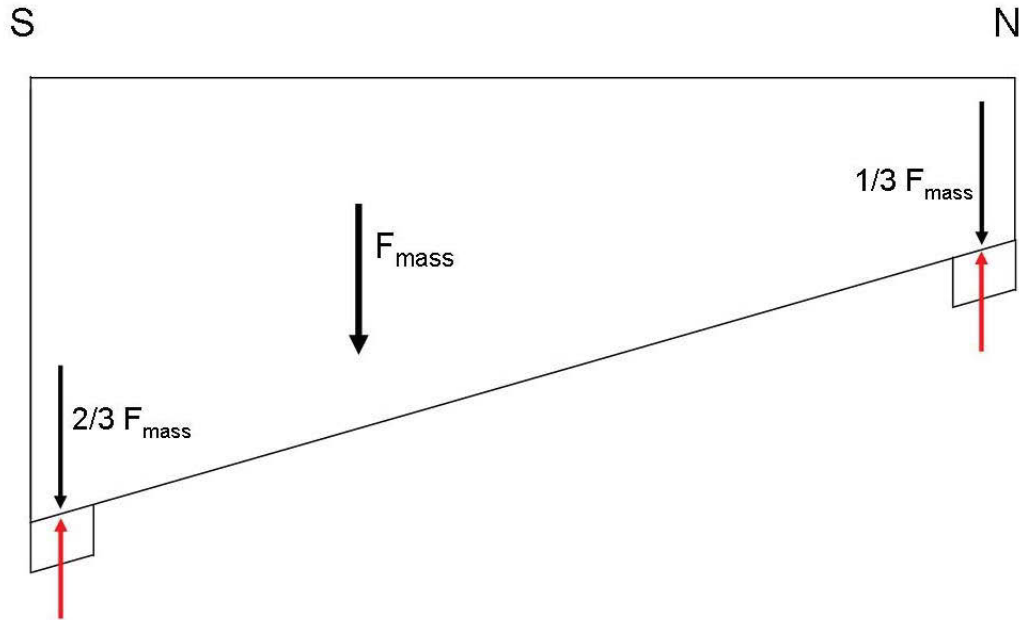


Figure 147: Sketch forces acting on barrier pillars

To calculate the capability or rather the area of the pillar which is necessary to apply the force, the basic approach of the definition of the strength is used (see Formula 35).

$$\sigma = \frac{F}{A} \quad \text{(Formula 35)}$$

σ ...	Strength	[MPa]
F...	Force	[N]
A...	Area	[m ²]

The strength of the rock mass is derived by the in Figure 148 presented graph by E. Hoek (2004).

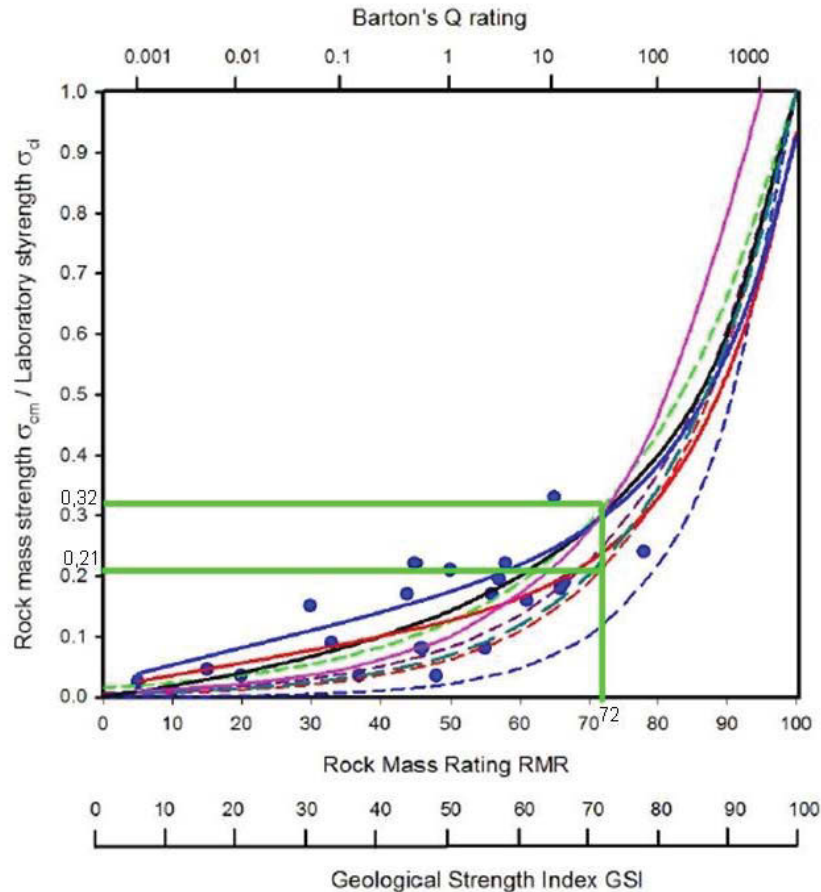


Figure 148: Estimation of the rock mass strength (cp. Hoek E. 2004, p. 2)

As shown in Figure 148 the estimation for the rock mass strength is determined by the RMR by Bieniawski (RMR = 72 [-], see chapter 7.2.1.2.1) and the uniaxial compressive strength which was derived at the laboratory tests ($\sigma_c = 200$ [MPa], see chapter 5.1.1). Therefore an estimated strength of the rock mass results in the range between 42 and 64 [MPa] is resulting. For the further calculations the average of 53 [MPa] is taken for the rock mass strength.

The area of the barrier pillar north is 5 [m²]. The horizontal width of 5 [m] is determined by the distance between the border of the current mine south and the major fault "17m". The used distance is taken at the detected outcrop of the major fault in the center of the current mine and based on the measurement in Surpac (see Figure 149).

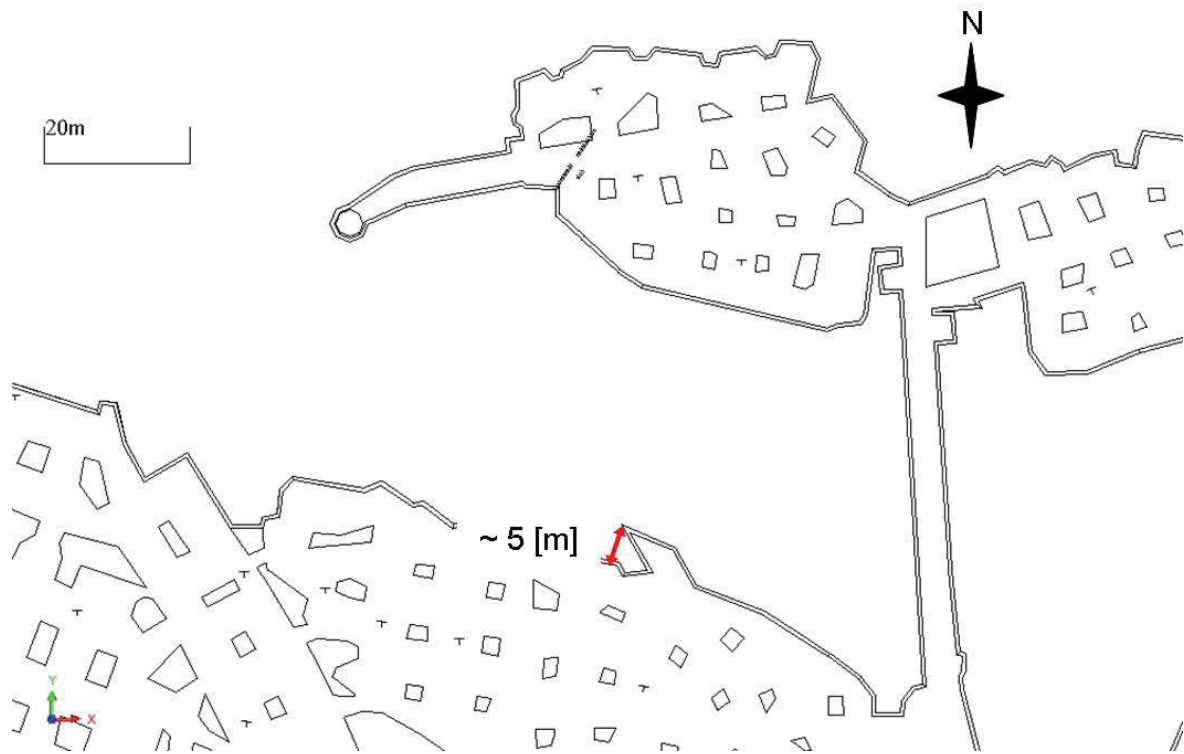


Figure 149: Width of barrier pillar north: current mining area south to major fault “17m”

With the area and the strength of the rock mass the force applied by the barrier pillar north can be calculated by transforming Formula 35. A factor of safety (FOS) of 3 is used. The values and the result are summarized in Table 51.

Width	5	[m]
length	1	[m]
A_{pillar}	5	[m²]
σ_{cm}/σ_c	0,21	[-]
	0,32	[-]
UCS	200	[MPa]
$\sigma_{cm}(0,21)$	42	[MPa]
$\sigma_{cm}(0,32)$	64	[MPa]
$\sigma_{cm,average}$	53	[MPa]
FOS	3	[-]
F_{pillar,north}	88,3	[MN]

Table 51: Values and result of barrier pillar north, south field

As shown in the table above, the capable force of the barrier pillar north is 88,3 [MN] including a factor of safety of 3 [-]. The load, based on the simplified model, is 71 [MN]. According to this approach the barrier pillar is capable to stand the force acting on it ($F_{pillar,north} / F > 1$).

To determine the necessary width of the barrier pillar south the force acting on the pillar and the determined strength of the rock mass is used. The factor of safety is set, as for barrier pillar north, to 3 [-]. The used values and the resulting necessary area/width of the barrier pillar south is presented in Table 52.

Force	143	[MN]
$\sigma_{cm,average}$	53	[MPa]
FOS	3	[-]
Area/Width	8	[m²] / [m]

Table 52: Values and result for barrier pillar south, south field

As shown in the table above, the width of the barrier pillar south has to have a horizontal width of 8 [m] to apply the force acting on it, including a factor of safety of 3 [-].

The above presented results are first approaches. If the major fault “south” differs in position and dip, a recalibration is mandatory. If the average length of the global viewed mass “sitting” on the mine changes, the force acting on the barrier pillars changes as well. Furthermore the used rock mass strength was determined on basis of the, at the current mining situation found rock mass rating (RMR) by Bieniawski. The possibility is given that the value of the RMR decreases by a zone of distraction near the fault introduced by the presence and the influence of the major fault south. Furthermore, through the alignment of the main development south the possibility is given that a fault of the, at the fieldwork detected fault system (60/010; see chapter 4.2.4), runs parallel within the southern wall. Even if no outcrop is present at the wall a major “wedge” over the whole length of the main development could arise. These facts underline the importance of determining the position and the rock quality of the surrounding rock mass by at least core drilling. If a fault runs parallel to the main development within the wall, the barrier pillar between the development and the major fault “17m” has to be adapted in that manner, that no safety issue concerning the wedge arises and massive support measurements are prevented. Therefore the above presented 8 [m] width has to be increased. A decrease is not valid.

7.6 Support

The height of the current mining operation is 3,2 [m] and at the current only isolated roof areas are supported. As shown in chapter 7, the height of the planned future mining operation will be between 6 and 12 [m]. Therefore a systematic support is suggested, because in 6 to 12 [m] high rooms, the visibility of the roof and therefore the possibility to check the roof/walls, in example in terms of movement, is not given. Furthermore the fact that employees are entering these rooms for mining, underlines the importance of appropriate support.

At this point it has to be highlighted that the subject support, has to be handled with great care. A simple stone fall from the roof will result in deadly injuries if employees are affected.

In the following the support for the roof, the walls and the floor will be discussed separately. The suggestions for the support of the roof and the wall will be done in that manner that first the systematic support, which should be applied in any case is presented. Additionally the support for special cases will be shown.

It has to be mentioned that the following presented suggestions are first approaches and basic solutions. Only with detailed surveying, like geological mapping, a detailed statement concerning the support can be done. Not every situation is possible to describe at this stage. The main influencing point will be the appearance and the frequency of the geological discontinuities. Based on the observed and surveyed geological discontinuities at the current mining area, basically no statement can be given in terms of regular frequency and meeting of them. Only by surveying at the development and mining itself, the faults and joints can be detected, hazardous situations can be recognized and a higher certainty against failure in any kind can be gained.

Before the detailed investigations are presented the basic calculation for the anchor length after Hoek is quoted (see Formula 36; cp. Hoek 2007, chapter 3, p.18).

$$L = \frac{2 + 0,15 * B}{ESR} \quad \text{(Formula 36)}$$

L...	Anchor length	[m]
B...	Room width	[m]
ESR...	Excavation support ratio	[-]

With a width of the room of 8 [m] (see chapter 7.2) and an Excavation support ratio (ESR) of 1,6 [-] (C = permanent openings, Barton, cp. Løset 1997, p. 26) a theoretical anchor length of 2 [m] results.

As exemplary anchor type a SN – anchor with 20 [mm] diameter and a load at yield strength of 157 [kN] (BSt 500 S) is taken for the further calculation. (cp. Minova 2010, p. 4). This anchor can be used as active (pre-stressed) resin anchor, which is the suggested anchor type, since resin anchors are used and installed in the current mining area. The pre-stressed resin anchor is an active anchor and increases the shear forces within the layers. Furthermore, only one anchor type and one way of installation is suggested to standardize the handling of the anchoring and improve therefore the certainty of appropriate installation.

7.6.1 Support roof

The support for the roof of the main development and the stope is viewed separately, since the dipping of the layers according to the alignment of the roof is different.

7.6.1.1 General support roof – main development

The general roof support for the main development is shown in Figure 150. This support is valid for the in Figure 150 presented virgin roof, where the roof area cuts horizontal the layering of the deposit.

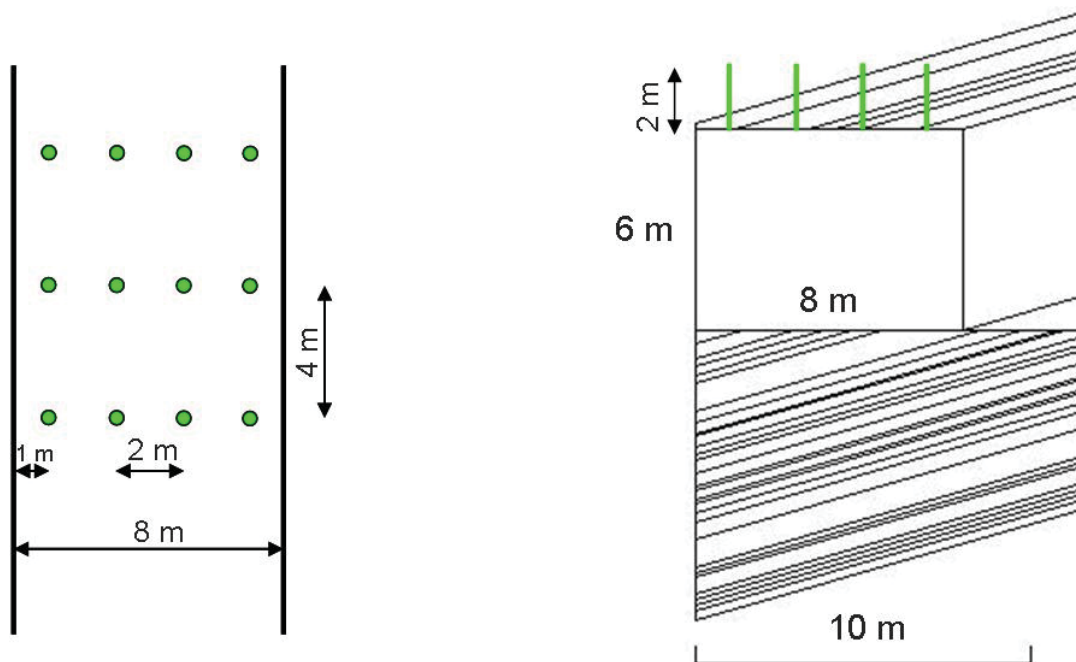


Figure 150: General support main development, roof

The support of the roof of the main development is mainly for stone fall protection. Considering the high uniaxial compressive strength and the high bending tension strength, the virgin roof at the main development is seen as stable. However the possibility is given that single stones, especially at the sharp edges drop out (cut: horizontal roof area – layer). Therefore the above presented outlay of anchors (green) is installed including a net, which is fixed by the anchors. The anchors are installed

vertically. Since the duration of the opening of the main development is uncertain, but at least several years, a corrosion resistant net is suggested.

The in Figure 167 presented anchor density of 0,125 anchors per square meter [A/m²] is equal to provide a plate of falling, with a thickness of 0,37 [m] at a factor of safety of 2 [-], which is similar to the first roof layer. The calculation is done by the basic approach below (see Formula 37).

$$FOS = \frac{F_{Anchor}}{F_{Plate}} \quad \text{(Formula 37)}$$

FOS...	Factor of safety	[-]
F _{Anchor} ...	Load at yield strength, anchor	[N]
F _{Plate} ...	Force from roof plate	[N]

The force of the plate is calculated after:

$$F_{Plate} = V * g * \rho \quad \text{(Formula 38)}$$

F _{Plate} ...	Force from roof plate	[N]
V...	Volume of plate	[m ³]
g...	Grav. Acceleration	[m/s ²]
ρ...	Density	[kg/m ³]

The calculation is based on the in chapter 7.6 presented SN – anchor with a load at yield strength of 157 [kN]. If the anchor type is changing a recalculation has to be done.

The support is mainly for stone fall protection and therefore the anchor length can be reduced to a length of 1,5 [m]. The installation of the anchor is done, for example, in this manner that after removing the first cut blocks, according to the roof, the arising working “platform” is used as basis for the drilling and installation of the anchor(s) and the net. Thereby the advantage arises that the support is installed as soon as possible and the temporary span width is decreased compared to the final one. Furthermore the next raise happens mostly under supported conditions. It is suggested that the width of the net is > 10 [m], so that the edges of the net can be fixed by the anchors of the general support of the wall (see chapter 7.6.2.1). Therefore the whole room width, including the edges (roof – wall) is supported against stone fall.

If unfavorable situations, concerning the quality of the roof (and also the wall), appear, straps are suggested to be installed additionally to the anchors and the net. The straps

are fixed with the anchors of the general roof support or by additional placed anchors. In Figure 151 two examples/sketches of straps are presented. The examples do not apply to the mine of Mazy and are used for illustration.

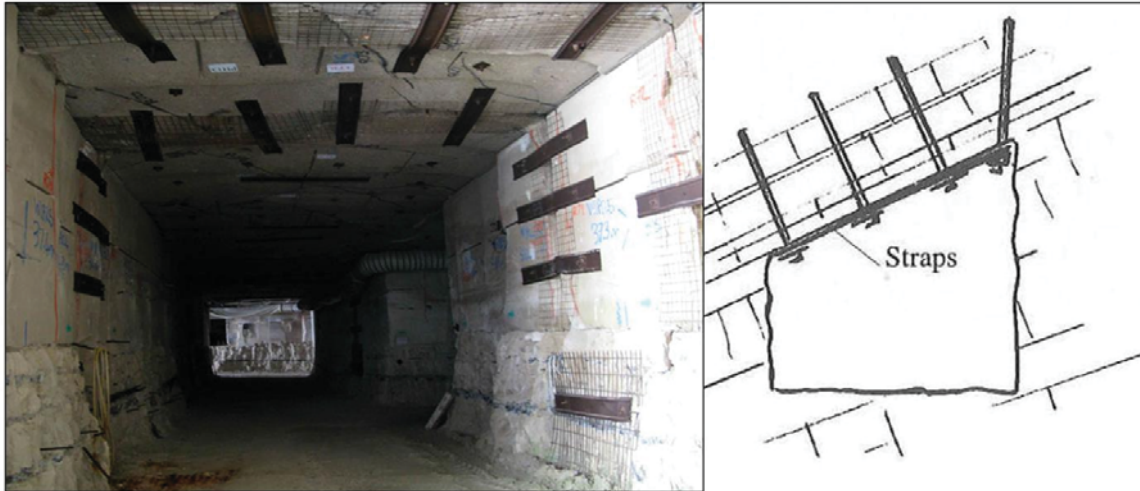


Figure 151: Example and illustration of installed straps (LEFT: cp. STONE Project 2011⁶; RIGHT: cp. Hoek 1995, p. 130)

⁶ Source: <http://www.stoneproject.org/3-quarry-workers.html> (01.08.2012)

7.6.1.2 General support roof – stope

Basically no support has to be applied for the virgin roof at the stope, since:

1. The classification systems (see chapter 7.2.1)
2. The cantilever beam calculation (see chapter 7.2.2)
3. The maximum unsupported span (see below and cp Hoek 2007, chapter 3, p. 18)

result, with a span width of 8 [m], as stable. The maximum unsupported span width by Hoek (2007) is calculated by the excavation support ratio (ESR) of 1,6 and the Q-value by Barton, which is determined at the classification system (see chapter 7.2.1.3.1) and results in 8,4 [m] (see Formula 39)

$$L_{\max.\text{un supported}} = 2 * ESR * Q^{0,4} \quad \text{(Formula 39)}$$

$L_{\max.\text{un supported}}$...	Maximum unsupported span width	[m]
ESR...	Excavation support ratio	[-]
Q...	Q-Value, Barton see chapter 7.2.1.3.1	[-]

Considering that the room height at the stope is between 6 and 12 [m], a stone fall protection as at the main development is suggested (see chapter 7.6.1.1 and Figure 152).

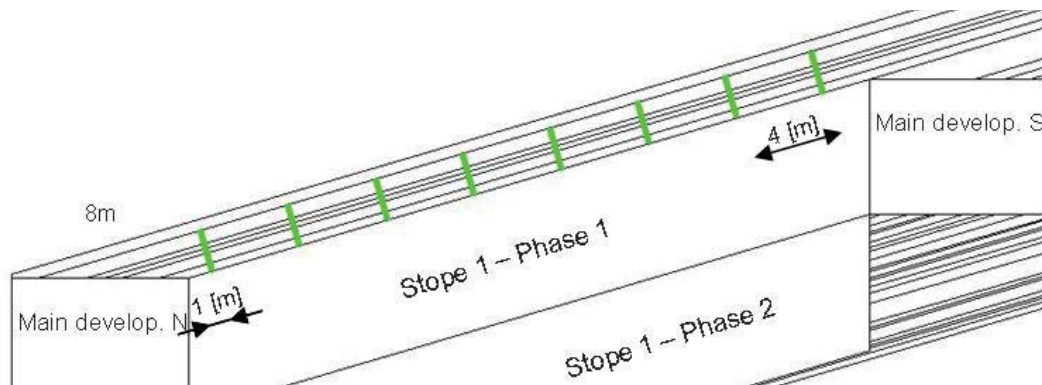


Figure 152: General support stope, roof

The net for the stope, which is fixed by the resin anchors, has not to be compulsive corrosion resistant, since the residence time is less as at the main development.

7.6.1.3 Special roof support

In the following special cases are presented, which require additional treatment. As already mentioned in the chapters before, this are only exemplary cases, which were detected during the thesis and no security of completeness is given. A detailed surveying at the development and mining itself, increases the certainty of indicating safety issues concerning support and give the base for proper reaction on these issues.

Basically two special mechanism of local failure of the roof were detected during the fieldwork. Once a single plate within the roof which has no abutments and is cut free by geological discontinuities and secondly a roof plate with exceeding width. Additionally the basic calculation of a wedge within the roof will be added.

1) Roof plate

As detected in the current mine the possibility is given that geological discontinuities concur in that manner that an isolated roof plate appears which has no abutment. A sketch is shown in Figure 153, where a section of the mapped geological discontinuities from the current mining area is superimposed on the plan view of the future mining area south. This example is used to present the basic calculation.

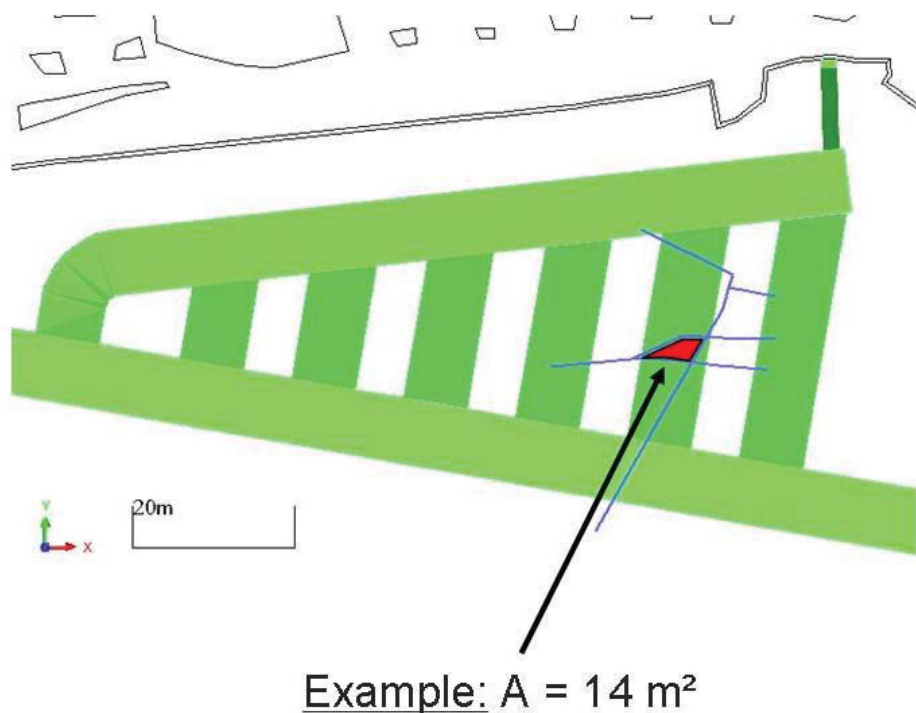


Figure 153: Sketch special case, roof plate

As shown in the figure above, the possibility is given and was observed during the fieldwork, that an isolated roof plate with no abutment arises. Furthermore the width of the roof plate from the example in Figure 153 is < 4 [m] (according to the distance of the anchor rows; general support, see chapter 7.6.1.1 and 7.6.1.2) and therefore the possibility is given that it is situated between the anchor row distance of the general support of the roof. Even if the plate is supported, in example by one anchor of the general roof support, the possibility of failure is given if the weight of the plate exceeds the load at yield strength of 157 [kN] of the anchor in reference of the factor of safety. This results in a special case which requires an additional support. Therefore the basic calculation is used to determine the force (see Formula 36, chapter 7.6.1.2), induced by the plate, against the force applied by the anchor, which results in the factor of safety. By transforming the basic calculation the anchor amount is resulting (see Formula 40).

$$AA = \frac{F_{Plate} * FOS}{F_{Anchor}} \quad (\text{Formula 40})$$

AA...	Anchor amount	[-]
FOS...	Factor of safety	[-]
F _{Anchor} ...	Load at yield strength, anchor	[N]
F _{Plate} ...	Force from roof plate	[N]

The force from the roof plate is calculated after Formula 37, chapter 7.6.1.2. For the calculation of the anchor amount (AA) the thickness of the first two roof layers, with a thickness of 0,89 [m], is taken into consideration. Since the effect of a failure of the roof plate is server if staff is affected, the factor of safety is set to 2 [-] (cp. Hoek 1995, p 9). With these constraints the anchor amount is calculated (see Table 53).

Area	A	14	[m ²]	1)
Layerthickness	t	0,89	[m]	
Volume	V	12,46	[m ³]	
Density	ρ	2,69	[t/m ³]	
Grav. Acc	g	9,81	[m/s ²]	
Force	F	329	[kN]	
Factor of safety	FOS	2	[-]	2)
Anchor strength	AS	157	[kN/A]	3)
Anchor amount (calc)	AA	4,19	[AA]	
Anchor amount (suggested)	>	5	[AA]	
Anchor density	AD	0,30	[A/m ²]	

Table 53: Calculation of the anchor amount, special case, roof plate

1) Estimated influenced layer thickness

2) Factor of safety suggested by Hoek (cp. Hoek 1995, p 9)

3) SN – anchor with 20 [mm] diameter and a load at yield strength of 157 [kN] (BSt 500 S) is taken for the further calculation. (cp. Minova 2010, p. 4)

As shown in the table above, the calculated anchor amount is 4,19 [-]. The suggested anchor amount is therefore 5 anchors.

The calculation constraints for the calculation of the roof plate remain the same, except the area of the plate. By changing the area the anchor amount is changing as well. Therefore the anchor amount can be plotted against the area of the plate (see Figure 154).

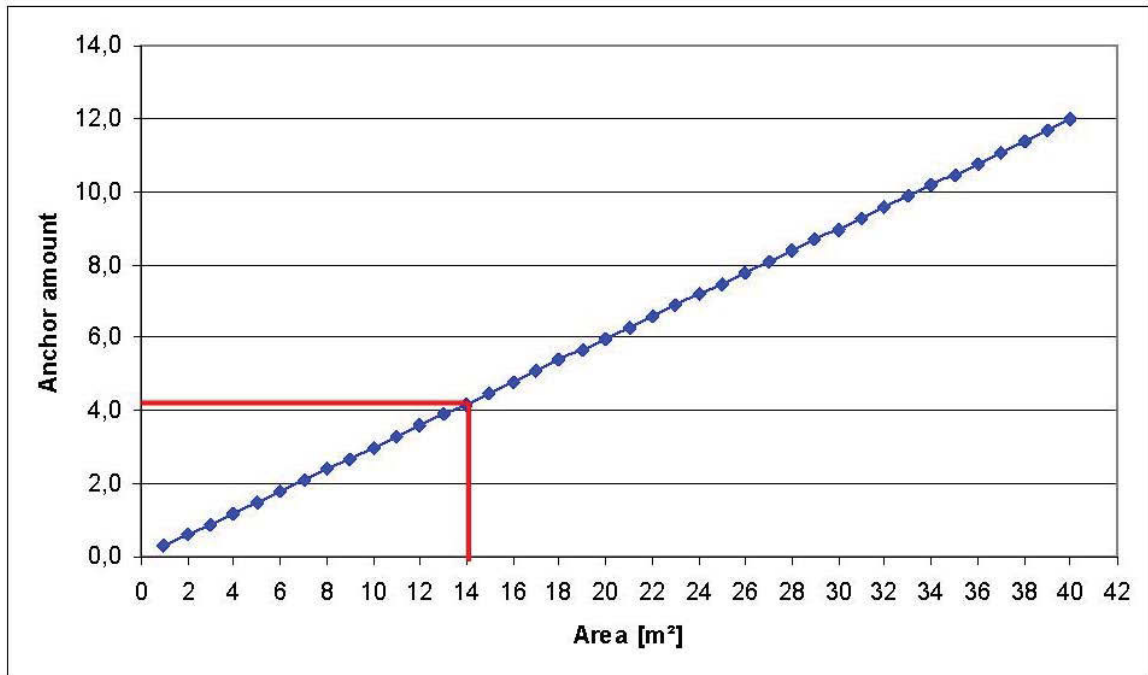


Figure 154: Anchor amount for roof plate, special case

If the anchor type is changed the presented calculation and the derived diagram (see Figure 154) remains invalid. Therefore a recalculation has to be done.

As anchor length 2 [m] are suggested (see chapter 7.6.1).

3) Wedges

Additionally the special case “wedge” is presented. Besides the layering, 3 different systems of geological discontinuities are present in the current mining area and the assumption is taken that they will be also present in the future mining area (see chapter 4.2.4). Therefore the possibility is given that the geological discontinuities concur in that manner that wedges arise. The program UNWEDGE⁷ was used to simulate and calculate wedges within the roof (and walls). The results are not used and mentioned at this point, since the results represent the maximum possible wedge which is possible with the 4 geological discontinuities and therefore not realistic or too pessimistic. Although the possibility for arising wedges is given, which have to be detected by geological mapping at the development and the mining itself, the basic calculation with an example is presented in the following.

As example a wedge with a volume of 19 [m³] is taken which results with a density of 2,69 [t/m³] in a wedge with a weight of 50 [t]. The basic calculation approach, as for the roof plate, is used to calculate the necessary anchor amount to prevent the wedge of falling, in reference at the factor of safety (see chapter 7.6.1.3; “roof plate”). As for the roof plate the force applied by the anchors is contrasted to the force given by the wedge (incl. the factor of safety). Since the nomenclature is different the formula for the anchor amount is presented below (see Formula 41).

$$AA = \frac{F_{Wedge} * FOS}{F_{Anchor}} \quad \text{(Formula 41)}$$

AA...	Anchor amount	[-]
FOS...	Factor of safety	[-]
F _{Anchor} ...	Load at yield strength, anchor	[N]
F _{Wedge} ...	Force from wedge	[N]

The calculation of the anchor amount (AA) is presented in Table 54, by using the previous mentioned values. The for the calculation used anchor type is the same as in the other chapters mentioned one (see chapter 7.6).

⁷ UNWEDGE is a 3D stability analysis and visualization program for underground excavations in rock containing intersecting structural discontinuities (cp. <http://www.rocscience.com/products/10/Unwedge> (31.07.2012) – by Roc Science – software tools for rock and soil. <http://www.rocscience.com>

Volume	V	19	[m ³]
Density	ρ	2,69	[t/m ³]
Weight	W	50	[t]
Grav. Acc	g	9,81	[m/s ²]
Force	F	490,5	[kN]
Factor of Safety	FOS	2	[-] 1)
Anchorstrength	AS	157	[kN/A] 2)
Anchor Amount	AA	6,25	[AA]
	>	7	[AA]

Table 54: Results for special case, wedge

1) Factor of safety suggested by Hoek (cp. Hoek 1995, p 9)

2) SN – anchor with 20 [mm] diameter and a load at yield strength of 157 [kN] (BSt 500 S) is taken for the further calculation. (cp. Minova 2010, p. 4)

The suggested installation of the anchors should be done in that manner that the length within the wedge (L_w) and the length in the ribside (L_r) is at least 1 [m] (cp. Hoek 1995, p. 61 f). A sketch is presented in Figure 156.

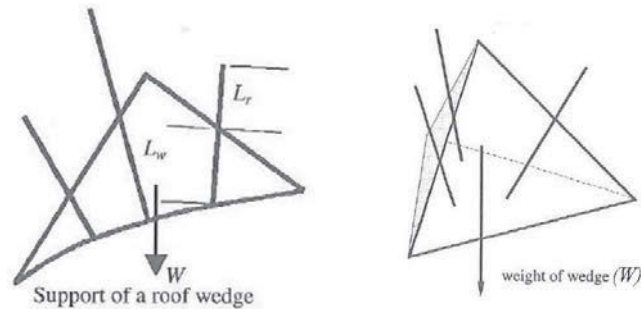


Figure 156: Special case, wedge, sketch of support installation (cp. Hoek 1995, p. 61)

The in the figure above presented left part represents a sketch of a homogeneous wedge and therefore looks different as the possible arising wedge in the future mining area.

If the anchor type is changed a recalculation has to be done. If, for instance, an anchor type with a higher anchor strength is used, the anchor amount is reduced.

7.6.2 Support walls

7.6.2.1 General support wall

In this chapter the general support for the walls in the main development and the stopes is presented. The virgin walls remain as stable. If, in example, the pillar is cut across by a geological discontinuity, the area at the outcrop has to be supported against stone fall, since the possibility is given that at the disturbed zone, single stones drop out of the structure of the pillar or walls.

An example of the pillar between stope 1 and 2 including a fault of the fault system “ksys95”, with a dip direction of 110 [°] and a dip of 85 [°] (see chapter 4.2.4), is presented in Figure 157.

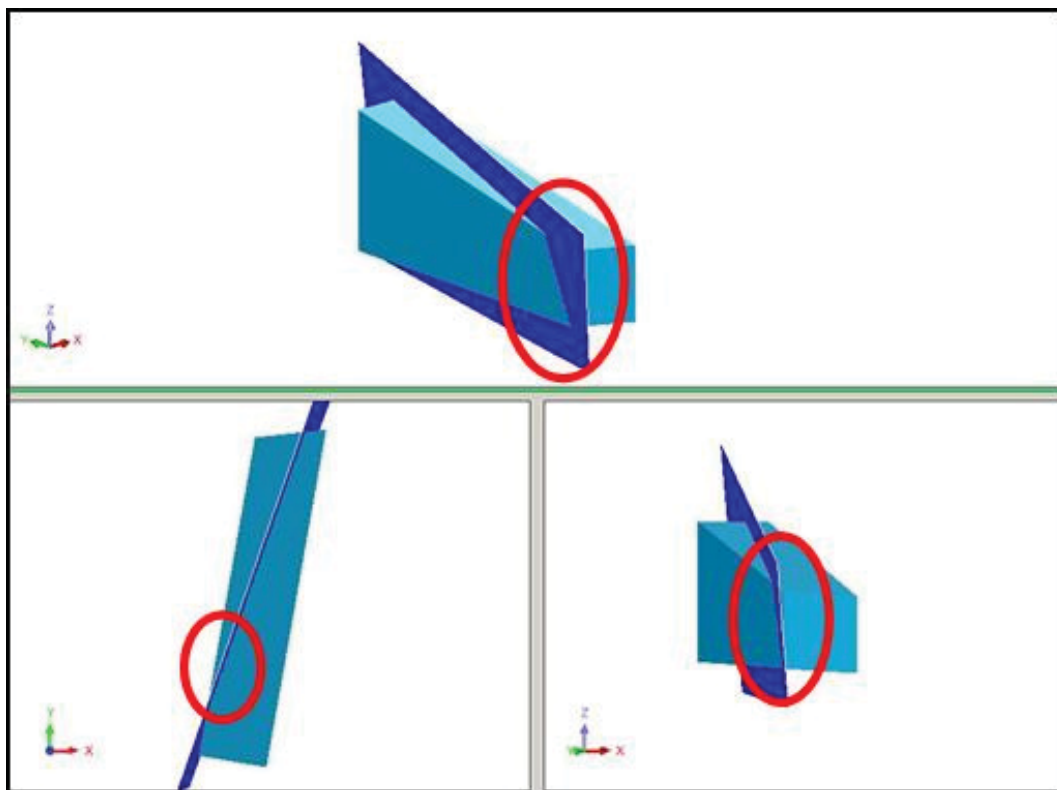


Figure 157: Strip pillar with fault, Surpac

The red circles in the figure above, exemplarily highlight possible stone fall areas. Due to the fact that the visibility in 6 to 12 [m] high rooms is decreased or non given and therefore a detection of loose material, a general support against stone fall is suggested which should be applied for each wall (main development and stope). In Figure 158 the suggested general support is presented.

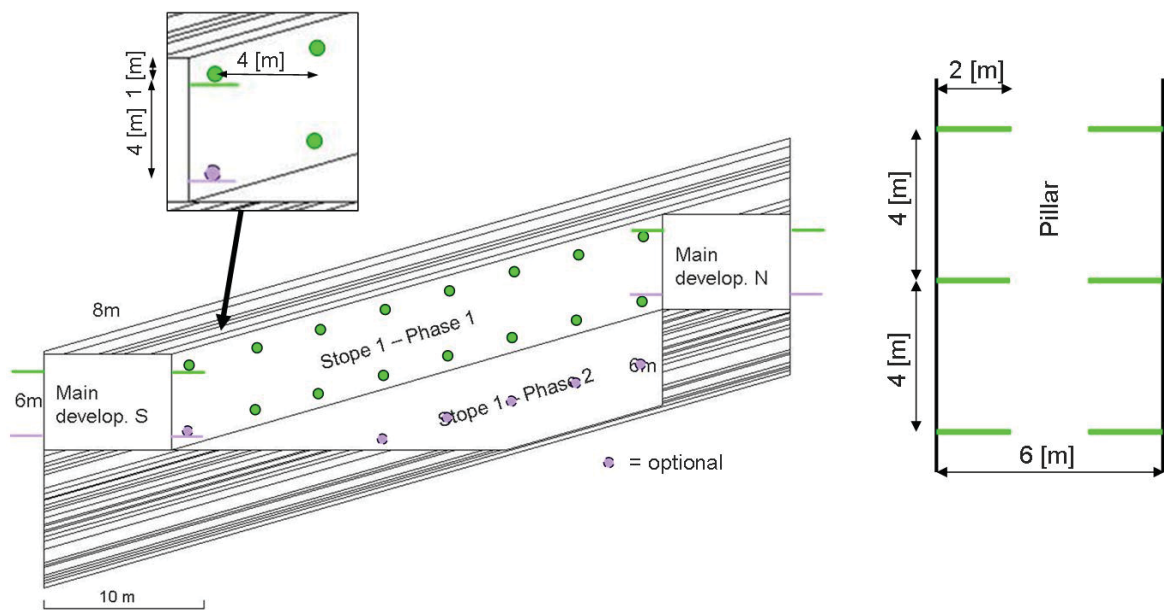


Figure 158: General support for the walls

The in the figure above presented support for the walls is installed in that manner that in 6 [m] high rooms (main development and stope 1 – phase 1) one anchor row 1 [m] below the roof is set. The distance between the anchors is 4 [m]. The main purpose of the anchors is to fix the net, which covers the whole wall. If a stone falls out of the wall, it is prevented by the net to fall into the middle of the room and slides between net and wall down to the edge floor – wall. This results in the suggestion, that the staff must not stay at the walls, except it is strictly necessary (maintenance,...).

The anchor row at the top of the wall additionally fixes the overlapping net of the general support of the roof (see chapter 7.6.1.1 and 7.6.1.2) and therefore the whole roof, including the edges (wall – roof), is covered and supported against stone fall.

After phase 1 at the stope, is extracted and phase 2 is started to be mined, an additional row of anchors is suggested. The anchors are set 1 [m] above of the floor of phase 1. With this anchor row either the ongoing net from phase 1 is fixed and/or a new net is fixed additionally if the net length of phase 1 is too short to reach the final height of the stope.

The presented purple anchor row (see Figure 158) is optional for heavy disturbed areas.

The net for the main development should be, as for the roof, corrosion resistant, since the lifetime is uncertain. The net for the stope has not to be compulsive corrosion resistant, since the residence time is less as at the main development. The lifetime of the main development and the stope is mainly depending on the yearly extraction amount.

The anchor length can be reduced to 1 [m] if the anchor, in combination with the net, is only set for stone fall protection. If the anchor takes over a further duty, in example reinforce small rock wedges, the anchor length should remain at least, as shown in Figure

158, with 2 [m]. The validity of the length of the anchor has to be determined at the development and mining itself, in example, by geological mapping.

With the in chapter 7.6.1 presented general support of the roof and the above presented support for the walls, the main development could look similar to the in Figure 159 presented illustration. (Note: The amount and the installation of the support as well as the profile of the stope are not applying in any kind to the mine Mazy. It serves only as an illustration, to gain an impression of the final look.)



Figure 159: Example/Illustration of possible final lookout of main development including support (Tensor 2012⁸)

⁸ Source: <http://www.tensor.co.uk/Applications/Mining-Roof-and-Wall-Support#>, (01.08.2012)

7.6.2.2 Special wall support - wedges

Besides the general wall support for stone fall protection, an additional support for possible wedges is presented. The design of the support of wedges is presented on hand of the example below. It has to be noted that this example shows the approach to a solution and design and does not replace a detailed surveying at the development and the mining itself. Only with a geological mapping, wedges and possible (not here mentioned) safety issues can be detected and reacted on it. At this stage no security of completeness in case of special cases can be given.

The outlay for the support for wedges within the walls is presented on hand of the example of the strip pillar between stope 1 and 2. The pillar is cut through by a fault of the fault system "ssys010" (see chapter 4.2.4). The dip direction of the in Figure 160 presented fault is 10 [°] and the dip 60 [°].

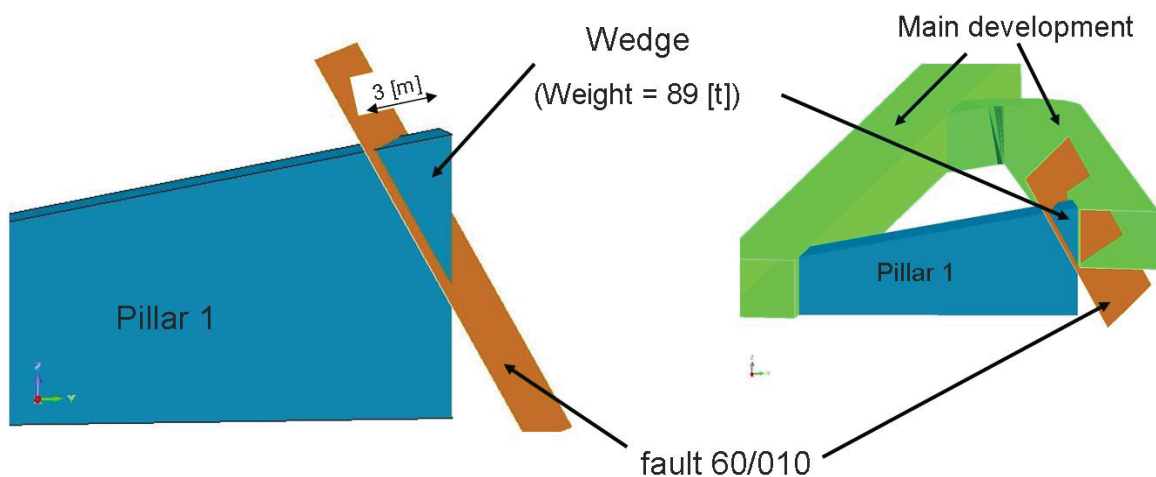


Figure 160: Special case wall, wedge, example, Surpac

As shown in the figure above, the possibility is given that wedges arise. The example above shows that the fault cuts through the end of pillar 1 (between stope 1 and 2). The alignment of the fault results that no abutment for the wedge is present. If the fault is filled with clayey material the remaining force against sliding is the connection between the layers and therefore the sliding is possible. To prevent a safety issue, the from Hoek (1980) suggested formula is used to calculate the necessary force which prevents the wedge from sliding (see Formula 42; cp Hoek 1980, p. 248).

$$T = \frac{W * (FOS * \sin(\psi) - \cos(\psi) * \tan(\phi) - c * A)}{\cos(\theta) * \tan(\phi) + FOS * \sin(\theta)} \quad (\text{Formula 42})$$

T...	Total load of anchors	[N]
W...	Weight of block	[N]
FOS...	Factor of Safety	[-]
Ψ...	Dip of sliding surface	[°]
Φ...	Angle between the plunge of the anchor and the normal to the sliding surface	[°]
c...	Cohesion	[Pa]
A...	Area of sliding plane	[m²]
Θ...	friction angle of sliding plane	[°]

Before the formula is presented in detail the append ant sketch is presented in Figure 161.

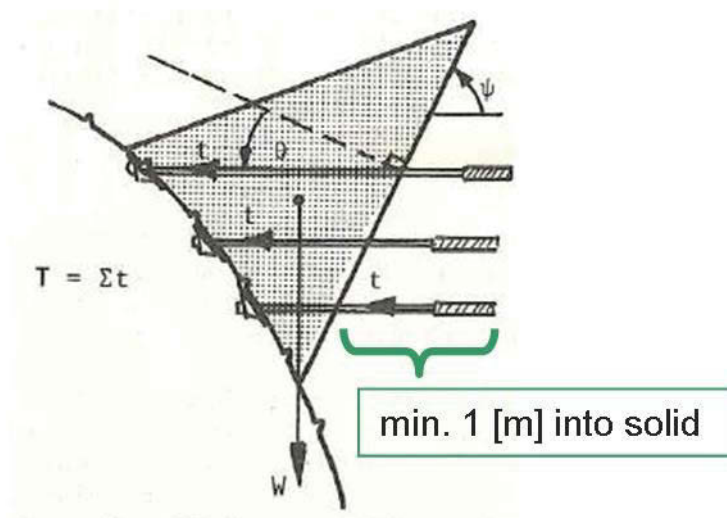


Figure 161: Sketch of support to reinforce a wedge against sliding (cp. Hoek 1980, p. 247)

As shown in the sketch in Figure 161 the total load of the anchors (T, see Formula 42) is the sum of the load of each anchor. The “weight” (W) of the block is the volume times the density times the gravitational acceleration. The volume of the block for the in Figure 160 presented example was read out by Surpac and amounts 33 [m³] and therefore a weight (W) of 871 [N] result. The factor of safety (FOS) is set to 2, since, especially for this example, the main development would be affected. As dip for the sliding surface (ψ), the dip of the fault is used.

When the wedge is shaped in that manner that the sliding would occur along the line of intersection of two planes, the presented formula gives a first approximation of the required support. The dip or plunge of the line of intersection of the 2 planes should be used as ψ . (cp. Hoek 1980, p. 248).

The friction angle (Φ) of the sliding plane is estimated with 15 [°], which is the friction angle of the filling of the fault and therefore, in this example, the friction angle of clayey material. The cohesion (c) is estimated with 0 [Pa]. (cp. Hoek 2007, chapter 4, p. 11)

The area of the sliding plane (A) of the example was determined with Surpac and amounts 28 [m²]. Due to the fact that the cohesion is 0 [Pa], the term “c*A” remains 0 [N] and therefore no force against sliding is resulting by cohesion.

The angle between the plunge of the anchor and the normal of the sliding surface (θ) is around 30 [°] in this example. The angle is resulting by the assumption that the anchors are installed perpendicular to the wall.

As shown in Figure 161 the same suggestion is done as for wedges within the roof. The length of the anchor through the wedge (if possible) and the length of the anchor in the ribside should be at least 1 [m]. It has to be determined in each single case which anchor length is sufficient to reinforce the wedge. (see chapter 7.6.1.3, “wedges” and cp. Hoek 1995, p. 61 f).

With the above presented values the anchor amount with a load at yield strength of 157 [kN]⁹ can be calculated (see Table 55).

Weight of wedge (W)	89	[t]
	871	[kN]
Area of sliding plane (A)	28	[m ²]
Dip of sliding surface (ψ)	60	[°]
Angle between anchor and the normal to sliding surface (θ)	30	[°]
Chesion (c)	0	[N/m ²]
Friction angel (φ)	15	[°]
Factor of Safety (FOS)	2	[-] 1)
Load of the anchor (T)	1129,5	[kN]
Excavation Face Area	28,0	[m ²]
Load per m ²	40,3	[kN/m ²]
Anchor strength	157,0	[kN/A] 2)
Anchor density	0,26	[A/m ²]
Anchor amount	7,2	[A]

Table 55: Results of anchor amount for special case wedge, wall

⁹ A detailed description of the anchor type as presented in chapter 7.6

As shown in the table above an anchor amount of 7,2 is resulting. Therefore an anchor amount of 8 anchors is suggested to reinforce the wedge against sliding. The anchor length is depending on the thickness of the wedge at the position where the anchor is installed. Near the roof the thickness of the wedge is between 3 and 1,6 [m]. Therefore an anchor length for the anchors near the roof of at least 4 [m] is suggested, depending if other influencing constraints are present (further geological discontinuities, etc.). The anchor should be installed in a regular distribution, although with concentration on the greatest thickness (in this example near the roof). A suggestion of the distribution of the anchors for the example is shown in Figure 162, based on the front view of the wedge (Note: it is a sketch)

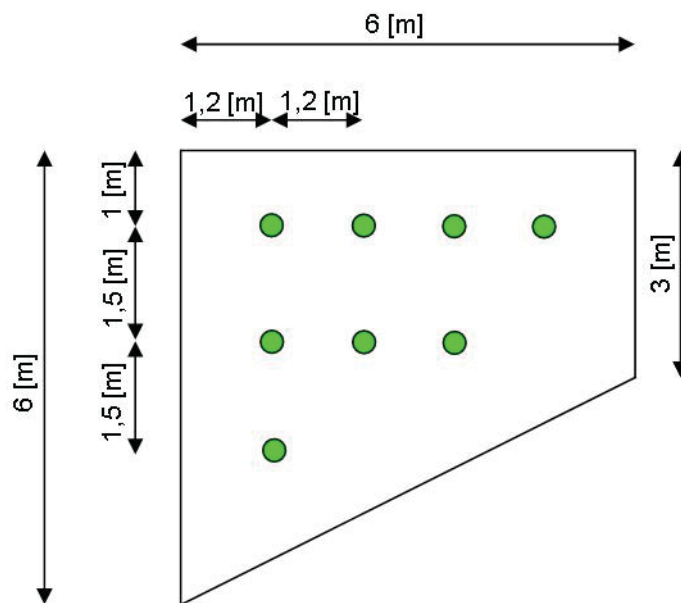


Figure 162: Anchor distribution, special case wedge, wall, plan view, sketch

7.6.3 Support floor

At the main development north the floor has to be supported since the profile (side view) cuts through the layers in that manner that single layers are not connected to the ribs side. Therefore a support to increase the shear forces and to connect those “loose” layers is suggested. The design of the support is presented in Figure 163.

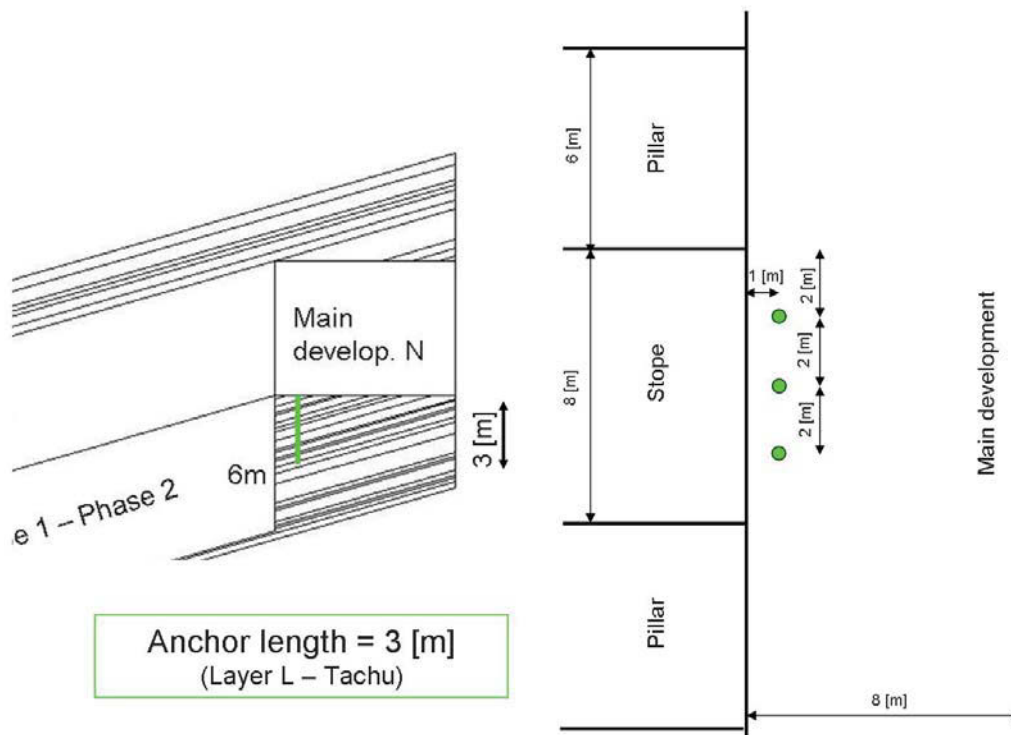


Figure 163: Support floor

As shown in the figure above the anchors with a length of 3 [m] reach 5 layers (Layer L – Tachu) which are connected to the ribs side. By installing the support the layers above Layer L are reinforced and connected to the layers below. A anchor row with 1 [m] distance from the edge “end” of stope – main development north, with a distance to each other of 2 [m], is suggested.

This support covers the virgin state of the floor of the main development. If geological discontinuities are present a review of the situation has to be done and the support adapted in a proper way.

It is suggested that the installation of the anchors is done before phase 2 at the stopes is applied. This results that mining phase 2 happens under reinforced conditions.

As anchor type the same active resin anchors as for the rest of the support (roof and wall) are suggested. An example for an anchor is presented in chapter 7.6.

7.7 Summary – south

In this chapter the layout of the possible future mining area south of variant “12 [m]” is summarized. This summary presents only a short overview of the determined basic dimensions and pays no attention on the necessary constraints (see chapter 7– 7.6.3).

The width of the room is 8 [m] (see chapter 7.2) at a mining height of around 6 [m] to 12 [m], dependent of the chosen variant (see chapter 7.4.1). The strip pillar has a width of 6 [m] and is situated nearly into north – south direction (see chapter 7.4).

The inclination of the main development south is about 3 [°] and of the main development north around 1 [°] into the east. The inclination of the stope of phase 1 is around 11 [°] and of phase 2 around 1 [°] into the south. (see chapter 7.4)

Between the main development north and the current mining area a barrier pillar of 8 [m] is installed (see chapter 7.4). The barrier pillar between the main development south and the major fault “south” is at the current data bases 8 [m] (see chapter 7.5).

As already mentioned in the previous chapters, with the determination of the exact position of the major fault “south”, as well as gaining knowledge of the rock mass conditions near the fault, by core drilling, the design and outlay of the future mining area south has to be recalibrated. The presented values represent a first approach and have to be adapted to the real situation. Furthermore, through the alignment of the main development south the possibility is given that a fault of the, at the fieldwork detected fault system (60/010; see chapter 4.2.4), runs parallel within the southern wall. Even if no outcrop is present at the wall a major “wedge” over the whole length of the main development could arise. These facts underline the importance of determining the position and the rock quality of the surrounding rock mass by at least core drilling.

8 Northfield

In this chapter the access and the outlay of the future mining area north is presented. The basis of the north field is presented in chapter 6.6 (see Figure 109), and used to determine the detailed design of the future mining area north. As described in chapter 6.6, the basis was developed by following the alignment of the current mining area north. It is suggested to perform a drilling program to gain certainty of the position of the deposit.

As stated from sides of the company, the outlay of the pillars and the rooms are done for the total thickness of the deposit – 12 [m]. The model within this thesis is done for the first phase which considers the extraction of the lower 6 [m], since the quality of the upper layers is questionable in terms of sale-ability caused by the nearness to the surface and therefore the possible weakened quality.

The superordinated long-term mine development intends that first the future mining area south is mined and afterwards the future mining area north. Therefore the presented outlay represents the apportionment of the investigations which were done for the future mining area south to the area north. Additionally the borders of a possible expansion into the north and west are not defined. This result, that only the basic outlay and the alignment of the access is presented. It is suggested that with the experience, which is collected by mining the future mining area south, the future mining area is redesigned and recalibrated.

8.1 Access to future mining area north

From the basic access within the current mining area (see chapter 6.7) the access to the possible future mining area north is designed. The profile is 5x5 [m]. The basic alignment (green) is shown in Figure 164, on hand of the plan view of the mine.

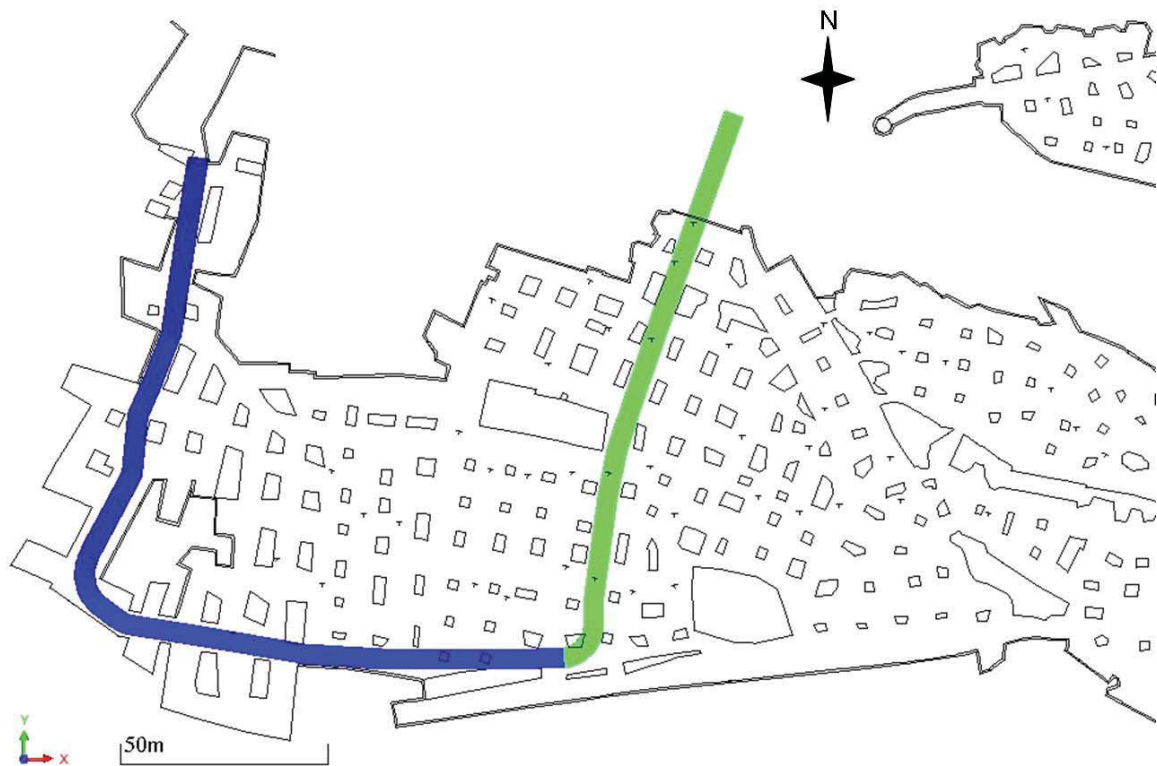


Figure 164: Access to the future mining area north, alignment, overview

To reach the lower levels of the future mining area, the access submerges under the floor of the current mining area (see Figure 165).

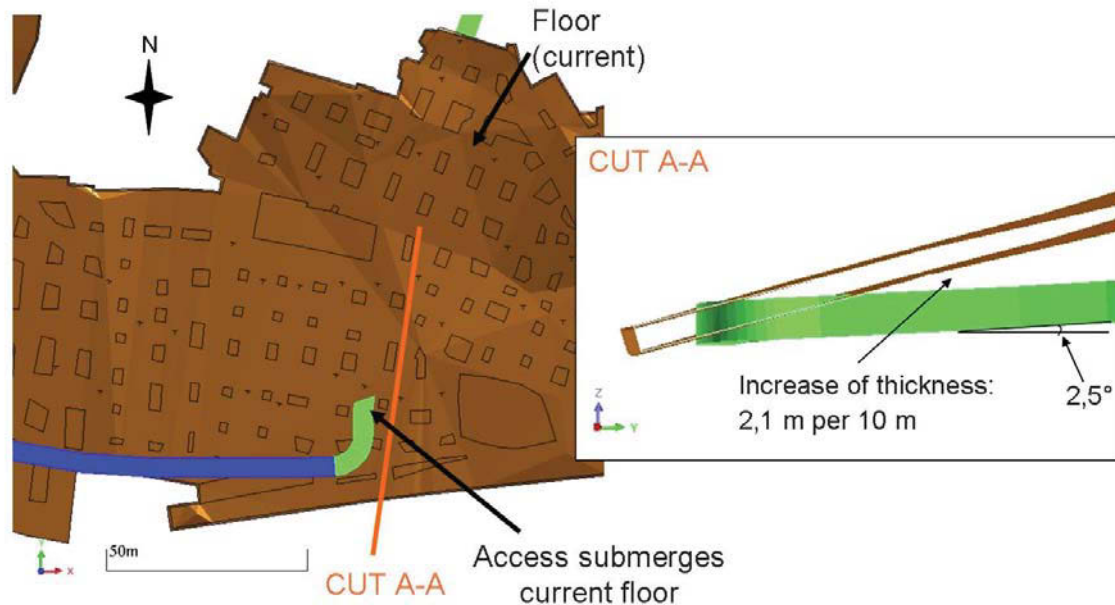


Figure 165: Alignment access to future mining area north, point of submerge and side view

The alignment is set in that manner that no pillar of the current mining area is undermined. To reach the point where the access submerges, the backfill (see chapter 4.3.1) has to be removed. The outlay of a proper support for this area is not part of the master thesis, although it is mentioned at this point. The support has to prevent any movement of the remaining backfill in the current mine especially against falling into the access. Furthermore the sharp edge of the remaining layers, where the access submerges, has to be supported in that manner that the roof (or floor of current mine) does not collapse. A collapse would additionally affect again the backfill of the current mine in this area. The walls need a general stone fall protection, since the final height at the point where the access submerge is $\sim 8,3$ [m] (= height of access + vertical height of room, current mine).

As shown in Figure 165 (left part), the thickness of the layer between the roof of the access and the floor of the current mine increases with 2,1 [m] per 10 [m] horizontal development. The access has a constant inclination of 2,5 [°] into the south. The inclination causes that the possible incoming water is directed into the south.

The cut through the major fault “17m” is not part of the master thesis but some suggestions or possible tasks are mentioned at this point. The access cuts through the major fault “17m” (see chapter 4.3.4.3) nearly perpendicular. The profile should be as downsized as possible at the cut through, to minimize the necessary support. Although, the size of the profile has to be big enough, to ensure that the planned machinery can pass through safely. Similar to the connection passage of the north and the south field of the current mining area, the need for a heavy reinforcement is probable. Furthermore it has to be considered that the rock mass at and near the fault can be heavily disordered and the water income can increase. If the rock mass is disordered in that manner that a

safe opening or passing through is not possible, an anticipatory reinforcement could be necessary. In any case an experienced expertise is suggested to be present at the cut through the fault. The placing of this issue to an external should be taken into consideration.

8.2 Outlay – future mining area north

After passing the major fault “17m” the access leads after 8 [m] (horizontal) into the main development south for the future mining area north. The alignment of the main development south runs parallel to the major fault with a horizontal distance of 8 [m], which represents the barrier pillar. The distance of 8 [m] is the same as for the barrier pillar south in the future mining area south (see chapter 7.5). Although the calculation of barrier pillar between the major fault “17m” and the main development south (north field) is less than 8 [m] due to the fact of less overburden – after the similar simplified model as in chapter 7.5 – this distance is seen to be adequate. Nevertheless the determined thickness of the barrier pillar is, as for the future mining area south, a first estimation and is strongly depending on the dominating situation of the distraction and quality of the rock mass by the influence of the major fault “17m”.

Since the mining method remains the same, the outlay is similar to the outlay for the south field. Strip pillars with a local alignment perpendicular to the main development and a global alignment nearly into dip direction (~ south). As already mentioned in chapter 8, the outlay of the dimensions are done for the whole thickness of the deposit (12 [m]), although the 3D model is designed for the first phase of superordinate mining sequence, which foresees the extraction of the lower 6 [m]. The design was done “only” for the lower layers since, according to the statement of the company, the quality of the upper layers is questionable due to the reason of the lower thickness of the overburden.

The width of the room is set to 8 [m] (with a height of 6 [m]), based on the results of the investigation for the room width at the south field (see chapter 7.2). The assumption has been taken that a similar quality of the roof strata is present in the future mining area north. To prove this assumption a geological mapping during the mining activities is suggested with a following update and recalibration of the found situation.

The thickness of the strip pillars remains with 6 [m]. Although the thickness of the overburden is less ($H_{\text{overburden,south,max}} = 75$ [m]; $H_{\text{overburden,north,max}} = 43$ [m]) and as a consequence thereof the vertical stress (σ_v) is decreased, a lower width of the pillars is resulting out of the theoretical calculations. Nevertheless a width to height ratio smaller 0,5 [-] is not suggested. Esterhuizen proposes that slender pillars with a width to height ration smaller than 0,8 [-] should be avoided due to their sensitivity to the presence of angular discontinuities (cp. Esterhuizen 2011, p. 49). In this case the undershoot of the width to height ratio is countered with a high factor of safety (FOS (43[m]) = 9,8 [-]; including a mitigation after Esterhuizen of 43 [%] for joint band 2, 85/110). Nevertheless a geological mapping is inevitable to react on possible unfavorable constellations of faults and joints influencing the pillar. If an unfavorable constellation occurs the width of the pillar has to be increased in that manner that stability is ensured.

With the previous mentioned values the outlay of the future mining field north is presented in Figure 166.

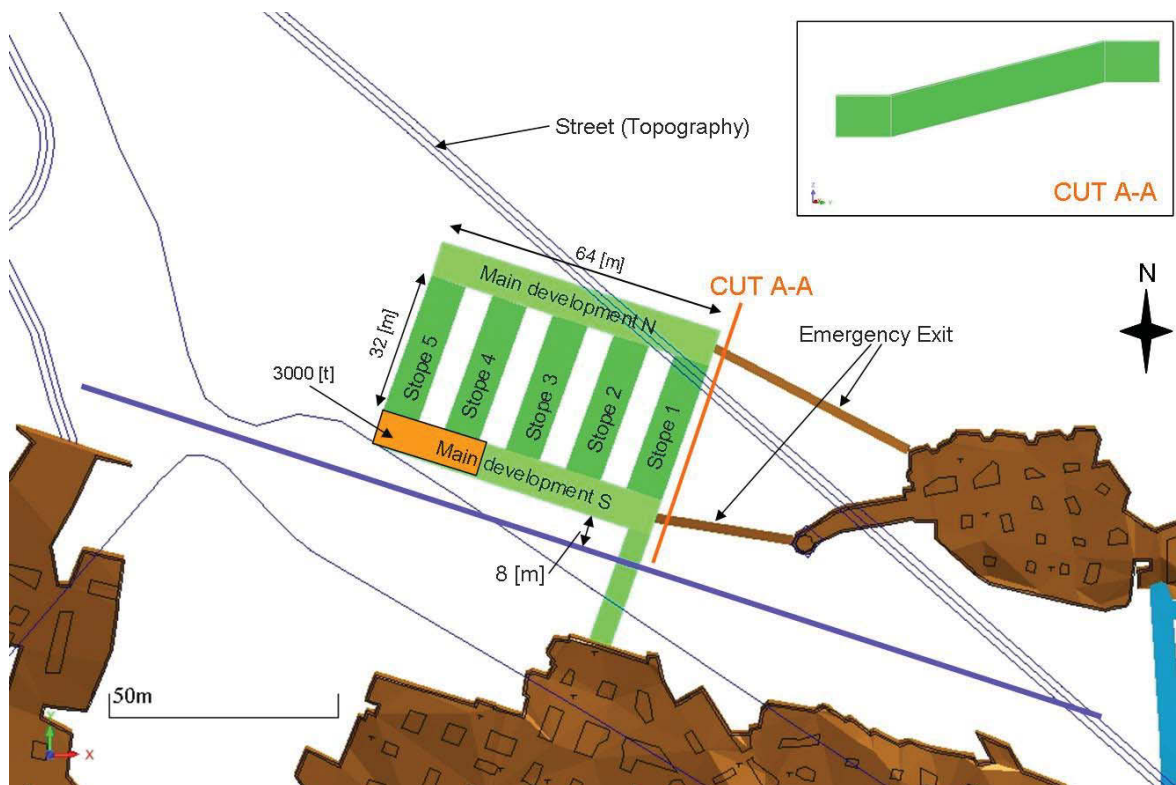


Figure 166: Outlay future mining area north

In the right corner in Figure 166 the profile or side view of the extraction is presented. As already mentioned the design in the 3D model is done only for the extraction of the lower layer (6 [m]) of the deposit.

The main developments have an inclination of ~ 5 [°] into the south – east. The stopes have an inclination of 14 [°] into \sim south. This concludes that the possible incoming water amount is conflating in the south – east and is guided by the access from the north field to the current northern border of the current mining area. From there the water is guided by the existing water flow direction to the main catch of the water collection at the current mining area and can be used as additional saleable water amount.

The determination of the length of the stopes (32 [m]) was influenced by two constraints. The first constraint is the geomechanical classification system and therefore the stability of the roof. As for the future mining area south, the stopes remain in the stable areas of the used classification systems with a viewed length of 40 [m] at a width of 8 [m] (see chapter 7.2). The viewed length results by taking two times the half span of the main developments into account ($32 + 2 \cdot 4$ [m]). The second constraint was stated by the company, that the design and outlay should not exceed with great distance the alignment of the street running on the surface (see Figure 166).

After five stopes a barrier pillar is suggested. This suggestion limits the length of the main development to 64 [m]. Globally seen, the in Figure 166 shown outlay represents a module. A second module into the west was not added since the border of the entrance is determining the limit into the west expansion. If the constraint concerning the border of the street is suspended, a further expansion into the north is possible. Although a limit concerning the through the dipping and the alignment of the deposit resulting decrease of thickness to the overburden into the north is set. The company stated that a minimum thickness of the overburden of 20 [m] has to be left. In the presented outlay the thickness of the overburden, according to the current Surpac model, is ~ 32 [m], pertaining to the western edge of the main development north. If the full thickness of the deposit is mined, the thickness of the overburden decreases to 26 [m]. Therefore it is questionable if a second module is applicable into the north. A possibility is that from the main development north, of the presented outlay, single stopes are headed into north until the limit of 20 [m] thickness of the overburden is reached and/or the quality drops due to the nearness of the surface.

Although the following possibility is excluded for further investigations within this thesis due to law regulations and ownership constraints, it is mentioned at this point. Through the nearness of the deposit to the surface a change form underground mining into open pit mining should be considered as a possibility and rechecked before the project “future mining area north” is realized. The change of underground to open pit mining would increase recovery to nearly 100 [%]. This includes that the quality of the material through the nearness of the surface is given.

According to the in Figure 166 presented outlay or module following volume can be extracted (see Table 56).

Future mining area north		
Main development north	3058	[m ³]
Main development south	3058	[m ³]
Stope 1	1482	[m ³]
Stope 2	1482	[m ³]
Stope 3	1482	[m ³]
Stope 4	1482	[m ³]
Stope 5	1482	[m ³]
Sum	13526	[m ³]
	36385	[t]

Table 56: Volume of outlay for future mining area north

As shown in the table above, the possible resources are 36.385 [t] This figure represents the theoretical value with no loss included (100 [%]). For the conversion from [m³] to [t] the in the laboratory tests gained density of 2,69 [t/m³] is used.

At the current mine ~ 60 [%] loss occurs, related to the complete mining height of 3,2 [m] (incl. the blasted “layer”). Since the mining method is changing from blasting and cutting to

exclusive cutting, a figure for the loss is not known at this stage and therefore the total possible extractable material is quoted.

Starting from the main developments, two emergency exits to the current mining area north are suggested, with the alignment presented in Figure 166. The emergency exit north has, based on the presented outlay, a slope length of ~48 [m] and an inclination of 5 [°] into the west. The emergency exit south has a slope length of 31 [m] and an inclination of 16 [°] into the west. The designed profile is 2x2 [m]. If the borders of the future mining area north are defined and known, the possibility of a shaft in the north – west should be taken into consideration. A shaft, with the proper installation (ladder), would replace one emergency exit from the current outlay and furthermore sustain the ventilation.

The support of the walls and the roof of the possible future mining area north are equal to the suggestions for the possible future mining area south (see chapter 7.6). The for the future mining area south presented suggestions in terms of support are only first approaches and the given examples do not claim to be exhaustive. Only with a geological mapping and an adequate supervision of the advancing and previous extraction, the possibility is given to reduce safety hazards and to react probably to unfavorable constellations and situations.

At this point it has to be mentioned that due to the support and the change of phase 1 (north: lower layers; south: upper layers), the upper layers and blocks are perforated by the drill holes for installing the anchors of phase 1. The two main questions, concerning the fact of perforation are once, if the drilling decreases the saleability of the layers above and secondly if the layers above are saleable at all, concerning the quality. These two questions have to be solved before implementing the plan for the future mining area north by further investigations (e.g. core drilling).

8.3 Summary – north

In this chapter the layout of the possible future mining area north is summarized. This summary presents only a short overview of the determined basic dimensions and pays no attention on the necessary constraints (see chapter 8– 8.2).

The width of the room is 8 [m], as for the future mining area south (see chapter 7.2). The mining height is around 6 [m], since the layout for the future mining area north is only done for the lower levels. The strip pillar has a width of 6 [m] and is situated nearly into north – south direction (see chapter 8.2).

The main developments have a length of 64 [m] and an inclination of around 5 [°] into the east. The stopes have a length of 32 [m] and an inclination of around 14 [°] into the south. (see Figure 166, chapter 8.2)

The barrier pillar between the major fault “17 [m]” and the main development south has a width of 8 [m] (see chapter 8.2).

As for the future mining area south, the presented values are first approaches and have to be recalibrated by taking the real situation, e.g. rock mass, into consideration.

9 General Safety aspects

In this chapter the during the thesis detected and recognized main improvements in terms of safety are listed, although the topic “safety” was no superficial point within this thesis and the fieldwork. These below mentioned points are suggestions and neither surrogate any kind of risk assessment or detailed investigations in terms of safety nor is claimed to be complete. Furthermore a detailed explanation of the equipment and the suggestions is not done within thesis.

The suggested improvements are summarized in 4 fields and presented below.

9.1 Equipment employees

During the fieldwork it was recognized that improvements in terms of safety direct on the staff is possible. Suggested further main equipment for each miner is:

- Self rescue kit
- Mine lamps
- Safety boots (according to the current state of technology)
- Ear protection (according to the current state of technology)

Ad 1. A self rescue kit is a small unit which delivers, dependent on the model, for a certain time respirable air in case of emergency. The kit is carried on the person or is placed on an immediately reachable position. It is suggested for each worker for the current mining operation and especially for the future mining operation. If the bad weathers are increasing, in example by a fire at the drilling rig, a secure escape has to be guaranteed to reach one of the 3 basically possible exits (entrance, main- and weather shaft). The time to reach one of the exits is increasing with the use of the self rescue kit and therefore significant time is won for the safe escape and the self rescue by the miner itself. Especially for the future mining areas, where the duration to reach one exit is increasing by increasing distance, the importance and the necessity is given. An example of a closed, unpacked and “in use” self rescue kit is shown in Figure 167.



Figure 167: Self rescue kit, closed (left), unpacked (middle), in use (right); (cp. Dräger 2012)

Ad 2. At the moment the staff uses hand carried torches. The use of a torch at the current mining area is not permanent required since at the working area fixed floodlights are installed. However a fixed mine lamp on the helmet is suggested so that a source of light is given in case of a malfunction of the power supply. Furthermore, by using mine lamps, both hands are available for use (e.g. for using self rescue kit).

9.2 Installations

To improve the orientation at the set routing cords in the northern secondary or emergency exit (see Figure 168), additional cones are suggested to install.

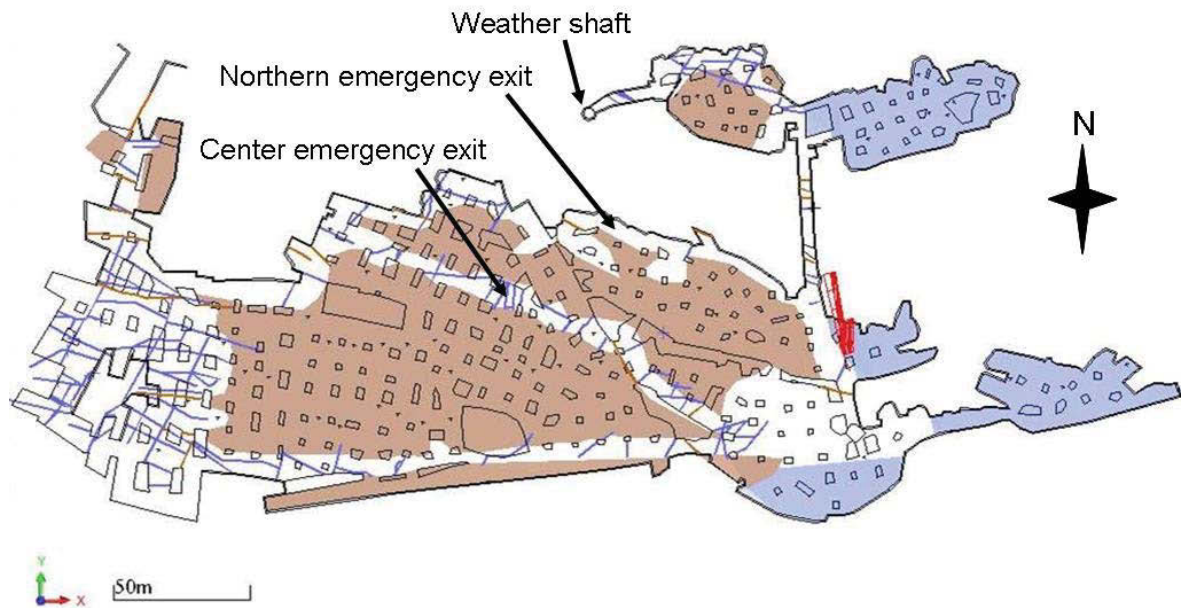


Figure 168: Position of northern emergency exit, plan view, Surpac

The routing cord is installed to ensure in case of emergency and visibility of the surrounding (e.g.: smoke, failure of torch,...) a safe guidance to another exit. The installation of the cones ensure the knowledge of the direction which someone goes, by sliding with the hand over the head of the cone to the bottom of the cone back on the routing cord. A at the fieldwork taken photo of the routing cord and a sketch of the installed cones is presented in Figure 169.

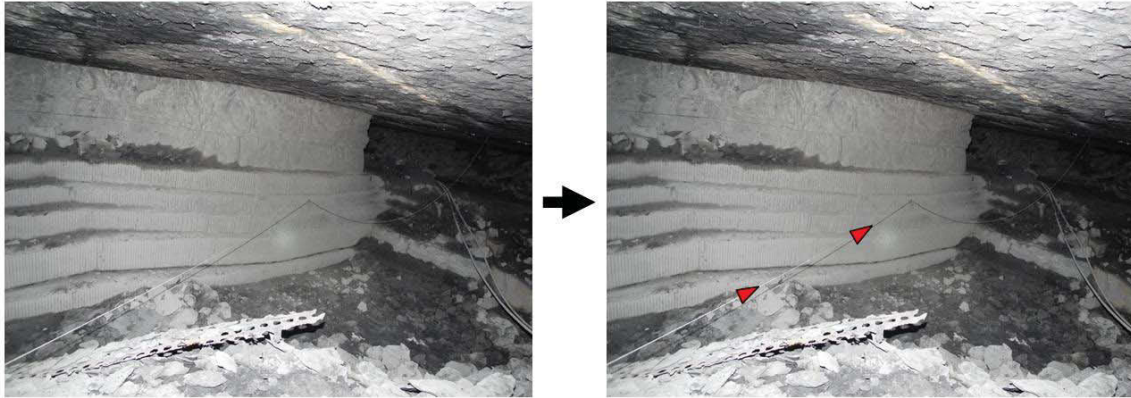


Figure 169: Routing cord and cones (right: current; left: suggestion)

Additionally it is suggested to install a routing cord inclusive cones also at the center emergency exit (see Figure 168). The direction in which the cones are leading, are mainly dependent on the direction of weathering and have to be (re-)evaluated, especially if the future mining operations are performed.

The installation of the cones and the additional routing cord only make sense in combination with a self rescue kit (see chapter 9.1). If, in example, a fire decreases the view to a minimum by the arising fume and therefore the amount of bad weathers within the mine increase to a toxicological concentration, the secure use of the routing cords, and the save escape, is only given if the supply with fresh air (self rescue kit) is given for the escaping person. This underlines the necessity of self rescue kits.

At the weather shaft (see Figure 168) the fan for the weathering of the current mining operation is placed (see Figure 170).



Figure 170: Fan at the weather shaft

The weather shaft represents besides the main shaft and the entrance the theoretically third exit. To ensure a safe accessibility a bypass, in form of a door, at the ventilator and a ladder in the weather shaft is suggested.

9.3 Weathering

Although it is not part of the thesis it has to be mentioned at this point that by applying the design for the future mining areas, the concept of the weathering has to be adapted and redesigned.

With the realization of the future mining areas, the geometry, concerning the weathering, changes and therefore the current ventilation is seen as insufficient. The capacity of the current ventilator has to be checked if it has the ability to ensure an adequate weathering. An auxiliary ventilation has to be considered at the development and the mining in separated mine workings (e.g. access to future mining areas). Furthermore the planned new diesel machinery represents an additional source of bad weathers (exhaust gases) and a further source for fire. These above mentioned aspects, besides further ones, have to be taken into consideration to layout an adequate ventilation system, to ensure safe working. In any case, a gas measuring equipment is suggested, to check the weathers on the way to and at the working place.

9.4 Additional machinery

At the current mining area the mining height is 3,2 [m]. Within this height the reachability of the roof is possible by using the current equipment. In the future mining areas the room height is at least 6 [m] and therefore an additional equipment to reach the roof safely is suggested. The reachability of the roof is necessary to control and install in example support and supply (like ventilation ducts, electricity,...). In the following, basic ideas are presented of possible equipment. No concerns in terms of dimensions have been taken and the examples only represent basic possibilities. No security of completeness is given. Furthermore no considerations in terms of equipment for the staff to ensure the safe use of the presented examples have been done.

The simplest equipment is a framework as shown in Figure 171.



Figure 171: Additional equipment, framework (cp. Accipo 2006¹⁰)

To use the framework the floor has to be almost horizontal and therefore this equipment can only be used in the main development south and north of the future mining area south.

The next example is a chain mounted lifting platform which is designed for uneven ground conditions, including inclinations (see Figure 172).

¹⁰ Source: <http://www.accipo.de/products/Gerueste/Stabilo-Profi-Fahrgerueste/Geruest-KRAUSE-Stabilo-Serie-5000-25-AH-530-m.html> (10.08.2012)



Figure 172: Additional equipment, chain mounted lifting platform (cp GL Arbeitsbühnen Verleih¹¹)

The chain mounted lifting platform is, depending on the model, basically in all the future mining areas applicable.

The third example is a on the boom of the wheel loader mounted working platform. The in Figure 173 shown picture is only exemplary to highlight the concept. If a lifting platform is available for the planed wheel loader, has to be cleared up with the final producer of it.

¹¹Source: http://www.gl-verleih.de/Vermietung/Arbeitsbuehnen/LEO_30_T_28.html?product_id=105 (10.08.2012)



Figure 173: Additional equipment, lifting platform mounted on the loader, exemplary (cp. Kran & Hebetchnik 2007¹²)

The applicability of the in Figure 173 shown working platform within the future mining areas, is connected to the applicability of the loader. Up to now the question remains unclear up to which inclination a wheel loader, as exemplary presented in chapter 6.1, is able to work in safe conditions. Furthermore it has to be questioned, if drilling (e.g. anchors) is possible from the extended platform.

¹² Source: <http://www.kran-und-hebetchnik.de/news/arbeitsbuehnen/did1085250/arbeitsbuehne-als-anbauloesung.html> (10.08.2012)

10 Discussion

The proposed outlays for the possible future mining area south and north (see chapter 7 and 8) represent a first approach. Especially at possible future mining area south the position of the major fault “south” is crucial. It is suggested to perform an exploration, by core drilling, to determine the exact position of the major fault “south” and to gain knowledge of the rock mass at and near the fault. Furthermore, due to the final layout, the possibility is given that a geological discontinuity runs parallel to the main development south. Only by detecting such discontinuities, e.g. by core drilling, the main development can be (re-)placed in that manner that an unfavorable geomechanical situation is prevented. With this obtained information the outlay can be adapted and adjusted to the real situation.

At the possible future mining area north a core drilling program (e.g. from surface) is suggested to gain knowledge of the position of the deposit. The outlay, presented in chapter 8, is based on the assumption that the deposit is following the alignment of the current mining area north. Additionally, the cut through the major fault “17m” represents a challenging project which has to be handled with great care and the necessary expertise and experience (see chapter 8.1).

Furthermore a core drilling program is suggested to ensure the position of the abandoned mine in the west to the current mining area (see chapter 4.3.4.2 and 6.4).

The suitability of the planned deployed machinery (see chapter 6.1), which are preferred from the company, has to be rechecked. The maximum height of the wheel loader which the bucket can enter the cut blocks parallel to the floor of this machine is 4,26 [m] (cp. Volvo 2007, p. 30) – at a mining height of around 6 [m]. How far the loader can lift the first uppermost block, at a nominal load of around 10 [t], will strongly depend on the cutting geometry. Furthermore no statement can be given at this stage up to which angle/inclination the wheel loader can operate, especially in the stopes which evince the greatest inclinations (11 – 14 [°]).

To ensure that the new mining method and as a consequence thereof the increasing mining dimensions, can be performed as safely as possible, a detailed geological mapping and a supervision of the operation is inevitable. Due to the fact that the heights of the pillars increase, the influences of the geological discontinuities increase as well. Only with a detailed ongoing investigation a reaction on unfavorable constellations can be done. With the mapping, the performed dimensioning has to be evaluated and, with regard of the mapping gained intelligence, complemented.

A special focus has to be put on the support. Since the mining height is increasing, the view ability of the roof and walls are decreasing. The presented support or reinforcement within this thesis is suggested as regular support and takes no unfavourable constellations

of geological discontinuities into consideration (see chapter 7.6). Only with a detailed surveying and a geological mapping the support, besides the regular presented one, can be set in the right position and with the correct amount. Furthermore a recheck from time to time, of the installed support in terms of correct installation, movement, loosening, etc. should be done to gain knowledge and to complement the reinforcement.

As already mentioned a special focus has to be set on the weathering (see chapter 9.3). Due to the changing geometry of the mine and the deployed new machinery the current weathering has to be recalibrated and adapted to ensure a safe working. The forced and the possible auxiliary ventilation have to be modulated so that a proper ventilation is ensured.

Another factor which has to be considered is the factor human. The current staff is used to a mining height of 3,2 [m] and over the years, used mining method. With the enlargement of the mining height (6 [m] up to 12 [m]) and in combination with the new and, most notably, bigger machinery, an education program should be implemented. Since at the current mining operation only occasional reinforcement is installed, an education concerning the regular installation and placing of support for the future mining areas should be performed. An assimilation time to this new situation has to be allowed concerning the new mining method, the new machinery, the regular installation of the support and the new weathering.

The move to the new mining fields offers many challenges and changes – but with the proposed procedures and a proper surveillance, a save and efficient mining operation is possible and one of the last underground mining operations in Belgium looks forward to a sustainable future.

11 Bibliography

Accipo: Gerüst KRAUSE Stabilo Serie 5000 2,5 AH 5,30 m, 2006, <http://www.accipo.de/products/Gerueste/Stabilo-Profi-Fahrgerueste/Geruest-KRAUSE-Stabilo-Serie-5000-25-AH-530-m.html> (10.08.2012)

Bieniawski, Z.T.: Rock Mechanics Design in Mining and Tunneling, A.A. Balkema, 1984

Brady, B.H.G. and Brown, E.T.: Rock mechanics for underground mining, 3rd edition, Springer, 2005

Brady, T. et al: Empirical approaches for weak rock masses, National Institute for Occupational Safety and Health (NISOH), <http://www.cdc.gov/niosh/mining/pubs/pdfs/eafwr.pdf> (08.06.2012)

Diederichs, M.S. and Kaiser, P.K.: Stability of large excavations in laminated hard rock masses: the voussoir analogue revisited, International Journal of Rock Mechanics and Mining Sciences 36, 1999, p. 97 - 117

Dräger: Dräger Oxy 6000 Sauerstoffselbstretter, http://www.draeger.com/AT/de/products/personal_protection/escape/self_rescuer/cin_oxy_6000.jsp (26.04.2012)

Esterhuizen, G.S.: Pillar strength in underground stone mines in the United States, International Journal of Rock Mechanics & Mining Sciences 48, 2011, p. 42 - 50

Eymer, W.: Grundlagen der Erdbewegung, 2. Aufl, Kirschbaum Verlag GmbH, 2006

Galiotto, R.: Luce e Matereia, 2011

GL Arbeitsbühnen Verleih: Ketten-Arbeitsbühne Leo 30 T, http://www.gl-verleih.de/Vermietung/Arbeitsbuehnen/LEO_30_T_28.html?product_id=105 (10.08.2012)

González-Nicieza, C., Álvarez-Fernández, M. I., and Menéndez-Díaz, A. and Álvarez-Vigil, A. E.: A Comparative Analysis of Pillar Design Methods and its Application to Marble Mines, Springer-Verlag, 2006

Hoek, E. and Brown, E.T.: Underground Excavations in Rock, The Institution of Mining Metallurgy, London, 1980

Hoek, E.: Estimates of rock mass strength, Discussion paper # 4, 2004

Hoek, E. et al: Support of Underground Excavations in Hard Rock, A.A. Balkema, Rotterdam, 1995

Hoek, E.: Rock engineering – course notes by Evert Hoek, 2007

Kran & Hebetchnik: Arbeitsbühne als Anbaulösung, 2007, <http://www.kran-und-hebetchnik.de/news/arbeitsbuehnen/did1085250/arbeitsbuehne-als-anbauloesung.html> (10.08.2012)

Laubscher, D.H.: A geomechanics classification system for rating of rock mass in mine design, Journal of the South African institute of mining and metallurgy, vol. 90, no. 10, 1990, p. 257-273

Løset, F.: Engineering Geology – Practical Use of the Q-Method, Norwegian Geotechnical Institute (NGI), 592046-4, 1997

Martin, C.D. and Maybee, W.G.: the strength of hard-rock pillars, International Journal of Rock & Mechanics & Mining Sciences 37, 2000

Minova: Minova BWZ Bolting range – Standard bolt systems, 2010

Österreichisches Normungsinstitut (ON): ÖNORM B 3124 – 5, 1981

Prinz, H. and Strauß, R.: Ingenieurgeologie, 5th ed., Spektrum Akademischer Verlag Heidelberg, 2011

Salamon, M.D.G.: The Role of Pillars in Mining, in: Rock Mechanics in Mining Practice, Budavari S., The South African Institute of Mining and Metallurgy, 1983, p. 173 - 200

Stewart, S.B.V. and Forsyth, W.W.: The Mathew's method for open stope design, CIM Bulletin, volume 88, No. 992, 1995, p. 45 – 53

STONE Project: Techniques → Stone workers → 3 Quarry Workers, 2011, <http://www.stoneproject.org/3-quarry-workers.html> (01.08.2012)

Tensar: Mining Roof and Wall support, 2012, <http://www.tensar.co.uk/Applications/Mining-Roof-and-Wall-Support#> (01.08.2012)

Villaescusa, E. et al.: Predicting underground stability using a hangingwall stability rating, in: Environmental and Safety Concerns in Underground Construction, Balkema, 1997, p. 171 - 176

Volvo: Volvo wheel loaders L150F, L180F, L220F, Ref. No. 21 B 100 2739, 2007

12 List of figures

Figure 1:	Plan view total, executive summary	2
Figure 2:	Distorting mirrors (Galiotto 2011, p. 39)	3
Figure 3:	Naming of mining areas.....	5
Figure 4:	Location of the mine 1, Google maps 2012.....	6
Figure 5:	Location of the mine, Google maps 2012.....	7
Figure 6:	Location of the mine 3, Google maps 2012.....	8
Figure 7:	Location of the mine 4, plan view, Surpac.....	9
Figure 8:	Location of the mine 5, Surpac	10
Figure 9:	Overburden, Entrance	11
Figure 10:	Sketch of recorded geological structure	12
Figure 11:	Terminal point: south field – connection passage (north direction).....	13
Figure 12:	Layer Cr – T, connection passage (east wall)	14
Figure 13:	Geological structure, total deposit, sketch.....	15
Figure 14:	Major Fault „17m“, outcrops	16
Figure 15:	Support major fault „17m“, connection passage.....	17
Figure 16:	Outcrop entrance, Major fault „17m“	18
Figure 17:	Major Fault „17m“, 3D, Surpac, 1	19
Figure 18:	Major Fault „17m“, 3D, Surpac, 2.....	19
Figure 19:	Major fault „south“, alignment, Surpac	20
Figure 20:	Major Faults „inside“	21
Figure 21:	Major Faults „inside“ example	21
Figure 22:	Major fault „inside“; photo number: 1738.....	22
Figure 23:	Major fault „inside“; photo number: 1760.....	23
Figure 24:	Major fault „inside“; photo number: 1427.....	23
Figure 25:	Major fault „inside“; photo number: 1464.....	24
Figure 26:	Geoelectric, Dipole H.....	25
Figure 27:	Geoelectric, Dipole V	26
Figure 28:	Geological discontinuities, overview	27

Figure 29:	Distance distribution, discontinuities	28
Figure 30:	Data „ksys195“ sorted in classes	29
Figure 31:	Data „ksys95“ sorted in classes	29
Figure 32:	Mining method	30
Figure 33:	Cut vs. drilled remaining pillars	31
Figure 34:	Examples of backfill	31
Figure 35:	Backfilled areas	32
Figure 36:	Ventilator, at weather shaft	33
Figure 37:	Processing.....	33
Figure 38:	Mine Plan 2007, AutoCAD	34
Figure 39:	Mine Plan 2007, Surpac.....	35
Figure 40:	Mine Plan 2011, Surpac.....	36
Figure 41:	Enlargement of current mining area.....	36
Figure 42:	Example spot heights, AutoCAD 2007	37
Figure 43:	Basis for roof area mine south	38
Figure 44:	Spot heights field south – connection passage, AutoCAD 2007	39
Figure 45:	3D model, current status, Surpac, 2011	40
Figure 46:	Mine Plan 2007 incl. streets and buildings, AutoCAD	41
Figure 47:	Comparison incomplete (left, from Figure 46) and complete and used one (right, from Figure 40, chapter 4.3.2.1) mine plan 2007, AutoCAD	42
Figure 48:	Topography, Surpac	42
Figure 49:	Topography incl. ortho – photo, Surpac	43
Figure 50:	Historical development, north field, photo number: 1489.....	44
Figure 51:	Historical dev., south field, shaft and east, photo Nr.: 1494, 1495.....	45
Figure 52:	Historical dev., south field, west, photo number: 1496	45
Figure 53:	Water collection and catch areas	47
Figure 54:	Position abandoned mine to Mazy	48
Figure 55:	Major faults „17m“ and „south“	49
Figure 56:	Pressure syndromes, overview	50
Figure 57:	Example pressure syndrome, photo nr.: 1431.....	51
Figure 58:	Pressure syndrome, entrance, photo nr.: 1394	52

Figure 59:	Pillar cut though by fault and joint	53
Figure 60:	Exposed roof plates	54
Figure 61:	BBK 81 – 2, before testing	58
Figure 62:	BBK 81 – 3, before testing	59
Figure 63:	Average results UCS of layers	62
Figure 64:	Total average results UCS of layers.....	62
Figure 65:	Experimental setup (cp. ÖNORM B 3124-5, p 3)	64
Figure 66:	Bending tension strength, entire	66
Figure 67:	TAT irregular pillar sketch (cp. Hoek E. and Brown E.T. 1980, p. 114).....	69
Figure 68:	TAT square pillar sketch (cp. Hoek and Brown 1980, p. 114).....	70
Figure 69:	TAT rectangular pillar sketch (cp. Hoek and Brown 1980, p. 114).....	71
Figure 70:	TAT strip pillar sketch (cp. Hoek and Brown 1980, p. 114).....	72
Figure 71:	Location Pillar 10, Surpac.....	73
Figure 72:	Pillar strength formulas, comparison of different approaches (cp. Martin and Maybee 2000, p. 1240)	75
Figure 73:	Sketch vertical-normal load, σ_p	78
Figure 74:	Thickness overburden	79
Figure 75:	Rock column areas	80
Figure 76:	Deformation of beam and spring (cp. Salamon 1983, p176)	82
Figure 77:	Effect on the panel width (cp. Salamon 1983, p178)	83
Figure 78:	Effect on panel width, section of alignment map	84
Figure 79:	Results incl. reduction.....	86
Figure 80:	Viewed areas for geomechanical classification system, current situation, current mining area south	89
Figure 81:	Bedding plane break frequency, HSR (cp. Villaescusa 1997, p 173).....	91
Figure 82:	Number of joint set and continuity, HSR (cp. Villaescusa 1997, p 173)	92
Figure 83:	Normal induced stresses, HSR (cp. Villaescusa 1997, p 174).....	92
Figure 84:	Table for Blast damage, HSR (cp. Villaescusa 1997, p 174).....	93
Figure 85:	Bench stope stability chart, HSR, current situation (cp. Villaescusa 1997, p 176)	94
Figure 86:	Classification table, Bieniawski (cp. Hoek 2007, chapter 3, p. 9).....	96
Figure 87:	Design span curve, Brady, RMR, current situation (cp. Brady, p. 2).....	98

Figure 88:	Adjustment for mining applications, Laubscher, current situation (cp. Bieniawski 1984, p. 119).....	99
Figure 89:	Stability diagram, Laubscher, current mining situation (cp. Laubscher 1990, p. 270)	102
Figure 90:	Diagram for support, Barton, current situation (cp. Løset 1997, p. 28) ...	106
Figure 91:	Planes for the rock stress factor (A), sketch, area 1	108
Figure 92:	Diagram to estimate induced stresses in hangingwalls (cp. Stewart and Forsyth 1995, p 52).....	109
Figure 93:	Rock stress factor (A), (cp. Stewart and Forsyth 1995, p 50)	110
Figure 94:	Rock defect orientation factor (B), (cp. Stewart and Forsyth 1995, p 50)	111
Figure 95:	Design surface orientation factor (C), (cp. Stewart and Forsyth 1995, p 51)	111
Figure 96:	Stability diagram Mathew's, current situation (cp. Stewart and Forsyth 1995, p 49)	113
Figure 97:	Cantilever beam, sketch	116
Figure 98:	Cantilever profile, sketch.....	117
Figure 99:	Example partly open and filled joint, pillar 3, photo nr.: 1413	122
Figure 100:	GU70-3-R, sketch at driving position.....	124
Figure 101:	GU70-3-R, sketch at cutting position.....	125
Figure 102:	GU70-3-R, sketch of cutting phases	126
Figure 103:	GU70 R-XC, working angle.....	127
Figure 104:	Volvo L220 F, sketch and naming of dimensions (cp. Volvo 2007, p. 30).....	128
Figure 105:	GU50 SC, sketch at working configuration.....	130
Figure 106:	Alignment of the access (brown) to the lower levels within the existing mining area, sketch, Surpac.....	131
Figure 107:	Future mining area south, basis, Surpac.....	134
Figure 108:	Future mining area north, current situation, Surpac	136
Figure 109:	Future mining area north, basis, Surpac	137
Figure 110:	Basic alignment of access, Surpac	138
Figure 111:	Cut A-A, access, sketch.....	139
Figure 112:	Cut B-B, access, sketch.....	139

Figure 113:	Anticipated result, south field, plan view, Surpac	140
Figure 114:	Profile, side view, south	141
Figure 115:	Access to south field, Surpac.....	143
Figure 116:	Exploration stope	144
Figure 117:	Barrier pillar, access south, viewed areas	145
Figure 118:	Viewed areas, classification systems, future mining area south	147
Figure 119:	Bench stope stability chart, HSR, future mining area south (cp. Villaescusa 1997, p 176)	149
Figure 120:	Design span curve, Brady, RMR, future mining area south (cp. Brady, p. 2)	151
Figure 121:	Stability diagram, Laubscher, future mining area south (cp. Laubscher 1990, p. 270)	153
Figure 122:	Diagram for support, Barton, future mining area south (cp. Løset 1997, p. 28)	156
Figure 123:	Change Factor B, Mathew's, future mining area south (cp. Stewart and Forsyth 1995, p 50).....	157
Figure 124:	Stability diagram Mathew's, future mining area south (cp. Stewart and Forsyth 1995, p 49).....	159
Figure 125:	Pillar 1 incl. joint, future mining area south, Surpac.....	163
Figure 126:	Mitigation of the pillar strength through discontinuities, strip pillar 1 (cp. Esterhuizen 2011, p. 47).....	164
Figure 127:	Result strip pillar 1 incl. mitigation, chart Esterhuizen, future mining area south (cp. Esterhuizen 2011, p. 49)	165
Figure 128:	Mitigation of the pillar strength through discontinuities, strip pillar 1; 5 [m] width (cp. Esterhuizen 2011, p. 47).....	166
Figure 129:	Result strip pillar 1, 5 [m] width, incl. mitigation, chart Esterhuizen, future mining area south (cp. Esterhuizen 2011, p. 49).....	167
Figure 130:	Square pillar 6x6x12m incl. geological discontinuity systems.....	168
Figure 131:	Mitigation of the pillar strength through discontinuities, square pillar, 6x6 [m] (cp. Esterhuizen 2011, p. 47)	168
Figure 132:	Outlay future mining area south, plan view, Surpac	170
Figure 133:	Pillar connection point, south, sketch	170
Figure 134:	Profile, side view, south	171
Figure 135:	Future mining area south, 3D views, Surpac.....	173

Figure 136:	Cut N-S, Stope 1, profile, Surpac.....	174
Figure 137:	Determination of possible minable volume.....	174
Figure 138:	Results comparison, incl. mitigation, chart Esterhuizen, future mining area south (cp. Esterhuizen 2011, p. 49)	178
Figure 139:	Variant „6 [m] A“, plan view, Surpac.....	179
Figure 140:	Variant „6 [m] B“, plan view, Surpac.....	179
Figure 141:	Variant „3,2 [m]“, plan view, Surpac	179
Figure 142:	Contrast profile Surpac (left) against profile theoretical (right).....	180
Figure 143:	Sketch for volume comparison, variant „12 [m]“	181
Figure 144:	Results of comparison/contrast of volumes by different variants.....	183
Figure 145:	Sketch for necessary length to reach total possible height of lower layers	184
Figure 146:	Mass on southern mine, sketch, Surpac	186
Figure 147:	Sketch forces acting on barrier pillars	187
Figure 148:	Estimation of the rock mass strength (cp. Hoek E. 2004, p. 2).....	188
Figure 149:	Width of barrier pillar north: current mining area south to major fault “17m”	189
Figure 150:	General support main development, roof	193
Figure 151:	Example and illustration of installed straps (LEFT: cp. STONE Project 2011; RIGHT: cp. Hoek 1995, p. 130).....	195
Figure 152:	General support stope, roof	196
Figure 153:	Sketch special case, roof plate	198
Figure 154:	Anchor amount for roof plate, special case	200
Figure 155:	Sketch special case, exceeding width of roof plate	201
Figure 156:	Special case, wedge, sketch of support installation (cp. Hoek 1995, p. 61)..	203
Figure 157:	Strip pillar with fault, Surpac	204
Figure 158:	General support for the walls	205
Figure 159:	Example/Illustration of possible final lookout of main development including support (Tensar 2012)	206
Figure 160:	Special case wall, wedge, example, Surpac	207
Figure 161:	Sketch of support to reinforce a wedge against sliding (cp. Hoek 1980, p. 247)	208

Figure 162:	Anchor distribution, special case wedge, wall, plan view, sketch	210
Figure 163:	Support floor	211
Figure 164:	Access to the future mining area north, alignment, overview	214
Figure 165:	Alignment access to future mining area north, point of submerge and side view	215
Figure 166:	Outlay future mining area north.....	218
Figure 167:	Self rescue kit, closed (right), unpacked (middle), in use (right); (cp. Dräger 2012)	223
Figure 168:	Position of northern emergency exit, plan view, Surpac.....	224
Figure 169:	Routing cord and cones (right: current; left: suggestion)	225
Figure 170:	Fan at the weather shaft	226
Figure 171:	Additional equipment, framework (cp. Accipo 2006)	228
Figure 172:	Additional equipment, chain mounted lifting platform (cp GL Arbeitsbühnen Verleih)	229
Figure 173:	Additional equipment, lifting platform mounted on the loader, exemplary (cp. Kran & Hebetchnik 2007)	230

13 List of tables

Table 1:	Data distance distribution, discontinuities	28
Table 2:	Base Material	55
Table 3:	Results UCS.....	57
Table 4:	Average results of UCS	61
Table 5:	Results bending tension strength.....	65
Table 6:	Sp, pillar design formulae for hard rock (cp. González-Nicieza et al 2006, p. 424)	68
Table 7:	Contrast of the area of the pillar results, pillar 10	77
Table 8:	Contrast of results, effective width pillar 10.....	77
Table 9:	Results of pillar 10, stability calculation.....	81
Table 10:	Results with reduced σ_p , pillar 10.....	85
Table 11:	Dimensions of viewed areas, classification system, current situation.....	89
Table 12:	Calculation of bedding plane breaks / meter	91
Table 13:	Summary, HSR rating, current situation.....	93
Table 14:	Hydraulic radius, HSR, current situation	93
Table 15:	Results RMR, current situation	97
Table 16:	Critical span or design span, Brady, current situation	98
Table 17:	Adjustment of weathering, Laubscher, current situation (cp. Laubscher 1990, p. 264)	100
Table 18:	Adjustment of joint orientation, Laubscher, current situation (cp. Laubscher 1990, p. 265)	100
Table 19:	Adjustment of blasting, Laubscher, current situation (cp. Laubscher 1990, p. 266)	100
Table 20:	Summary, MRMR, Laubscher, current situation.....	101
Table 21:	Summary, Q-System, current situation	104
Table 22:	Excavation Support Ratio (ESR), Barton, current situation (cp. Løset 1997, p. 26)	105
Table 23:	Results equivalent dimension (y), Barton, current situation.....	106
Table 24:	Used constants for calculating the stability number (N).....	112

Table 25:	Stability number, summary, current situation	112
Table 26:	Summary of classification systems	115
Table 27:	Volvo L220 F, dimensions (cp. Volvo 2007, p 24 – 33)	128
Table 28:	Final dimensions, planned machinery	129
Table 29:	Calculation of FOS of the pillar at the south access (east)	145
Table 30:	HSR rating, future mining area south	148
Table 31:	Hydraulic radius, HSR, future mining area south	148
Table 32:	RMR, future mining area south	150
Table 33:	Critical span or design span, Brady, future mining area south	150
Table 34:	MRMR, Laubscher, future mining area south	152
Table 35:	Q-Value, Barton, future mining area south	155
Table 36:	Equivalent dimension (y), Barton, future mining area south	155
Table 37:	Stability Number (N), Mathew's, future mining area south	158
Table 38:	Summary of the global dimensioning of the room width	161
Table 39:	Input parameters, pillar design, future mining area south	162
Table 40:	Result strip pillar 1, future mining area south	163
Table 41:	Result strip pillar 1 incl. mitigation after Esterhuizen, future mining area south	164
Table 42:	Result strip pillar 1; 5 [m] width, incl. mitigation after Esterhuizen, future mining area south	166
Table 43:	Result square pillar; 6x6 [m] area, incl. mitigation after Esterhuizen, future mining area south	169
Table 44:	Inclinations, future mining area south	172
Table 45:	Possible resources, future mining area south, Surpac	175
Table 46:	Input parameters, pillar design, comparison to other variants	177
Table 47:	Comparison dimensions variant „12[m]”; “6 [m] A”; “6 [m] B”; “3,2 [m]”	177
Table 48:	Contrast of different variants by volume	180
Table 49:	Input parameters for the volume calculation, comparison of variants	183
Table 50:	Values and the average result of the height and the length of the mass, mining area south	186
Table 51:	Values and result of barrier pillar north, south field	189
Table 52:	Values and result for barrier pillar south, south field	190

Table 53:	Calculation of the anchor amount, special case, roof plate	199
Table 54:	Results for special case, wedge	203
Table 55:	Results of anchor amount for special case wedge, wall	209
Table 56:	Volume of outlay for future mining area north	219

14 List of abbreviations and definitions

A	Rock stress factor
AA	Anchor amount
A_B	Adjustment blasting effects
AD	Anchor density
A_{JO}	Adjustment joint orientation
A	Dip (of stope)
A_{MS}	Adjustment mining induced stress
A_p	Area pillar
a_p	Width pillar
A_{RC}	Tributary area / area of rock column
a_s	Width specimen
A_w	Adjustment weathering
B	Rock defect orientation factor
BBK	Bergbaukunde
BTS	Bending tension strength
C	Design surface orientation factor
C	cohesion
c'	Residual cohesion
CD	Compact Disc
C_p	Compare
E	Area extraction ratio
E	Youngs modul
e.g.	exempli gratia
ESR	Excavation support ratio

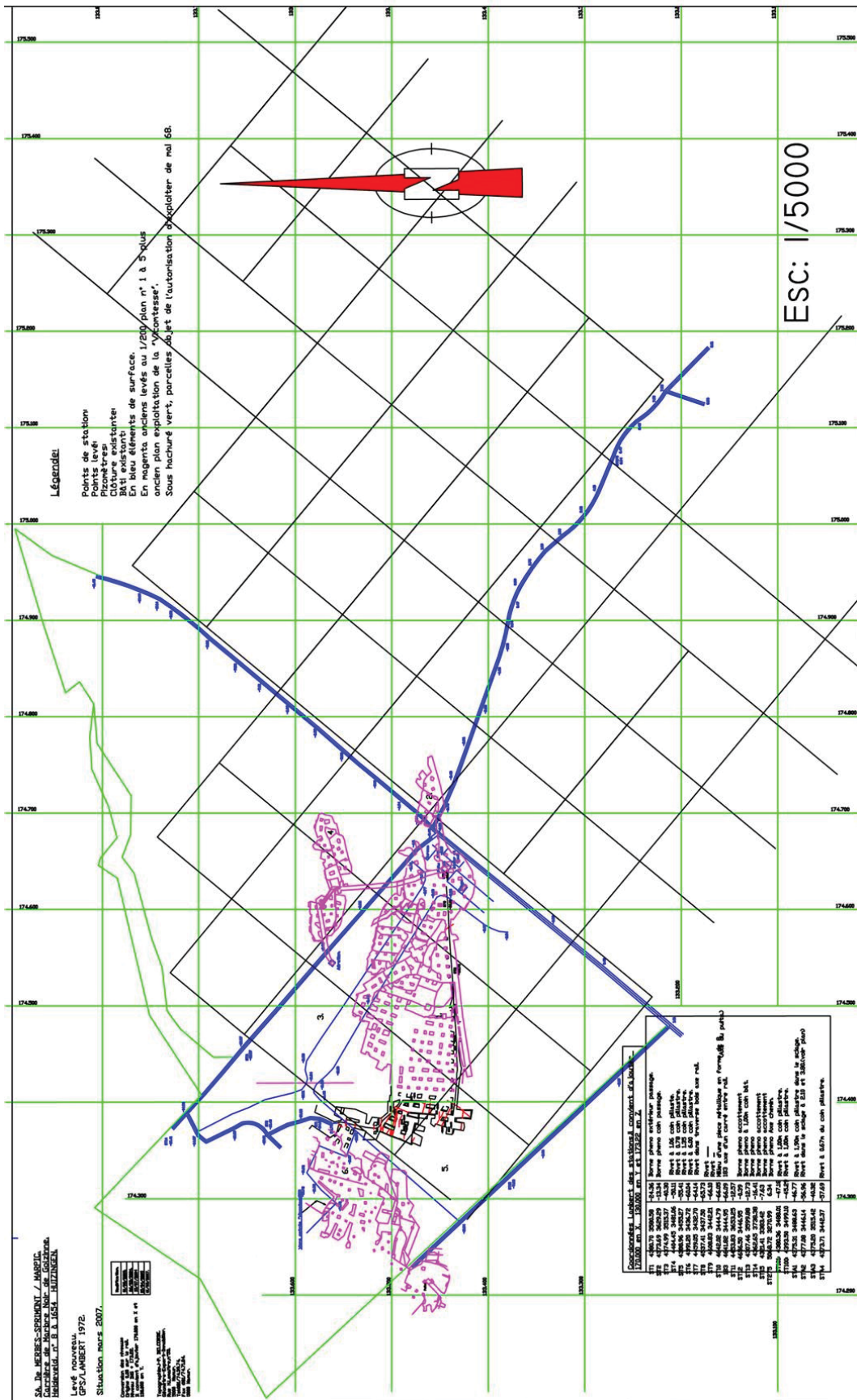
Fault	<u>Definition:</u> Faults are discontinuities with vertical and/or horizontal relative motion (cp. Prinz and Strauß 2011, p. 127)
FOS	Factor of safety
H_p	Height pillar
H_s	Height specimen
HSR	Hangingwall stability rating
J_a	Joint alteration number
J_n	Joint set number
Joint	<u>Definition:</u> Joints are planar discontinuities, which occur due different loading, without clearly evident shifting along the failure plane (cp. Prinz and Strauß 2011, p. 118)
J_r	Joint roughness number
J_w	Joint water reduction factor
K	Ratio horizontal stress to vertical stress
L	Length
MRMR	Mining rock mass rating
M_y	Bending moment
N	Stability number
NGI	Norwegian Geotechnical Institute
Nr.	Number
P	Rigid distributed load
Φ	Friction angle
Pty Ltd	Proprietary limited company
Q	Virgin vertical stress
q_0	Uniformity distributed load
R	Circumference
ρ	Density

RMR	Rock mass rating
RQD	Rock quality designation
σ_b	Bending tension strength
σ_c	Uniaxial compressive strength
σ_H	Horizontal stress
σ_i	Induced stress
σ_n	Normal stress
σ_p	Load acting on pillar
σ_T	Shear stress
σ_v	Primary in situ stress / vertical stress
SN	Store-Norfors (location in Norway)
S_p	Strength of the pillar
SRF	Stress reduction factor
S_0	Reduced uniaxial compressive strength
T	Mineable thickness
T	Total load of the anchors
TAT	Tributary Area Theory
UCS	Uniaxial compressive strength
V_p	Volume pillar
V_s	Volume specimen
W	Weight
w_e	Effective Width
W_p	Width pillar
W_y	Moment of resistance
W_0	Width room
Y	Equivalent dimension

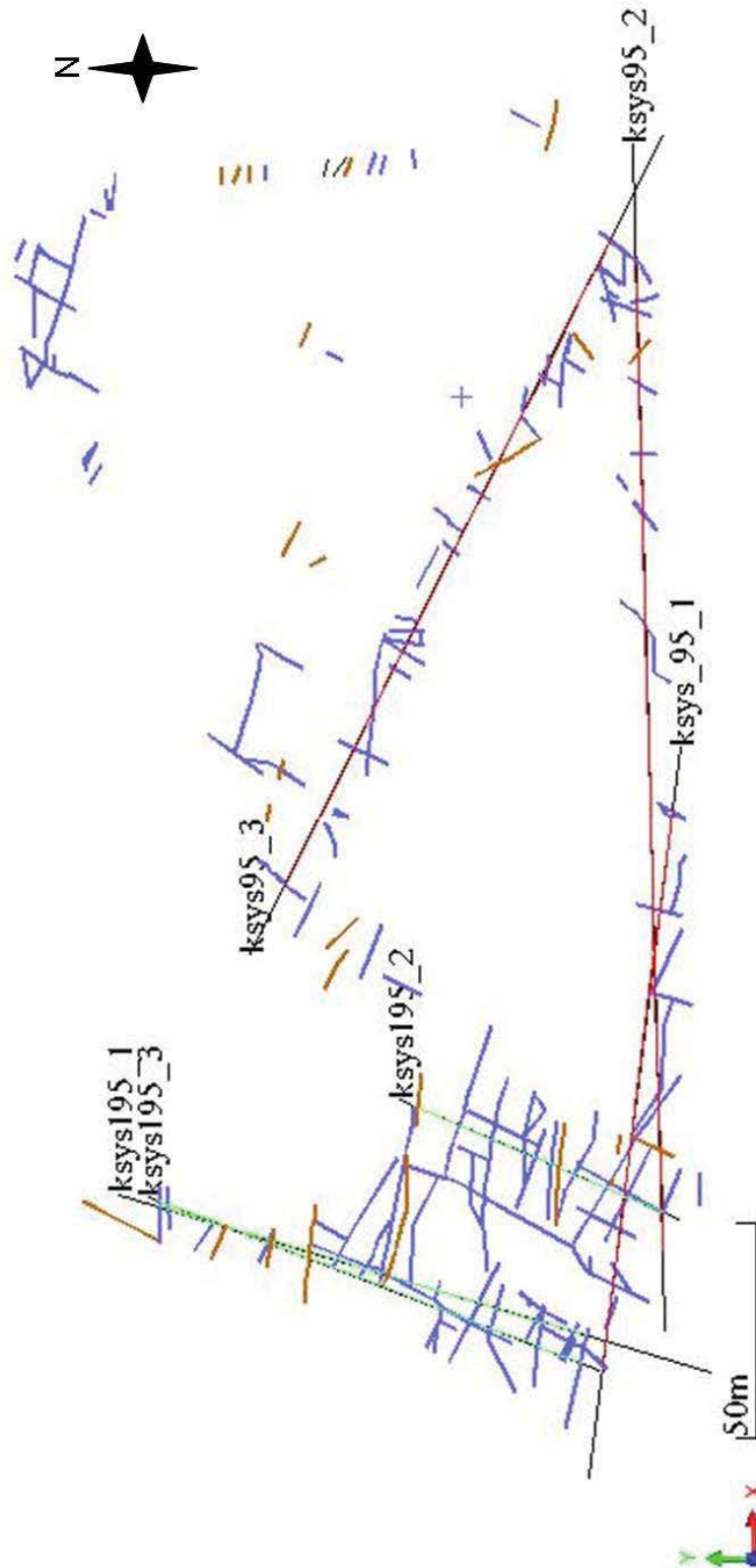
15.2 Provided Map of the company – left part, enlarged



15.3 Provided Map of the company – right part, enlarged



15.4 Discontinuities distance distribution – overview map

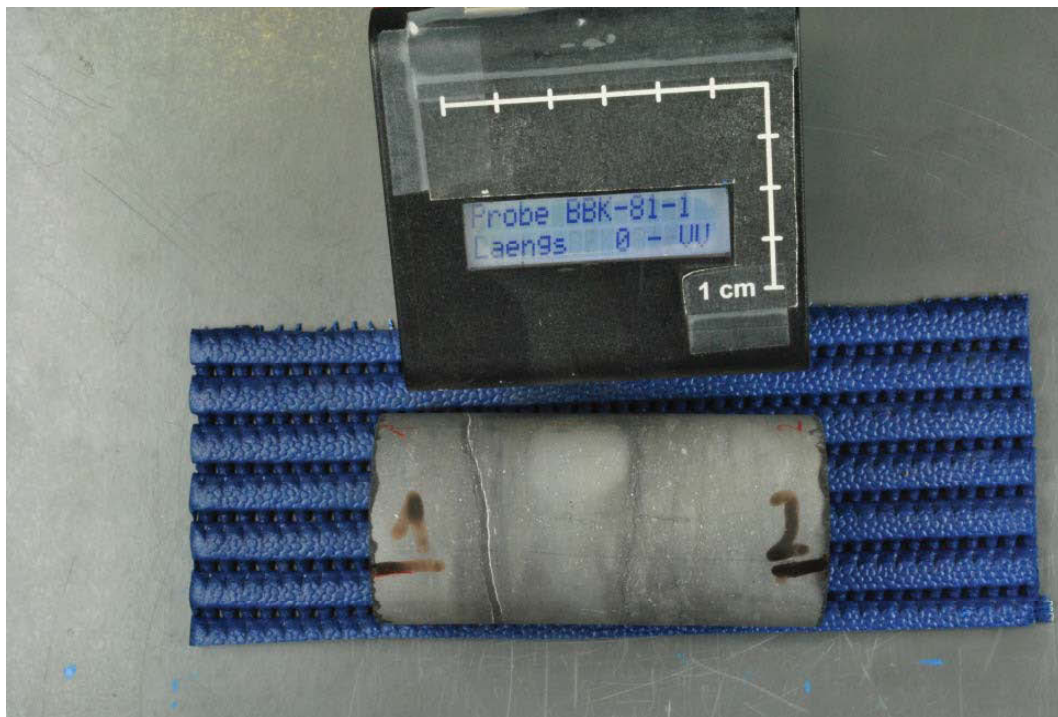


15.5 Exemplary photo documentation for UCS laboratory tests

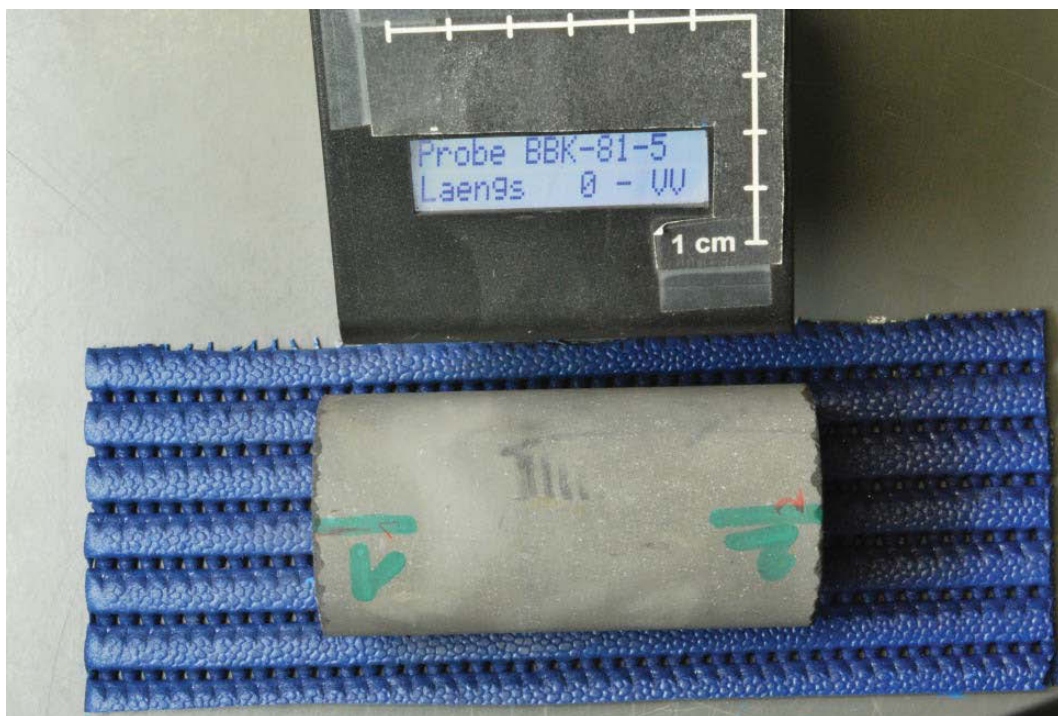
15.5.1 BBK 81 – base material



15.5.2 BBK 81-1 – sample – perpendicular to layering



15.5.3 BBK 81-5 – sample – parallel to layering



15.6.2 Pillar 44 – 265 (only Database 3 available)

Nr. (Pillar)		Cirumference (U_p)	Area pillar (A_p)	Ent- width (w_e)	A_{RC}	$H_{\text{overburden}}$	S_p (Hedley)	σ_p (with σ_n)	FOS (Hedley)	Effect panel width		FOS (Hedley) mitigated
		Map	Map	Map	Tributary Area	Height overburden	Map	Map	Map	value mitigation [-]	Percent (to 4) [%]	Map
		[m]	[m ²]	[m]	[m ²]	[m]	[MPa]	[MPa]	[-]			[-]
44	roof		5,80	2,41	76,64	38,45	74,82	12,85	5,82	2,50	0,63	9,32
	floor	13,50	10,05	2,98	76,64	38,45	83,18	7,42	11,21	2,50	0,63	17,94
45	roof		2,55	1,60	62,28	40,92	60,93	25,26	2,41	2,80	0,70	3,45
	floor	8,41	4,42	2,10	62,28	40,92	69,89	14,59	4,79	2,80	0,70	6,84
46	roof		5,06	2,25	82,42	48,36	72,30	19,93	3,63	3,00	0,75	4,84
	floor	12,25	8,76	2,86	82,42	48,36	81,53	11,51	7,08	3,00	0,75	9,44
47	roof		2,22	1,49	68,58	50,58	58,83	39,57	1,49	2,80	0,70	2,12
	floor	7,86	3,84	1,95	68,58	50,58	67,39	22,86	2,95	2,80	0,70	4,21
48	roof		2,57	1,60	83,73	52,76	61,03	43,48	1,40	2,50	0,63	2,25
	floor	9,05	4,45	1,97	83,73	52,76	67,60	25,12	2,69	2,50	0,63	4,31
49	roof		9,28	3,05	114,76	39,18	84,14	12,26	6,86	2,45	0,61	11,21
	floor	17,76	16,07	3,62	114,76	39,18	91,71	7,08	12,95	2,45	0,61	21,15
50	roof		5,16	2,27	108,15	43,05	72,66	22,81	3,19	2,60	0,65	4,90
	floor	12,14	8,94	2,95	108,15	43,05	82,73	13,18	6,28	2,60	0,65	9,66
51	roof		4,75	2,18	81,80	44,89	71,15	19,57	3,64	2,80	0,70	5,19
	floor	11,54	8,22	2,85	81,80	44,89	81,37	11,30	7,20	2,80	0,70	10,28
52	roof		6,43	2,54	99,59	47,44	76,76	18,59	4,13	2,80	0,70	5,90
	floor	13,56	11,13	3,28	99,59	47,44	87,34	10,74	8,13	2,80	0,70	11,62
53	roof		10,59	3,25	131,29	50,30	86,95	15,78	5,51	2,60	0,65	8,48
	floor	18,65	18,33	3,93	131,29	50,30	95,58	9,12	10,48	2,60	0,65	16,13
54	roof		3,75	1,94	93,57	53,78	67,07	33,97	1,97	2,45	0,61	3,22
	floor	10,72	6,49	2,42	93,57	53,78	75,01	19,62	3,82	2,45	0,61	6,24
55	roof		9,82	3,13	151,79	39,75	85,34	15,54	5,49	2,30	0,58	9,55
	floor	18,79	17,01	3,62	151,79	39,75	91,73	8,97	10,22	2,30	0,58	17,77
56	roof		9,88	3,14	130,21	42,58	85,47	14,19	6,02	2,50	0,63	9,63
	floor	16,55	17,11	4,14	130,21	42,58	98,02	8,20	11,96	2,50	0,63	19,13
57	roof		11,26	3,36	144,01	46,42	88,31	15,02	5,88	2,60	0,65	9,05
	floor	18,73	19,50	4,16	144,01	46,42	98,37	8,67	11,34	2,60	0,65	17,45
58	roof		5,37	2,32	108,77	50,58	73,38	25,91	2,83	2,50	0,63	4,53
	floor	13,26	9,30	2,81	108,77	50,58	80,74	14,97	5,39	2,50	0,63	8,63
59	roof		3,30	1,82	98,94	53,76	64,99	40,73	1,60	2,45	0,61	2,60
	floor	12,21	5,72	1,87	98,94	53,76	65,99	23,53	2,80	2,45	0,61	4,58
60	roof		9,18	3,03	87,58	28,97	83,91	6,99	12,00	2,25	0,56	21,34
	floor	16,04	15,90	3,97	87,58	28,97	95,99	4,04	23,77	2,25	0,56	42,27
61	roof		4,46	2,11	73,76	31,37	70,07	13,11	5,34	2,40	0,60	8,91
	floor	11,23	7,73	2,75	73,76	31,37	79,99	7,57	10,56	2,40	0,60	17,60
62	roof		5,26	2,29	91,58	34,77	73,01	15,31	4,77	2,25	0,56	8,48
	floor	12,48	9,11	2,92	91,58	34,77	82,37	8,84	9,31	2,25	0,56	16,56
63	roof		178,57	13,36	762,49	40,91	176,21	4,42	39,87	BP	BP	BP
	floor	84,38	309,17	14,66	762,49	40,91	184,54	2,55	72,29	BP	BP	BP
64	roof		3,10	1,76	86,17	42,96	63,94	30,25	2,11	2,45	0,61	3,45
	floor	9,29	5,36	2,31	86,17	42,96	73,23	17,47	4,19	2,45	0,61	6,84
65	roof		3,04	1,74	82,35	45,36	63,64	31,11	2,05	2,60	0,65	3,15
	floor	9,18	5,26	2,29	82,35	45,36	72,98	17,97	4,06	2,60	0,65	6,25
66	roof		4,84	2,20	101,63	47,79	71,50	25,39	2,82	2,80	0,70	4,02
	floor	11,87	8,38	2,82	101,63	47,79	81,00	14,66	5,52	2,80	0,70	7,89
67	roof		2,95	1,72	92,91	50,79	63,18	40,45	1,56	2,80	0,70	2,23
	floor	9,05	5,11	2,26	92,91	50,79	72,44	23,37	3,10	2,80	0,70	4,43
68	roof		2,48	1,57	70,13	53,32	60,48	38,18	1,58	2,60	0,65	2,44
	floor	8,33	4,29	2,06	70,13	53,32	69,19	22,05	3,14	2,60	0,65	4,83
69	roof		2,36	1,54	62,72	55,80	59,76	37,48	1,59	2,45	0,61	2,60
	floor	8,09	4,09	2,02	62,72	55,80	68,55	21,65	3,17	2,45	0,61	5,17
70	roof		8,54	2,92	82,28	30,26	82,40	7,38	11,17	2,10	0,53	21,27
	floor	15,41	14,78	3,84	82,28	30,26	94,42	4,26	22,15	2,10	0,53	42,19
71	roof		9,72	3,12	149,46	34,55	85,10	13,45	6,33	2,10	0,53	12,05
	floor	18,61	16,82	3,62	149,46	34,55	91,65	7,77	11,80	2,10	0,53	22,47
72	roof		2,68	1,64	85,10	43,80	61,68	35,19	1,75	2,45	0,61	2,86
	floor	8,62	4,64	2,15	85,10	43,80	70,73	20,32	3,48	2,45	0,61	5,68
73	roof		2,52	1,59	78,29	46,33	60,76	36,36	1,67	2,60	0,65	2,57
	floor	8,36	4,37	2,09	78,29	46,33	69,70	21,00	3,32	2,60	0,65	5,11
74	roof		5,84	2,42	98,66	48,81	74,93	20,86	3,59	2,80	0,70	5,13
	floor	13,09	10,11	3,09	98,66	48,81	84,73	12,05	7,03	2,80	0,70	10,04
75	roof		2,70	1,64	81,44	52,04	61,81	39,67	1,56	2,80	0,70	2,23
	floor	8,66	4,68	2,16	81,44	52,04	70,87	22,91	3,09	2,80	0,70	4,42

Nr. (Pillar)		Cirumference (U _n)	Area pillar (A _n)	Eff. width	A _{RC}	H _{overburden}	S _p (Hedlev)	σ _p (with σ _n)	FOS (Hedlev)	Effect panel width	FOS (Hedley) mitigated	
		Map	Map	Map	Tributary Area	Height overburden	Map	Map	Map	value mitigation	Percent (to 4)	Map
		[m]	[m ²]	[m]	[m ²]	[m]	[MPa]	[MPa]	[-]	[-]	[%]	[-]
76	roof		2,91	1,71	74,54	54,59	62,96	35,37	1,78	2,60	0,65	2,74
	floor	9,00	5,04	2,24	74,54	54,59	72,14	20,43	3,53	2,60	0,65	5,43
77	roof		2,50	1,58	54,71	56,93	60,62	31,51	1,92	2,45	0,61	3,14
	floor	8,37	4,33	2,07	54,71	56,93	69,34	18,20	3,81	2,45	0,61	6,22
78	roof		70,43	8,39	319,56	58,34	139,64	6,70	20,85	BP	BP	BP
	floor	64,32	121,93	7,58	319,56	58,34	132,74	3,87	34,31	BP	BP	BP
79	roof		13,26	3,64	77,90	31,51	91,98	4,69	19,63	2,25	0,56	34,90
	floor	19,61	22,95	4,68	77,90	31,51	104,29	2,71	38,54	2,25	0,56	68,51
80	roof		5,71	2,39	61,96	33,24	74,50	9,13	8,16	2,40	0,60	13,60
	floor	13,37	9,88	2,96	61,96	33,24	82,87	5,27	15,71	2,40	0,60	26,19
81	roof		16,90	4,11	134,31	36,19	97,74	7,28	13,43	2,25	0,56	23,88
	floor	21,86	29,26	5,35	134,31	36,19	111,54	4,20	26,54	2,25	0,56	47,18
82	roof		3,64	1,91	88,72	45,15	66,58	27,85	2,39	2,30	0,58	4,16
	floor	10,20	6,30	2,47	88,72	45,15	75,77	16,09	4,71	2,30	0,58	8,19
83	roof		2,64	1,62	79,58	47,50	61,44	36,23	1,70	2,50	0,63	2,71
	floor	8,56	4,57	2,14	79,58	47,50	70,44	20,93	3,37	2,50	0,63	5,39
84	roof		6,54	2,56	101,29	49,91	77,10	19,55	3,94	2,60	0,65	6,07
	floor	13,66	11,33	3,32	101,29	49,91	87,80	11,29	7,78	2,60	0,65	11,96
85	roof		6,37	2,52	107,54	53,10	76,58	22,68	3,38	2,50	0,63	5,40
	floor	14,44	11,03	3,06	107,54	53,10	84,26	13,10	6,43	2,50	0,63	10,29
86	roof		7,14	2,67	120,43	56,59	78,79	24,16	3,26	2,30	0,58	5,67
	floor	14,32	12,36	3,45	120,43	56,59	89,57	13,95	6,42	2,30	0,58	11,16
87	roof		3,36	1,83	61,45	29,23	65,24	13,54	4,82	2,30	0,58	8,38
	floor	10,21	5,81	2,28	61,45	29,23	72,73	7,82	9,30	2,30	0,58	16,17
88	roof		13,94	3,73	103,53	31,28	93,15	5,88	15,85	2,50	0,63	25,36
	floor	21,06	24,14	4,58	103,53	31,28	103,22	3,39	30,41	2,50	0,63	48,66
89	roof		7,12	2,67	88,25	34,76	78,75	10,90	7,23	2,50	0,63	11,56
	floor	14,82	12,33	3,33	88,25	34,76	87,94	6,29	13,97	2,50	0,63	22,35
90	roof		8,72	2,95	107,58	37,96	82,82	11,85	6,99	2,30	0,58	12,15
	floor	17,72	15,09	3,41	107,58	37,96	88,97	6,85	12,99	2,30	0,58	22,60
91	roof		5,86	2,42	116,43	46,67	74,99	23,47	3,19	2,45	0,61	5,22
	floor	12,76	10,14	3,18	116,43	46,67	85,94	13,56	6,34	2,45	0,61	10,35
92	roof		3,91	1,98	75,31	49,44	67,78	24,09	2,81	2,60	0,65	4,33
	floor	10,64	6,77	2,55	75,31	49,44	76,90	13,91	5,53	2,60	0,65	8,50
93	roof		8,17	2,86	112,45	51,34	81,49	17,89	4,56	2,80	0,70	6,51
	floor	15,12	14,14	3,74	112,45	51,34	93,23	10,33	9,02	2,80	0,70	12,89
94	roof		3,78	1,94	100,64	54,84	67,20	36,97	1,82	2,80	0,70	2,60
	floor	10,28	6,54	2,54	100,64	54,84	76,90	21,35	3,60	2,80	0,70	5,14
95	roof		6,80	2,61	90,91	57,90	77,84	19,59	3,97	2,60	0,65	6,11
	floor	14,10	11,77	3,34	90,91	57,90	88,08	11,32	7,78	2,60	0,65	11,97
96	roof		6,85	2,62	104,65	60,62	77,98	23,43	3,33	2,45	0,61	5,43
	floor	21,97	11,86	2,16	104,65	60,62	70,83	13,53	5,23	2,45	0,61	8,54
97	roof		6,69	2,59	83,58	30,73	77,52	9,72	7,98	2,60	0,65	12,27
	floor	13,63	11,58	3,40	83,58	30,73	88,86	5,61	15,83	2,60	0,65	24,36
98	roof		19,16	4,38	135,93	33,04	100,85	5,93	17,00	3,10	0,78	21,94
	floor	24,23	33,17	5,48	135,93	33,04	112,80	3,43	32,92	3,10	0,78	42,48
99	roof		6,76	2,60	102,59	36,73	77,74	14,09	5,52	3,10	0,78	7,12
	floor	14,72	11,71	3,18	102,59	36,73	85,99	8,14	10,56	3,10	0,78	13,63
100	roof		7,75	2,78	107,68	40,59	80,42	14,28	5,63	2,50	0,63	9,01
	floor	15,56	13,41	3,45	107,68	40,59	89,50	8,25	10,85	2,50	0,63	17,36
101	roof		7,14	2,67	119,18	44,17	78,79	18,66	4,22	2,50	0,63	6,76
	floor	16,15	12,36	3,06	119,18	44,17	84,34	10,78	7,83	2,50	0,63	12,52
102	roof		6,38	2,53	90,29	47,59	76,60	17,05	4,49	2,50	0,63	7,19
	floor	13,31	11,04	3,32	90,29	47,59	87,80	9,85	8,92	2,50	0,63	14,27
103	roof		8,94	2,99	129,10	51,76	83,35	18,91	4,41	3,10	0,78	5,69
	floor	18,68	15,48	3,31	129,10	51,76	87,76	10,92	8,04	3,10	0,78	10,37
104	roof		2,96	1,72	81,49	55,29	63,21	38,55	1,64	3,10	0,78	2,12
	floor	9,05	5,12	2,26	81,49	55,29	72,51	22,27	3,26	3,10	0,78	4,20
105	roof		3,21	1,79	67,92	58,32	64,53	31,21	2,07	3,10	0,78	2,67
	floor	9,43	5,56	2,36	67,92	58,32	74,03	18,03	4,11	3,10	0,78	5,30
106	roof		10,14	3,18	90,60	32,01	86,02	7,23	11,89	2,60	0,65	18,29
	floor	17,79	17,56	3,95	90,60	32,01	95,78	4,18	22,92	2,60	0,65	35,26
107	roof		28,01	5,29	176,40	34,71	110,89	5,53	20,05	2,45	0,61	32,73
	floor	36,55	48,49	5,31	176,40	34,71	111,04	3,20	34,76	2,45	0,61	56,74
108	roof		8,30	2,88	95,85	39,11	81,82	11,43	7,16	3,25	0,81	8,81
	floor	16,00	14,37	3,59	95,85	39,11	91,36	6,60	13,84	3,25	0,81	17,04
109	roof		6,23	2,50	92,01	43,06	76,16	16,09	4,73	3,10	0,78	6,11
	floor	13,31	10,79	3,24	92,01	43,06	86,80	9,29	9,34	3,10	0,78	12,05
110	roof		7,49	2,74	91,09	46,03	79,75	14,16	5,63	3,10	0,78	7,27
	floor	14,61	12,97	3,55	91,09	46,03	90,84	8,18	11,10	3,10	0,78	14,33
111	roof		2,95	1,72	68,77	48,15	63,18	28,39	2,23	3,10	0,78	2,87
	floor	9,04	5,11	2,26	68,77	48,15	72,48	16,40	4,42	3,10	0,78	5,70

Nr. (Pillar)		Cirumference (U _n)	Area pillar (A _n)	Eff. width	A _{RC}	H _{overburden}	S _p (Hedlev)	σ _p (with σ _n)	FOS (Hedlev)	Effect panel width	FOS (Hedlev) mitigated	
		Map	Map	Map	Tributary Area	Height overburden	Map	Map	Map	value mitigation	Percent (to 4)	Map
		[m]	[m ²]	[m]	[m ²]	[m]	[MPa]	[MPa]	[-]	[-]	[%]	[-]
112	roof		2,65	1,63	64,26	49,63	61,48	30,50	2,02	3,10	0,78	2,60
	floor	8,57	4,58	2,14	64,26	49,63	70,48	17,62	4,00	3,10	0,78	5,16
113	roof		8,10	2,85	109,78	53,09	81,33	18,20	4,47	2,50	0,63	7,15
	floor	18,68	14,03	3,00	109,78	53,09	83,55	10,51	7,95	2,50	0,63	12,72
114	roof		9,54	3,09	99,17	57,19	84,71	15,05	5,63	2,50	0,63	9,01
	floor	16,57	16,51	3,99	99,17	57,19	96,23	8,69	11,07	2,50	0,63	17,71
115	roof		4,64	2,15	66,73	58,91	70,76	21,42	3,30	3,10	0,78	4,26
	floor	12,02	8,04	2,68	66,73	58,91	78,85	12,37	6,37	3,10	0,78	8,22
116	roof		18,82	4,34	144,26	61,09	100,40	11,85	8,48	2,10	0,53	16,14
	floor	41,24	32,59	3,16	144,26	61,09	85,70	6,84	12,53	2,10	0,53	23,86
117	roof		5,26	2,29	83,11	34,86	72,99	13,95	5,23	2,50	0,63	8,37
	floor	13,63	9,10	2,67	83,11	34,86	78,77	8,06	9,78	2,50	0,63	15,65
118	roof		8,26	2,87	66,80	38,67	81,72	7,91	10,33	2,50	0,63	16,52
	floor	14,46	14,30	3,96	66,80	38,67	95,87	4,57	20,98	2,50	0,63	33,56
119	roof		7,68	2,77	97,16	41,30	80,24	13,23	6,07	2,60	0,65	9,33
	floor	14,83	13,29	3,58	97,16	41,30	91,26	7,64	11,95	2,60	0,65	18,38
120	roof		9,64	3,10	102,81	44,80	84,94	12,09	7,03	2,80	0,70	10,04
	floor	16,43	16,69	4,06	102,81	44,80	97,17	6,98	13,91	2,80	0,70	19,88
121	roof		7,80	2,79	99,72	48,48	80,55	15,69	5,14	2,80	0,70	7,34
	floor	15,16	13,50	3,56	99,72	48,48	90,98	9,06	10,04	2,80	0,70	14,34
122	roof		4,34	2,08	78,70	50,56	69,59	23,18	3,00	2,60	0,65	4,62
	floor	11,17	7,52	2,69	78,70	50,56	79,10	13,39	5,91	2,60	0,65	9,09
123	roof		17,13	4,14	111,64	52,40	98,06	8,64	11,35	2,45	0,61	18,52
	floor	21,11	29,65	5,62	111,64	52,40	114,26	4,99	22,89	2,45	0,61	37,37
124	roof		199,26	14,12	643,28	57,86	181,11	4,73	38,32	BP	BP	BP
	floor	72,77	344,98	18,96	643,28	57,86	209,91	2,73	76,90	BP	BP	BP
125	roof		4,11	2,03	42,67	59,51	68,64	15,62	4,39	2,10	0,53	8,37
	floor	11,19	7,12	2,55	42,67	59,51	76,90	9,02	8,52	2,10	0,53	16,23
126	roof		4,33	2,08	74,30	37,22	69,54	16,15	4,31	2,50	0,63	6,89
	floor	12,98	7,50	2,31	74,30	37,22	73,28	9,33	7,85	2,50	0,63	12,57
127	roof		12,79	3,58	92,38	41,55	91,15	7,59	12,00	2,80	0,70	17,15
	floor	19,39	22,14	4,57	92,38	41,55	103,02	4,39	23,48	2,80	0,70	33,55
128	roof		3,66	1,91	89,69	45,23	66,66	28,07	2,37	3,00	0,75	3,17
	floor	11,60	6,33	2,18	89,69	45,23	71,22	16,21	4,39	3,00	0,75	5,86
129	roof		10,86	3,30	90,24	48,57	87,51	10,21	8,57	3,10	0,78	11,06
	floor	17,45	18,81	4,31	90,24	48,57	100,09	5,90	16,98	3,10	0,78	21,91
130	roof		2,85	1,69	36,78	50,42	62,65	16,44	3,81	3,00	0,75	5,08
	floor	9,20	4,94	2,15	36,78	50,42	70,64	9,50	7,44	3,00	0,75	9,92
131	roof		10,19	3,19	102,00	51,22	86,12	12,97	6,64	2,80	0,70	9,48
	floor	17,12	17,64	4,12	102,00	51,22	97,86	7,49	13,06	2,80	0,70	18,66
132	roof		3,72	1,93	58,94	53,40	66,94	21,41	3,13	2,50	0,63	5,00
	floor	10,75	6,44	2,40	58,94	53,40	74,62	12,37	6,03	2,50	0,63	9,66
133	roof		3,76	1,94	74,70	39,19	67,12	19,70	3,41	2,00	0,50	6,81
	floor	10,27	6,51	2,54	74,70	39,19	76,76	11,38	6,75	2,80	0,70	9,64
134	roof		5,59	2,36	72,65	43,13	74,10	14,20	5,22	3,10	0,78	6,74
	floor	16,06	9,67	2,41	72,65	43,13	74,81	8,20	9,12	3,10	0,78	11,77
135	roof		3,70	1,92	46,20	45,04	66,86	14,22	4,70	3,20	0,80	5,88
	floor	10,23	6,41	2,51	46,20	45,04	76,31	8,21	9,29	3,20	0,80	11,61
136	roof		5,38	2,32	72,77	49,52	73,40	16,96	4,33	3,20	0,80	5,41
	floor	13,17	9,31	2,83	72,77	49,52	81,06	9,79	8,28	3,20	0,80	10,35
137	roof		2,68	1,64	46,14	51,24	61,68	22,32	2,76	3,10	0,78	3,57
	floor	8,72	4,64	2,13	46,14	51,24	70,33	12,89	5,45	3,10	0,78	7,04
138	roof		3,65	1,91	78,06	52,41	66,63	28,36	2,35	2,80	0,70	3,36
	floor	10,11	6,32	2,50	78,06	52,41	76,22	16,38	4,65	2,80	0,70	6,65
139	roof		3,01	1,73	71,27	54,45	63,49	32,63	1,95	2,50	0,63	3,11
	floor	9,18	5,21	2,27	71,27	54,45	72,63	18,85	3,85	2,50	0,63	6,17
140	roof		6,45	2,54	50,78	36,17	76,82	7,20	10,67	2,25	0,56	18,96
	floor	14,16	11,17	3,16	50,78	36,17	85,63	4,16	20,58	2,25	0,56	36,59
141	roof		12,50	3,54	91,44	39,36	90,65	7,28	12,45	2,40	0,60	20,75
	floor	24,30	21,65	3,56	91,44	39,36	91,00	4,21	21,63	2,40	0,60	36,06
142	roof		3,47	1,86	88,50	41,97	65,77	27,12	2,43	2,50	0,63	3,88
	floor	9,83	6,00	2,44	88,50	41,97	75,32	15,66	4,81	2,50	0,63	7,69
143	roof		3,64	1,91	57,41	47,48	66,58	18,95	3,51	3,10	0,78	4,53
	floor	10,19	6,30	2,47	57,41	47,48	75,80	10,95	6,92	3,10	0,78	8,93
144	roof		14,95	3,87	147,58	51,34	94,79	12,82	7,39	3,00	0,75	9,86
	floor	21,08	25,89	4,91	147,58	51,34	106,84	7,41	14,43	3,00	0,75	19,24
145	roof		3,50	1,87	77,06	54,15	65,93	30,17	2,19	2,80	0,70	3,12
	floor	9,87	6,06	2,46	77,06	54,15	75,54	17,42	4,34	2,80	0,70	6,19
146	roof		8,57	2,93	87,04	55,76	82,48	14,33	5,76	2,50	0,63	9,21
	floor	15,46	14,84	3,84	87,04	55,76	94,45	8,27	11,41	2,50	0,63	18,26
147	roof		8,62	2,94	108,30	36,92	82,59	11,74	7,04	2,50	0,63	11,26
	floor	21,68	14,92	2,75	108,30	36,92	79,98	6,78	11,80	2,50	0,63	18,87

Nr. (Pillar)		Cirumference (U _n)	Area pillar (A _n)	Eff. width	A _{RC}	H _{overburden}	S _p (Hedlev)	σ _p (with σ _n)	FOS (Hedlev)	Effect panel width		FOS (Hedley) mitigated
		Map	Map	Map	Tributary Area	Height overburden	Map	Map	Map	value mitigation	Percent (to 4)	Map
		[m]	[m ²]	[m]	[m ²]	[m]	[MPa]	[MPa]	[-]	[-]	[%]	[-]
148	roof		5,04	2,24	69,71	39,04	72,21	13,67	5,28	2,80	0,70	7,55
	floor	11,81	8,72	2,95	69,71	39,04	82,84	7,90	10,49	2,80	0,70	14,99
149	roof		16,44	4,06	126,10	41,25	97,07	8,00	12,13	2,25	0,56	21,56
	floor	28,84	28,47	3,95	126,10	41,25	95,79	4,62	20,72	2,25	0,56	36,83
150	roof		3,80	1,95	76,06	47,68	67,30	24,15	2,79	2,50	0,63	4,46
	floor	10,68	6,58	2,46	76,06	47,68	75,67	13,95	5,43	2,50	0,63	8,68
151	roof		7,65	2,77	101,44	50,09	80,16	16,81	4,77	2,50	0,63	7,63
	floor	14,81	13,24	3,58	101,44	50,09	91,15	9,71	9,39	2,50	0,63	15,02
152	roof		5,54	2,35	99,62	53,51	73,97	24,32	3,04	2,50	0,63	4,87
	floor	13,20	9,60	2,91	99,62	53,51	82,22	14,05	5,85	2,50	0,63	9,36
153	roof		6,69	2,59	113,87	55,36	77,52	23,85	3,25	3,10	0,78	4,19
	floor	14,33	11,58	3,23	113,87	55,36	86,66	13,77	6,29	3,10	0,78	8,12
154	roof		9,07	3,01	120,47	57,50	83,66	19,32	4,33	2,30	0,58	7,53
	floor	16,20	15,71	3,88	120,47	57,50	94,94	11,16	8,51	2,30	0,58	14,80
155	roof		2,89	1,70	88,15	60,24	62,84	46,52	1,35	2,30	0,58	2,35
	floor	9,22	5,00	2,17	88,15	60,24	71,00	26,87	2,64	2,30	0,58	4,59
156	roof		2,46	1,57	77,84	38,24	60,37	30,61	1,97	2,25	0,56	3,51
	floor	8,47	4,26	2,01	77,84	38,24	68,37	17,68	3,87	2,25	0,56	6,87
157	roof		3,03	1,74	88,20	41,04	63,58	30,26	2,10	2,40	0,60	3,50
	floor	9,30	5,24	2,25	88,20	41,04	72,37	17,48	4,14	2,40	0,60	6,90
158	roof		2,49	1,58	63,90	43,52	60,55	28,27	2,14	2,25	0,56	3,81
	floor	8,33	4,31	2,07	63,90	43,52	69,35	16,33	4,25	2,25	0,56	7,55
159	roof		76,34	8,74	298,67	47,25	142,48	4,68	30,46	BP	BP	BP
	floor	53,02	132,17	9,97	298,67	47,25	152,21	2,70	56,34	BP	BP	BP
160	roof		5,39	2,32	72,86	52,14	73,46	17,82	4,12	2,30	0,58	7,17
	floor	13,66	9,34	2,73	72,86	52,14	79,72	10,29	7,75	2,30	0,58	13,47
161	roof		3,02	1,74	63,91	54,33	63,52	29,14	2,18	2,50	0,63	3,49
	floor	9,18	5,22	2,27	63,91	54,33	72,70	16,83	4,32	2,50	0,63	6,91
162	roof		2,24	1,50	82,28	56,30	58,94	52,44	1,12	2,60	0,65	1,73
	floor	8,35	3,87	1,85	82,28	56,30	65,63	30,29	2,17	2,60	0,65	3,33
163	roof		2,62	1,62	86,94	57,81	61,34	48,49	1,26	2,50	0,63	2,02
	floor	8,53	4,54	2,13	86,94	57,81	70,33	28,01	2,51	2,50	0,63	4,02
164	roof		1,50	1,23	90,86	61,12	53,36	93,57	0,57	2,30	0,58	0,99
	floor	6,76	2,60	1,54	90,86	61,12	59,79	54,05	1,11	2,30	0,58	1,92
165	roof		2,63	1,62	57,66	38,28	61,41	21,20	2,90	2,25	0,56	5,15
	floor	8,56	4,56	2,13	57,66	38,28	70,36	12,25	5,75	2,25	0,56	10,21
166	roof		3,10	1,76	73,23	40,97	63,94	24,52	2,61	2,40	0,60	4,35
	floor	9,27	5,36	2,31	73,23	40,97	73,31	14,16	5,18	2,40	0,60	8,63
167	roof		2,06	1,44	82,20	43,73	57,76	44,11	1,31	2,25	0,56	2,33
	floor	7,59	3,57	1,88	82,20	43,73	66,12	25,48	2,60	2,25	0,56	4,61
168	roof		3,09	1,76	48,69	51,90	63,91	20,69	3,09	2,30	0,58	5,37
	floor	10,43	5,35	2,05	48,69	51,90	69,05	11,95	5,78	2,30	0,58	10,05
169	roof		3,38	1,84	86,94	58,45	65,35	38,05	1,72	2,50	0,63	2,75
	floor	9,70	5,85	2,41	86,94	58,45	74,87	21,98	3,41	2,50	0,63	5,45
170	roof		2,92	1,71	93,22	60,76	63,00	49,13	1,28	2,30	0,58	2,23
	floor	9,33	5,05	2,17	93,22	60,76	70,93	28,38	2,50	2,30	0,58	4,35
171	roof		3,34	1,83	83,37	58,44	65,16	36,93	1,76	2,40	0,60	2,94
	floor	9,70	5,78	2,38	83,37	58,44	74,42	21,33	3,49	2,40	0,60	5,82
172	roof		1,72	1,31	104,00	61,10	55,21	93,41	0,59	2,25	0,56	1,05
	floor	7,28	2,98	1,64	104,00	61,10	61,68	53,95	1,14	2,25	0,56	2,03
173	roof		3,68	1,92	76,70	61,39	66,76	32,38	2,06	2,10	0,53	3,93
	floor	10,41	6,37	2,45	76,70	61,39	75,41	18,70	4,03	2,10	0,53	7,68
174	roof		114,66	10,71	460,69	59,05	157,74	6,00	26,28	BP	BP	BP
	floor	77,53	198,52	10,24	460,69	59,05	154,27	3,47	44,49	BP	BP	BP
175	roof		6,07	2,46	74,46	39,63	75,66	12,30	6,15	2,25	0,56	10,94
	floor	13,39	10,51	3,14	74,46	39,63	85,41	7,10	12,02	2,25	0,56	21,38
176	roof		2,93	1,71	76,25	42,49	63,06	27,99	2,25	2,40	0,60	3,75
	floor	9,13	5,07	2,22	76,25	42,49	71,84	16,17	4,44	2,40	0,60	7,41
177	roof		3,29	1,81	73,00	45,37	64,93	25,46	2,55	2,25	0,56	4,53
	floor	9,48	5,70	2,41	73,00	45,37	74,76	14,70	5,08	2,25	0,56	9,04
178	roof		143,18	11,97	719,59	52,29	166,74	6,65	25,08	BP	BP	BP
	floor	131,12	247,89	7,56	719,59	52,29	132,56	3,84	34,52	BP	BP	BP
179	roof		2,31	1,52	75,66	40,19	59,43	33,30	1,78	2,25	0,56	3,17
	floor	8,64	4,00	1,85	75,66	40,19	65,60	19,24	3,41	2,25	0,56	6,06
180	roof		2,06	1,43	76,30	43,28	57,72	40,63	1,42	2,40	0,60	2,37
	floor	7,59	3,56	1,88	76,30	43,28	66,03	23,47	2,81	2,40	0,60	4,69
181	roof		2,47	1,57	84,42	45,65	60,41	39,54	1,53	2,25	0,56	2,72
	floor	8,54	4,27	2,00	84,42	45,65	68,17	22,84	2,99	2,25	0,56	5,31
182	roof		2,54	1,59	90,11	42,44	60,86	38,08	1,60	2,25	0,56	2,84
	floor	8,42	4,40	2,09	90,11	42,44	69,69	21,99	3,17	2,25	0,56	5,63
183	roof		2,84	1,69	52,37	42,41	62,59	19,77	3,17	2,30	0,58	5,50
	floor	8,89	4,92	2,21	52,37	42,41	71,72	11,42	6,28	2,30	0,58	10,92

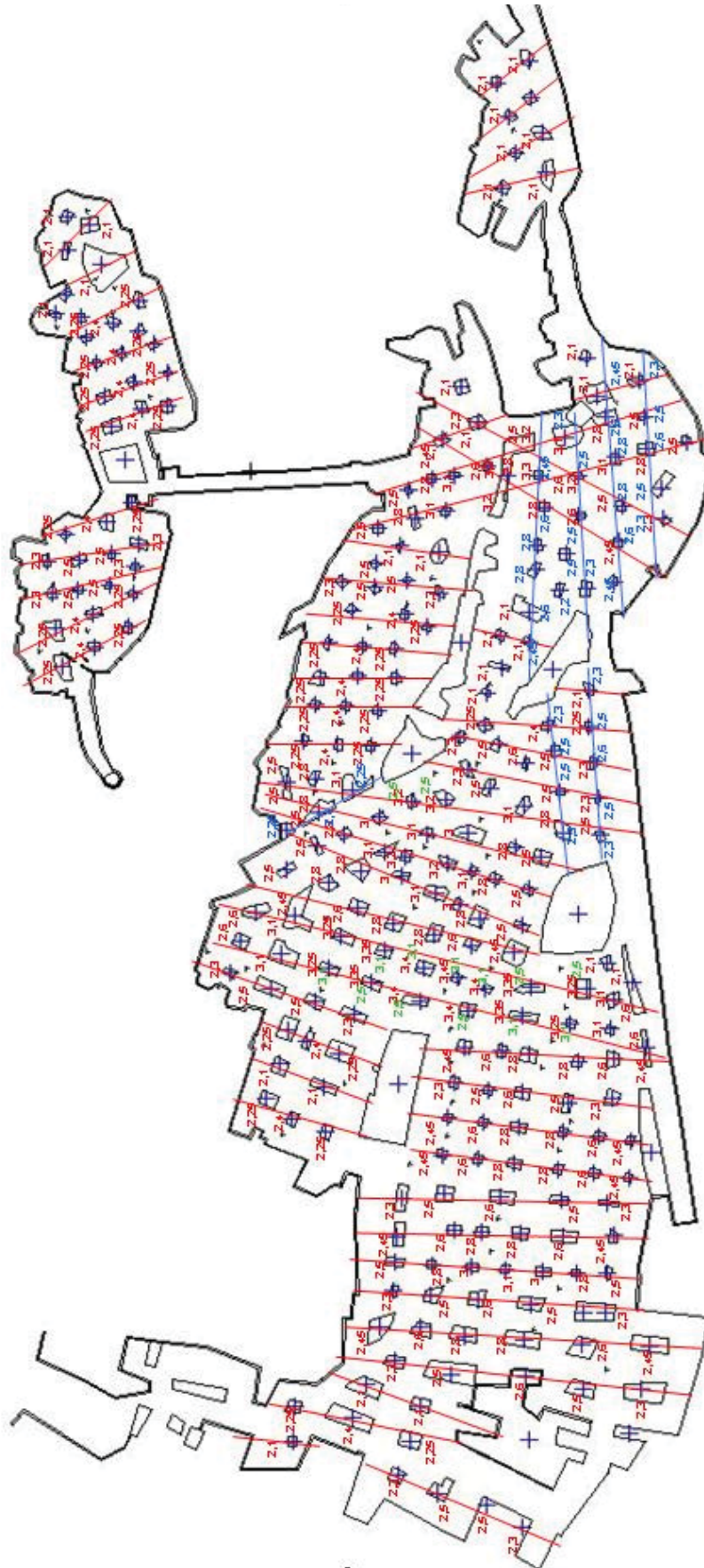
Nr. (Pillar)		Cirumference (U _n)	Area pillar (A _n)	Eff. width	A _{RC}	H _{overburden}	S _p (Hedlev)	σ _p (with σ _n)	FOS (Hedlev)	Effect panel width		FOS (Hedley) mitigated
		Map	Map	Map	Tributary Area	Height overburden	Map	Map	Map	value mitigation	Percent (to 4)	Map
		[m]	[m ²]	[m]	[m ²]	[m]	[MPa]	[MPa]	[-]	[-]	[%]	[-]
184	roof		2,24	1,50	64,44	44,82	58,98	32,61	1,81	2,50	0,63	2,89
	floor	7,92	3,88	1,96	64,44	44,82	67,48	18,84	3,58	2,50	0,63	5,73
185	roof		2,63	1,62	81,15	46,99	61,37	36,71	1,67	2,40	0,60	2,79
	floor	8,55	4,55	2,13	81,15	46,99	70,33	21,20	3,32	2,40	0,60	5,53
186	roof		1,77	1,33	58,97	48,39	55,62	40,71	1,37	2,25	0,56	2,43
	floor	7,75	3,07	1,58	58,97	48,39	60,68	23,52	2,58	2,25	0,56	4,59
187	roof		2,15	1,47	64,74	45,24	58,36	34,49	1,69	2,50	0,63	2,71
	floor	8,09	3,72	1,84	64,74	45,24	65,37	19,92	3,28	2,50	0,63	5,25
188	roof		2,07	1,44	79,02	47,55	57,80	45,98	1,26	2,50	0,63	2,01
	floor	7,63	3,58	1,88	79,02	47,55	66,04	26,56	2,49	2,50	0,63	3,98
189	roof		3,29	1,81	65,49	49,92	64,90	25,17	2,58	2,30	0,58	4,48
	floor	9,82	5,69	2,32	65,49	49,92	73,39	14,54	5,05	2,30	0,58	8,78
190	roof		2,99	1,73	53,67	45,97	63,37	20,90	3,03	2,50	0,63	4,85
	floor	9,17	5,17	2,26	53,67	45,97	72,39	12,07	6,00	2,50	0,63	9,59
191	roof		1,58	1,26	50,33	47,37	54,02	38,26	1,41	2,10	0,53	2,69
	floor	7,16	2,73	1,53	50,33	47,37	59,53	22,10	2,69	2,10	0,53	5,13
192	roof		11,83	3,44	120,78	50,52	89,40	13,05	6,85	2,10	0,53	13,05
	floor	17,55	20,48	4,67	120,78	50,52	104,14	7,54	13,82	2,10	0,53	26,32
193	roof		2,92	1,71	54,99	55,47	63,03	26,41	2,39	2,10	0,53	4,55
	floor	9,01	5,06	2,25	54,99	55,47	72,25	15,25	4,74	2,10	0,53	9,02
194	roof		16,48	4,06	147,64	57,52	97,12	13,04	7,45	2,10	0,53	14,19
	floor	25,29	28,53	4,51	147,64	57,52	102,40	7,53	13,60	2,10	0,53	25,90
195	roof		4,62	2,15	78,68	58,45	70,67	25,18	2,81	2,80	0,70	4,01
	floor	11,51	8,00	2,78	78,68	58,45	80,37	14,55	5,53	2,80	0,70	7,89
196	roof		5,08	2,25	104,94	60,81	72,36	31,80	2,28	2,50	0,63	3,64
	floor	11,89	8,79	2,96	104,94	60,81	82,89	18,37	4,51	2,50	0,63	7,22
197	roof		5,10	2,26	91,03	49,04	72,44	22,15	3,27	2,80	0,70	4,67
	floor	14,98	8,83	2,36	91,03	49,04	74,02	12,79	5,79	2,80	0,70	8,27
198	roof		2,59	1,61	75,53	51,37	61,14	37,94	1,61	3,10	0,78	2,08
	floor	8,47	4,48	2,12	75,53	51,37	70,11	21,91	3,20	3,10	0,78	4,13
199	roof		3,17	1,78	67,39	59,02	64,32	31,74	2,03	2,80	0,70	2,90
	floor	9,50	5,49	2,31	67,39	59,02	73,29	18,33	4,00	2,80	0,70	5,71
200	roof		3,14	1,77	68,72	63,59	64,18	35,19	1,82	2,45	0,61	2,98
	floor	9,00	5,44	2,42	68,72	63,59	74,95	20,32	3,69	2,45	0,61	6,02
201	roof		2,58	1,61	110,31	64,27	61,10	69,47	0,88	2,45	0,61	1,44
	floor	8,47	4,47	2,11	110,31	64,27	70,04	40,13	1,75	2,45	0,61	2,85
	roof	not assigned										
203	roof		3,39	1,84	98,48	66,76	65,41	49,06	1,33	2,50	0,63	2,13
	floor	9,80	5,87	2,40	98,48	66,76	74,61	28,34	2,63	2,50	0,63	4,21
204	roof		2,62	1,62	98,50	70,58	61,34	67,08	0,91	2,30	0,58	1,59
	floor	8,54	4,54	2,13	98,50	70,58	70,29	38,75	1,81	2,30	0,58	3,16
205	roof		9,50	3,08	144,19	70,47	84,63	27,06	3,13	2,50	0,63	5,00
	floor	18,41	16,45	3,57	144,19	70,47	91,13	15,63	5,83	2,50	0,63	9,33
206	roof		6,33	2,52	87,97	69,39	76,46	24,40	3,13	2,60	0,65	4,82
	floor	13,43	10,96	3,26	87,97	69,39	87,09	14,09	6,18	2,60	0,65	9,51
207	roof		2,78	1,67	82,37	69,05	62,27	51,69	1,20	2,50	0,63	1,93
	floor	8,83	4,82	2,18	82,37	69,05	71,23	29,86	2,39	2,50	0,63	3,82
208	roof		4,61	2,15	74,03	68,75	70,65	27,90	2,53	2,10	0,53	4,82
	floor	11,81	7,99	2,71	74,03	68,75	79,30	16,12	4,92	2,10	0,53	9,37
209	roof		2,96	1,72	68,09	71,73	63,21	41,79	1,51	2,50	0,63	2,42
	floor	9,10	5,12	2,25	68,09	71,73	72,31	24,14	3,00	2,50	0,63	4,79
210	roof		1,76	1,33	50,82	49,12	55,53	35,85	1,55	2,50	0,63	2,48
	floor	7,15	3,05	1,71	50,82	49,12	62,97	20,71	3,04	2,50	0,63	4,87
211	roof		2,22	1,49	50,12	51,15	58,86	29,17	2,02	2,80	0,70	2,88
	floor	7,85	3,85	1,96	50,12	51,15	67,52	16,85	4,01	2,80	0,70	5,72
212	roof		2,18	1,48	75,52	53,06	58,59	46,44	1,26	3,10	0,78	1,63
	floor	7,97	3,78	1,90	75,52	53,06	66,39	26,82	2,48	3,10	0,78	3,19
213	roof		2,13	1,46	70,11	55,96	58,20	46,70	1,25	2,60	0,65	1,92
	floor	7,73	3,68	1,90	70,11	55,96	66,52	26,97	2,47	2,60	0,65	3,79
214	roof		42,30	6,50	286,13	57,33	122,93	9,81	12,53	2,50	0,63	20,05
	floor	59,00	73,24	4,97	286,13	57,33	107,41	5,67	18,95	2,50	0,63	30,33
215	roof		3,07	1,75	95,30	59,66	63,82	46,82	1,36	2,60	0,65	2,10
	floor	9,24	5,32	2,30	95,30	59,66	73,15	27,04	2,71	2,60	0,65	4,16
216	roof		1,99	1,41	102,95	61,86	57,23	81,09	0,71	2,50	0,63	1,13
	floor	7,43	3,44	1,85	102,95	61,86	65,60	46,84	1,40	2,50	0,63	2,24
217	roof		2,41	1,55	75,09	60,11	60,09	47,30	1,27	2,45	0,61	2,07
	floor	8,20	4,18	2,04	75,09	60,11	68,83	27,32	2,52	2,45	0,61	4,11
218	roof		2,14	1,46	109,50	63,99	58,32	82,73	0,70	2,50	0,63	1,13
	floor	7,75	3,71	1,91	109,50	63,99	66,70	47,79	1,40	2,50	0,63	2,23
219	roof		3,63	1,90	100,98	67,58	66,52	47,60	1,40	2,00	0,50	2,79
	floor	10,15	6,28	2,47	100,98	67,58	75,83	27,49	2,76	2,80	0,70	3,94

Nr. (Pillar)		Cirumference (U _n)	Area pillar (A _n)	Eff. width	A _{RC}	H _{overburden}	S _p (Hedlev)	σ _p (with σ _n)	FOS (Hedlev)	Effect panel width	FOS (Hedlev) mitigated	
		Map	Map	Map	Tributary Area	Height overburden	Map	Map	Map	value mitigation	Percent (to 4)	Map
		[m]	[m ²]	[m]	[m ²]	[m]	[MPa]	[MPa]	[-]	[-]	[%]	[-]
220	roof		3,97	1,99	90,40	52,63	68,03	30,34	2,24	2,10	0,53	4,27
	floor	10,78	6,87	2,55	90,40	52,63	76,96	17,52	4,39	2,10	0,53	8,37
221	roof		5,94	2,44	101,11	55,69	75,26	23,97	3,14	2,10	0,53	5,98
	floor	12,85	10,29	3,20	101,11	55,69	86,27	13,84	6,23	2,10	0,53	11,87
222	roof		6,09	2,47	100,69	56,31	75,73	23,54	3,22	2,10	0,53	6,13
	floor	12,84	10,55	3,29	100,69	56,31	87,39	13,60	6,43	2,10	0,53	12,24
223	roof		20,19	4,49	126,35	63,75	102,18	10,10	10,12	2,30	0,58	17,60
	floor	22,38	34,95	6,25	126,35	63,75	120,48	5,83	20,66	2,30	0,58	35,93
224	roof		12,14	3,48	91,77	66,83	89,97	12,79	7,04	2,60	0,65	10,82
	floor	18,87	21,01	4,45	91,77	66,83	101,73	7,39	13,77	2,60	0,65	21,19
225	roof		15,33	3,92	97,87	66,41	95,38	10,73	8,89	2,10	0,53	16,93
	floor	20,52	26,54	5,17	97,87	66,41	109,64	6,20	17,69	2,10	0,53	33,70
226	roof		3,22	1,79	76,01	65,43	64,56	39,11	1,65	2,10	0,53	3,14
	floor	9,04	5,57	2,46	76,01	65,43	75,68	22,59	3,35	2,10	0,53	6,38
227	roof		4,36	2,09	87,34	57,58	69,66	29,18	2,39	2,10	0,53	4,55
	floor	11,09	7,55	2,72	87,34	57,58	79,55	16,85	4,72	2,10	0,53	8,99
228	roof		12,19	3,49	110,56	61,38	90,08	14,08	6,40	2,10	0,53	12,18
	floor	20,35	21,11	4,15	110,56	61,38	98,19	8,13	12,07	2,10	0,53	22,99
229	roof		2,80	1,67	80,78	58,93	62,36	42,99	1,45	2,10	0,53	2,76
	floor	9,04	4,85	2,15	80,78	58,93	70,61	24,83	2,84	2,10	0,53	5,42
230	roof		3,11	1,76	56,85	59,31	64,03	27,41	2,34	2,10	0,53	4,45
	floor	8,89	5,39	2,43	56,85	59,31	75,07	15,83	4,74	2,10	0,53	9,03
231	roof		7,02	2,65	79,14	61,60	78,47	17,56	4,47	2,10	0,53	8,51
	floor	14,16	12,16	3,44	79,14	61,60	89,34	10,14	8,81	2,10	0,53	16,78
232	roof		3,86	1,97	79,75	60,84	67,58	31,77	2,13	2,10	0,53	4,05
	floor	10,37	6,69	2,58	79,75	60,84	77,43	18,35	4,22	2,10	0,53	8,04
233	roof		3,55	1,88	67,54	58,76	66,15	28,31	2,34	2,10	0,53	4,45
	floor	9,97	6,14	2,46	67,54	58,76	75,66	16,35	4,63	2,10	0,53	8,81
234	roof		5,90	2,43	82,86	61,72	75,12	21,94	3,42	2,10	0,53	6,52
	floor	12,57	10,21	3,25	82,86	61,72	86,89	12,67	6,86	2,10	0,53	13,06
235	roof		3,52	1,88	75,65	44,87	66,04	24,38	2,71	2,40	0,60	4,52
	floor	9,92	6,10	2,46	75,65	44,87	75,60	14,08	5,37	2,40	0,60	8,95
236	roof		4,42	2,10	72,04	45,30	69,89	18,69	3,74	2,40	0,60	6,23
	floor	11,49	7,65	2,66	72,04	45,30	78,66	10,79	7,29	2,40	0,60	12,15
237	roof		2,50	1,58	53,00	44,54	60,62	23,88	2,54	2,50	0,63	4,06
	floor	8,72	4,33	1,99	53,00	44,54	67,94	13,80	4,92	2,50	0,63	7,88
238	roof		4,78	2,19	63,22	45,30	71,26	15,17	4,70	2,50	0,63	7,52
	floor	11,48	8,27	2,88	63,22	45,30	81,83	8,76	9,34	2,50	0,63	14,94
239	roof		1,84	1,36	47,30	47,22	56,16	30,67	1,83	2,50	0,63	2,93
	floor	7,19	3,19	1,77	47,30	47,22	64,22	17,72	3,62	2,50	0,63	5,80
240	roof		1,92	1,39	58,98	48,12	56,77	37,34	1,52	2,30	0,58	2,64
	floor	7,59	3,33	1,75	58,98	48,12	63,86	21,57	2,96	2,30	0,58	5,15
241	roof		2,76	1,66	70,08	48,49	62,14	31,15	2,00	2,25	0,56	3,55
	floor	8,92	4,78	2,14	70,08	48,49	70,57	17,99	3,92	2,25	0,56	6,97
242	roof		2,13	1,46	42,98	49,16	58,20	25,15	2,31	2,25	0,56	4,11
	floor	7,59	3,68	1,94	42,98	49,16	67,13	14,53	4,62	2,25	0,56	8,22
243	roof		2,08	1,44	47,84	49,88	57,88	29,03	1,99	2,30	0,58	3,47
	floor	7,67	3,60	1,88	47,84	49,88	66,05	16,77	3,94	2,30	0,58	6,85
244	roof		6,86	2,62	73,56	49,75	78,00	13,51	5,78	2,50	0,63	9,24
	floor	14,24	11,87	3,33	73,56	49,75	88,02	7,80	11,28	2,50	0,63	18,05
245	roof		50,68	7,12	174,23	48,38	128,61	4,21	30,56	2,10	0,53	58,22
	floor	37,90	87,74	9,26	174,23	48,38	146,69	2,43	60,35	2,10	0,53	114,95
246	roof		8,49	2,91	79,85	47,61	82,28	11,33	7,26	2,25	0,56	12,91
	floor	15,74	14,70	3,74	79,85	47,61	93,17	6,54	14,24	2,25	0,56	25,31
247	roof		5,12	2,26	72,65	47,63	72,52	17,09	4,24	2,25	0,56	7,54
	floor	12,14	8,87	2,92	72,65	47,63	82,41	9,87	8,35	2,25	0,56	14,84
248	roof		4,26	2,06	53,48	49,51	69,26	15,72	4,41	2,40	0,60	7,34
	floor	11,13	7,38	2,65	53,48	49,51	78,50	9,08	8,65	2,40	0,60	14,41
249	roof		4,38	2,09	56,06	51,51	69,73	16,69	4,18	2,25	0,56	7,43
	floor	11,14	7,58	2,72	56,06	51,51	79,52	9,64	8,25	2,25	0,56	14,67
250	roof		1,95	1,40	44,96	49,66	56,98	28,94	1,97	2,25	0,56	3,50
	floor	7,38	3,38	1,83	44,96	49,66	65,24	16,71	3,90	2,25	0,56	6,94
251	roof		2,79	1,67	55,66	50,28	62,30	25,38	2,45	2,40	0,60	4,09
	floor	8,75	4,83	2,21	55,66	50,28	71,63	14,66	4,89	2,40	0,60	8,14
252	roof		1,85	1,36	55,24	52,70	56,25	39,73	1,42	2,25	0,56	2,52
	floor	7,32	3,21	1,75	55,24	52,70	63,84	22,95	2,78	2,25	0,56	4,95
253	roof		2,48	1,57	36,30	49,00	60,48	18,16	3,33	2,25	0,56	5,92
	floor	8,48	4,29	2,02	36,30	49,00	68,57	10,49	6,54	2,25	0,56	11,62
254	roof		2,50	1,58	60,68	50,98	60,62	31,30	1,94	2,40	0,60	3,23
	floor	8,43	4,33	2,05	60,68	50,98	69,09	18,08	3,82	2,40	0,60	6,37
255	roof		2,48	1,57	46,51	52,43	60,48	24,90	2,43	2,25	0,56	4,32
	floor	8,34	4,29	2,06	46,51	52,43	69,14	14,38	4,81	2,25	0,56	8,55

Nr. (Pillar)		Cirumference (U_p)	Area pillar (A_p)	Eff. width	A_{RC}	$H_{overburden}$	S_p (Hedlev)	σ_p (with σ_n)	FOS (Hedlev)	Effect panel width		FOS (Hedley) mitigated
		Map	Map	Map	Tributary Area	Height overburden	Map	Map	Map	value mitigation	Percent (to 4)	Map
		[m]	[m ²]	[m]	[m ²]	[m]	[MPa]	[MPa]	[-]	[-]	[%]	[-]
256	roof		2,15	1,47	33,74	46,86	58,36	18,62	3,13	2,10	0,53	5,97
	floor	8,67	3,72	1,72	33,74	46,86	63,15	10,75	5,87	2,10	0,53	11,19
257	roof		2,23	1,49	37,65	48,46	58,90	20,71	2,84	2,25	0,56	5,06
	floor	7,87	3,86	1,96	37,65	48,46	67,52	11,96	5,64	2,25	0,56	10,04
258	roof		4,00	2,00	78,70	50,22	68,16	25,02	2,72	2,40	0,60	4,54
	floor	10,93	6,92	2,53	78,70	50,22	76,71	14,45	5,31	2,40	0,60	8,85
259	roof		3,05	1,75	47,67	51,69	63,70	20,44	3,12	2,25	0,56	5,54
	floor	9,34	5,28	2,26	47,67	51,69	72,49	11,81	6,14	2,25	0,56	10,91
260	roof		5,32	2,31	53,05	51,39	73,21	12,97	5,65	2,25	0,56	10,04
	floor	12,11	9,21	3,04	53,05	51,39	84,07	7,49	11,22	2,25	0,56	19,96
261	roof		49,09	7,01	219,29	48,86	127,60	5,52	23,11	2,10	0,53	44,02
	floor	37,92	85,00	8,97	219,29	48,86	144,34	3,19	45,26	2,10	0,53	86,21
262	roof		2,55	1,60	68,22	47,25	60,93	31,94	1,91	2,10	0,53	3,63
	floor	9,06	4,42	1,95	68,22	47,25	67,34	18,45	3,65	2,10	0,53	6,95
263	roof		4,35	2,09	57,95	47,05	69,61	15,86	4,39	2,10	0,53	8,36
	floor	12,77	7,53	2,36	57,95	47,05	74,03	9,16	8,08	2,10	0,53	15,39
264	roof		3,71	1,93	40,18	47,81	66,92	13,09	5,11	2,10	0,53	9,74
	floor	10,43	6,43	2,47	40,18	47,81	75,70	7,56	10,01	2,10	0,53	19,07
265	roof		9,92	3,15	62,80	48,93	85,54	7,84	10,91	2,10	0,53	20,78
	floor	16,75	17,17	4,10	62,80	48,93	97,61	4,53	21,55	2,10	0,53	41,06

Note: "BP" = Barrier Pillar

15.7 Effect on the panel width – alignment map



15.8 Calculation rock quality designation (RQD – value)

Layer	Thickness Layer	> 10 [cm]
[-]	[cm]	[cm]
Croutes calcaires et base des calcaires de Falnuée très probable	120	120
	24	24
	16	16
	13	13
	21	21
	14	14
	23	23
Croutes et Rachets	18	18
	16	16
	24	24
	15	15
	1,5	0
"34"	7	0
	2	0
	14	14
Croutes	17	17
	25	25
	33	33
	27	27
	25	25
Raches	4	0
	6	0
	30	30
Male	30	30
*)	4	0
Croute	11	11
Croute	13	13
nouveau banc	34	34
Banc vif	15	15
Croutes et Rachets	32	32
	7	0
	20	20
Croutes	10	0
*)	0	0
Croutes	10	0
Mâle	33	33
Croutes	3	0
	2	0
A	48	48
*)	0	0
R	61	61
AB	22	22
nouveau banc	0	0
AC	46	46
	5	0
BB	38	38
Sum	937,5	865

Note: “*)” = No name and/or thickness is available according to the from the company provided data (“Coupe Veine inf+fotos.xls”; see data CD)

15.9 Tables for Barton's – Q-System

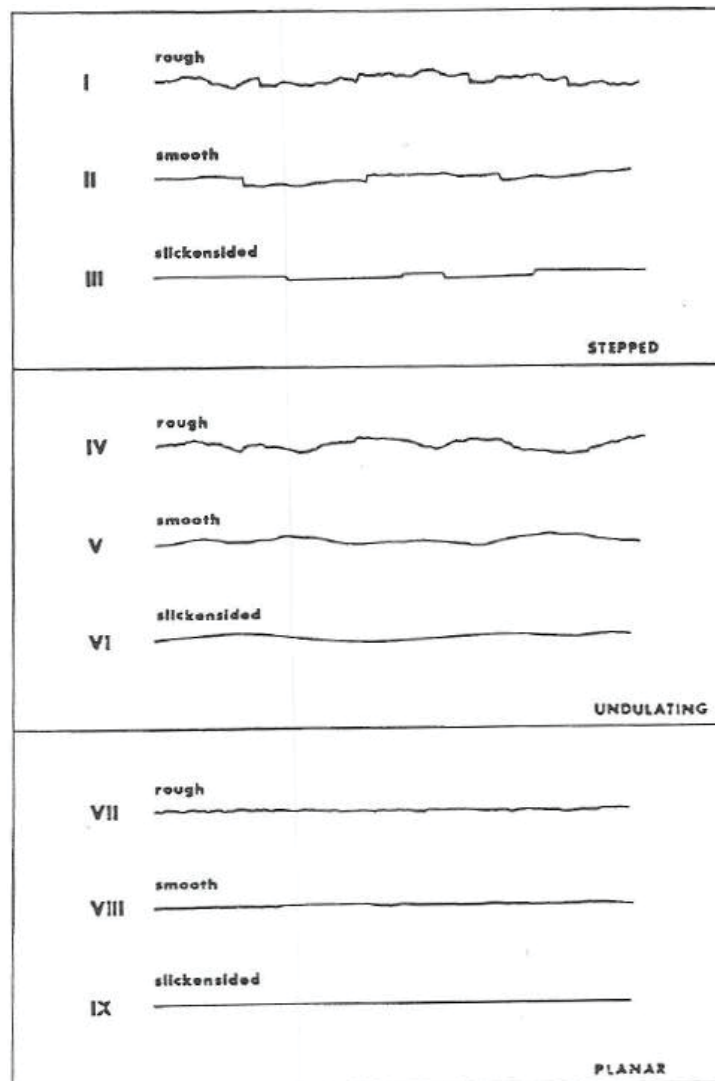
Note: The source for the following used tables is:

Løset, F.: Engineering Geology – Practical Use of the Q-Method, Norwegian Geotechnical Institute (NGI), 592046-4, 1997, p. 7 -26

1 RQD (Rock Quality Designation)		RQD
A	Very poor (> 27 joints per m^3)	0-25
B	Poor (20-27 joints per m^3)	25-50
C	Fair (13-19 joints per m^3)	50-75
D	Good (8-12 joints per m^3)	75-90
E	Excellent (0-7 joints per m^3)	90-100
Note: i) Where RQD is reported or measured as ≤ 10 (including 0) the value 10 is used to evaluate the Q-value ii) RQD-intervals of 5, <i>i.e.</i> 100, 95, 90, <i>etc.</i> , are sufficiently accurate		

2 Joint Set Number		J_n
A	Massive, no or few joints	0.5-1.0
B	One joint set	2
C	One joint set plus random joints	3
D	Two joint sets	4
E	Two joint sets plus random joints	6
F	Three joint sets	9
G	Three joint sets plus random joints	12
H	Four or more joint sets, random heavily jointed "sugar cube", <i>etc.</i>	15
J	Crushed rock, earthlike	20
Note: i) For intersections, use $3 \times J_n$ ii) For portals, use $2 \times J_n$		

3 Joint Roughness Number		J_r
<i>a) Rock-wall contact, and</i>		
<i>b) Rock-wall contact before 10 cm</i>		
A	Discontinuous joints	4
B	Rough or irregular, undulating	3
C	Smooth, undulating,	2
D	Slickensided, undulating	1.5
E	Rough, irregular, planar	1.5
F	Smooth, planar	1
G	Slickensided, planar	0.5
Note: Description refers to small scale features and intermediate scale features, in that order.		
<i>c) No rock-wall contact when sheared</i>		
H	Zone containing clay minerals thick enough to prevent rock-wall contact	1
J	Sandy, gravelly or crushed zone thick enough to prevent rock-wall contact	1
Note: i) Add 1 if the mean spacing of the relevant joint set is greater than 3m. ii) J _r = 0.5 can be used for planar slickensided joints having lineations, provided the lineations are oriented in the estimated sliding direction.		



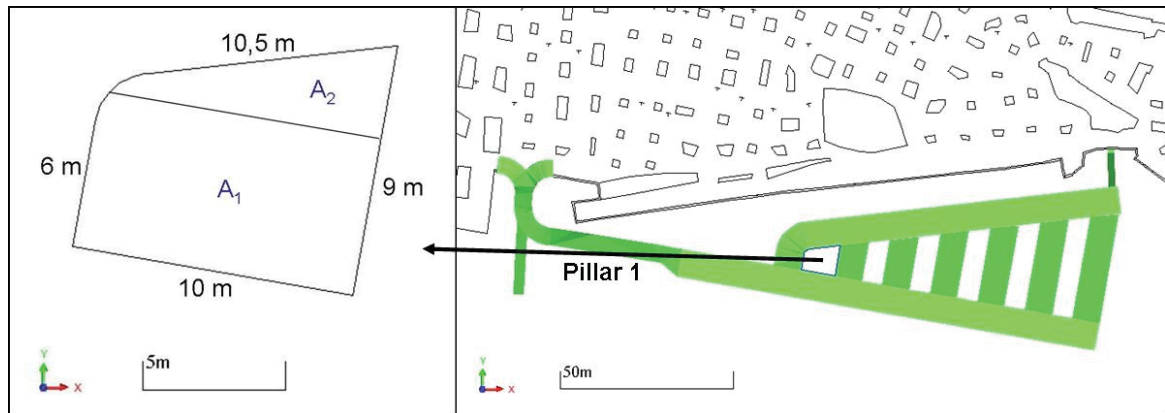
4 Joint Alteration Number		ϕ_r approx	J_a
<i>a) Rock-wall contact (no mineral fillings, only coatings)</i>			
A	Tightly healed, hard, non-softening, impermeable filling, <i>i.e.</i> , quartz or epidote.		0.75
B	Unaltered joint walls, surface staining only.	25-35°	1
C	Slightly altered joint walls. Non-softening mineral coatings; sandy particles, clay-free disintegrated rock, <i>etc.</i>	25-30°	2
D	Silty or sandy clay coatings, small clay fraction (non-softening).	20-25°	3
E	Softening or low friction clay mineral coatings, <i>i.e.</i> , kaolinite or mica. Also chlorite, talc gypsum, graphite, <i>etc.</i> , and small quantities of swelling clays.	8-16°	4
<i>b) Rock-wall contact before 10 cm shear (thin mineral fillings)</i>			
F	Sandy particles, clay-free disintegrated rock, <i>etc.</i>	25-30°	4
G	Strongly over-consolidated, non-softening, clay mineral fillings (continuous, but <5mm thickness).	16-24°	6
H	Medium or low over-consolidation, softening, clay mineral fillings (continuous, but <5mm thickness).	12-16°	8
J	Swelling-clay fillings, <i>i.e.</i> , montmorillonite (continuous, but <5mm thickness). Value of J_a depends on percent of swelling clay-size particles.	6-12°	8-12
<i>c) No rock-wall contact when sheared (thick mineral fillings)</i>			
K	Zones or bands of disintegrated or crushed rock. Strongly over-consolidated.	6-24°	6
L	Zones or bands of clay, disintegrated or crushed rock. Medium or low over-consolidation or softening fillings.	12-16°	8
M	Zones or bands of clay, disintegrated or crushed rock. Swelling clay. J_a depends on percent of swelling clay-size particles.	6-12°	8-12
N	Thick continuous zones or bands of clay. Strongly over-consolidated.	6-122°	10
O	Thick, continuous zones or bands of clay. Medium to low over-consolidation.	16-24°	13
P	Thick, continuous zones or bands with clay. Swelling clay. J_a depends on percent of swelling clay-size particles	12-16°	13-20

5 Joint Water Reduction Factor		J_w
A	Dry excavations or minor inflow, i. e. < 5 l/min locally (humid or a few drippings)	1.0
B	Medium inflow or pressure, occasional outwash of joint fillings (many drippings)	0.66
C	Large inflow or high pressure in competent rock with unfilled joints.	0.5
D	Large inflow or high pressure, considerable outwash of joint fillings.	0.33
E	Exceptionally high inflow or water pressure at blasting, decaying with time.	0.2-0.1
F	Exceptionally high inflow or water pressure continuing without noticeable decay.	0.1-0.05
Note: i) Factors C to F are crude estimates. Increase J _w if drainage measures are installed. ii) Special problems caused by ice formation are not considered.		

6 Stress Reduction Factor		SRF
<i>a) Weakness zones intersecting excavation, which may cause loosening of rock mass when tunnel is excavated</i>		
A	Multiple occurrences of weakness zones containing clay or chemically disintegrated, very loose surrounding rock (any depth)	10
B	Single weakness zones containing clay or chemically disintegrated rock (depth of excavation ≤ 50m)	5
C	Single weakness zones containing clay or chemically disintegrated rock (depth of excavation > 50m)	2.5
D	Multiple shear zones in competent rock (clay-free) loose surrounding rock (any depth)	7.5
E	Single shear zones in competent rock (clay-free) (depth of excavation ≤ 50m)	5.0
F	Single shear zones in competent rock (clay-free) (depth of excavation > 50m)	2.5
G	Loose, open joints, heavily jointed or "sugar cube", etc. (any depth)	5.0
Note: i) Reduce these values of SRF by 25-50% if the relevant shear zones only influence but do not intersect the excavation.		

<i>b) Competent rock, stress problems</i>		σ_c/σ_1	σ_θ/σ_c	SRF
H	Low stress, near surface, open joints	>200	<0.01-0.3	2.5
J	Medium stress, favourable stress condition	200-10	0.01-0.3	1
K	High stress, very tight structure. Usually favourable to stability, may be unfavourable to wall stability	10-5	0.3-0.4	0.5-2
L	Moderate slabbing after > hour in massive rock	5-3	0.5-0.65	5-50
M	Slabbing and rock burst after a few minutes in massive rock	3-2	0.65-1	50-200
N	Heavy rock burst and immediate dynamic deformation in massive rock	<2	>1	200-400
<p>Note: ii) For strongly anisotropic virgin stress field (if measured): when $5 \leq \sigma_1/\sigma_3 \leq 10$, reduce σ_c to $0.75 \sigma_c$. When $\sigma_1/\sigma_3 > 10$, reduce σ_c to $0.5 \sigma_c$, where σ_c = unconfined compression strength, σ_1 and σ_3 are the major and minor principal stresses, and σ_θ = maximum tangential stress (estimated from elastic theory).</p> <p>iii) Few case records available where depth of crown below surface is less than span width. Suggest SRF increase from 2.5 to 5 for such cases (see H).</p>				
<i>c) Squeezing rock: plastic flow on incompetent rock under the influence of high pressure</i>			σ_θ/σ_c	SRF
O	Mild squeezing rock pressure		1-5	5-10
P	Heavy squeezing rock pressure		>5	10-20
<p>Note: iv) Cases of squeezing rock may occur for depth $H < 350Q^{1/3}$ (Singh <i>et al.</i>, 1992). Rock mass compression strength can be estimated from $Q = 0.7\gamma Q^{1/3}$ (MPa) where γ = rock density in kN/m^3 (Singh, 1993).</p>				
<i>d) Swelling rock: chemical swelling activity depending on the presence of water</i>				SRF
R	Mild swelling rock pressure			5-10
S	Heavy swelling rock pressure			10-15

15.10 Calculation of pillar 1, future mining area south



Input parameters		
σ_c	200,00	[MPa]
H_p	6,00	[m]
$H_{\text{overburden}}$	65,00	[m]
ρ	2690,00	[kg/m ³]
Room width	8,00	[m]

Pillar		
a_p	6	[m]
b_p	10	[m]
c_p	9	[m]
d_p	10,44	[m]
A_1	60	[m ²]
A_2	15	[m ²]
A_p	75	[m ²]

Rockcolumn		
a_{rc}	14	[m]
b_{rc}	18,00	[m]
c_{rc}	17,00	[m]
d_{rc}	18,44	[m]
A_1	252	[m ²]
A_2	27	[m ²]
A_{rc}	279	[m ²]

σ_p (irregular)	6,38	[MPa]
------------------------	------	-------

U_p	35,44	[m]
w_e	8,47	[m]

w_e/H_p	1,41	[-]
S_p (Hedley)	87,73	[MPa]
Mitigation after Esterhuizen for 60 [°]	22	[%]
S_p (mitigated)	68,43	[MPa]

FOS =	11	[-]
-------	----	-----

15.11 Values for the calculation of the example for volume comparison/contrast of different Variants, future mining area south

Width_{deposit}	"Var 12"	"Var 6m A"	"Var 6m B"	"Var 3,2m"
[m]	[m³]	[m³]	[m³]	[m³]
20	20880	16860	17520	11264
25	27840	21075	21900	14080
30	34800	25290	26280	16896
35	41760	29505	30660	19712
40	48720	33720	35040	22528
45	55680	37935	39420	25344
50	62640	42150	43800	28160
55	69600	46365	48180	30976
60	76560	50580	52560	33792
65	83520	54795	56940	36608
70	90480	59010	61320	39424
75	97440	63225	65700	42240
80	104400	67440	70080	45056
85	111360	71655	74460	47872
90	118320	75870	78840	50688
95	125280	80085	83220	53504
100	132240	84300	87600	56320

15.12 Fieldwork report

The complete fieldwork report is added in the following (see next page). The fieldwork was done from the 23rd to the 29th of October 2011. The in the report at the annex added maps, which were used during the fieldwork to mark and quote the investigations and the results, are attached at the enclosed data CD of the thesis. The maps are attached at the report to round the results off and to have a printed overview. The maps attached at the data CD are of greater quality and therefore of higher resolution.

The photo documentation which was done at the fieldwork is attached as well at the data CD. The photo numbers are marked at the maps including the direction and the position of the taken photo.

Report

Fieldwork Mazy, Golzinne (BEL)

Vielkind Moritz Stefan, BSc

Date(24/11/2011)



Chair of Mining Engineering and Mineral Economics
Department Mineral Resources and Petroleum Engineering
Motanuniversitaet Leoben

A-8700 LEOBEN, Franz Josef Straße 18
Phone: +43/(0)3842-402-2001
Fax: +43/(0)3842-402-2002
bergbau@unileoben.ac.at

Table of contents

Table of contents	II
1 Introduction	1
2 Program of the Field Work	2
2.1 Photo documentation of the mining area	4
2.2 Surveying of the rock pillars	4
2.3 Documentation of pressure symptoms and signs of loosening	5
2.4 Documentation of the layer structure	5
2.5 Documentation of the major fault system “17m”	5
2.6 Recording of the dominant geological discontinuities	6
2.7 Surveying	6
2.8 Identification of the backfilled areas	6
2.9 Rock samples of the material	7
3 List of figures	8
4 Annex	I
4.1 Results DISTO D5 - Pillars	I
4.2 Results of the documentation of the Layer structure	III
4.3 Results Point Load Test – blasted layers (between BB and U)	IV
4.4 Results Schmidhammer	V
4.5 Maps used at the fieldwork	VI
4.5.1 Overview - results	VI
4.5.2 Overview – table of content	VII
4.5.3 Map part 1	VIII
4.5.4 Map part 2	IX
4.5.5 Map part 3	X
4.5.6 Map part 4	XI
4.5.7 Map part 5	XII
4.5.8 Map part 6	XIII
4.5.9 Map part 7	XIV
4.5.10 Map part 8	XV
4.5.11 Map part 9	XVI
4.5.12 Map part 10	XVII
4.5.13 Map part 11	XVIII
4.5.14 Map part 21	XIX
4.5.15 Map part 22	XX

4.5.16 Map part 23	XXI
4.5.17 Map part 24	XXII
4.5.18 Map part 31	XXIII
4.5.19 Map part 32	XXIV
4.5.20 Map part 33	XXV
4.5.21 Map part 34	XXVI
4.5.22 Map part 41	XXVII
4.5.23 Map part 42	XXVIII
4.5.24 Map part 43	XXIX
4.5.25 Map part 51	XXX
4.5.26 Map part 52	XXXI
4.5.27 Map part 53	XXXII
4.5.28 Map part 61	XXXIII
4.5.29 Map part 01	XXXIV
4.5.30 Map part 02	XXXV
4.5.31 Map part 03	XXXVI
4.5.32 Map part S01	XXXVII
4.5.33 Map part S02	XXXVIII

1 Introduction

From the 23rd of October to the 29th of October 2011 the company Solobema (S.A. de Merbes-Sprimont) gave us the opportunity to do the for the master thesis necessary field work.

In the following, the work and investigations, including the results, which was done at the field work, is listed. Within this report no details concerning the company, mining, the mine itself or the interpretation of the gained results is done. For the further comprehensibility it is crucial to state the used designation of the areas of the underground mine (see Figure 1).

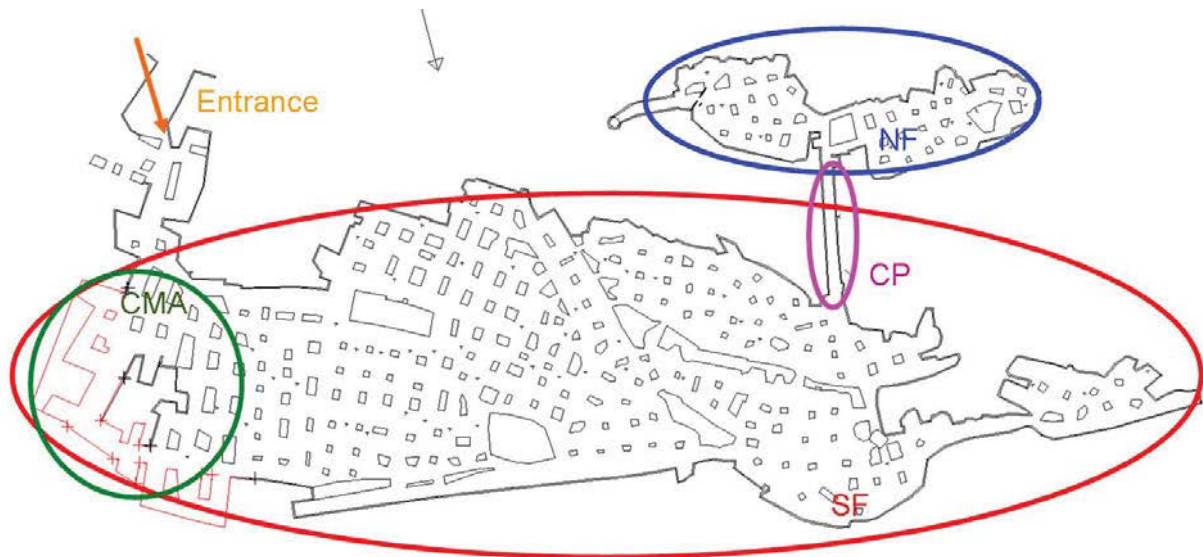


Figure 1: Planview, designation of areas

SF...	South Field
NF...	North Field
CMA...	Current Mining Area
CP...	Connection Passage

Note: Figure 1 is the planview of the mine. This material was provided by the company. In the South-West the progress (CMA) from the last years (red lines) has been adapted – based on the measurements taken during the fieldwork.

2 Program of the Field Work

In the following sub chapters the major points of the field work will be presented. The main focus is to give an overview of the work and the investigations which were made during the fieldwork. In this paper only the gained results of the measurements are presented which are used as major database for the master thesis. No interpretation of the results will be done.

In the following the digitalized results, marked in the plan view of the mine is presented (see Figure 2).

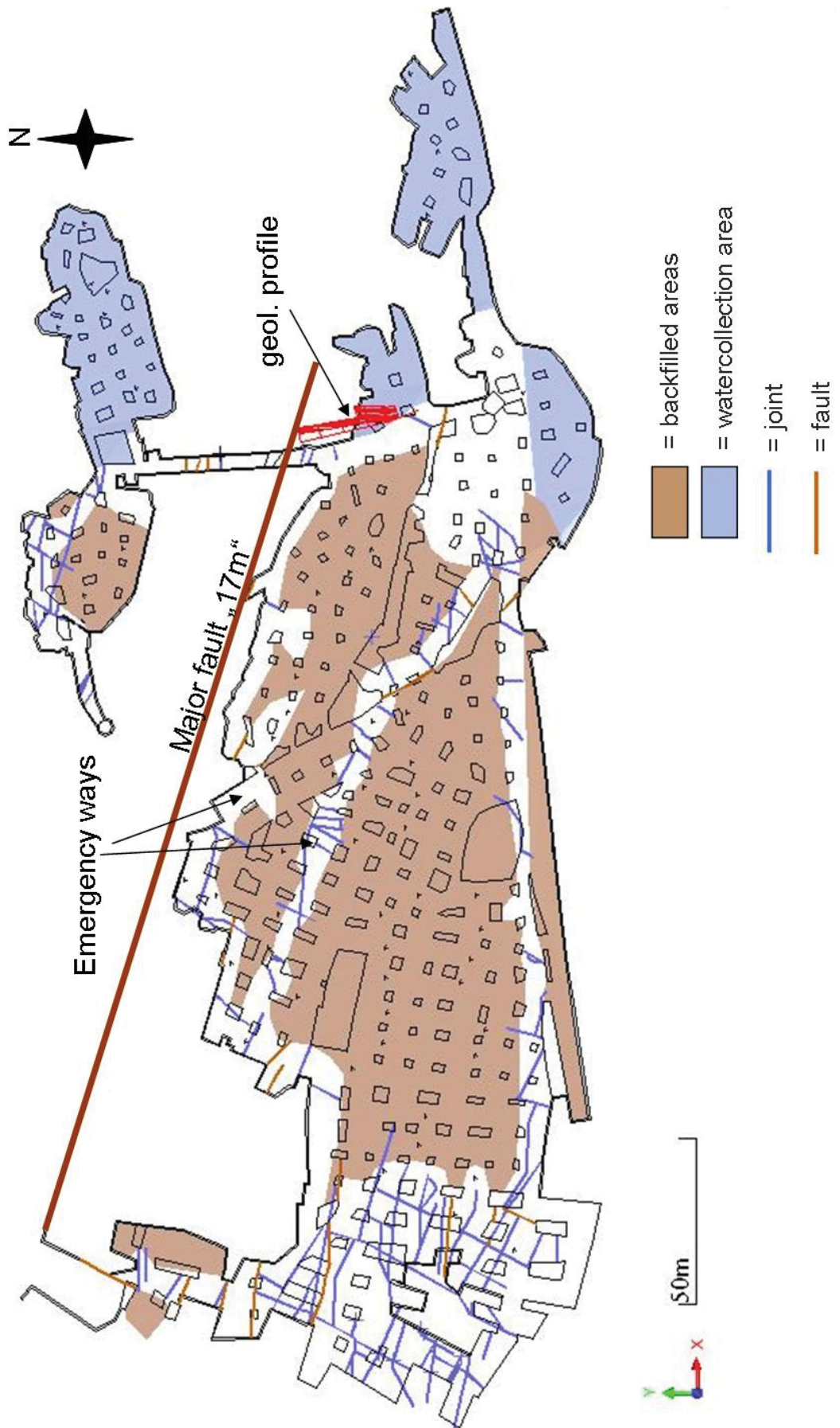


Figure 2: Results of the fieldwork marked in the map of the mine (planview)

2.1 Photo documentation of the mining area

Around 650 photos were made and marked in the maps during the field work. The main focus of the photo documentation was on pillars. Where possible, the photos were taken from all 4 sides. Besides the pillars, photos from the backfilling, dominant geological discontinuities, layers, infrastructure and important information (e.g.: marking of layers or pressure symptoms) were taken.

The reason was on the one hand to gain a comparison database for the future to recognize if some movements or differences had taken place. On the other hand the photo documentation builds a help for the work of the master thesis (review and control). The photos are attached on the data CD of the master thesis.

2.2 Surveying of the rock pillars

An important part of the field work was the surveying of the rock pillars. The focuses of the measurements were the heights (total and blasted) and the area of the cross section (floor, middle and roof) of the pillars. The measurements were made with a laser based distance meter (Leica DISTO D5) in the accessible areas and with a Trimble S6 (see also chapter 2.7).

This data is necessary inter alia for the safety calculations and it builds a control to the correctness of the existing map.

The major part of the measurements was near the current mining area. The results of the measurements with the laser guided distance meter are added in the Annex (see chapter 4.1). The pillar numbers of the measured pillars and allocation of the in the Annex mentioned side lengths are marked in the used enlarged maps of the provided map of the company (see Annex, chapter 4.5).

2.3 Documentation of pressure symptoms and signs of loosening

Within the photo documentation pressure symptoms were recorded and marked in the used enlarged maps to get an impression and overview of the distribution and density of pressure symptoms of the pillars (see Annex, chapter 4.5).

2.4 Documentation of the layer structure

In the connection passage of the North- and South-field (see Figure 1) the order, the thickness and the dip of the layers were investigated (after the major fault in direction south). The measurement was possible since the dip of the connection passage (~ 2 [°]) is lower than the dip of the layering (~ 14 [°]) and therefore it “cuts” through the layers. This data is used to gain a geological profile of the deposit. Furthermore it gives a better understanding of the deposit. The measurements are marked in the used enlarged maps as well listed in the Annex (see chapter 4.5 and 4.2).

2.5 Documentation of the major fault system “17m”

The major fault “17m”, which shifts the north field from the south field, was detected at 3 areas. Once at the connection passage, secondly at the northern center of the south field and at the entrance. The dip is 70 [°] and the dip direction is 34 [°]. The alignment is shown in Figure 2.

2.6 Recording of the dominant geological discontinuities

A special focus was to identify and record the geological discontinuities in terms of position, dip and dip direction. This was done at most of the passable mining area, with special concentration at the current mining area (West). In the emergency or secondary ways the documentation was only done partly since due to the low heights of the rooms (backfilled) the visibility of the roof was decreased. The secondary ways are located in the center of the south field of the current mining area in the north and in the middle of the mine (see Figure 2).

2.7 Surveying

One part of the surveying was done outside the portal (North-west) to get measured points of the walls, the street and terrain edges, which can be implemented in the 3D model. The second part of the surveying was done underground (with connection to the surface) to gain following information:

1. Countercheck of the existing map
2. Edges of the whole pillar on the base of measured points (to built some pillars in the 3D model)
3. Countercheck of the area of the cross section of the pillars

It has to be mentioned, that only a small part at the current mining area has been surveyed. The surveying was done with a Trimble S6 by a local surveying. No connection to the Belgian surveying system was done.

2.8 Identification of the backfilled areas

During the fieldwork, the alignment of the backfill, where possible, has been recorded and marked in the maps. The main problem is that height of the backfilling varies. The access to the center of the south field e.g. was not possible due to the fact that the backfilling reaches narrow or completely to the roof. Some areas in the center could have been reached by crawling but the duration of the stay in Belgium was too short and it was not the main focus of the fieldwork.

2.9 Rock samples of the material

To gain the geomechanical parameters, which are necessary for the stability and safety calculations, rock samples have been taken to Leoben for further testing. 6 samples were prepared from the company and one sample was taken from the blasted material. The dimensions of the samples are ~ 20*20*20 [cm]. The prepared specimens were taken from the following layers (nomenclature is equal to the company's):

- BB (the first layer from the roof)
- U, C, D, E, F (material of value, lower part of the pillar)

Additionally the layers U, C, D, E, F were tested with the Schmidt hammer to get a first impression of the geomechanical parameters. To gain values of the blasted material (layers between BB and U), besides the taken sample, the Point Load Test was performed on samples of the blasted material within the mine. The results of these tests are added in the Annex (see chapter 4.3 and 4.4).

3 List of figures

Figure 1: Planview, designation of areas 1

Figure 2: Results of the fieldwork marked in the map of the mine (planview) 3

4 Annex

4.1 Results DISTO D5 - Pillars

Nr.		a [m]	b [m]	c [m]	d [m]	Height [m]	Sidenote
1	roof	3,19	2,81	2,18	2,8	3,2	
	floor	3,63	3,66	3	3,2	1,3	
2	roof	2,44	1,9	1,69	1,97	3,2	
	floor	2,86	3,09			1,5	
3	roof	3,79	10,97	2,26	10,31	3,2	
	floor	4,37	11,66	3,69	10,86	1,3	
4	roof	7,52	2,72	4,6	4,2	3,2	
	floor	9,3	4,27	5,47	5,52	1,3	
5	roof	4,01	2,49	3,14	2,34	3,2	
	floor	5,34	3,27	3,53	3,06	1,3	
6	roof	5,72	5,3	3,77	6,33	3,2	
	floor		6,54	5,32	6,81	1,3	
7	roof	2,9	2,9	2,2	2,22	3,2	
	floor	3,4		2,8	3,48	1,3	
8	roof	3,23	2,65	3,02	2,86	3,2	
	floor		3,64	4,59		1,35	
9	roof	1,89	2,53	3,74	2,5	3,2	
	floor	2,97	3,52	4,98	3,8	1,34	
10	roof	3,66	2,88	3,44	2,42	3,19	
	floor	4,27	3,16	4,87	3,4	1,31	
11	roof	2,72	4,4	2,82	4,34	3,18	
	floor	3,64	5,21	3,69	5,09	1,27	
12	roof	2,78	3,02	1,74	2,22	3,21	
	floor	3,38	3,45	3,09	3,28	1,32	
13	roof	1,03	2,37	2,57	2,54		
	floor	2,04	2,5	2,19	3,84		
14	roof	3,94	4,56	e	f		
	floor	4,84	5,91	e	f		
15	roof	3,6	2,74	3,14	2,57		
	floor						
15 a	roof						
	floor						
16	roof	11,55	4,8	10,6	3,14	3,2	
	floor	11,94	5,81	11,9	4,35	1,31	
17	roof	2,4	4,42	2,6	5,16	3,21	
	floor	3,64	5,39	3,65	6,36	1,32	
18	roof	3,41	2,96	2,7	2,98	3,26	
	floor	4,19	3,9	3,48	4,2	1,33	
19	roof	2,39	1,82			3,23	
	floor	3,35				1,35	
20	roof	2,19					
	floor	2,64					

21	roof	7,27	2,81	7,38	1,53	3,2	
	floor	8,69	4,02	9,57	3	1,33	
22	roof	2,21	7,87	2,81	9,19	3,23	
	floor					1,34	
23	roof	5,94	2,09			3,21	
	floor	6,64	3,07			1,33	
24	roof	2,47	3,19			3,24	
	floor	3,32		10,74		1,33	
25	roof	4,22	2,89	2,77		3,24	
	floor		4,22			1,33	
26	roof	3,14	4,87	3,07	5,52	3,17	
	floor	4,61	5,62	4,29	6,79	1,27	
27	roof	3,23	5,26	2,43	4,48	3,25	
	floor	4,19	7,1	3,82	5,25	1,34	
28	roof	3,32				3,23	
	floor	3,8				1,33	
29	roof	3,24				3,22	
	floor					1,33	
30	roof	1,86				3,23	
	floor					1,33	
31	roof	1,26	2,36	2,86		3,02	versintert
	floor	1,74	2,25	3,3		1,32	
32	roof	1,62	1,85	1,08		3,14	
	floor		2,29			1,33	
33	roof	1,39	2,82	1	2,92	3,13	
	floor	2,19	3,47	1,68	3,91	1,32	
34	roof	2,22	2,82	4,61	2,2	2,95	versintert
	floor	3,27	3,12	5,73	2,63	1,32	
35	roof	1,03	6,63	4,63	5,49	3,05	versintert
	floor	1,23	7,38	5,09	6,89	1,31	
36	roof	1,62	3,7	3,15	1,27	3,16	
	floor	1,97				1,32	
37	roof	6,74	e				
	floor						
38	roof	3,81	3,7	2,16	2,7	2,76	backfill
	floor	4,37	4,04	2,6	2,97	1,33	
39	roof	3,01	2,95			3,17	backfill
	floor		3,62			1,29	
40	roof	1,57	1,91				backfill
	floor	2,03	2,21			1,31	
41	roof	1,13					backfill
	floor	1,73				1,35	
42	roof	1,8	1,7	2,2			
	floor	2,55				1,35	
43	roof	3,23					
	floor					1,35	

4.2 Results of the documentation of the Layer structure

	Layer [-]	Height		Sum [cm]	
		vertical Height [cm]	Height perpendicular to the dip [cm]		
Current mining area	Layer Blasted = 130		130		
	U = 38		38		
	C = 32		32		
	D = 36		36		
	E = 56		56		
	F = 36		36		
			328	328	
		-----	-----	-----	
	G = 70	70	67,1		
	H = 44	44	42,2		
	I2 = 25	25	24,0		
	I1 = 25	25	24,0		
	M = 25	25	24,0		
	Ma = 85	85	81,5		
x = 85 (CrMa, D1,...)	0	0,0			
	274	262,7	262,7		
	-----	-----	-----		
	CrMa = 13	13	12,5		
	D1 = 22	22	21,1		
	D2 = 31	31	29,7		
	C = 8	8	7,7		
	14" = 34	34	32,6		
	9' = 25	25	24,0		
	HH = 18	18	17,3		
	K = 38	38	36,4		
	x3 = 20 (Cr)	0	0,0		
	-----	0	0,0		
at 22.9 [m]		0	0,0		
	Cr = 41	41	39,3		
	L(5') = 9	9	8,6		
	M(6') = 30	30	28,8		
	Cr = 9	9	8,6		
	PPP = 33	33	31,6		
	Tachu = 24	24	23,0		
	x2 = 38 (MM)	0	0,0		
	-----	0	0,0		
at 30 [m]		0	0,0		
	MM = 50	50	47,9		
	Cr = 85	85	81,5		
	Q12 = 19	19	18,2		
	Q13 = 12	12	11,5		
	x4 = 13 (Cr)	0	0,0		
	-----	0	0,0		
at 36.2 [m]		0	0,0		
	Q12 = 19	0	0,0		
	Q13 = 12	0	0,0		
	Cr = 51	51	48,9		
	Amour = 20	20	19,2		
	Coral Coriandre = 12.5	12,5	12,0		
	S = 21	21	20,1		
	T = 25	25	24,0		
	x5 = 30	0	0,0		
		630,5	604,5	604,5	
	-----	-----	-----		
			Sum	1195,2	

4.3 Results Point Load Test – blasted layers (between BB and U)

Sample	Area					Result	Foto Nr.	Info
	H	B		L				
		B1	B2	L1	L2			
	[cm]	[cm]	[cm]	[cm]	[cm]			
1	4	5		5,5		40,7	1777	
2	4	4,5		9,5	7	51,2	1778	
3	4,2	5	5	7	8	37,8	1779	
4	4,5	5,5	7	10		68,3	1780	dolomitic
5	4	14,5		5	6	50	1781	
6	4,5	6,5		10		37,4	1783	
7	5,5	10,5		7		41,4	1786	
8	3,5	6,5		7,5		25,9	1788	
9	3,8	9		9		39,5	1789	
10	4,5	5		11		52,6	1791	

4.4 Results Schmidhammer

Schmidhammer Model L2, horizontal 27.10.2011

Pillar 11	Layer				
	U	C	D	E	F
1	40	39	39	42	38
2	43	43	41	46	38
3	43	43	39	43	40
4	41	38	39	4	41
5	44	42	42	45	40
6	40	42	38	47	41
7	40	42	39	43	41
8	42	38	39	40	43
9	45	38	39	40	40
10	43	39	40	44	43

Schmidhammer Model N-9, horizontal 28.10.2011

Pillar 11	Layer				
	U	C	D	E	F
1	59	56	51	52	58
2	57	56	53	53	58
3	54	54	52	54	57
4	51	54	51	53	56
5	52	54	53	51	56
6	54	52	54	50	58
7	54	54	54	54	56
8	53	55	52	54	57
9	56	51	52	53	58
10	59	55	54	52	55

Pillar 3 Layer

Pillar 3	Layer				
	U	C	D	E	F
1	42	46	43	41	41
2	43	45	45	45	39
3	39	44	45	44	41
4	43	44	46	43	40
5	43	45	45	44	38
6	44	44	45	42	41
7	48	46	46	44	39
8	47	42	46	46	40
9	46	42	44	41	40
10	47	43	44	40	42

Pillar 3 Layer

Pillar 3	Layer				
	U	C	D	E	F
1	55	53	58	54	52
2	55	54	58	54	57
3	50	54	55	57	53
4	52	56	55	57	56
5	55	56	55	57	55
6	55	56	55	56	56
7	52	55	56	56	56
8	55	54	55	54	55
9	53	55	54	56	55
10	55	55	55	56	52

Pillar 10 Layer

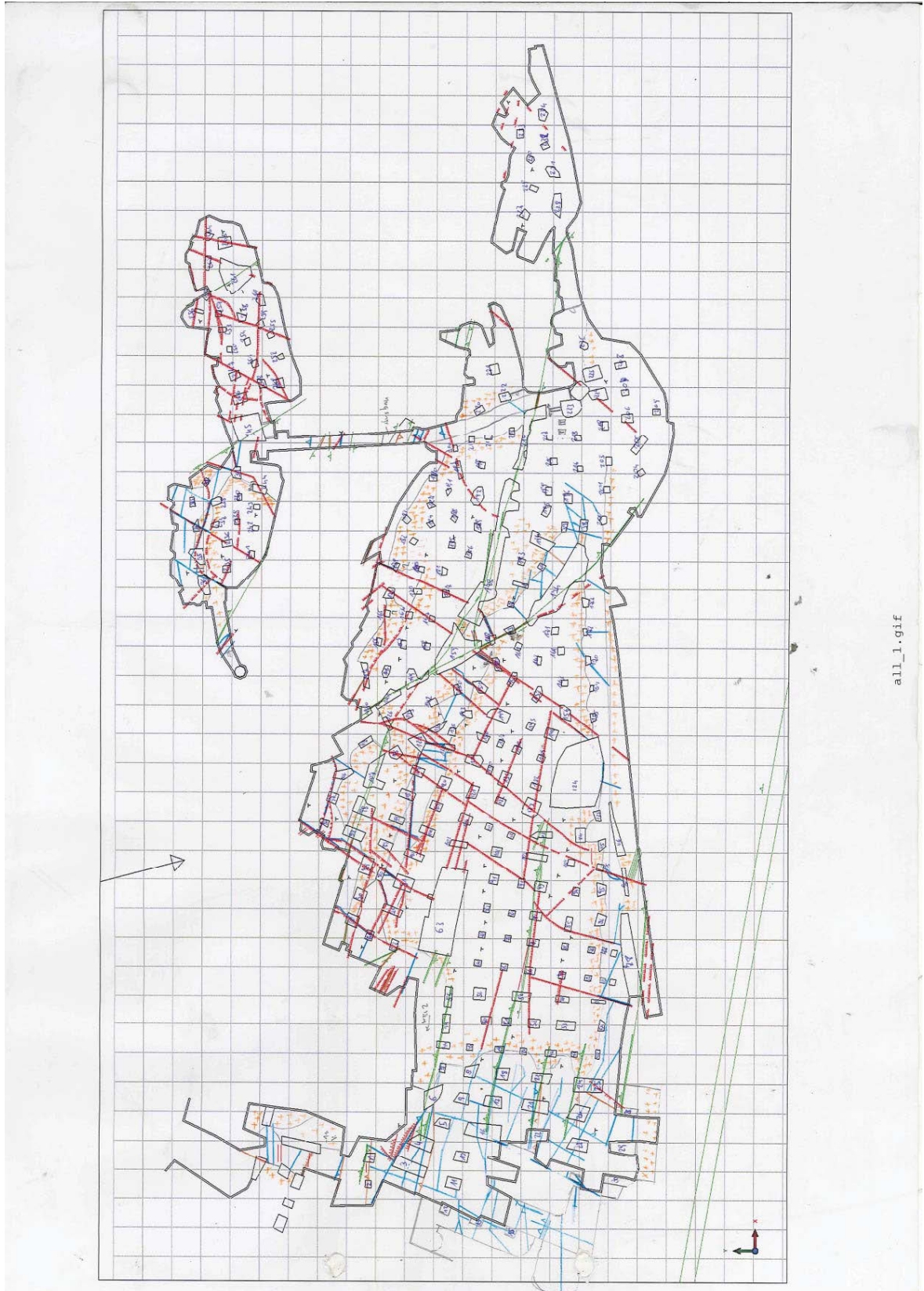
Pillar 10	Layer				
	U	C	D	E	F
1	42	43	45	40	40
2	47	44	41	41	39
3	48	44	45	39	36
4	44	44	47	40	42
5	45	42	38	42	34
6	42	42	42	39	41
7	45	42	43	40	36
8	43	42	46	40	36
9	44	43	39	42	39
10	47	42	44	42	42

Pillar 10 Layer

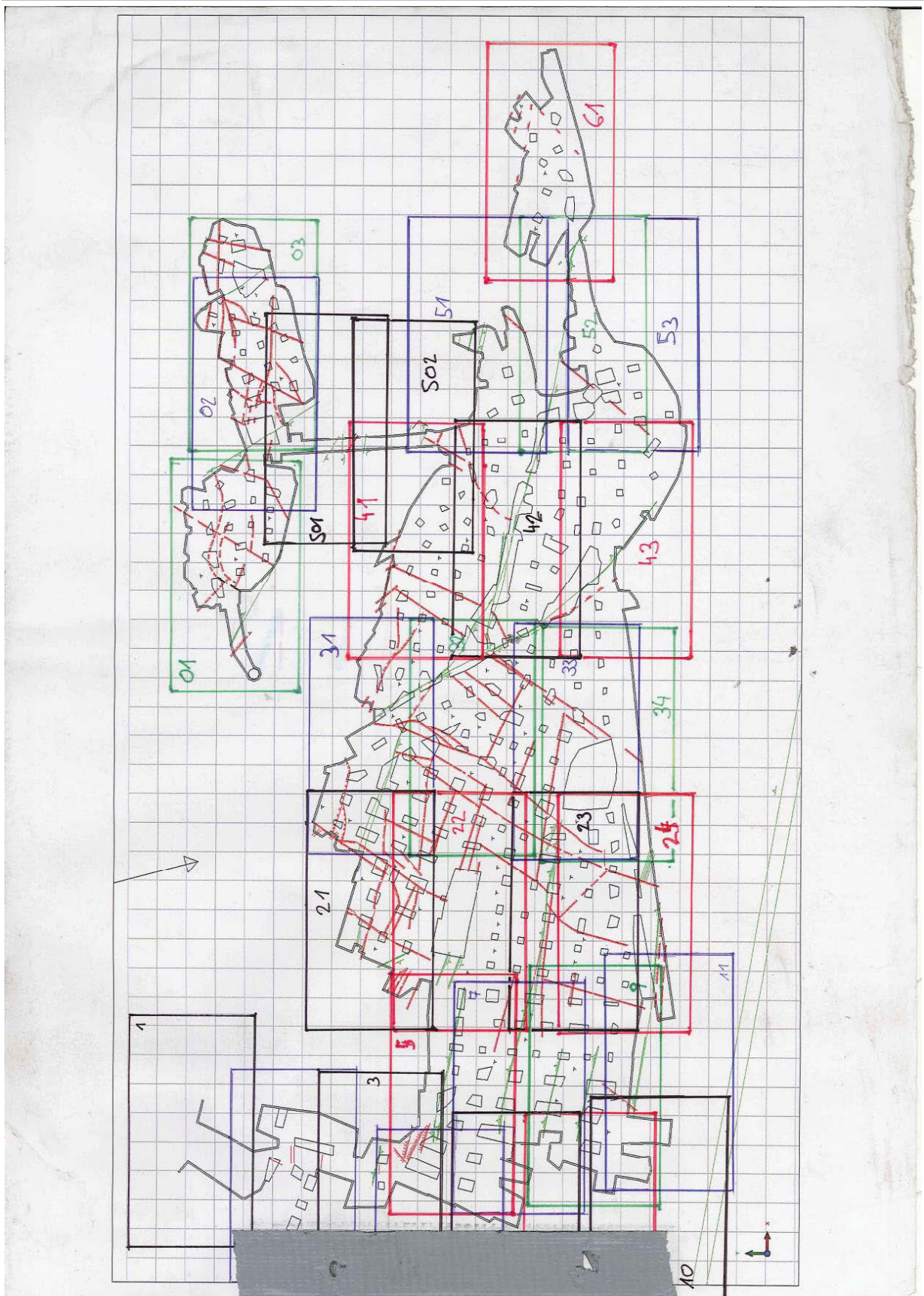
Pillar 10	Layer				
	U	C	D	E	F
1	54	55	56	54	57
2	55	57	56	53	58
3	53	55	57	54	58
4	55	56	56	53	58
5	54	55	55	55	58
6	52	57	52	56	56
7	52	54	53	56	56
8	55	55	53	53	57
9	56	56	58	57	57
10	54	57	55	52	56

4.5 Maps used at the fieldwork

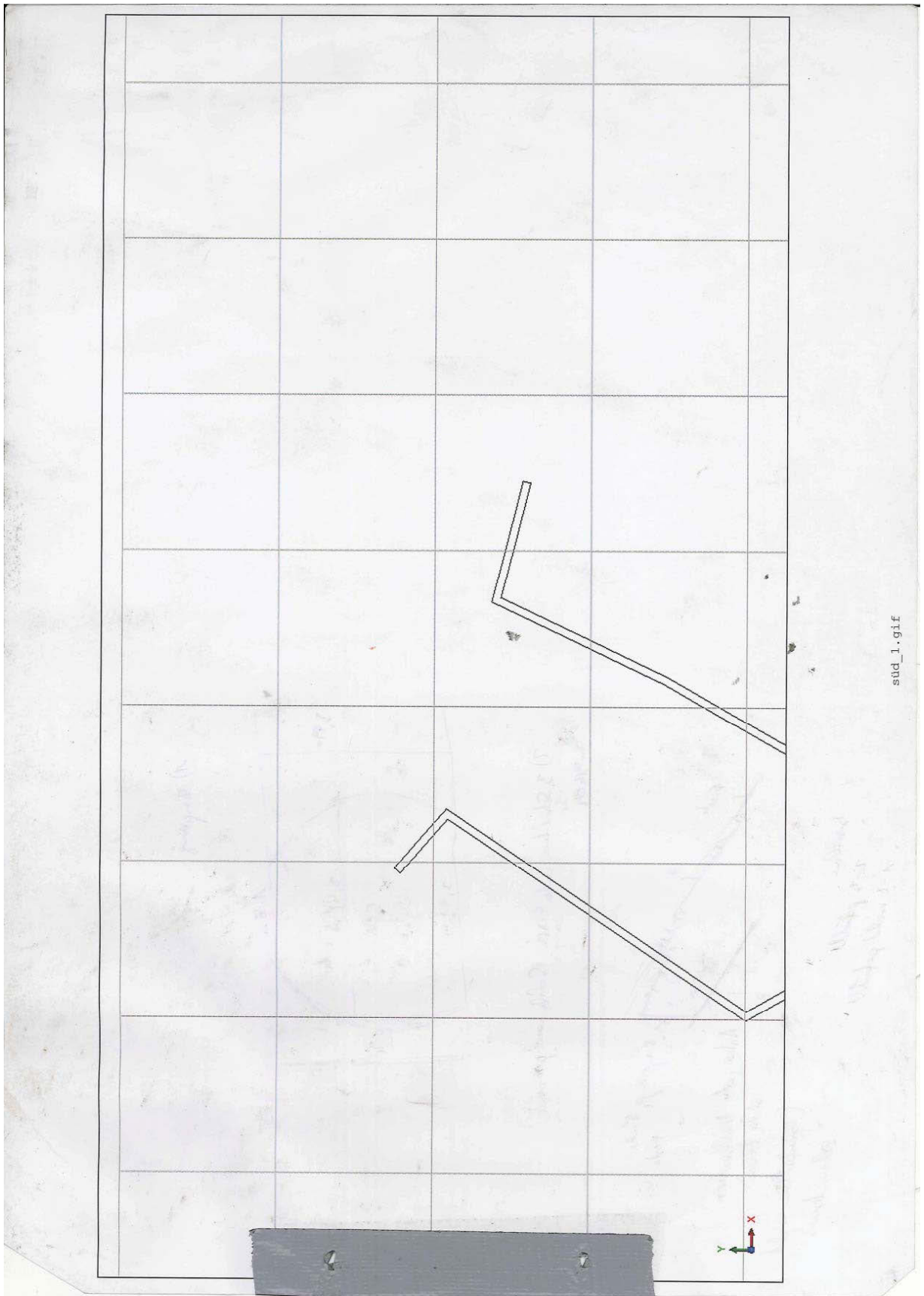
4.5.1 Overview - results



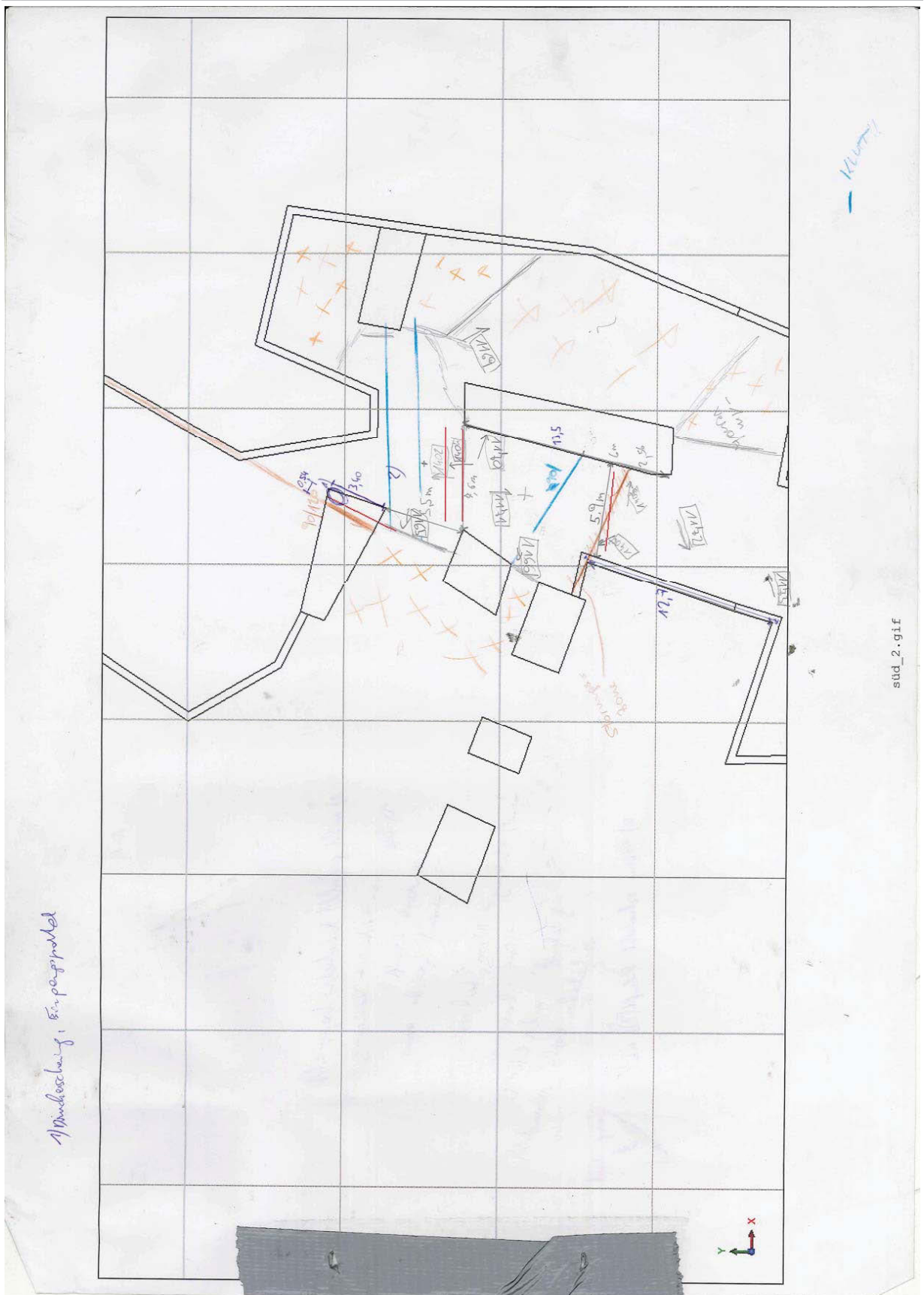
4.5.2 Overview – table of content



4.5.3 Map part 1



4.5.4 Map part 2



std_2.gif

4.5.6 Map part 4



sud_4.gif

4.5.9 Map part 7

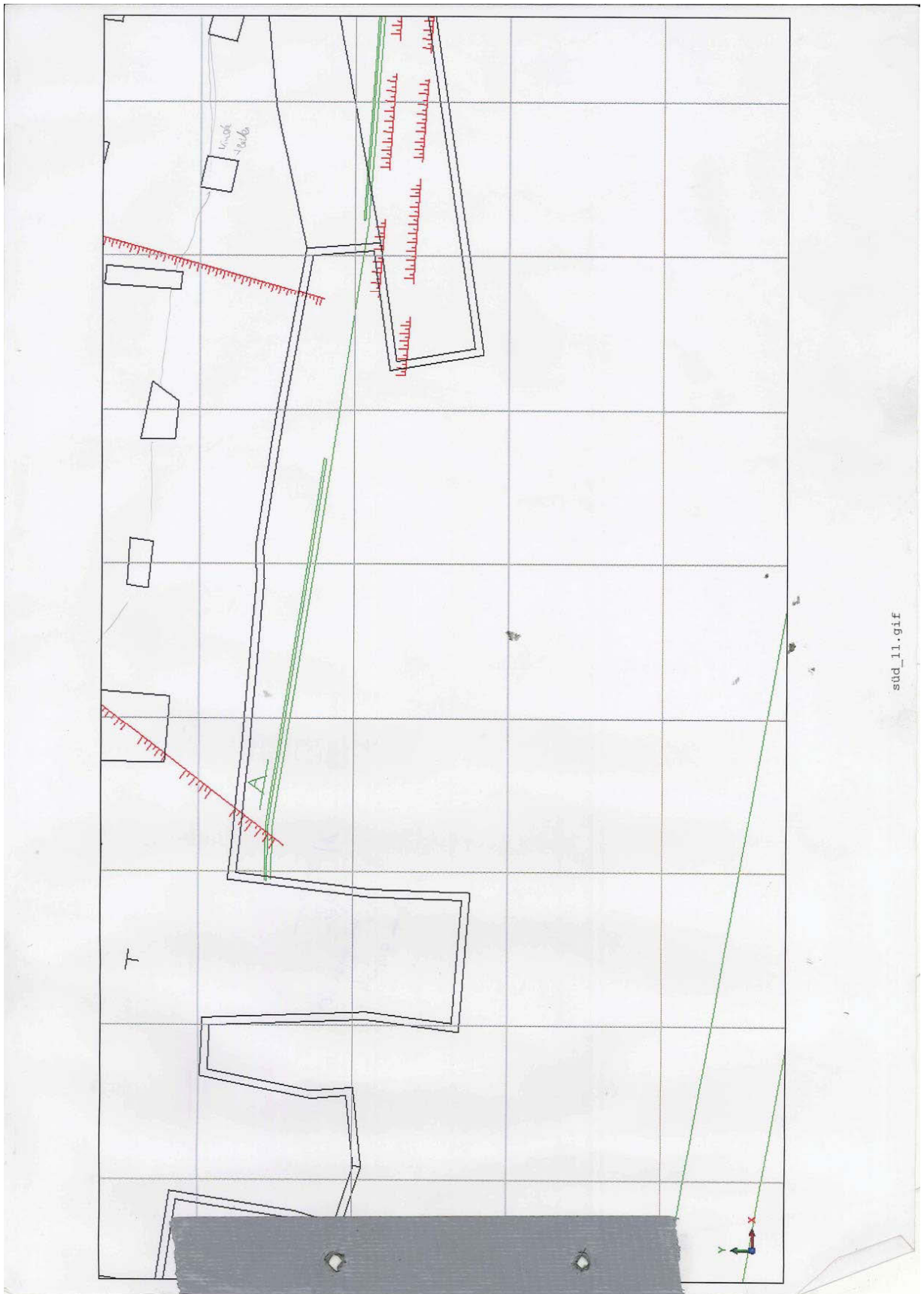


sud_7.gif

4.5.11 Map part 9



4.5.13 Map part 11

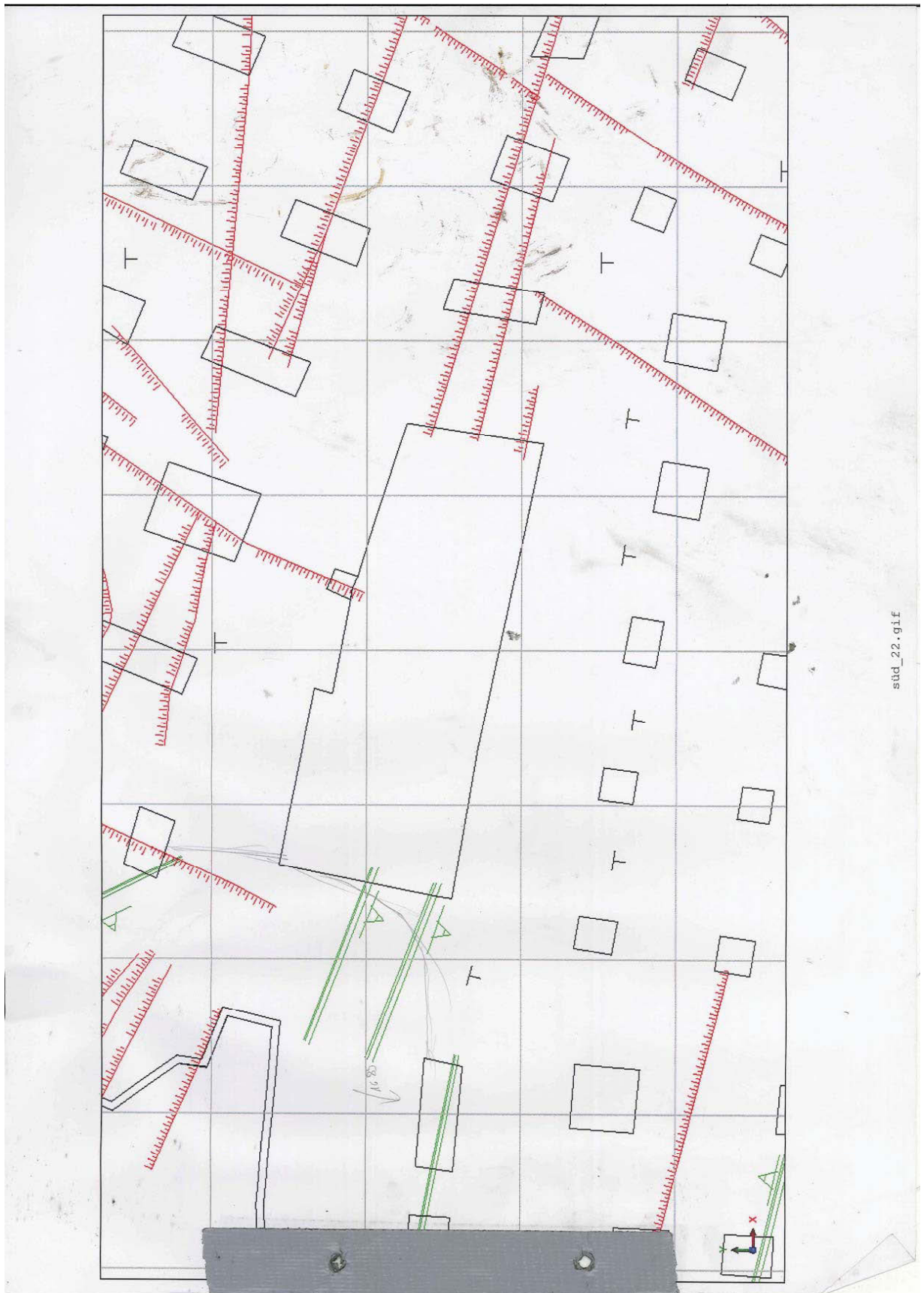


4.5.14 Map part 21

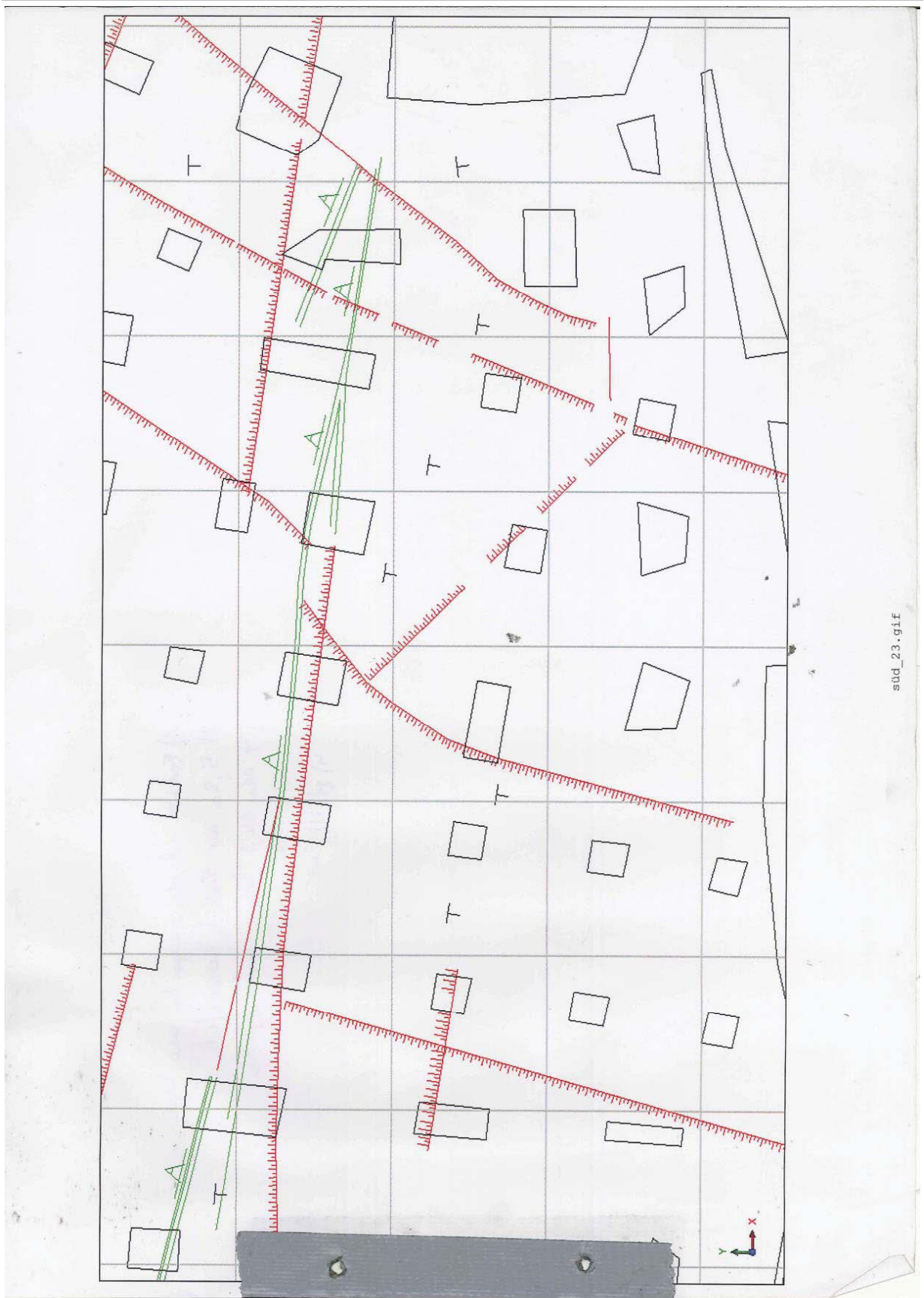


sud_21.gif

4.5.15 Map part 22



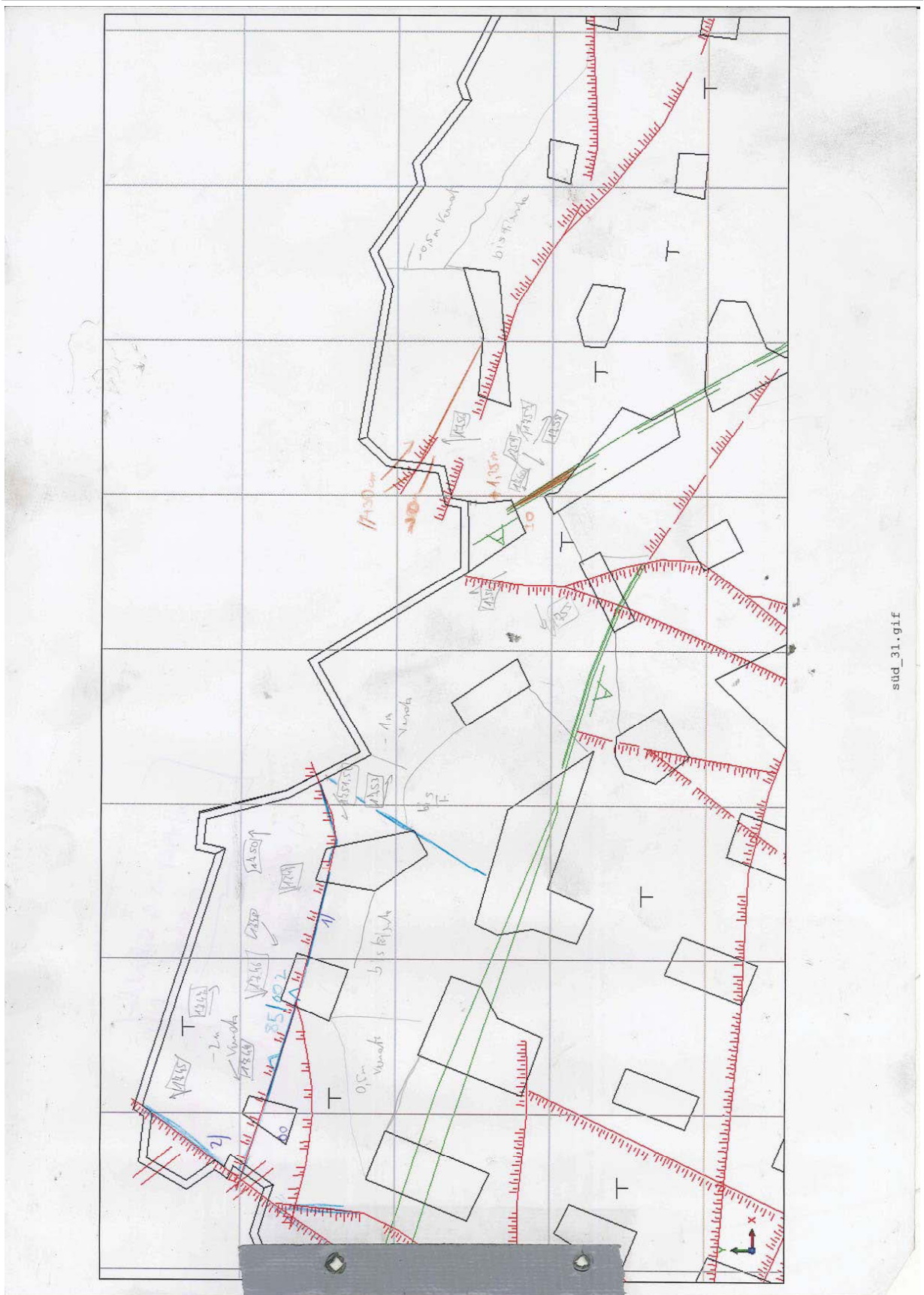
4.5.16 Map part 23



4.5.17 Map part 24

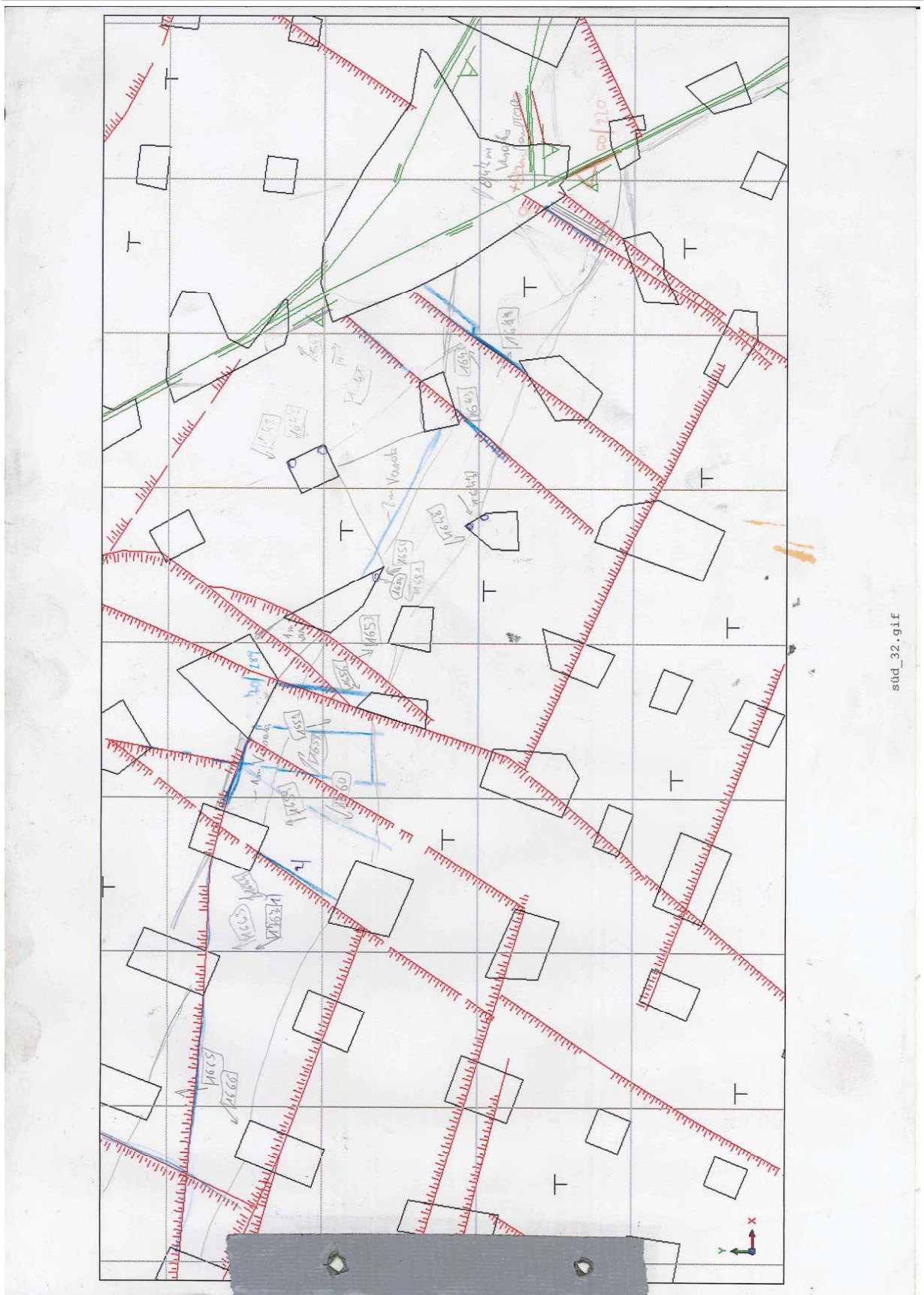


4.5.18 Map part 31



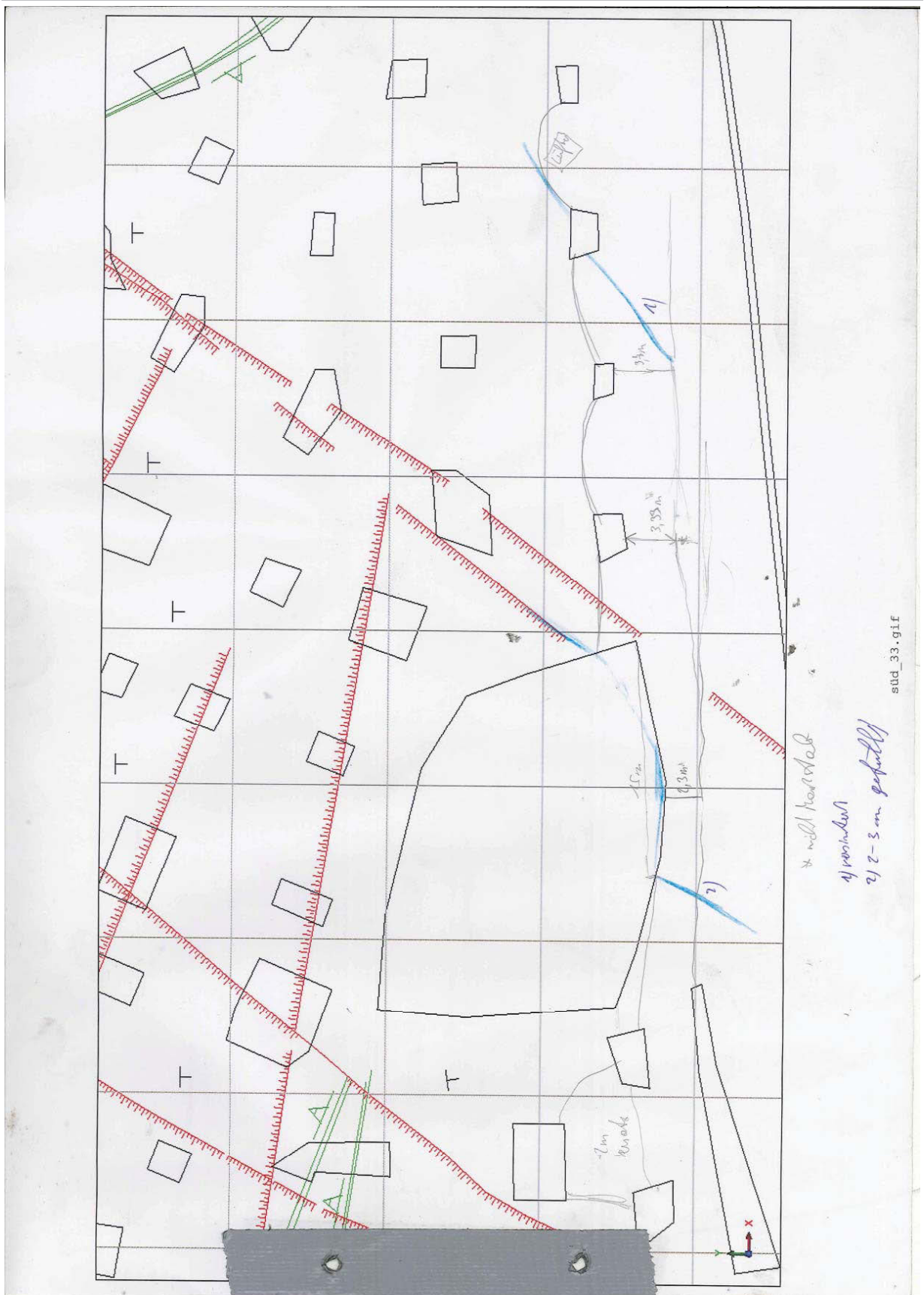
sud_31.gif

4.5.19 Map part 32

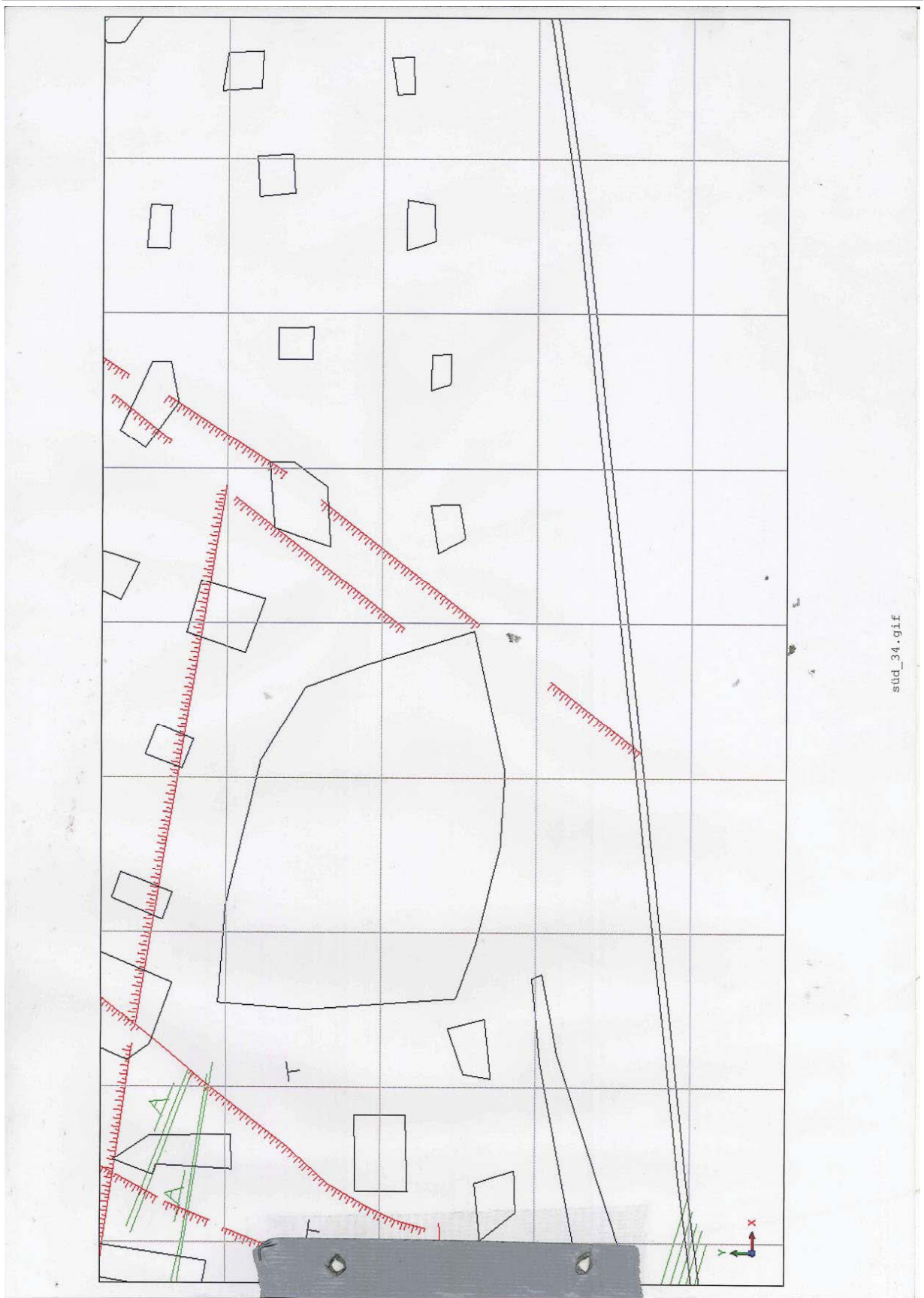


sud_32.gif

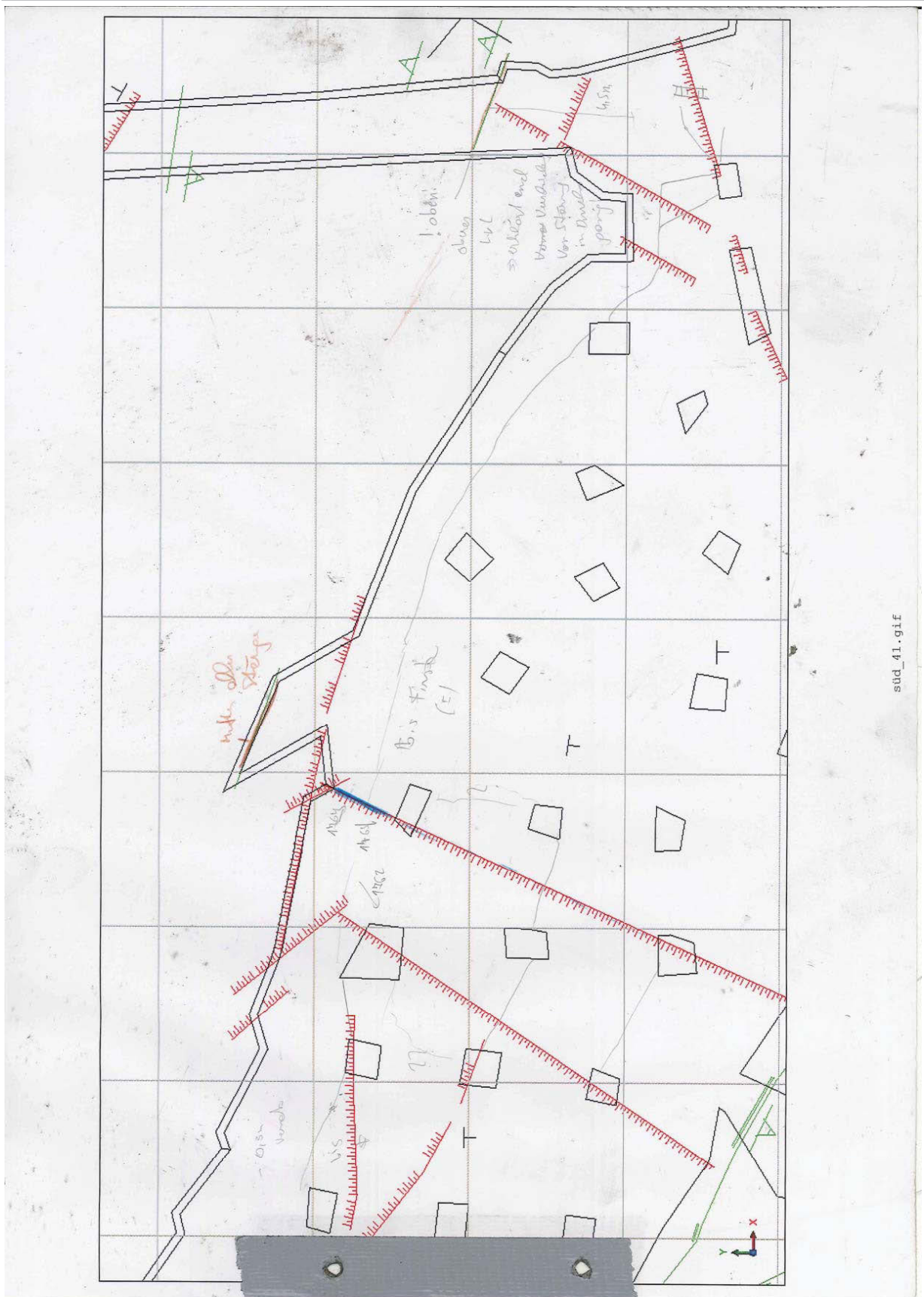
4.5.20 Map part 33



4.5.21 Map part 34



4.5.22 Map part 41



4.5.24 Map part 43



stud_43.gif

4.5.27 Map part 53



4.5.28 Map part 61



4.5.29 Map part 01



4.5.31 Map part 03

